

UC Berkeley

SEMM Reports Series

Title

Large deflection analysis of plates

Permalink

<https://escholarship.org/uc/item/3f56p42t>

Author

Murray, David

Publication Date

1967-09-01

REPORT NO.
67-44

STRUCTURES AND MATERIALS RESEARCH
DEPARTMENT OF CIVIL ENGINEERING

LARGE DEFLECTION ANALYSIS OF PLATES

By
D. W. MURRAY

REPORT TO
NATIONAL SCIENCE FOUNDATION
NSF GRANT GK-75

SEPTEMBER 1967

STRUCTURAL ENGINEERING LABORATORY
UNIVERSITY OF CALIFORNIA
BERKELEY CALIFORNIA

Structures and Materials Research
Department of Civil Engineering

LARGE DEFLECTION ANALYSIS OF PLATES

by

D. W. Murray

Graduate Student

E. L. Wilson

Faculty Investigator

Structural Engineering Laboratory
University of California
Berkeley, California

September 1967

ABSTRACT

A brief introduction to the finite element concept and a formulation of classical large deflection plate equations is presented. A general approach to large deflection problems of elastic structures, based on an equilibrium balance between the resisting forces of the final structural configuration and the applied loads, is discussed. The details of a finite element formulation for large deflection plate problems are developed. This development makes use of the constant strain triangle (CST) for in-plane deformation and the linear curvature compatible triangle with nine degrees of freedom (LCCT-9) for out-of-plane deformations. Results of solutions using this technique are compared with typical solutions achieved by the use of classical plate equations. The concept of geometric stiffness is discussed and formulated so that it is applicable to plate problems. The formulation is applied to solve problems where elastic plates with varying support conditions are loaded into post-buckling configurations. The formulation of the plate problem for nonlinear material properties is discussed and an approximate method is developed. Examples of its application are presented.

ACKNOWLEDGMENTS

This work was carried out during the course of study for a Ph.D. degree in Civil Engineering at the University of California in Berkeley.

The author wishes to express his deep appreciation to Professor E. L. Wilson for his supervision, patience and support throughout the course of this work. In addition he would like to express his appreciation to Professors R. W. Clough and R. J. DeVogelaere for serving as members of his thesis committee.

This work would not have been possible without the generous support of the University of California Computer Center which subsidized the computer time necessary for extensive program development.

In addition the author would like to express his appreciation to the many graduate students and colleagues at the University of California who contributed, through their discussions, to the development of this work. In particular the timely suggestions of Dr. C. A. Felippa are gratefully acknowledged.

Finally, the author would like to give special thanks to his wife and family for their patience and fortitude in foregoing the normal fruits of life during this period.

CONTENTS

	Page
ABSTRACT	ii
ACKNOWLEDGMENTS	iii
NOMENCLATURE AND LIST OF SYMBOLS	vii
INTRODUCTION	1
Chapter	
1. FORMULATION OF PLATE EQUATIONS	4
1.1 Introduction	4
1.2 Relation of the Large Deflection Plate Problem to Nonlinear Theory of Elasticity	5
1.3 Formulation of Equations	6
1.3.1 Displacement Formulation of the Equations of Elasticity	6
1.3.2 The Strain-Displacement Relations	7
1.3.3 Restrictions on the Displacement Field-- Kirchoff Assumptions	10
1.3.4 The Constitutive Relations and the Strain Displacement Equations	13
1.3.5 The Equilibrium Equations	16
1.3.6 Derivation of Plate Equations	22
1.4 Summary of Plate Assumptions	27
2. A LARGE DEFLECTION FINITE ELEMENT ANALYSIS OF PLATES	30
2.1 Selection of a Finite Element Idealization	30
2.1.1 A Review of Basic Concepts	30
2.1.2 A Survey of Element Development	33
2.1.3 Selection of Element for this Analysis	34
2.2 A General Approach to Large Deflection Analysis	37
2.3 The Stiffness Formulation	40
2.3.1 Stiffness Formulation for Linear Structures	42
2.3.2 Incremental Stiffness	43
2.3.3 An Approximate Stiffness	46
2.3.4 The Direct Stiffness Procedure	47

Chapter	Page
2.4 The Element Stiffness	48
2.5 Derivation of Stiffness for In-Plane Deformations . . .	54
2.6 Derivation of Stiffness for Out-of-Plane Deformations .	55
2.7 Evaluation of Element Deformations	56
2.8 Evaluation of Element Forces	61
2.9 Global Transformation, Assembly and Iteration	62
2.10 Solution of Equations	65
2.11 Applications	66
2.11.1 Inextensional Bending	66
2.11.2 Cylindrical Bending	68
2.11.3 Simply Supported Plate - Uniform Load	70
2.11.4 Clamped Square Plate - Uniform Load	76
2.11.5 Post-Buckling Behavior of a Cantilevered Plate	76
2.12 Discussion of Results - Stresses	79
3 THE GEOMETRIC STIFFNESS	92
3.1 Introduction	92
3.2 Formulation of a "Complete" Geometric Stiffness for Two-Dimensional Elements	94
3.3 Geometric Stiffness Matrix for Influence of In-Plane Forces on Bending Stiffness	100
3.4 Applications	101
3.4.1 Post-Buckling of a Cantilevered Plate	101
3.4.2 Post-Buckling Behavior of a Square Plate	103
3.4.3 Post-Buckling of a Simulated Flange Plante	108
3.4.4 Post-Buckling of a Simply Supported Rectangular Plate With an Aspect Ratio of 1.75	111
3.4.5 Discussion	111
4 VARIABLE MATERIAL PROPERTIES	115
4.1 Introduction	115
4.1.a Material Properties	115
4.1.b Numerical Computations	116

Chapter	Page
4.1.c The Displacement Model	116
4.1.d Discussion	117
4.2 Stiffness Formulation for Variable Material Properties	118
4.2.1 The Element Stiffness	118
4.2.2 Incremental Stiffness, Geometric Stiffness and Stress Determination	120
4.3 A General Solution Technique Including Nonlinear Material Effects	121
4.4 An Approximate Method of Including Nonlinear Material Effect	125
4.4.a A Nonlinear Elastic Constitutive Relationship	125
4.4.b Derivation of Element Stiffness Matrix	127
4.5 Solution Procedure	131
4.6 Application	131
4.6.1 Moment Curvature	131
4.6.2 Cylindrical Bending of $\frac{1}{2}$ inch Plate	135
4.6.3 Cylindrical Bending of 0.1 inch Plate	135
4.7 Discussion of Analysis for Nonlinear Materials	135
5 PROGRAMMING	141
5.1 Program Outline	141
5.2 Computational effort	143
6 SUMMARY AND CONCLUSIONS	144
REFERENCES	145
APPENDIX A	148
APPENDIX B	155
APPENDIX C	164
APPENDIX D	189

NOMENCLATURE AND LIST OF SYMBOLS

Symbols have been defined as they appear in the text. However it has not been possible to maintain uniform symbology throughout since in some sections special emphasis has been required. Wherever possible this is noted below. The tilde (\sim) indicates the quantity is a function of the spatial co-ordinates. A subscript 0 indicates the quantity is referred to the middle surface or to a configuration referred to as the "initial" configuration.

- a_i - directed projections of sides of triangle on x axis
- a_{ij} - direction cosines of displaced co-ordinate system
- A - plan area of triangle
- A_k, A^k - plan area of subtriangle
- A_{ij} - area of triangle formed by joining corners i and j with the origin
- $[A]$ - matrix relating $\{\Delta\tilde{\epsilon}^P\}$ and $\{\Delta\tilde{\epsilon}\}$
- b_i - directed projections of sides of triangle on y axis
- B - $\frac{Eh}{1-\nu^2}$ in Chapter 1; Subscript indicating Bending
- $[\tilde{B}], [\tilde{B}_\Delta]$ - matrices of functions to define strains from nodal point displacements
- $[B_e], [B_o]$ - matrices arising in determination of nodal curvatures from nodal displacements
- c - distance from middle surface to center of stiffness
- C_i - $\cos \gamma_i$

$[\tilde{C}]$	- constitutive matrix
$[\bar{C}]$	- constitutive matrix of linear elasticity in Chapter 4
d_i	- dimension of triangle (see Appendices C and D)
D	- $\frac{Eh^3}{12(1-\nu^2)}$
$[\tilde{D}], [\tilde{D}_\Delta], [\tilde{D}_k]$	- matrices of functions to define displacement field from nodal displacements
E	- subscript indicating P, B order of nodal vectors
e	- subscript indicating "corner order" of nodal vector
e_{ij}	- Cauchy infinitesimal strain tensor
E, E_T, E_s	- elastic moduli; normal, tangent and secant, respectively
E_{ij}	- Green's strain tensor
\hat{e}_i, \hat{E}_i	- unit base vectors
f	- arbitrary function of triangular co-ordinates
$\{F\}, F_i$	- body force vector and its components per unit of mass
h	- thickness of plate
h_i	- height of triangle
i	- index with range of 3
I	- moment of inertia
I_3	- 3×3 identity matrix
j	- index with range of 3

- $[K], [K_G], [K_D], [K_I]$ - stiffness matrices: normal, geometric, displaced, incremental, in-plane, bending, corner order (local), coupling PB, corner order, secant, and tangent, respectively
- $[K_P], [K_B], [\bar{K}], [K_{PB}]$
- $[K_e], [K_s], [K_T]$
- l_i - length of side of triangle
- $[L], [L_E]$ - numerical matrices arising from integration of interpolation functions
- $\{\tilde{m}\}, \tilde{m}_x, \tilde{m}_y, \tilde{m}_{xy}$ - vector of stress couples and its components
- M_x, M_y, M_{xy} - stress couples in Chapter 1
- M_x, M_y, M_X, M_Y - nodal moments about the x, y, X, Y axes respectively
- $[\tilde{M}]$ - matrix of functions to determine stress couples from nodal displacements
- n_i - co-ordinate measure normal to side l_i
- $\{\tilde{n}\}, \tilde{n}_x, \tilde{n}_y, \tilde{n}_{xy}$ - vector of stress resultants and its components
- $[\tilde{N}]$ - matrix of functions to determine stress resultants from nodal displacements
- $N_\alpha, N_{\alpha\beta}$ - stress resultants in Chapters 1 and 3
- o - subscript indicating middle surface; subscript indicating initial configuration, or centroid
- P - subscript for in-Plane nodal quantities
- $P_x, P_y, P_z, P_X, P_Y, P_Z$ - nodal forces in x, y, z, X, Y, Z, directions respectively
- $[P]$ - constitutive matrix for elastic-plastic material
- q - uniform pressure normal to plate surface
- Q_α - shear resultants

$[Q], [\bar{Q}]$

- numerical matrices arising from integration of interpolation functions

$[Q_0], [Q_k]$

- matrices arising in condensing nodal displacements of center point of triangle

$\{r\}, \{r_k\}$

- nodal displacements of structure and element k

$\{r_E\}, \{r_P\}, \{r_B\}$

- element nodal displacements (see subscripts E, P, B)

$\{r_{P_c}^k\}, \{r_{B_c}^k\}, \{r_{B_c}^k\}$

- element nodal displacements: on plane $z = c$, and for subtriangle k with 10 and 9 degrees of freedom, respectively

$\{r_0\}$

- nodal displacement for centroid of triangle

$\{\bar{r}_e\}, \{\bar{r}_i\}, \{r_e\}, \{r_i\}$

- corner order of element nodal displacements in local and global co-ordinates respectively

\vec{r}, \vec{r}^*

- position vector before deformation in global and local co-ordinates respectively

$\{R\}, \{R_f\}, \{R_s\}$

- applied generalized forces for structure

$\{R_k\}, \{R_{fk}\}, \{R_{sk}\}$

- applied generalized forces for element k

$\{R_E\}, \{R_P\}, \{R_B\}$

- element nodal forces (see subscripts E, P, B)

$\{\bar{R}_e\}, \{\bar{R}_i\}, \{R_e\}, \{R_i\}$

- corner order of element forces in local and global co-ordinates respectively

\vec{R}^*

- position vector for displaced reference element

$s, ds, ds_0; s_i$

- length measure; side co-ordinate (Appendix D)

S, S_0, dS

- area measure

S_i

- $\sin \gamma_i$

S_{ij}

- Kirchoff stress tensor

$\{T\}, T_i$

- surface traction vector and its components

$[T_c]$

- corner transformation matrix

- $dT_i, dT_i^{(u)}, dT_i^{(v)}, dT_i^{(z)}$ - force vector on element of surface area dS
- $\{\tilde{u}\}, \tilde{u}_i$ - general displacement vector and its components
- \tilde{u} - displacement in x direction
- $\{u\}$ - nodal vector of u displacements
- \tilde{U} - displacement in X direction
- $\{U\}, U_i$ - nodal vector of U displacements and its components
- \tilde{v} - displacements in y direction
- $\{v\}, v_i$ - nodal vector of v displacements and its components
- V, dV, V_k, dV_k - volume measures
- \tilde{V} - displacement in Y direction
- $\{V\}, V_i$ - nodal vector of V displacements and its components
- \tilde{w} - displacement in z direction
- $\{w\}, w_i$ - nodal vector of w displacements and its components
- $\{w_x^{k_i}, w_y^{k_i}, w_{xi}, w_{yi}\}$ - nodal vectors of first derivatives of w and their components
- \tilde{W}, W_i - displacement in Z direction and nodal values
- $[\bar{W}_{x1}], [\bar{W}_{x0}], [W_x], [W_y]$ - matrices specifying nodal slopes in terms of nodal displacements
- x, X - global and local co-ordinates respectively: In Chapter 1, undeformed and deformed co-ordinates respectively *
- x^*, X^* - undeformed co-ordinates before and after displacement †
- X_x^*, Y_y^* - derivatives of co-ordinate transformation ‡
- \bar{x}, \bar{y} - see * (above)
- \bar{x}^*, \bar{y}^* - see † (above)
- \bar{y}_x^*, \bar{y}_y^* - see ‡ (above)

z, Z	- see * (above)
z^*, Z^*	- see † (above)
α	- index with range 2; range of 3 in Appendix A
β	- index with range of 2; range of 3 in Appendix A
δ_{xy}, δ_i	- shearing stress: angle of side i with x axis
$\Gamma, \Gamma_0, \Delta\Gamma$	- configuration of structure
δ, Δ, Δ^k	- variation, increment, and correction for deformation of side k, respectively
$\tilde{\epsilon}_i, \{\tilde{\epsilon}\}, \epsilon^P, \epsilon^E$	- engineering strain, strain vector, plastic and elastic strain respectively
$\bar{\epsilon}, \bar{\epsilon}^P$	- effective strains
$\{\zeta\}, \zeta_i$	- vector of triangular co-ordinates and its components
θ_x, θ_y	- nodal rotations
$\{\theta_x\}, \{\theta_y\}, \{\theta\}$	- vectors of nodal rotations
$\theta_{s\alpha}^k$	- end slope of side k of triangle
$[\Lambda_\alpha], [\Lambda_\beta]$	- matrices of functions for geometric stiffness
λ_i	- = d_i/l_i
μ_i	- = $1 - \lambda_i$
ν	- Poisson's ratio
$\pi_\epsilon, \pi_\epsilon^P, \pi_\sigma$	- strain and stress invariants
$\rho, \bar{\rho}$	- density; position vector after deformation
$\tilde{\sigma}_i, \{\tilde{\sigma}\}, \tilde{\sigma}_x, \tilde{\sigma}_y, \tilde{\sigma}_{xy}$	- Eulerian stress tensor; stress vector and its components
$\bar{\sigma}$	- effective stress
$\{\varphi_u\}, \{\varphi_v\}, \{\varphi_w\},$ $\{\varphi_u^k\}, \{\varphi_w^k\}$	- interpolation functions for u, v, w displacements - subtriangle interpolation functions

- ϕ_x, ϕ_y - nodal rotations
- $\{\tilde{\epsilon}\}, \tilde{\epsilon}_{xx}, \tilde{\epsilon}_{yy}, 2\tilde{\epsilon}_{xy}$ - curvature vector and its components
- $\{\epsilon\}, \{\epsilon_i\}$ - nodal curvature vectors
- ω_{ij} - infinitesimal rotation tensor
- ,
- *
- footnote symbol; virtual quantity; undeformed value
- ∇^2 - harmonic operator
- ∇^4 - biharmonic operator

INTRODUCTION

In the last decade the introduction of high speed digital computers has had a profound effect on the field of structural analysis. The availability of such machines has enabled engineers to solve problems which were intractable before. In order to efficiently utilize such powerful tools, matrix formulation, together with generalized concepts of stiffness and flexibility have become the common base of communication in structural engineering.

In the field of continuum mechanics the effect has not been so pronounced but the computer has led to intensive activity in developing techniques in which the behavior of a continuum can be represented by a discretized system. One technique of this type has been the representation of a continuum by a model consisting of a finite number of "elements." This technique is known as the "finite element" method. If the problem is formulated on the basis of a variational principle, the finite element method is equivalent to a Rayleigh-Ritz procedure in which the domain of a set of trial functions is restricted to the volume of an element and the same trial functions are used in the domain of each element. The finite element method is therefore sometimes referred to as an "extended Ritz method."

This dissertation develops a finite element method of analysis for plate structures including the effects of large deformations.[†]

The analysis is based on approximating the actual plate structure by an idealized model composed of triangular finite elements. A detailed

[†] The meaning of the term "large deformations" in the context of this work is discussed in section 1.2.

discussion of the concept of finite element representation of a two-dimensional continuum, and a review of recent developments in this field, has been presented by Felippa [1][†] and others, and will not be repeated here. A short review of the basic concepts is contained in section 2.1.

The particular finite element model adopted for this investigation assumes that in-plane deformation produces constant strain in each element while out-of-plane deformation produces a linear variation of curvature throughout the element (discontinuous along lines connecting the corners with the centroid). This is equivalent to combining the behavior of two previously developed elements: the constant strain triangle (CST) and the linear curvature compatible triangle with nine degrees of freedom (LCCT-9). The application of the constant strain triangle to problems of plane stress and plane strain, and the application of linear curvature compatible triangles to problems of plate bending, has been presented elsewhere [2, 3]. The details of coupling the behavior of these elements together to solve problems involving large deflection of plate structures are dealt with here.

The method is applicable to problems in which the membrane and bending effects both contribute to the carrying capacity of the structure. The solution technique is iterative and the effects of the initial stress may be optionally included to give a more accurate estimate of incremental stiffness. This is advantageous in investigating post buckling behavior. Since deformation in these structures often exceeds the proportional limit of the material, an approximate method of including the effect of nonlinear material behavior has been included.

[†] Numbers in square brackets refer to references listed at the end.

The finite element approach in general has a number of advantages over more classical solution methods. Once it is formulated for a particular type of element it is applicable to arbitrary geometries, loading and boundary conditions. In addition, there is no difficulty in principle in extending the formulation to problems involving incremental analysis, variation of material properties or step-by-step dynamic analysis. For large deflection plate problems, the formulation presented in this dissertation possesses the additional advantage that it is not subject to the geometric restrictions on slopes that are present in the classical formulation of the plate equations.

The method presented here is based on the simplest finite element model that gives a reasonable representation of the macroscopic behavior of a plate. Further developments are to be expected upon the introduction of higher order elements, better inter-element compatibility, refined geometric relationships, and extension to problems of the type mentioned in the paragraph above. In addition it appears feasible to investigate the construction of an element stiffness which couples the in-plane and out-of-plane behavior at the element level.

1. FORMULATION OF PLATE EQUATIONS

1.1 Introduction

In order to evaluate the effectiveness of the finite element approach, results are usually compared with those obtained by "classical methods" of solution for typical problems.[†] In formulating this finite element approach to large deflection plate problems, most of the assumptions are similar to, but not always identical with, those of classical plate theory. Because of this it is advantageous to review the development of the classical plate equations so that the assumptions associated with the two approaches may be compared.

In formulating the plate equations either a physical or a variational approach may be used. The physical approach will be followed since it best suits the purpose of this discussion. Two alternative developments are available:

- (a) the three dimensional elasticity equations may be reduced to two dimensional equations by imposing the assumptions of plate theory, or,
- (b) the plate equations may be set up directly from two dimensional relationships.

We adopt the former approach because it leads to a more direct evaluation of the approximations involved. The development follows that outlined by Fung [4] but more emphasis is placed on physical interpretation in an effort to gain a better appreciation of the factors involved.

[†] See section 2.1.1.

1.2 Relation of the Large Deflection Plate Problem to Nonlinear Theory of Elasticity

The nonlinear theory of elasticity considers nonlinearities which arise from finite deformation. Finite deformation implies finite engineering strain or finite rotation or both. When deformations are finite it is necessary to specify whether stresses and strains are referred to the original configuration (Lagrangian description) or the deformed configuration (Eulerian description). Equilibrium must be established in the deformed configuration while the geometry and boundary conditions are usually specified in the original configuration. When the Lagrangian description is used the kinematic equations are simple but the equilibrium equations are complicated. When the Eulerian description is used the equilibrium equations are simple but the kinematic equations are complicated [4]. Solution of such general equations is difficult but specific problems can be solved using numerical incremental techniques [1, 5].

The large deflection plate problem belongs to a special class of finite deformation problems in which the engineering strains, but not the rotations, can be considered as infinitesimal. The physical consideration which differentiates between large and small deflection plate theories is the stretching of the middle surface as a result of out-of-plane deformations. This stretching results in the development of "membrane" stresses which are not accounted for in small deflection theory. Small deflection theory can be considered adequate "only if the stresses corresponding to the stretching of the middle surface are small in comparison with the maximum bending stresses." This will be true "if the deflections of the plate from its initial plane or from a true developable surface are small in comparison with the thickness of the plate"* [6, 7].

* Quotations are from pages 48 and 49 of Timoshenko [6].

Accepting the first quotation above as the distinguishing feature separating "large" from "small" deflection theory of plates, the limit of applicability of small deflection theory cannot be associated with any absolute geometric restriction on displacements or rotations. It is generally accepted that the limit is reached when the ratio of maximum deflection to thickness of plate attains a value of $1/3$ to $1/2$, although this can be influenced by such factors as boundary conditions and the type of curvature developed in the plate.

The formulation of large deflection plate equations, by reducing the three dimensional elasticity equations to two dimensional equations, requires the distinction to be made between stress tensors referred to deformed configuration and stress tensors referred to the initial configuration. Since some readers may not be familiar with the stress tensors required, a brief review of their definition and relation to the present development is given in Appendix A.

1.3 Formulation of Equations

1.3.1 Displacement Formulation of the Equations of Elasticity

The governing equations for plate problems are formulated with displacements as the dependent variables. The displacement formulation of three dimensional elasticity requires the use of the following sets of equations:

- (a) Equilibrium equations
- (b) Strain-displacement equations
- (c) Constitutive equations

Substitution of the strain-displacement equations into the constitutive equations and subsequent substitution of the constitutive equations into the equilibrium equations yields the displacement equations of equilibrium,

which, together with the boundary conditions, are sufficient to properly specify static elasticity problems. Since displacements are the dependent variables the compatibility conditions are automatically satisfied if the solution is sufficiently differentiable.

The familiar small deflection plate equation

$$\nabla^4 w = \frac{q}{D} \quad (1-1)$$

where w is the deflection of the middle surface of the plate normal to the original plane of the plate, q is the distributed load, and $D = \frac{Eh^3}{12(1 - \nu^2)}$, is the expression of the equilibrium requirement normal to the original plane of the plate. This simple equation results because of the assumptions made in constraining the displacement field. These assumptions permit the displacements contributing to the bending behavior of the plate to be expressed in terms of the single dependent variable, w .

The object of this chapter is to examine the assumptions involved in reducing the three dimensional equations of elasticity to a set of simpler two dimensional equations which we will refer to as a set of "plate equations." The assumptions associated with the reduction of each of the sets of equations (a), (b) and (c) are examined in the following sections. Rectangular cartesian co-ordinates and cartesian tensor notation are used throughout but conventional engineering nomenclature is used when it is desirable to write equations in full.

1.3.2 The Strain-Displacement Relations

The measure of deformation usually used in solid mechanics is one-half the difference between the square of the distance between two adjacent material points after deformation and the square of the distance between the same material points before deformation. This leads to the following

relation (see Fig. 1.1).

$$\frac{ds^2 - ds_0^2}{2} = \frac{1}{2} (u_{i,j} + u_{j,i} + u_{k,i} u_{k,j}) dx_i dx_j = E_{ij} dx_i dx_j \quad (1-2)$$

where u_i are the displacements in the co-ordinate directions,

ds is the distance between the two material points after deformation,

ds_0 is the distance between the two points before deformation,

x_i are the co-ordinates of the point Q before deformation,

$x_i + dx_i$ are the coordinates of the point P before deformation, and

$$E_{ij} = \frac{1}{2} (u_{i,j} + u_{j,i} + u_{k,i} u_{k,j}) \quad (1-3)$$

is known as Green's strain tensor or the Lagrangian finite strain tensor.

By defining two other quantities, e_{ij} and ω_{ij} , equation (1-3) can be written as

$$E_{ij} = e_{ij} + \frac{1}{2} (e_{ki} - \omega_{ki})(e_{kj} - \omega_{kj}) \quad (1-4)$$

where $e_{ij} = \frac{1}{2} (u_{i,j} + u_{j,i})$ is known as Cauchy's strain tensor or the Lagrangian infinitesimal strain tensor, and $\omega_{ij} = \frac{1}{2} (u_{j,i} - u_{i,j})$ is known as the infinitesimal rotation tensor.

The following properties of the quantities defined above follow directly from their definition:

- (i) e_{ij} and ω_{ij} are linear functions of the displacement gradients and E_{ij} is a quadratic function of the displacement gradients.
- (ii) E_{ij} and e_{ij} are symmetric while ω_{ij} is antisymmetric.

If the magnitudes of the displacement gradients, $u_{i,j}$, are restricted so that they are small quantities of the order

$$u_{i,j} \ll 1, \quad (1-5)$$

the product terms in (1-3) become small quantities of the second order and Green's strain tensor reduces to Cauchy's strain tensor. Under these circumstances the following physical interpretation can be made:

- (a) The components of e_{ij} can be identified with the conventional engineering strains (ϵ and γ) as follows

$$\langle e_{11} \ e_{22} \ e_{33} \ 2e_{12} \ 2e_{23} \ 2e_{31} \rangle = \langle E_{xx} \ E_{yy} \ E_{zz} \ \gamma_{xy} \ \gamma_{yz} \ \gamma_{zx} \rangle \quad (1-6)$$

- (b) The components ω_{ij} can be related to the infinitesimal average rigid body rotation of the element.

Since higher order product terms in (1-3) imply higher order product terms in (1-4), this indicates that both engineering strains and average rotations are small quantities of the first order under restrictions (1-5). Restrictions (1-5) may therefore be stated in the alternative form

$$e_{ij} \ll 1 \quad \text{and} \quad \omega_{ij} \ll 1. \quad (1-7)$$

Restrictions (1-5) or (1-7) are the assumptions used in deriving the equations of linear elasticity.

In large deflection plate theory the restrictions (1-5) are relaxed for the gradients of the out-of-plane displacement component, w . The engineering strain components can no longer be identified as in (1-6) but must now be approximated by the components of Green's strain tensor. Under these circumstances the identification is as follows

$$\langle E_{11} \ E_{22} \ E_{33} \ 2E_{12} \ 2E_{23} \ 2E_{31} \rangle = \langle \epsilon_{xx} \ \epsilon_{yy} \ \epsilon_{zz} \ \gamma_{xy} \ \gamma_{yz} \ \gamma_{zx} \rangle \quad (1-8)$$

where ϵ_{xx} , are the engineering strains associated with line elements oriented in the co-ordinate directions before deformation. Equation (1-8) is valid, providing ϵ_{ij} and $\gamma_{ij} \ll 1$, regardless of the magnitude of the displacement gradients (see Appendix A).

The explicit form of equations (1-4), which is used for plate formulation, will be developed after a discussion of the restrictions on the displacement field and the constitutive equations which are presented in the next two sections.

1.3.3 Restrictions on the Displacement Field--Kirchoff Assumptions

In order to derive the two dimensional plate equations, from the three dimensional equations of elasticity, constraints are placed on the displacement field. These constraints may be stated as follows:

- (1) Material points lying on normals to the middle surface before deformation remain in a straight line after deformation. This is usually abbreviated to "normals remain straight,"
- (2) The straight line through the material points referred to in (1) above, is also normal to the middle surface after deformation. This is usually abbreviated to "normals remain normal."
- (3) The strain in the direction of the normal can be neglected in establishing the displacement of a material point.
- (4) The slope of the middle surface remains small.

Assumptions 1, 2 and 3 above are usually referred to as the "Kirchoff assumptions."

Applying assumptions 1, 3, and 4, the horizontal displacements of a typical point, A, may be expressed as (see Fig. 1.2b)

$$u_A(x, y, z) = u_0 + z_A (u, z)_0 \quad (1-9)$$

$$v_A(x, y, z) = v_0 + z_A (v, z)_0$$

where the subscript 0 refers to middle surface values and therefore u_0 , v_0 , $(u, z)_0$ and $(v, z)_0$ are functions of x and y only. Assumptions 3 and 4 are required for equations (1-9) since no distinction is made between

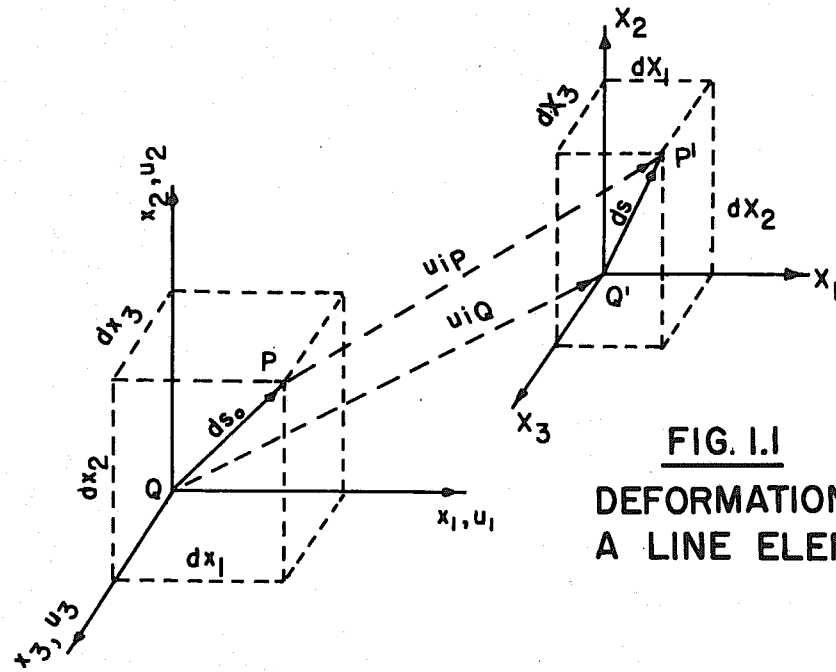


FIG. I.1
DEFORMATION OF
A LINE ELEMENT

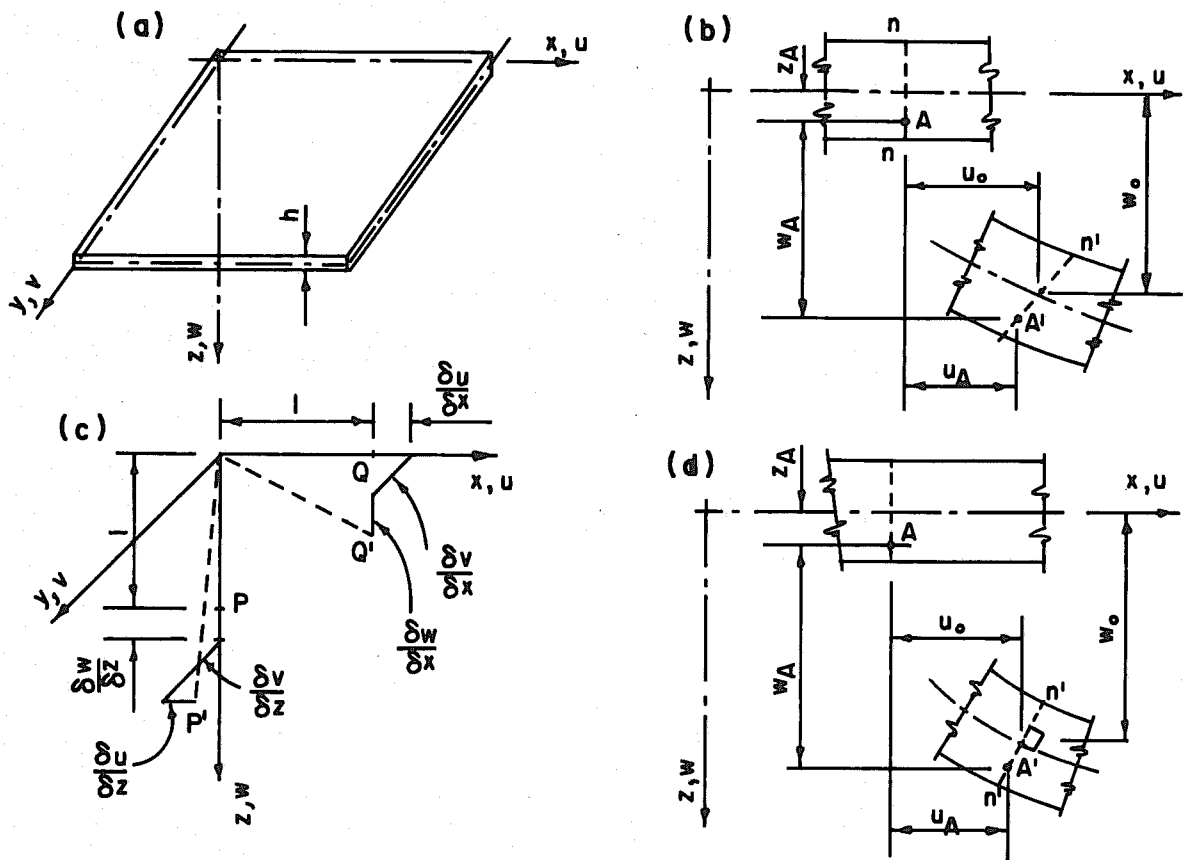


FIG. I.2
DEFORMATION IN A
PLATE ELEMENT

the vertical projection of O-A' and z_A .

Applying assumption 2, using equations (1-9) and evaluating at the middle surface yields

$$(2 E_{xz})_0 = (u_{,z})_0 (1 + u_{0,x}) + (w_{,x})_0 (1 + w_{,z})_0 + (v_{,z})_0 v_{0,x} = 0 \quad (1-9a)$$

$$(2 E_{yz})_0 = (v_{,z})_0 (1 + v_{0,y}) + (w_{,y})_0 (1 + w_{,z})_0 + (u_{,z})_0 u_{0,y} = 0$$

These equations express the condition, in the form of a scalar product, that, at the middle surface, lines originally located along the coordinate axes remain at right angles. This is illustrated in Fig. 1.2c and Fig. 1.2d.

If the quantities

$$w_{,x}, w_{,y}, u_{,z}, v_{,z} < 1$$

are regarded as small quantities of first order, such that products of these quantities are of the same order as the engineering strains (second order), then the quantities

$$u_{0,x}, v_{0,y} \ll 1$$

cannot be greater than second order. If restrictions are now placed on the quantities

$$w_{,z}, u_{0,y}, v_{0,x} \ll 1$$

such that they are small quantities of the same order as the engineering strains (second order) then equations (1-9a) reduce to the following first order equations, correct up to second order,

$$(u_{,z})_0 = -w_{0,x}$$

$$(v_{,z})_0 = -w_{0,y}$$

Under these circumstances, equations (1-9) can be written as

$$\begin{aligned}
 u(x, y, z) &= u_0 - z \omega_{0,x} \\
 v(x, y, z) &= v_0 - z \omega_{0,y}
 \end{aligned}
 \tag{1-10}$$

In addition, since $w_{0,x}$ and $w_{0,y}$ are first order quantities, we have the relation

$$w(x, y) = w_0(x, y) \tag{1-11}$$

which is correct up to small quantities of the second order.

Equations (1-10) and (1-11) are a mathematical expression of the constraints on the displacement field. They express the displacement of the three dimensional structure in terms of the dependent variables u_0 , v_0 , and w_0 which are functions of only two spatial co-ordinates.

1.3.4 The Constitutive Relations and the Strain Displacement Equations

We confine our discussion here to linearly elastic materials. In the finite element approach more general material properties will be considered. The most general form of the constitutive equations for a linear elastic material is given by the relation (see Appendix A).

$$S_{ij} = C_{ijkl} E_{kl} \tag{1-12}$$

where S_{ij} is the Kirchoff stress tensor,

E_{kl} is Green's strain tensor, and

C_{ijkl} are the elastic moduli which satisfy the relations

$$\begin{aligned}
 C_{ijkl} &= C_{jikl} \\
 C_{ijkl} &= C_{ijlk} \\
 C_{ijkl} &= C_{klij}
 \end{aligned}
 \tag{1-13}$$

The interchange of indexes is established by the symmetry of the stress and strain tensors and the assumption of the existence of a strain energy density function. Introduction of symmetries reduces the number of independent moduli. We will confine ourselves here to an isotropic elastic material for which there are only two elastic constants and the six independent components of stress are related to the six independent components of strain by the equations

$$\begin{pmatrix} S_{xx} \\ S_{yy} \\ S_{zz} \\ S_{xy} \\ S_{yz} \\ S_{zx} \end{pmatrix} = \begin{bmatrix} C_1 & C_2 & C_2 & \cdot & \cdot & \cdot \\ & C_1 & C_2 & \cdot & \cdot & \cdot \\ & & C_1 & \cdot & \cdot & \cdot \\ & & & C_3 & \cdot & \cdot \\ & & & & C_3 & \cdot \\ & \text{SYM.} & & & & C_3 \end{bmatrix} \begin{pmatrix} E_{xx} \\ E_{yy} \\ E_{zz} \\ 2E_{xy} \\ 2E_{yz} \\ 2E_{zx} \end{pmatrix} \quad (1-14)$$

$$\text{where } C_1 = \frac{E(1-\nu)}{(1+\nu)(1-2\nu)}, \quad C_2 = \frac{E\nu}{(1+\nu)(1-2\nu)} \quad \text{and} \quad C_3 = \frac{E}{2(1+\nu)}.$$

To reduce these equations to two dimensional form it is assumed that the normal stress S_{zz} remains small and is negligible compared to the stresses on the x and y planes. In addition, assumption 2 of section 1.3.3, which leads to equations (1-10), sets E_{yz} and $E_{zx} = 0$. The stresses S_{yz} and S_{zx} therefore cannot be determined from strains, though their existence is required for equilibrium, and can be omitted from the above relationship. (This situation is analogous to simple beam theory where shearing stresses must also be determined from equilibrium considerations.)

The conditions $S_{zz} = S_{yz} = S_{zx} = 0$ define a plane stress condition and by virtue of the discussion above it is assumed that each horizontal

layer of a plate element may be considered to be in a state of plane stress. The constitutive relations therefore become

$$\begin{Bmatrix} S_{xx} \\ S_{yy} \\ S_{xy} \end{Bmatrix} = \begin{bmatrix} 1 & \nu & 0 \\ \nu & 1 & 0 \\ 0 & 0 & \frac{1-\nu}{2} \end{bmatrix} \begin{Bmatrix} E_{xx} \\ E_{yy} \\ 2E_{xy} \end{Bmatrix} \quad (1-15)$$

The number of strain components required to define the relevant stresses in the plate has therefore been reduced to three.

Returning now to the strain displacement relations discussed in section 1.3.2, the three strain components required in (1-15) are

$$\begin{aligned} E_{xx} &= u_{,x} + \frac{1}{2}(u_{,x}^2 + v_{,x}^2 + w_{,x}^2) \\ E_{yy} &= v_{,y} + \frac{1}{2}(u_{,y}^2 + v_{,y}^2 + w_{,y}^2) \\ 2E_{xy} &= u_{,y} + v_{,x} + u_{,x}u_{,y} + v_{,x}v_{,y} + w_{,x}w_{,y} \end{aligned} \quad (1-16)$$

Applying a similar set of assumptions as used in section 1.3.3, namely

$$w_{,x}, w_{,y} < 1$$

are small quantities of the first order, whose products are of the same order as $u_{,x}$ and $v_{,y}$ (second order),

i.e.,

$$u_{,x}, v_{,y} \ll 1,$$

and that

$$v_{,x}, u_{,y} \ll 1,$$

the strain displacement equations become

$$\begin{aligned}
 E_{xx} &= u_{,x} + \frac{1}{2} w_{,x}^2 \\
 E_{yy} &= v_{,y} + \frac{1}{2} w_{,y}^2 \\
 2E_{xy} &= u_{,y} + v_{,x} + w_{,x} w_{,y} .
 \end{aligned}
 \tag{1-17}$$

The physical effect of the w displacement gradients can now be easily seen if these terms are interpreted as the first term of cosine approximation for the difference between the inclined length and the projected length of a line element.

It should be noted that the assumption that engineering strains are small makes it unnecessary to differentiate between the Eulerian stress tensor, σ_{ij} , and the Kirchoff stress tensor, S_{ij} , when interpreting the results, providing the proper orientation is maintained in the interpretation.

1.3.5 The Equilibrium Equations

The three dimensional equilibrium equations for finite deformation problems in the Lagrangian description are contained in the expression (see Appendix A),

$$\frac{\partial}{\partial x_j} \left[S_{jk} \left(\delta_{ik} + \frac{\partial u_i}{\partial x_k} \right) \right] + \rho_0 F_{oi} = 0
 \tag{1-18}$$

where S_{jk} is the Kirchoff stress tensor. Assuming no body force to be acting, and writing these equations in expanded form yields

$$\frac{\partial}{\partial x} \left[S_{xx} \left(1 + \frac{\partial u}{\partial x}\right) + S_{xy} \frac{\partial u}{\partial y} + S_{xz} \frac{\partial u}{\partial z} \right] + \frac{\partial}{\partial y} \left[S_{yx} \left(1 + \frac{\partial u}{\partial x}\right) + S_{yy} \frac{\partial u}{\partial y} + S_{yz} \frac{\partial u}{\partial z} \right] + \frac{\partial}{\partial z} \left[S_{zx} \left(1 + \frac{\partial u}{\partial x}\right) + S_{zy} \frac{\partial u}{\partial y} + S_{zz} \frac{\partial u}{\partial z} \right] = 0.$$

$$\frac{\partial}{\partial x} \left[S_{xx} \frac{\partial v}{\partial x} + S_{xy} \left(1 + \frac{\partial v}{\partial y}\right) + S_{xz} \frac{\partial v}{\partial z} \right] + \frac{\partial}{\partial y} \left[S_{yx} \frac{\partial v}{\partial x} + S_{yy} \left(1 + \frac{\partial v}{\partial y}\right) + S_{yz} \frac{\partial v}{\partial z} \right] + \frac{\partial}{\partial z} \left[S_{zx} \frac{\partial v}{\partial x} + S_{zy} \left(1 + \frac{\partial v}{\partial y}\right) + S_{zz} \frac{\partial v}{\partial z} \right] = 0. \quad (1-19)$$

$$\frac{\partial}{\partial x} \left[S_{xx} \frac{\partial w}{\partial x} + S_{xy} \frac{\partial w}{\partial y} + S_{xz} \left(1 + \frac{\partial w}{\partial z}\right) \right] + \frac{\partial}{\partial y} \left[S_{yx} \frac{\partial w}{\partial x} + S_{yy} \frac{\partial w}{\partial y} + S_{yz} \left(1 + \frac{\partial w}{\partial z}\right) \right] + \frac{\partial}{\partial z} \left[S_{zx} \frac{\partial w}{\partial x} + S_{zy} \frac{\partial w}{\partial y} + S_{zz} \left(1 + \frac{\partial w}{\partial z}\right) \right] = 0.$$

Placing restrictions on the displacement field that are consistent with those used in arriving at the strain displacement relationships, namely

$$\frac{\partial u}{\partial x}, \frac{\partial v}{\partial y}, \frac{\partial w}{\partial z}, \frac{\partial v}{\partial x}, \frac{\partial w}{\partial y}, \frac{\partial w}{\partial z} \ll 1 \quad (1-19a)$$

and recalling that

$$\frac{\partial u}{\partial z} = - \frac{\partial w}{\partial x} \quad \text{and} \quad \frac{\partial v}{\partial z} = - \frac{\partial w}{\partial y},$$

these equations reduce to

$$\frac{\partial}{\partial x} \left[S_{xx} - S_{xz} \frac{\partial w}{\partial x} \right] + \frac{\partial}{\partial y} \left[S_{yx} - S_{yz} \frac{\partial w}{\partial x} \right] + \frac{\partial}{\partial z} \left[S_{zx} - S_{zz} \frac{\partial w}{\partial x} \right] = 0$$

$$\frac{\partial}{\partial x} \left[S_{xy} - S_{xz} \frac{\partial w}{\partial y} \right] + \frac{\partial}{\partial y} \left[S_{yy} - S_{yz} \frac{\partial w}{\partial y} \right] + \frac{\partial}{\partial z} \left[S_{zy} - S_{zz} \frac{\partial w}{\partial y} \right] = 0 \quad (1-20)$$

$$\frac{\partial}{\partial x} \left[S_{xx} \frac{\partial w}{\partial x} + S_{xy} \frac{\partial w}{\partial y} + S_{xz} \right] + \frac{\partial}{\partial y} \left[S_{yx} \frac{\partial w}{\partial x} + S_{yy} \frac{\partial w}{\partial y} + S_{yz} \right] + \frac{\partial}{\partial z} \left[S_{zx} \frac{\partial w}{\partial x} + S_{zy} \frac{\partial w}{\partial y} + S_{zz} \right] = 0$$

Since S_{ij} is a stress tensor defined with respect to the original configuration, these equations can be reduced to two dimensional form by integrating over the original thickness of the plate. For this purpose we define the "stress resultants"

$$\langle N_x \quad N_y \quad N_{xy} \quad N_{yx} \quad Q_x \quad Q_y \rangle = \int_{-\frac{h}{2}}^{\frac{h}{2}} \langle S_{xx} \quad S_{yy} \quad S_{xy} \quad S_{yx} \quad S_{xz} \quad S_{yz} \rangle dz \quad (1-21)$$

and the stress couples

$$\langle M_x \quad M_y \quad M_{xy} \quad M_{yx} \rangle = \int_{-\frac{h}{2}}^{\frac{h}{2}} \langle S_{xx} \quad S_{yy} \quad S_{xy} \quad S_{yx} \rangle z dz. \quad (1-22)$$

Since S_{ij} is a symmetric tensor, it follows from the definitions that

$$N_{xy} = N_{yx} \quad \text{and} \quad M_{xy} = M_{yx}.$$

Integrating equations (1-20) through the plate thickness yields

$$\frac{\partial}{\partial x} [N_x - Q_x \frac{\partial w}{\partial x}] + \frac{\partial}{\partial y} [N_{yx} - Q_y \frac{\partial w}{\partial x}] + [S_{yx} - S_{yz} \frac{\partial w}{\partial x}]_{-h/2}^{h/2} = 0.$$

$$\frac{\partial}{\partial x} [N_{xy} - Q_x \frac{\partial w}{\partial y}] + \frac{\partial}{\partial y} [N_y - Q_y \frac{\partial w}{\partial y}] + [S_{xy} - S_{yz} \frac{\partial w}{\partial x}]_{-h/2}^{h/2} = 0. \quad (1-23)$$

$$\begin{aligned} & \frac{\partial}{\partial x} [N_x \frac{\partial w}{\partial x} + N_{xy} \frac{\partial w}{\partial y} + Q_x] + \frac{\partial}{\partial y} [N_{yx} \frac{\partial w}{\partial x} + N_y \frac{\partial w}{\partial y} + Q_y] \\ & + [S_{yx} \frac{\partial w}{\partial x} + S_{yz} \frac{\partial w}{\partial y} + S_{zz}]_{-h/2}^{h/2} = 0. \end{aligned}$$

The stress resultants and stress couples can be interpreted physically as shown in Fig. 1.3a, b. It has also been demonstrated in Appendix A that the stress components S_{ij} , although referred to the original configuration, maintain the surface tractions at the same relative orientation to the material elements as in the deformed configuration. Equations (1-23) therefore express the transverse equilibrium requirements in the x, y, z

directions of a plate element in its deformed configuration and may be interpreted as shown in Fig. 1.3c. An inspection of the equilibrium of this element verifies this conclusion.

Further assumptions are now necessary in order to reduce equations (1-23) to the form required to derive the classical plate equations.

- (a) Load applied normal to the top surface of the plate is assumed to be the only nonzero surface traction in the final equilibrium position.

$$\text{i.e. } \left[S_{zx} \right]_{-\frac{h}{2}}^{\frac{h}{2}} = \left[S_{zy} \right]_{-\frac{h}{2}}^{\frac{h}{2}} = 0. \quad \text{and} \quad \left[S_{zz} \right]_{-\frac{h}{2}}^{\frac{h}{2}} = q.$$

- (b) The transverse shear resultants and S_{zz} are assumed to be at least an order of magnitude smaller than the in-plane stress resultants in the first two equations (1-23). Since these terms are multiplied by first order displacement quantities they are quantities of higher order and are discarded.

Equations (1-23) therefore become,

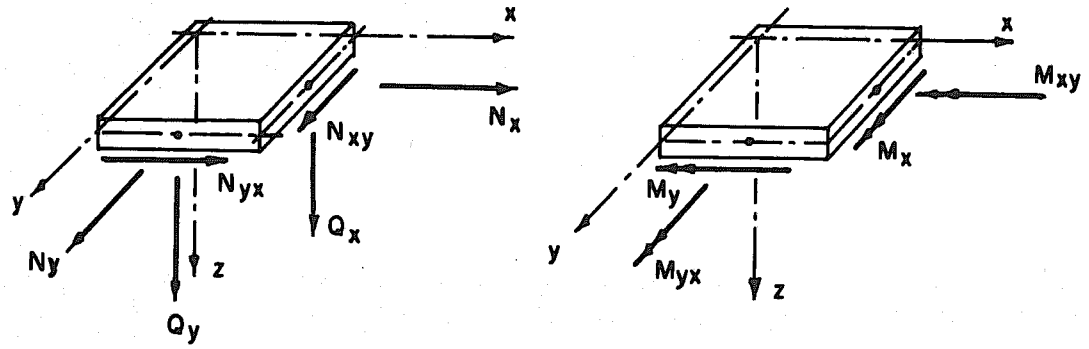
$$\begin{aligned} \frac{\partial}{\partial x} N_x + \frac{\partial}{\partial y} N_{yx} &= 0 \\ \frac{\partial}{\partial x} N_{xy} + \frac{\partial}{\partial y} N_y &= 0 \end{aligned} \tag{1-24}$$

$$\frac{\partial}{\partial x} Q_x + \frac{\partial}{\partial y} Q_y = - \left[q + N_x \frac{\partial^2 w}{\partial x^2} + 2 N_{xy} \frac{\partial^2 w}{\partial x \partial y} + N_y \frac{\partial^2 w}{\partial y^2} \right].$$

These are the equilibrium relationships between the stress resultants.

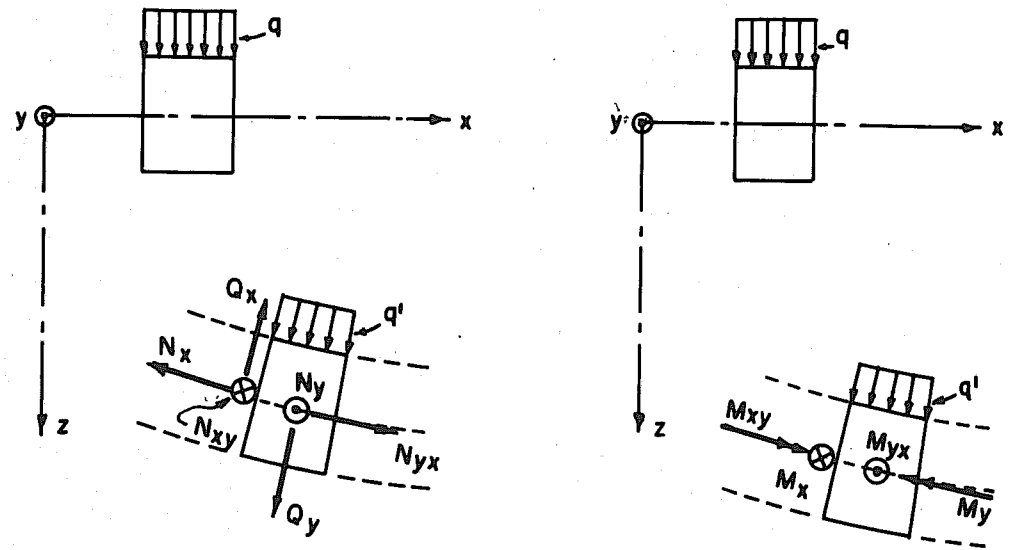
To derive equilibrium relationships between the stress couples, the first two equations (1-20) are multiplied by z and integrated through the thickness. In this operation the following approximations are made:

- (a) It is assumed the distribution of the stresses S_{xz} and S_{yz} are approximately symmetrical with respect to the middle surface so that



(a) STRESS RESULTANTS

(b) STRESS COUPLES



(c) STRESS RESULTANTS IN EQUILIBRIUM POSITION

(d) STRESS COUPLES IN EQUILIBRIUM POSITION

FIG. I.3 - STRESS RESULTANTS AND STRESS COUPLES

$$\int_{-\frac{h}{2}}^{\frac{h}{2}} S_{zx} dz = 0.$$

(b) The terms in the last bracket lead to an integration by parts.

For the second of these equations, the relation is

$$\int_{-\frac{h}{2}}^{\frac{h}{2}} z \frac{\partial}{\partial z} \left[S_{zx} - \frac{\partial w}{\partial z} S_{zz} \right] dz$$

$$= \left[S_{zx} - \frac{\partial w}{\partial z} S_{zz} \right]_{-\frac{h}{2}}^{\frac{h}{2}} - \int_{-\frac{h}{2}}^{\frac{h}{2}} \left[S_{zx} - \frac{\partial w}{\partial z} S_{zz} \right] dz.$$

Again the terms multiplied by displacement gradients are of higher order and surface values of S_{zy} vanish, so that this integral may be approximated by

$$- \int_{-\frac{h}{2}}^{\frac{h}{2}} S_{zx} dz = - Q_x.$$

The resulting equations are

$$\frac{\partial}{\partial x} M_x + \frac{\partial}{\partial y} M_{yx} - Q_x = 0$$

$$\frac{\partial}{\partial x} M_{xy} + \frac{\partial}{\partial y} M_y - Q_y = 0.$$

(1-26)

It should be noted that moment equilibrium about a line normal to the middle surface of an element, such as that shown in Fig. 1.3d, follows (at least to first order quantities) from the symmetry of the stress tensor S_{ij} , the assumption of small engineering strains, and a physical interpretation consistent with that above.

We now refer back to our discussion in section 1.3.4 where it was pointed out that, due to the second Kirchhoff assumption, the transverse shearing stresses cannot be established from material deformation but must be derived from equilibrium considerations after the other force quantities have been determined. Since a displacement formulation is

desired, the stress resultants Q_x and Q_y associated with these shears are eliminated by differentiating in the first of equations (1-26) with respect to x and the second with respect to y and substituting the results into the last of equations (1-24). This results in the following basic equilibrium equations.

$$\frac{\partial}{\partial x} N_x + \frac{\partial}{\partial y} N_{yx} = 0$$

$$\frac{\partial}{\partial x} N_{xy} + \frac{\partial}{\partial y} N_y = 0$$

(1-27)

$$\frac{\partial^2 M_x}{\partial x^2} + 2 \frac{\partial^2 M_{xy}}{\partial x \partial y} + \frac{\partial^2 M_y}{\partial y^2} = - \left[q + N_x \frac{\partial^2 w}{\partial x^2} + 2 N_{xy} \frac{\partial^2 w}{\partial x \partial y} + N_y \frac{\partial^2 w}{\partial y^2} \right].$$

These equations represent the equilibrium requirements for the sum of the forces in the x , y and z directions respectively.

1.3.6 Derivation of Plate Equations

Different forms of the plate equations can now be obtained by combining the equations developed in the preceding sections. The pertinent equations are summarized below.

(i) The Kirchoff Relations

$$u(x, y, z) = u_0(x, y) - z \omega_0(x, y),_{,x} \quad (1-10)$$

$$v(x, y, z) = v_0(x, y) - z \omega_0(x, y),_{,y} \quad (1-11)$$

$$w(x, y, z) = w_0(x, y)$$

(ii) The strain displacement relations

$$\begin{aligned}
 E_{xx} &= u_{,x} + \frac{1}{2} w_{,x}^2 \\
 E_{yy} &= v_{,y} + \frac{1}{2} w_{,y}^2
 \end{aligned}
 \tag{1-17}$$

$$2 E_{xy} = u_{,y} + v_{,x} + w_{,x} w_{,y}$$

(iii) The constitutive equations

$$\begin{Bmatrix} S_{xx} \\ S_{yy} \\ S_{yz} \end{Bmatrix} = \frac{E}{1-\nu^2} \begin{bmatrix} 1 & \nu & \cdot \\ \nu & 1 & \cdot \\ \cdot & \cdot & \frac{1-\nu}{2} \end{bmatrix} \begin{Bmatrix} E_{xx} \\ E_{yy} \\ 2E_{xy} \end{Bmatrix}
 \tag{1-15}$$

(iv) The equilibrium equations

$$N_{x,x} + N_{y,x,y} = 0$$

$$N_{y,y,x} + N_{y,y} = 0
 \tag{1-27}$$

$$M_{x,xx} + 2M_{xy,xy} + M_{y,yy} = -[q + N_x \omega_{o,xx} + 2N_{xy} \omega_{o,xy} + N_y \omega_{o,yy}]$$

A. The Small Deflection Plate Equations

The small deflection equations may be obtained by imposing restrictions (1-5) on all displacement gradients. The product terms in (1-17) may then be omitted since they are small quantities of higher order. Substituting equations (1-10) into the truncated equations (1-17) and then inserting this form of (1-17) into equations (1-15) yields the stress components in terms of the displacements of the middle surface. Integration of equations (1-15) through the thickness of the plate in accordance with definitions (1-21) and (1-22) yields the following expressions for stress resultants and stress couples.

$$\begin{Bmatrix} N_x \\ N_y \\ N_{xy} \end{Bmatrix} = B \begin{bmatrix} 1 & \cdot & \cdot & \nu \\ \nu & \cdot & \cdot & 1 \\ \cdot & \frac{1-\nu}{2} & \frac{1-\nu}{2} & \cdot \end{bmatrix} \begin{Bmatrix} u_{0,x} \\ u_{0,y} \\ v_{0,x} \\ v_{0,y} \end{Bmatrix} \quad (1-28)$$

and

$$\begin{Bmatrix} M_x \\ M_y \\ M_{xy} \end{Bmatrix} = -D \begin{bmatrix} 1 & \nu & \cdot \\ \nu & 1 & \cdot \\ \cdot & \cdot & \frac{1-\nu}{2} \end{bmatrix} \begin{Bmatrix} w_{0,xx} \\ w_{0,yy} \\ 2w_{0,xy} \end{Bmatrix} \quad (1-29)$$

Substitution of these results into (1-27) yields the plate equations

$$\begin{aligned} \nabla^2 u_0 - \frac{(1+\nu)}{2} (u_{0,yy} - v_{0,xy}) &= 0 \\ \nabla^2 v_0 - \frac{(1+\nu)}{2} (v_{0,xx} - u_{0,xy}) &= 0 \end{aligned} \quad (1-30)$$

$$\nabla^4 w_0 = \frac{1}{D} (q + N_x w_{0,xx} + 2N_{xy} w_{0,xy} + N_y w_{0,yy}) \quad (1-31)$$

where ∇^2 is the harmonic operator $\left(\frac{\partial^2}{\partial x^2} + \frac{\partial^2}{\partial y^2} \right)$ and

∇^4 is the biharmonic operator $\left(\frac{\partial^4}{\partial x^4} + 2 \frac{\partial^4}{\partial x^2 \partial y^2} + \frac{\partial^4}{\partial y^4} \right)$

Equations (1-30) are coupled together, since the dependent variables u_0 and v_0 appear in both, and represent the displacement equations of

equilibrium of the plane stress problem. Equation (1-31) is the equation from which the out-of-plane displacement component, w , can be determined and is uncoupled from equations (1-30). However the in-plane stress resultants are required to be known before equation (1-31) can be solved. If these stress resultants are zero throughout, then (1-31) reduces to the simplest form of plate bending equation

$$\nabla^4 w_0 = \frac{q}{D}$$

B. The von Karman Equations

The most important set of large deflection plate equations are known as the "von Karman equations." They may be obtained by retaining the product terms in equations (1-17) and following the same procedure as is used for developing the small deflection equations.

If this is done, the expressions for stress resultants and stress couples become

$$\begin{aligned} N_x &= B \left[\mathcal{M}_{0,x} + \frac{w_{0,x}^2}{2} + \nu \left(\mathcal{N}_{0,y} + \frac{w_{0,y}^2}{2} \right) \right] \\ N_y &= B \left[\mathcal{N}_{0,y} + \frac{w_{0,y}^2}{2} + \nu \left(\mathcal{M}_{0,x} + \frac{w_{0,x}^2}{2} \right) \right] \\ N_{xy} &= \left(\frac{1-\nu}{2} \right) B \left[\mathcal{M}_{0,y} + \mathcal{N}_{0,x} + w_{0,x} w_{0,y} \right] \end{aligned} \quad (1-32)$$

and

$$\begin{Bmatrix} M_x \\ M_y \\ M_{xy} \end{Bmatrix} = -D \begin{bmatrix} 1 & \nu & \cdot \\ \nu & 1 & \cdot \\ \cdot & \cdot & \frac{1-\nu}{2} \end{bmatrix} \begin{Bmatrix} w_{0,xx} \\ w_{0,yy} \\ 2 w_{0,xy} \end{Bmatrix} \quad (1-29)$$

Substitution of these results into the equilibrium equations (1-27) yields

$$\begin{aligned} \frac{\partial}{\partial x} [u_{0,x} + \nu v_{0,y} + \frac{1}{2} (w_{0,x}^2 + \nu w_{0,y}^2)] \\ + \frac{1-\nu}{2} \frac{\partial}{\partial y} [u_{0,y} + v_{0,x} + w_{0,x} w_{0,y}] = 0 \end{aligned} \quad (1-33)$$

$$\begin{aligned} \frac{\partial}{\partial y} [v_{0,y} + \nu u_{0,x} + \frac{1}{2} (w_{0,y}^2 + \nu w_{0,x}^2)] \\ + \frac{1-\nu}{2} \frac{\partial}{\partial x} [u_{0,y} + v_{0,x} + w_{0,x} w_{0,y}] = 0 \end{aligned} \quad (1-34)$$

where N_x , N_{xy} and N_y in equation (1-34) are represented by the expressions (1-32) in terms of the displacements u_0 , v_0 and w_0 .

The same interpretation can be associated with these equations as with the corresponding equations of the small deflection theory. However since equations (1-33) are now dependent on w_0 , they cannot be solved without also achieving a solution of (1-34) which in itself is dependent on u_0 and v_0 through the presence of the stress resultants N_x , N_y and N_{xy} . The three equations are therefore completely coupled and must be solved simultaneously.

Equations (1-33) may be satisfied by introducing a stress function and solving (1-34) simultaneously with the compatibility equations. However it serves no purpose to pursue this type of development here.

It is significant to notice that the only difference between the small deflection formulation and the large deflection formulation is the inclusion of the product terms in the strain displacement relationship. Physically these terms represent the stretching of the line elements due to out-of-plane displacements.

C. The Membrane Plate Equations

If a plate is supported in such a way that significant membrane forces can be developed, the membrane forces carry a proportionally greater share of the loading as the load is increased. For very thin plates at high loads an approximate formulation may be obtained by neglecting the contribution of bending to the carrying capacity of the plate. This is equivalent to setting $D = 0$ in equation (1-34). This approximate theory therefore requires the simultaneous solution of equations (1-33) and the equation

$$q + N_x w_{,xx} + 2N_{xy} w_{,xy} + N_y w_{,yy} = 0. \quad (1-35)$$

D. Inextensional Plate Equations

When the boundary conditions and loading on a plate are such that the plate can deform without developing significant membrane forces, the behavior of the plate may be approximated by neglecting middle surface strains, i.e., considering the middle surface "inextensible." A discussion of two approaches to this type of problem may be found in Borg [8] and Mansfield [7].

1.4 Summary of Plate Assumptions

A review of the preceding derivation indicates that the principal restrictions required in the formulation of the classical plate equations may be summarized as follows:

(a) $u_{,x}, u_{,y}, v_{,x}, v_{,y}, w_{,z} \ll 1$

are required to be small quantities of second order, and

$$(b) \quad w_{,x}, w_{,y} < 1$$

are required to be small quantities of first order such that the square of these quantities, which is of second order, is of the same order as the engineering strains and the quantities in (a).

Assumptions (a) and (b) are required to establish each of the following:

- (i) the Kirchoff equations (1-10) and (1-11),
- (ii) the strain displacement equations (1-17), and
- (iii) the equilibrium equations (1-27).

The above assumptions are those normally associated with the theory of "thin" plates. If the ratio of plate thickness to a characteristic lateral dimension of the plate is small (i.e., the plate is "thin"), the theory yields a satisfactory solution. For "thick" plates the Kirchoff assumptions are no longer applicable.

In the development of the finite element method which follows, restrictions (1-5) or (1-7) are placed on the displacement gradients with respect to the local co-ordinate system. However, since the local co-ordinate system translates and rotates with the element all of the above restrictions on displacement gradients may be removed with respect to the global reference frame. The principal limitation on the method, as formulated in the following sections, is that engineering strains remain small, i.e.,

$$\epsilon_{ij}, \gamma_{ij} \ll 1.$$

The finite element method, of course, introduces a set of approximations which are not present in classical theory, but results indicate that there

is a considerably wider range of application over which it can be expected to yield good results. This range can be expected to increase as more sophisticated elements are developed.

2. A LARGE DEFLECTION FINITE ELEMENT ANALYSIS OF PLATES

The analysis which is developed in this chapter is restricted to elastic structures. The development is carried out for a homogeneous, isotropic, linear elastic material and assumes small engineering strains throughout. However no conceptual difficulty is involved in extending the model to include inhomogeneous or nonlinear elastic material, or finite engineering strains. The method is extended in chapter four to include an approximate method of incorporating nonlinear material behavior. Although the method is developed for a particular type of finite element model, the concepts are general and applicable to other models.

2.1 Selection of a Finite Element Idealization

2.1.1 A Review of Basic Concepts

Recent progress in the field of finite element analysis has produced a large number of possibilities in selecting a scheme for idealizing a two-dimensional structure. Displacement, equilibrium, and mixed models have been developed. The purpose of any model is to approximate the behavior of the continuum, which has an infinite number of degrees of freedom, by an assumed behavior which can be defined by a finite number of degrees of freedom. To accomplish this the structure is divided into subregions and the behavior of each subregion is approximated by a linear combination of a finite number of independent functions whose range is restricted to the subregion. The number of independent functions determines the number of generalized co-ordinates or degrees of freedom associated with the subregion.

If the specified functions are used as a basis for representing displacements, the model is said to be a "displacement model." If the specified functions are used as a basis for representing stresses, the model is said to be an "equilibrium model." If the functions are used as partial bases, for both displacements and stresses, the model is said to be a "mixed model." For a completely linear system, de Veubeke [9] has used the principle of minimum potential energy to show that if complete compatibility is maintained at the interfaces of subregions, displacement models yield upper bounds to the stiffness coefficients; and has used the principle of complementary energy to show that if equilibrium is maintained at all points, equilibrium models yield lower bounds to the stiffness coefficients. If the class of functions is expanded to become "relatively complete"* with respect to the set of functions satisfying the boundary conditions of the assembled structure, the stiffness coefficients should converge to their proper values.

Since the process of expanding the class of functions to relative completeness has been generally impractical, a compromise has been attempted. The set of functions selected to represent the behavior of a subregion has been restricted to a limited number, and the convergence of the results has been studied as the size of the subregions is reduced. This technique usually requires the evaluation of finite element results by comparison with classical solutions of typical problems before the validity of the model and the degree of subdivision required for reliable application can be established.

* See Sokolnikoff [10], p. 407

Since displacement models are the most readily available and highly developed at the present time, equilibrium and mixed models were not seriously considered for this investigation.

Considerable progress has been made in establishing minimum requirements for a set of functions for displacement models which will produce convergence to the proper stiffness coefficients as the subdivision is refined. Felippa has summarized the requirements for plane stress analysis [1] and plate bending analysis [3] and also described a systematic procedure for constructing a set of basis functions by using interpolating polynomials. For this purpose it is useful to look at the subregions as a physical element. The displacement throughout the element is then specified by forming a linear combination of the basis functions or "shape" functions. The coefficient of each function becomes the generalized coordinate for that particular shape and is thus associated with a "degree of freedom." By making use of interpolation functions, each generalized co-ordinate can be identified with a physical displacement quantity at a particular location in the element (which is referred to as a nodal point or node). Compatibility between elements is established by locating the nodes on the boundaries between elements and imposing the same nodal displacement on all elements adjoining a particular node.

The simplest element that meets the minimum requirements for a given application is an element for which the number of degrees of freedom are just sufficient to maintain the minimum continuity requirements (compatibility with adjacent elements and internal continuity) and whose displacement functions can produce rigid body motions and the constant strain states ("completeness" property) associated with that application. When

additional degrees of freedom are provided the element is referred to as a "higher order" element. Higher order elements have the advantage of being able to represent a better approximation of the displacement with a coarser subdivision.

2.1.2 A Survey of Element Development

The element selected for large deflection plate analysis must be capable of representing both in-plane and out-of-plane deformation. This suggests combining the displacement patterns of existing elements which have been successful in the analysis of plane stress and plate bending. Triangular elements were the first type of element to achieve extensive use in the analysis of plane stress problems. The simplest element in this case is the constant strain triangle which has been dealt with by Wilson [2]. Higher order triangular elements have been developed by Felippa [1]. Triangular elements may be combined to produce quadrilateral elements of arbitrary shape [1].

In contrast to the plane stress problems, rectangular elements were the first type of elements to be successfully applied to the plate bending problem. Some of these elements have performed satisfactorily in spite of failure to satisfy some of the minimum completeness or continuity requirements. Clough and Tocher [11] have compared results of three rectangular elements and four types of triangular elements, including the first triangular element which satisfied the minimum continuity requirements. Bogner, Fox and Schmit [12] developed the first compatible and complete rectangular element. Felippa [3] has provided an alternative development of the Hsieh-Clough-Tocher triangular element stiffness and has systematically developed higher order compatible triangular plate bending elements

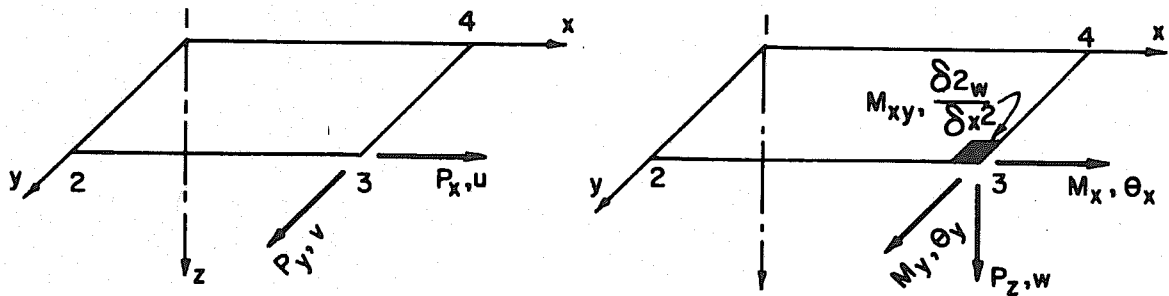
which may be assembled into arbitrary quadrilateral elements. Argyris [5] has developed a parallelogram element and introduced the concepts of natural co-ordinates, stresses and strains.

2.1.3 Selection of Element for this Analysis

The first element which was considered in this investigation was a rectangular element in which the out-of-plane displacements could be represented by the compatible and complete set of functions developed by Bogner, Fox and Schmit with 16 degrees of freedom. In addition, a linear variation of in-plane strain components could be achieved with 8 degrees of freedom (see Fig. 2.1). All degrees of freedom were associated with nodal displacements at the four corners. The disadvantages of this type of element may be listed as follows:*

- (a) Any rectangular element subjected to both in-plane and out-of-plane deformations becomes a warped surface after deformation in which the four nodal points no longer lie in a common plane. Since the solution technique is iterative, this presents problems of geometry and stiffness computation for the next load increment.
- (b) Although the out-of-plane and in-plane displacement functions each form a compatible system, displacements of the combined functions are incompatible unless displacements for all elements are referenced to a common plane.
- (c) The generalized forces associated with second derivative degrees of freedom do not correspond with readily identified physical force quantities and transformation of these quantities to a different set of coordinate axes introduces errors of unknown magnitude.

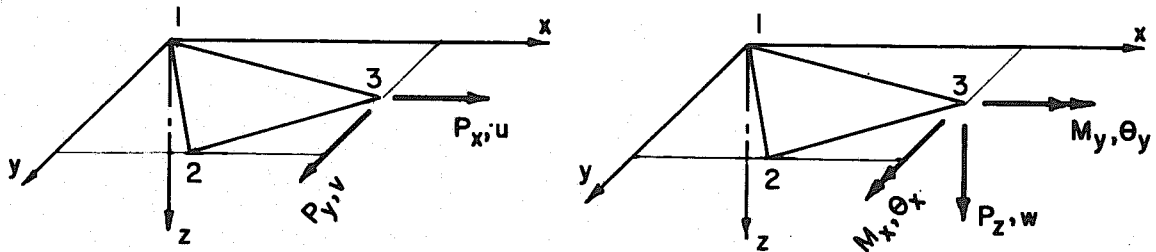
* These can be better appreciated after reading Section 2.2.



(a) IN-PLANE NODAL QUANTITIES AT NODE 3.

(b) OUT-OF-PLANE NODAL QUANTITIES AT NODE 3

FIG. 2.1 24 DEGREE OF FREEDOM RECTANGULAR ELEMENT



(a) IN PLANE NODAL QUANTITIES AT NODE 3

(b) OUT OF PLANE NODAL QUANTITIES AT NODE 3

FIG. 2.2 15 DEGREE OF FREEDOM TRIANGULAR ELEMENT

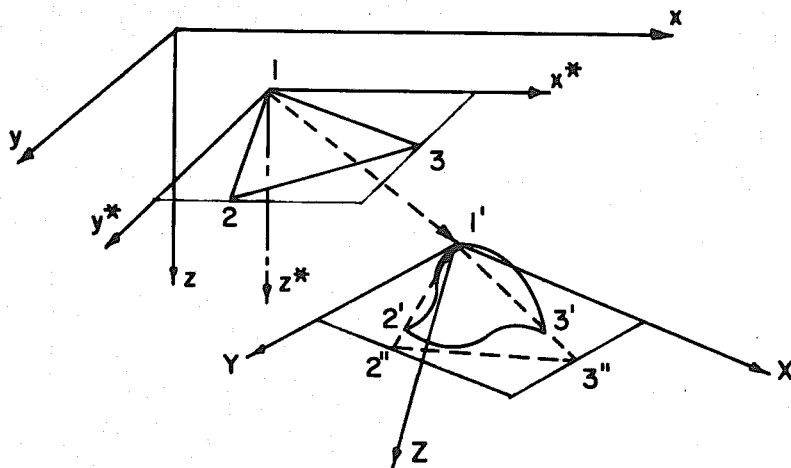


FIG. 2.3 COORDINATE SYSTEMS BEFORE AND AFTER DEFORMATION

- (d) The rectangular element is less flexible in representing arbitrary geometries and in refining mesh size in regions of high displacement gradient. (This objection can be eliminated by adopting an arbitrary quadrilateral element).

The element which was finally selected for this analysis assumes the in-plane deformation patterns are those associated with the constant strain triangle and the out-of-plane deformations are those associated with the linear curvature compatible triangle with nine degrees of freedom (see Fig. 2.2). This combination possesses the advantages:

- 1) In any deformed configuration the nodal points define a plane.
- 2) All nodal forces are readily identifiable physical force quantities.
- 3) The element is the simplest triangular element available which meets the minimum requirements for both in-plane and out-of-plane displacements.

It should be pointed out that this element does not produce compatible displacements when adjacent elements are referred to different reference planes. It thus has the same disadvantage as listed in (b) for the rectangular element. Results cannot therefore be interpreted as representing a bound on the true solution and the model must be verified by trial as discussed in Section 2.1.1.

In attempting to establish a truly compatible element for this type of problem it becomes apparent that the polynomials used to represent in-plane displacements must be of the same degree as those used to represent out-of-plane displacements. This gives rise to generalized nodal forces which cannot be associated with physical force components. In addition, Clough* has pointed out that compatibility along lines where a discontinuity

* Verbal communication from Prof. R. C. Clough, University of California

in reference planes occurs cannot be maintained without Reissner type shear deformation if in-plane shear deformation can occur and the nodal points do not lie on a developable surface. Carr [13] has recently combined a higher order in-plane element and the compatible triangular bending elements, with good results, for analysis of thin shells. However both types of incompatibility mentioned above are present in his model.

2.2 A General Approach to Large Deflection Analysis

The approach to large deflection problems which is used in this analysis will now be described. The method is illustrated with reference to the particular type of finite element model selected in section 2.1.3 but is completely general and is due to Wilson.[†] It has previously been applied to trusses and two dimensional frames [14] and is extended to plate bending in this dissertation.

In analyzing a large deflection problem we seek a structural configuration for our model in which the unbalanced internal forces are equilibrated by the applied external loads. We assume that the solution to the problem is unique (see Appendix B for a discussion of uniqueness) and it is therefore irrelevant how we arrive at the final configuration as long as the final configuration maintains an equilibrium balance.

Consider now an element which forms a part of a plate structure as shown in Fig. 2.3. Define the "global" co-ordinate system, which is a fixed set of axes for the entire structure, as the rectangular cartesian co-ordinate system, x, y, z . Define also the "local" co-ordinate system before deformation, x^*, y^*, z^* , and the "displaced local" co-ordinate

[†] Prof. E. L. Wilson, University of California, Berkeley.

system after deformation, X, Y, Z . The local co-ordinate system X, Y, Z is defined such that nodal points of the element after deformation ($1', 2', 3'$) lie in the X, Y plane, and is oriented in such a way that the "average rotation" of the element with respect to the local co-ordinate system is zero. The co-ordinate systems x^*, y^*, z^* and X, Y, Z can therefore be regarded as the same local system which translates and rotates with the element as the element is displaced.

The following procedure may be regarded as an algorithm for computing the equilibrium configuration.

1. Assume that the nodal locations have been specified in the global co-ordinate system, by some approximate method. From these locations, establish the displaced local co-ordinate system for the element in its deformed configuration.
2. Determine the element deformation with respect to the displaced local co-ordinate system.
3. Using the deformations and element stiffness defined with respect to the displaced local co-ordinate system, determine the element resisting forces.
4. Transform the element resisting forces and the element stiffness to the global system.
5. Repeat the steps 2, 3, and 4 for each element of the model and then sum the resisting forces and stiffness coefficients at each node. The difference between the resisting forces and the applied loads represents a set of unbalanced forces on the given configuration of the model.
6. Apply the set of unbalanced forces to the model in the configuration defined by the nodal locations in step 1 (the appropriate stiffness

has been determined in step 5) and solve for increments in the nodal displacements. This gives a new estimate of nodal locations.

7. Repeat steps 1 through 6 until the configuration of the model maintains an equilibrium balance with the applied loads.

Some general comments may now be made on this procedure.

- (a) Although displacements and displacement gradients may be large with respect to the global co-ordinate system, they may be reduced to arbitrarily small quantities with respect to the displaced local co-ordinate system by refining the subdivision, providing the engineering strains are small. Therefore strain-displacement equations referred to the displaced local co-ordinate system need not include the products of displacement gradients and small deflection plate theory is valid for the element (see sections 1.3.6, and 1.4).
- (b) Since the structural stiffness matrix is assembled using the current geometry the effect of change in structural configuration is included in the equilibrium equations.
- (c) Since the final configuration of the structure is always based on an equilibrium balance with the total applied loading, the assembled stiffness used to determine the displacement increments for the next iterate need not be exact. The only requirement on the assembled stiffness is that the displacement increments determined from it should ultimately lead to an equilibrium configuration (see section 2.3.3).

The principal disadvantage of this approach is the computational effort involved. Each iterate requires the complete solution of a small deflection problem. It is therefore essential that an efficient equation solver be available and that a reasonable estimate of the assembled stiffness matrix be attained.

2.3 The Stiffness Formulation

In solving structural problems by matrix techniques, two general methods have been developed, namely, the flexibility method and the stiffness method. The stiffness method, in the form of the direct stiffness assembly, has proved more versatile and easier to adapt to automatic programming techniques. It is therefore followed here.

This section develops the stiffness formulation in general terms,* assuming that the variation of internal strains and stresses can be specified throughout the structure in terms of the displacements of a finite number of nodal points. The detailed relationships between nodal displacements and internal effects will be developed for this particular model in subsequent sections.

The stiffness formulation can be derived from the principle of minimum potential energy or from the principle of virtual work. We select here the principle of virtual work since it is less restrictive than that of potential energy and intuitively more obvious. It is assumed throughout that engineering strains remain small and the structure remains elastic.

The principle of virtual work may be expressed as†

$$\int_V \tilde{\sigma}_{ij} \delta \tilde{\epsilon}_{ij} dV = \int_V \rho \tilde{F}_i \delta \tilde{u}_i dV + \int_{S_\sigma} \tilde{T}_i \delta \tilde{u}_i dS \quad (2-1)$$

* In general we assume $\{\tilde{u}\} = [\tilde{D}] \{r\}$ where $[\tilde{D}]$ is a matrix of functions which specify displacements throughout the structure and $\{\tilde{\epsilon}\} = [\tilde{B}] \{r\}$ where $[\tilde{B}]$ is a matrix of functions which specify the strains throughout the structure.

† See, for example, page 285 of Fung [4]. Equation (2-1) applies only for small deformation theory. The extension for large displacements is discussed later in the section.

where δ indicates a virtual variation,

\sim indicates the quantity is a variable function of the spatial co-ordinates

σ_{ij} is the stress tensor

ϵ_{ij} is the strain tensor

ρ is the mass per unit volume

u_i is the displacement vector

V is the volume of the body

S is the surface area

S_σ is the surface area on which stress boundary conditions are prescribes

T_i is the prescribed traction on S_σ , and

F_i is the body force per unit of mass.

Specializing this immediately for a structure in which the stress condition is confined to two dimensions, the equation of virtual work can be written as

$$\int_V \{\delta \tilde{\epsilon}\}^T \{\tilde{\sigma}\} dV = \int_V \rho \{\delta \tilde{u}\}^T \{\tilde{F}\} dV + \int_{S_\sigma} \{\delta \tilde{u}\}^T \{\tilde{T}\} dS \quad (2-2)$$

where

$$\begin{aligned} \{\tilde{\sigma}\}^T &= \langle \tilde{\sigma}_x & \tilde{\sigma}_y & \tilde{\tau}_{xy} \rangle \\ \{\tilde{\epsilon}\}^T &= \langle \tilde{\epsilon}_x & \tilde{\epsilon}_y & \tilde{\gamma}_{xy} \rangle \\ \{\tilde{u}\}^T &= \langle \tilde{u} & \tilde{v} & \tilde{w} \rangle \\ \{\tilde{F}\}^T &= \langle \tilde{F}_x & \tilde{F}_y & \tilde{F}_z \rangle \\ \text{and } \{\tilde{T}\}^T &= \langle \tilde{T}_x & \tilde{T}_y & \tilde{T}_z \rangle. \end{aligned} \quad (2-3)$$

2.3.1 Stiffness Formulation for Linear Structures

We assume it is possible to express the displacements and engineering strains throughout the structure as linear functions of m nodal displacements.

If we designate the nodal displacement vector as $\{r\}$, we can write

$$\text{and } \begin{matrix} \{ \tilde{u} \} \\ 3 \times 1 \end{matrix} = \begin{matrix} [\tilde{D}] \\ 3 \times m \quad m \times 1 \end{matrix} \{ r \} \quad (2-4)$$

$$\begin{matrix} \{ \tilde{\epsilon} \} \\ 3 \times 1 \end{matrix} = \begin{matrix} [\tilde{B}] \\ 3 \times m \quad m \times 1 \end{matrix} \{ r \} .$$

The constitutive relation can be expressed as

$$\begin{matrix} \{ \tilde{\sigma} \} \\ 3 \times 1 \end{matrix} = \begin{matrix} [\tilde{C}] \\ 3 \times 3 \quad 3 \times 1 \end{matrix} \{ \tilde{\epsilon} \} . \quad (2-5)$$

Noting that $\{ \delta \tilde{u} \} = [\tilde{D}] \{ \delta r \}$ and $\{ \delta \tilde{\epsilon} \} = [\tilde{B}] \{ \delta r \}$, the virtual work equation becomes

$$\{ \delta r \}^T \left[\int_V [\tilde{B}]^T [\tilde{C}] [\tilde{B}] dV \right] \{ r \} = \{ \delta r \}^T \left\{ \int_V [\tilde{D}]^T \{ \tilde{F} \} dV + \int_{S_\sigma} [\tilde{D}]^T \{ \tilde{T} \} dS \right\} . \quad (2-6)$$

Performing the integration, this can be expressed as

$$\{ \delta r \}^T [K] \{ r \} = \{ \delta r \}^T \{ \{ R_f \} + \{ R_s \} \} . \quad (2-7)$$

where $[K]$, $\{R_f\}$ and $\{R_s\}$ can be identified with the corresponding terms in equation (2-6). $[K]$ is known as the structure stiffness matrix and $\{R_f\}$ and $\{R_s\}$ are generalized forces associated with the body forces and surface forces respectively. Defining the total external force vector $\{R\}$, as

$$\{ R \} = \{ R_f \} + \{ R_s \} \quad (2-8)$$

and noting that $\{ \delta r \}$ is composed of arbitrary elements, equation (2-7)

becomes

$$[K] \{ r \} = \{ R \} .$$

This set of equations can now be solved for $\{r\}$, which can then be used to determine the stresses and strains at any point by using relations (2-4) and (2-5).

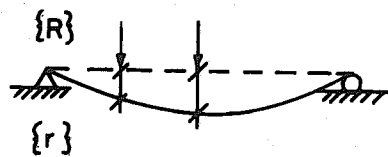
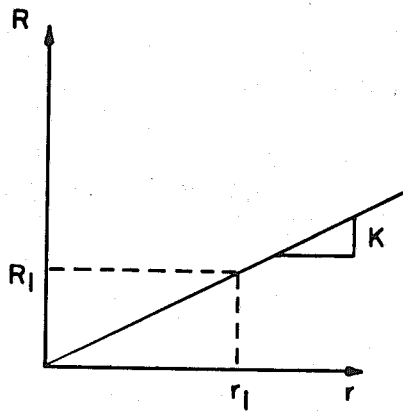
2.3.2 Incremental Stiffness*

The stiffness evaluated in section 2.3.1 applies only to a structure which is initially stress free and for which the field of engineering strains may be assumed to be a linear function of nodal displacements over the total range of these displacements. This behavior is illustrated schematically in Fig. 2.4a.

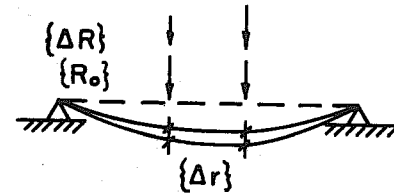
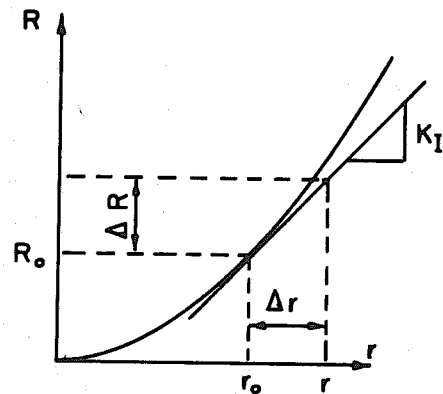
We now consider a structure for which the response is significantly nonlinear as illustrated schematically in Fig. 2.4b. In order to analyze such a structure the response may be approximated, in the region of an equilibrium configuration, by a linear relationship between increments in load and increments in displacement. The resulting stiffness matrix will be referred to as the "incremental stiffness."

In order to derive the incremental stiffness, assume a stable configuration is defined by the nodal displacements $\{r_0\}$ under the set of loads $\{R_0\}$. Consider an adjacent equilibrium position $\{r_0\} + \{\Delta r\}$ in equilibrium with the loads $\{R_0\} + \{\Delta R\}$. The principle of the virtual work now states that the virtual work must vanish in both the configuration $\{r_0\}$ and the configuration $\{r_0\} + \{\Delta r\}$, since both are equilibrium positions. However the situation is now more complex. We note that, for a proper formulation,

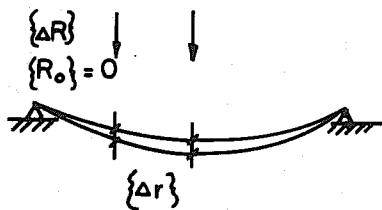
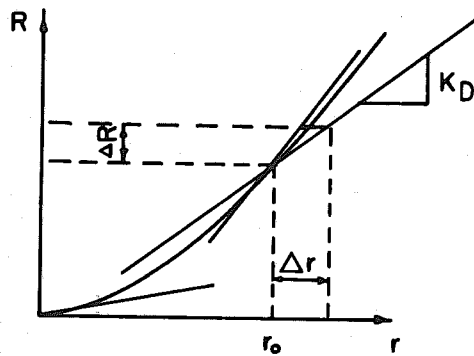
* The incremental stiffness, and its evaluation for this model, are treated in detail in Chapter 3. Details are omitted here since it is not necessary to have an "exact" evaluation of incremental stiffness in the application of this method.



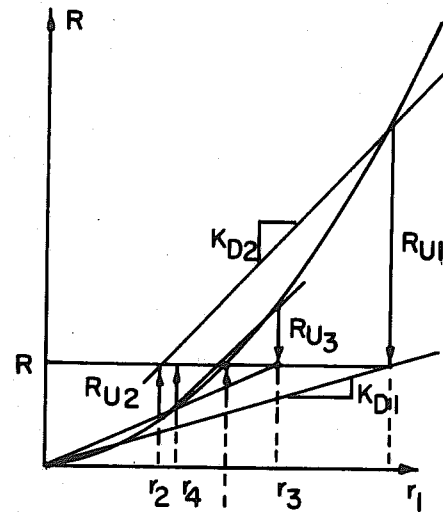
(a) CONVENTIONAL STIFFNESS



(b) INCREMENT OR TANGENT STIFFNESS



(c) DISPLACED STRUCTURE STIFFNESS



(d) ITERATION USING APPROXIMATE STIFFNESS K_D

FIG. 2.4 STRUCTURE STIFFNESSES

all virtual work quantities of the first order of magnitude should be included. Since an "initial" stress condition exists due to the presence of the loads $\{R_0\}$, the work of the initial stresses on second order virtual strains is of the same order of magnitude as the work of increments of stress on first order virtual strains.

A formulation of the incremental virtual work equation is carried out in Appendix B. The resulting equation may be expressed as[†]

$$\begin{aligned} \{\delta \Delta r\}^T \cdot \frac{1}{2} \left[\int_{V_0} \sum_{i=1}^3 \sum_{j=1}^3 \sigma_{ij0} \left[[\tilde{D}_{\Delta,i}]^T [\tilde{D}_{\Delta,j}] + [\tilde{D}_{\Delta,j}]^T [\tilde{D}_{\Delta,i}] \right] \alpha V_0 \right] \{\Delta r\} \\ + \{\delta \Delta r\}^T \left[\int_{V_0} [\tilde{B}_{\Delta}]^T [\tilde{C}] [\tilde{B}_{\Delta}] \alpha V_0 \right] \{\Delta r\} = \{\delta \Delta r\}^T \{\Delta R\} \end{aligned} \quad (2-9)$$

where σ_{ij0} is the stress condition in configuration $\{r_0\}$ and the subscript Δ indicates a matrix for incremental quantities referred to position $\{r_0\}$. We define the "geometric stiffness" matrix $[K_G]$ as the quantity between the vectors of nodal increments in the first term of equation (2-9), and $[K_D]$ as the quantity between the vectors of nodal increments in the second term. Equation (2-9) can then be written as

$$\{\delta \Delta r\}^T \left[[K_G] + [K_D] \right] \{\Delta r\} = \{\delta \Delta r\}^T \{\Delta R\}. \quad (2-10)$$

Since the vector $\{\delta \Delta r\}$ is arbitrary, this implies that

[†] Note that this formulation is easily extended to include thermal effects by the following procedure. Compute the internal thermal stress increments $\Delta\sigma_{ij0}$ and the associated external restraining forces $\{\Delta R_T\}$ by assuming the structure is completely restrained. The thermal stress increment is then added to the existing stress state σ_{ij0} and the increments in displacement $\{\Delta r\}$ are determined by applying an effective load of $\{\Delta R\} - \{\Delta R_T\}$. The stresses $\Delta\sigma_{ij}$ resulting from the increments of displacement are then added to $\sigma_{ij0} + \Delta\sigma_{ij0}$ to determine the resulting stress condition.

$$[K_G + K_D] \{\Delta r\} = \{\Delta R\}$$

or

$$[K_T] \{\Delta r\} = \{\Delta R\} . \quad (2-11)$$

The matrix $[K_T]$ is the incremental stiffness matrix for the configuration $\{r_0\}$.

2.3.3 An Approximate Stiffness

We now refer back to the discussion of Section 2.2 where it was pointed out that an exact evaluation of the incremental stiffness is not necessary because the procedure is iterative and the final configuration must satisfy an equilibrium balance with the total applied loads.

The evaluation of the instantaneous incremental stiffness $[K_T]$ (tangent stiffness) developed in Section 2.3.2 requires the evaluation of $[K_D]$ and $[K_G]$. The matrix $[K_D]$ represents the normal structural stiffness matrix of an unstressed structure in configuration $\{r_0\}$ for infinitesimal nodal displacements. It is illustrated schematically in Fig. 2.4c. The matrix $[K_G]$ represents the change in nodal forces due to the existence of a constant "initial" stress state as the geometric configuration of the structure is infinitesimally altered.

The evaluation of $[K_G]$ requires considerable computational effort and the results in Section 2.11 will show that an effective solution for many problems can be obtained by approximating the stiffness with $[K_D]$. The remainder of this chapter describes in detail how the problem is formulated on this basis. The iteration scheme for this type of solution is illustrated in Fig. 2.4d where numerical subscripts indicate the iterate number and R_u indicates the unbalanced load.

It should be emphasized here that the omission of the geometric stiffness matrix can be justified only because the procedure is iterative and

based on a final equilibrium balance. Any incremental solution, in which the structure develops both membrane and bending stresses, which does not include the effect of the geometric stiffness or does not evaluate the unbalanced forces with respect to the total applied load must be expected to diverge from the correct solution. Of the techniques available, the iterative technique provides closer control but is considerably more time consuming. In Chapter 3, both iteration and the geometric stiffness are combined in the solution process.

It should also be emphasized that the necessity of including the geometric stiffness depends primarily on the initial stress state rather than on the magnitude of the deformation. The nonlinear terms in the strain-displacement equations are always present but it is the existence of the initial stresses which makes them significant for infinitesimal displacement increments. This is best illustrated by a simple example such as the beam-column discussed in section 3.1. The term "initial stress" matrix is therefore probably a better name than "geometric stiffness" matrix.

2.3.4 The Direct Stiffness Procedure

The direct stiffness procedure refers to a method of forming the stiffness of an assemblage of elements when the stiffness of the individual elements are known. Referring to equation (2-6) the variation of strain, and the displacement components, throughout the structure are represented in the matrices $[\tilde{B}]$ and $[\tilde{D}]$ respectively. However, the integral over the entire structure can be evaluated by the sum of the integrals over each subregion. If $[\tilde{B}]_k$ and $[\tilde{D}]_k$ indicate the variation of strain and displacement throughout the element k , as a result of unit change in nodal displacements, then (2-6) can be replaced by the relation

$$\begin{aligned} \{S_r\}^T & \left[\sum_{k=1}^N \int_{V_k} [\tilde{B}]_k^T [\tilde{C}]_k [\tilde{B}]_k dV \right] \{r\} \\ & = \{S_r\}^T \left\{ \sum_{k=1}^N \int_{V_k} [\tilde{D}]_k^T \{F\} dV + \sum_{k=1}^N \int_{S_{\sigma k}} [\tilde{D}]_k^T \{\tilde{T}\} dS \right\} \end{aligned} \quad (2-12)$$

or

$$\left[\sum_{k=1}^N [K_k] \right] \{r\} = \left\{ \sum_{k=1}^N \{R_{fk}\} + \sum_{k=1}^N \{R_{sk}\} \right\}, \quad (2-13)$$

where $[K_k]$ is the stiffness of the element k and $\{R_{fk}\}$ and $\{R_{sk}\}$ are the generalized forces associated with the element k . A literal interpretation of (2-13) indicates that the stiffness of each element is developed in a matrix format which includes the total number of degrees of freedom of the structure. Since only nodal displacements for nodes on element k produce displacements in the element, this is an awkward procedure. The element stiffnesses are therefore developed independently for each element k , by considering only the displacements $\{r_k\}$, and the corresponding forces $\{R_k\}$, for the nodes located on that element. In the summation process, the elements of $\{r_k\}$ and $\{R_k\}$ are identified with the corresponding nodal quantities in $\{r\}$ and $\{R\}$. The process of identifying nodal quantities of the element with the corresponding nodal quantities of the structure, and adding the stiffness coefficients into the proper location in the structural stiffness matrix, is referred to as the "assembly" process.

2.4 The Element Stiffness[†]

A typical element for this finite element model is shown in Fig. 2.5.

We consider each corner to be a nodal point and number them in a

[†] Since in this chapter there is no need to differentiate between the type of stress and strain tensors, we revert to standard nomenclature. Strictly speaking however the stress and strain tensors we use are the Kirchoff and Green tensors, respectively.

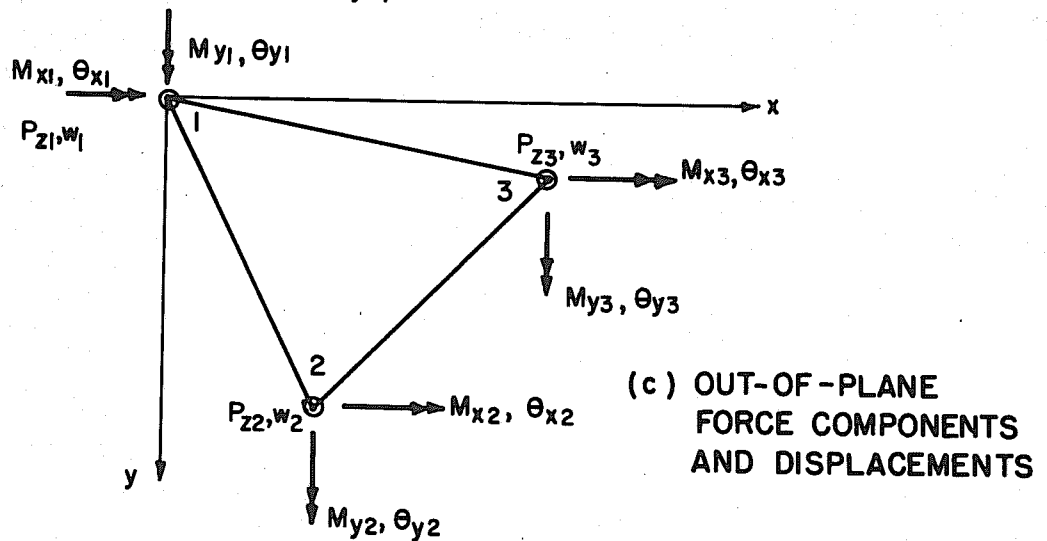
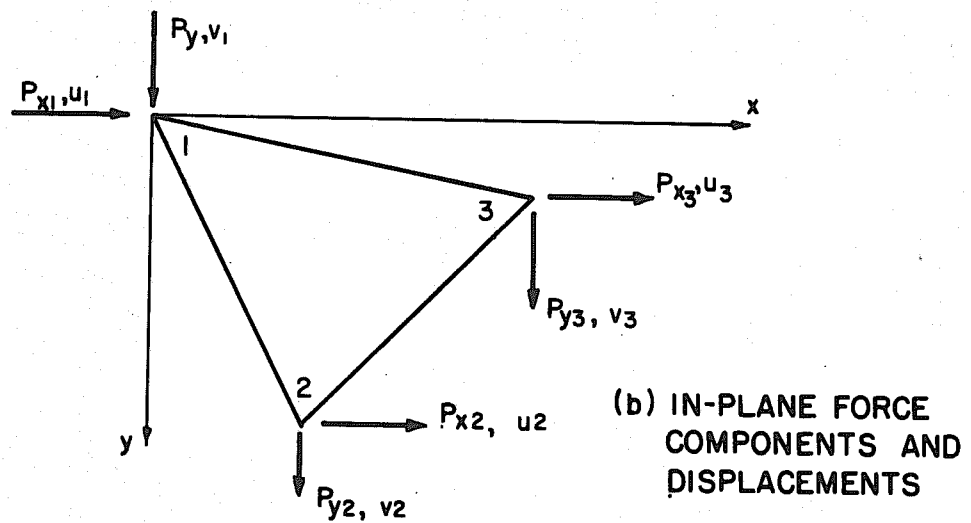
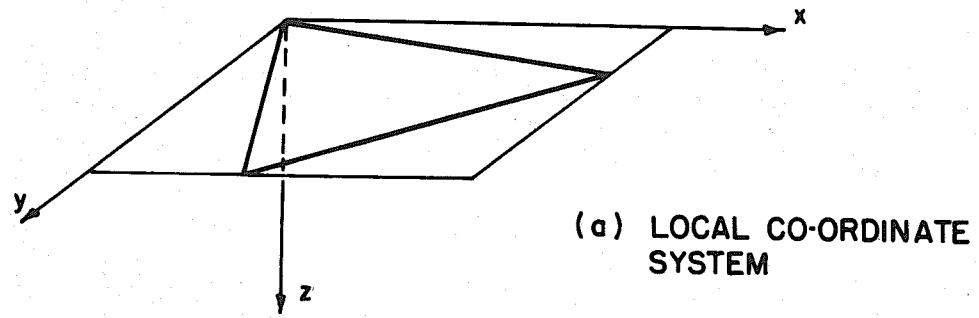


FIG. 2.5 NODAL QUANTITIES FOR DISPLACEMENT MODEL

counterclockwise manner. The nodal forces and displacements can be arranged in vectors. Define the nodal force vector, $\{R_E\}$, for the element, and

$\{R_P\}$ and $\{R_B\}$, as

$$\{R_E\}^T = \langle \{R_P\}^T \mid \{R_B\}^T \rangle$$

$= \langle P_{x1} \ P_{x2} \ P_{x3} \ P_{y1} \ P_{y2} \ P_{y3} \mid P_{z1} \ M_{x1} \ M_{y1} \ P_{z2} \ M_{x2} \ M_{y2} \ P_{z3} \ M_{x3} \ M_{y3} \rangle$
and the corresponding nodal displacement vector, $\{r_E\}$, and the vectors

$\{r_P\}$ and $\{r_B\}$, as

$$\{r_E\}^T = \langle \{r_P\}^T \mid \{r_B\}^T \rangle$$

$= \langle u_1 \ u_2 \ u_3 \ v_1 \ v_2 \ v_3 \mid w_1 \ \theta_{x1} \ \theta_{y1} \ w_2 \ \theta_{x2} \ \theta_{y2} \ w_3 \ \theta_{x3} \ \theta_{y3} \rangle$.

These nodal quantities are illustrated in Fig. 2.5. In general the subscript "P" will refer to quantities associated with in-Plane behavior, the subscript "B" will refer to quantities associated with Bending, and the subscript "E" will refer to quantities associated with the entire Element, ordered as above.

Recalling the Kirchoff relations [equations (1-10) and (1-11)] we may write the displacement of any point in terms of the middle surface quantities as*

$$\tilde{u} = \tilde{u}_0 - z \tilde{w}_{0,x}$$

$$\tilde{v} = \tilde{v}_0 - z \tilde{w}_{0,y}$$

$$\tilde{w} = \tilde{w}_0$$

(2-14)

* In the following a tilde (\sim) will be used to indicate a quantity which is a function of the co-ordinates to distinguish it from the corresponding nodal quantities. Since interpolation functions are always co-ordinate functions no tilde is used with them.

where the subscript 0 denotes a middle surface quantity which is a function of the co-ordinates x and y .

Since we are developing a displacement model it is now necessary to assume a variation of the quantities \tilde{u}_0 , \tilde{v}_0 , and \tilde{w}_0 over the area of the element. For the present we will not specify the form of these functions but simply describe the variation by the relations

$$\begin{aligned}\tilde{u}_0 &= \{\phi_u\}^T \{u\} \\ \tilde{v}_0 &= \{\phi_v\}^T \{v\} \\ \tilde{w}_0 &= \{\phi_w\}^T \{w\}\end{aligned}\quad (2-1)$$

where $\{u\}^T = \langle u_1 u_2 u_3 \rangle$, $\{v\}^T = \langle v_1 v_2 v_3 \rangle$, $\{w\} = \langle r_p \rangle$ and $\{\phi_u\}$, $\{\phi_v\}$ and $\{\phi_w\}$ are vectors whose elements are the shape functions associated with the corresponding sets of nodal displacements $\{u\}$, $\{v\}$, $\{w\}$, respectively.

The strain displacement relations are given by equations (1-16) of section 1. These relations are

$$\begin{aligned}\tilde{E}_{xx} &= \frac{\partial \tilde{u}}{\partial x} + \frac{1}{2} \left(\frac{\partial \tilde{u}^2}{\partial x} + \frac{\partial \tilde{v}^2}{\partial x} + \frac{\partial \tilde{w}^2}{\partial x} \right) \\ \tilde{E}_{yy} &= \frac{\partial \tilde{v}}{\partial y} + \frac{1}{2} \left(\frac{\partial \tilde{u}^2}{\partial y} + \frac{\partial \tilde{v}^2}{\partial y} + \frac{\partial \tilde{w}^2}{\partial y} \right) \\ 2\tilde{E}_{xy} &= \frac{\partial \tilde{u}}{\partial y} + \frac{\partial \tilde{v}}{\partial x} + \frac{\partial \tilde{u}}{\partial x} \frac{\partial \tilde{u}}{\partial y} + \frac{\partial \tilde{v}}{\partial x} \frac{\partial \tilde{v}}{\partial y} + \frac{\partial \tilde{w}}{\partial x} \frac{\partial \tilde{w}}{\partial y}.\end{aligned}\quad (1-16)$$

Assuming now that the products of all displacement gradients are small (see section 1.4 and 2.2) the strain displacement relations become those of linear elasticity, namely

$$\begin{aligned}\tilde{E}_{xx} &= \tilde{\epsilon}_{xx} = \frac{\partial \tilde{u}}{\partial x} \\ \tilde{E}_{yy} &= \tilde{\epsilon}_{yy} = \frac{\partial \tilde{v}}{\partial y} \\ 2\tilde{E}_{xy} &= \tilde{\gamma}_{xy} = \frac{\partial \tilde{v}}{\partial x} + \frac{\partial \tilde{u}}{\partial y}.\end{aligned}\quad (2-16)$$

Substituting equations (2-14) into equations (2-16) yields

$$\{\tilde{\epsilon}\} \equiv \begin{Bmatrix} \tilde{\epsilon}_{xx} \\ \tilde{\epsilon}_{yy} \\ \tilde{\gamma}_{xy} \end{Bmatrix} = \begin{Bmatrix} \tilde{u}_{0,x} \\ \tilde{v}_{0,y} \\ \tilde{u}_{0,x} + \tilde{v}_{0,y} \end{Bmatrix} - \gamma \begin{Bmatrix} \tilde{w}_{0,xx} \\ \tilde{w}_{0,yy} \\ 2\tilde{w}_{0,xy} \end{Bmatrix} = \{\tilde{\epsilon}_0\} - \gamma \{\tilde{\chi}\} \quad (2-17)$$

where

$$\begin{aligned} \{\tilde{\epsilon}\}^T &= \langle \tilde{\epsilon}_{xx} \quad \tilde{\epsilon}_{yy} \quad \tilde{\gamma}_{xy} \rangle \\ \{\tilde{\epsilon}_0\}^T &= \langle \tilde{u}_{0,x} \quad \tilde{v}_{0,y} \quad \tilde{u}_{0,x} + \tilde{v}_{0,y} \rangle \\ \text{and} \quad \{\tilde{\chi}\}^T &= \langle \tilde{w}_{0,xx} \quad \tilde{w}_{0,yy} \quad 2\tilde{w}_{0,xy} \rangle \end{aligned} \quad (2-18)$$

Equations (2-18) can now be expressed in terms of the nodal displacements by using equations (2-15). We then obtain

$$\{\tilde{\epsilon}_0\} = \begin{bmatrix} \{\phi_{u,x}\}^T & \cdot \\ \cdot & \{\phi_{v,y}\}^T \\ \{\phi_{u,y}\}^T & \{\phi_{v,x}\}^T \end{bmatrix} \begin{Bmatrix} \{u\} \\ \{v\} \end{Bmatrix} = [\tilde{B}_P] \{r_P\} \quad (2-19)$$

$$\{\tilde{\chi}\} = \begin{bmatrix} \{\phi_{w,xx}\}^T \\ \{\phi_{w,yy}\}^T \\ \{2\phi_{w,xy}\}^T \end{bmatrix} \{r_B\} = [\tilde{B}_B] \{r_B\} \quad (2-20)$$

Equations (2-19) and (2-20) define the matrices $[\tilde{B}_P]$ and $[\tilde{B}_B]$.

To determine the stiffness of the element we now apply the principle of virtual work. The generalized nodal forces $\{R_E\}$ which equilibrate a set of internal stresses $\{\tilde{\sigma}\}$, where $\{\tilde{\sigma}\}^T = \langle \tilde{\sigma}_x \tilde{\sigma}_y \tilde{\sigma}_{xy} \rangle$, are determined by the equation

$$\{r_E^*\}^T \{R_E\} = \int_V \{\tilde{\epsilon}^*\}^T \{\tilde{\sigma}\} dV. \quad (2-21)^\dagger$$

The two dimensional constitutive relation may be written as

$$\{\tilde{\sigma}\} = [\tilde{C}] \{\tilde{\epsilon}\}. \quad (2-22)$$

Substituting (2-22) in (2-21) and expressing $\{\tilde{\epsilon}\}$ and $\{\tilde{\epsilon}^*\}$ by relation (2-17), the virtual work equation becomes

$$\begin{aligned} \{r_E^*\}^T \{R_E\} &= \int_V \{ \{\tilde{\epsilon}_0^*\} - z \{\tilde{\chi}^*\} \}^T [\tilde{C}] \{ \{\tilde{\epsilon}_0\} - z \{\tilde{\chi}\} \} dV \\ &= \int_V \{\tilde{\epsilon}_0^*\}^T [\tilde{C}] \{\tilde{\epsilon}_0\} dV - \int_V z \{\tilde{\epsilon}_0^*\}^T [\tilde{C}] \{\tilde{\chi}\} dV \\ &\quad - \int_V z \{\tilde{\chi}^*\}^T [\tilde{C}] \{\tilde{\epsilon}_0\} dV + \int_V z^2 \{\tilde{\chi}^*\}^T [\tilde{C}] \{\tilde{\chi}\} dV \end{aligned} \quad (2-23)$$

If $[\tilde{C}]$ does not vary with z , the two center terms vanish when integrated through the depth of the section. Equation (2-23) therefore becomes

$$\begin{aligned} \{r_E^*\}^T \{R_E\} &= \{r_P^*\}^T \left[\int_V [\tilde{B}_P]^T [\tilde{C}] [\tilde{B}_P] dV \right] \{r_P\} \\ &\quad + \{r_B^*\}^T \left[\int_V z^2 [\tilde{B}_B]^T [\tilde{C}] [\tilde{B}_B] dV \right] \{r_B\} \end{aligned} \quad (2-24)$$

$$= \{r_P^*\}^T [K_P] \{r_P\} + \{r_B^*\}^T [K_B] \{r_B\} \quad (2-25a)$$

$$= \begin{Bmatrix} \{r_P^*\} \\ \{r_B^*\} \end{Bmatrix}^T \begin{bmatrix} K_P & \cdot \\ \cdot & K_B \end{bmatrix} \begin{Bmatrix} \{r_P\} \\ \{r_B\} \end{Bmatrix} \quad (2-25b)$$

$$= \{r_E^*\}^T [K_E] \{r_E\}. \quad (2-25c)$$

Since the virtual displacements are arbitrary, we have

[†] An asterisk * will be used to indicate virtual quantities in the remainder of this chapter.

$$\{R_E\} = [K_E]\{r_E\}, \quad (2-26)$$

where $[K_E]$ is the stiffness matrix of the element. The matrices $[K_P]$ and $[K_B]$ are the respective stiffness matrices for the in-plane and the out-of-plane nodal displacements, illustrated in Fig. 2.5, and are defined by the corresponding terms in equations (2-24) and (2-25a).

2.5 Derivation of Stiffness for In-Plane Deformations

The stiffness matrix for in-plane deformation has been denoted as $[K_P]$ in section 2.4. It is evaluated by carrying out the integration of the first term of Equation (2-24). However it is useful to carry out the integration of the stiffness matrix in a special order so that it is easier to recover the internal element forces after the nodal vector $\{r_E\}$ has been evaluated.

We define the vector of internal forces (stress resultants),

$$\{\tilde{m}\}^T = \langle \tilde{m}_x \quad \tilde{m}_y \quad \tilde{m}_{xy} \rangle = \int_{-\frac{h}{2}}^{\frac{h}{2}} \langle \tilde{\sigma}_x \quad \tilde{\sigma}_y \quad \tilde{\sigma}_{xy} \rangle dz. \quad (2-27)$$

Then

$$\begin{aligned} \{\tilde{m}\} &= \int_{-\frac{h}{2}}^{\frac{h}{2}} \{\tilde{\sigma}\} dz = \int_{-\frac{h}{2}}^{\frac{h}{2}} [\tilde{C}]\{\tilde{\epsilon}\} dz = \int_{-\frac{h}{2}}^{\frac{h}{2}} [\tilde{C}]\{\tilde{\epsilon}_0 - z\{\alpha\}\} dz \\ &= \int_{-\frac{h}{2}}^{\frac{h}{2}} [\tilde{C}]\{\tilde{\epsilon}_0\} dz = \int_{-\frac{h}{2}}^{\frac{h}{2}} [\tilde{C}][\tilde{B}_P] dz \{r_P\} = [\tilde{N}]\{r_P\} \end{aligned} \quad (2-28)$$

where $[\tilde{N}] = h[\tilde{C}][\tilde{B}_P]$, providing $[\tilde{C}]$ is not a function of z .

The stiffness $[K_P]$ can now be defined in terms of the matrix $[\tilde{N}]$.

From (2-25) we note the definition of $[K_P]$ is

$$[K_P] = \int_V [\tilde{B}_P]^T [\tilde{C}] [\tilde{B}_P] dV \quad (2-29)$$

where $[\tilde{B}_P]$ is the function of x and y only. Integrating through the thickness this equation can be written as

$$[K_P] = \int_A [\tilde{B}_P]^T [\tilde{N}] dA. \quad (2-30)$$

The stiffness $[K_P]$, for the nodal degrees of freedom we have chosen, is that of the constant strain triangle. This is one of the first finite elements stiffnesses developed and it appears in numerous publications. It is evaluated in Appendix C using triangular co-ordinates.

2.6 Derivation of Stiffness for Out-of-Plane Deformations

The stiffness matrix for out-of-plane deformations has been denoted as $[K_B]$ in section 2.4. It is evaluated by carrying out the integration of the second term in equation (2-24). However, as in the case of $[K_P]$, it is useful to carry out the integration so that the internal stress couples can be recovered after the nodal displacements are known. We define the stress couples

$$\{\tilde{m}\}^T = \langle \tilde{m}_x \quad \tilde{m}_y \quad \tilde{m}_{xy} \rangle = \int_{-\frac{h}{2}}^{\frac{h}{2}} -z \langle \tilde{\sigma}_{xx} \quad \tilde{\sigma}_{yy} \quad \tilde{\sigma}_{xy} \rangle dz. \quad (2-31)$$

The negative sign is included so that the stress couples are the conjugates of the curvature (that is, the product of a stress couple and its corresponding curvature is positive work).

Expressing $\{\tilde{\sigma}\}$ in equation (2-31) in terms of the nodal displacements we obtain

$$\{\tilde{m}\} = \int_{-\frac{h}{2}}^{\frac{h}{2}} -z \{\tilde{\sigma}\} dz = \int_{-\frac{h}{2}}^{\frac{h}{2}} -z [\tilde{C}] \{\tilde{\epsilon}_0\} - z \{\tilde{\chi}\} dz. \quad (2-32)$$

If $[\tilde{C}]$ is not a function of z , this reduces to

$$\begin{aligned} \{\tilde{m}\} &= \int_{-\frac{h}{2}}^{\frac{h}{2}} z^2 [\tilde{C}] \{\tilde{\epsilon}\} dz = \int_{-\frac{h}{2}}^{\frac{h}{2}} z^2 [\tilde{C}] [\tilde{B}_B] dz \{r_B\} \\ &= [\tilde{M}] \{r_B\} \end{aligned} \quad (2-33)$$

where $[\tilde{M}] = \frac{h^3}{12} [\tilde{C}] [\tilde{B}_B]$.

The stiffness matrix can now be written in terms of $[\tilde{M}]$. From equation (2-24),

$$[K_B] = \int_V z^2 [B_B]^T [\tilde{C}] [\tilde{B}_B] dV$$

which becomes

$$[K_B] = \int_A [\tilde{B}_B]^T [\tilde{M}] dA. \quad (2-34)$$

The stiffness matrix $[K_B]$, for the nodal degrees of freedom used in this model, is that for the Hsieh-Clough-Tocher element. It has been evaluated by Clough and Tocher [10] and also evaluated by Felippa [3] using triangular co-ordinates and interpolation functions. The procedure is outlined in Appendix C following the method of Felippa.

2.7 Evaluation of Element Deformations

We consider the element in a displaced and deformed configuration as shown in Fig. 2.6. Assume that the nodal displacements are known in the global co-ordinate system. In order to evaluate the element resisting forces it is necessary to evaluate the element deformations in the displaced local co-ordinate system, since nodal displacements and rotations, are assumed small with respect to the local system.

For this purpose we define the following co-ordinate systems (see Fig. 2.6) which describe a material point P.

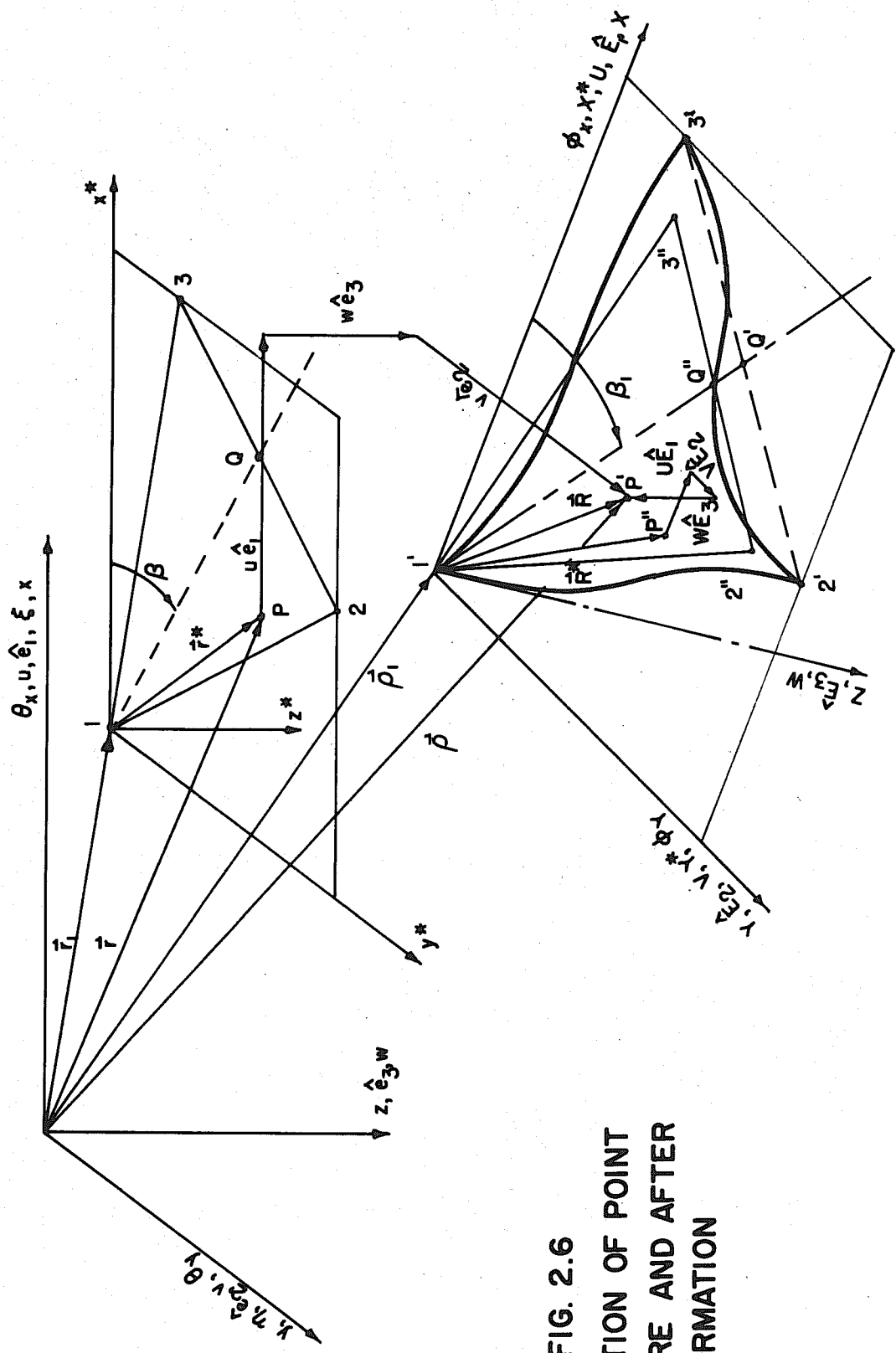


FIG. 2.6
LOCATION OF POINT
BEFORE AND AFTER
DEFORMATION

GLOBAL	x, y	Global co-ordinates of P in undeformed element in original position
CO-ORDINATES	ξ, η, ζ	Global co-ordinates of P' in deformed element (P → P')
LOCAL CO-ORDINATES	x^*, y^*	Local co-ordinates of P in undeformed element in original position
LOCAL CO-ORDINATES	X^*, Y^*	Local co-ordinates of P'' in displaced but undeformed element (referred to as the "reference element"). (P → P'')
AFTER DEFORMATION	X, Y, Z	Local co-ordinates of P' in displaced and deformed element (P → P').

In this section all capital letters apply to quantities associated with the displaced local co-ordinate system.

We adopt a vector approach, and describe the position of typical point P' after deformation, in both the global co-ordinate system and the displaced co-ordinate system.†

$$\vec{\rho} = \vec{r} + u \hat{e}_1 + v \hat{e}_2 + w \hat{e}_3 = \vec{\rho}' + \vec{R} = \vec{\rho}' + \vec{R} + U \hat{E}_1 + V \hat{E}_2 + W \hat{E}_3 \quad (2-35)$$

Using the relations

$$\vec{r} = \vec{r}_1 + \vec{r}^* = \vec{r}_1 + x^* \hat{e}_1 + y^* \hat{e}_2$$

and

$$\vec{\rho}' - \vec{r}_1 = u_1 \hat{e}_1 + v_1 \hat{e}_2 + w_1 \hat{e}_3,$$

equation (2-35) becomes

$$\begin{aligned} & (x^* + u - u_1) \hat{e}_1 + (y^* + v - v_1) \hat{e}_2 + (w - w_1) \hat{e}_3 \\ & = (X^* + U) \hat{E}_1 + (Y^* + V) \hat{E}_2 + W \hat{E}_3. \end{aligned} \quad (2-36)$$

† The symbol $\hat{\ }_$ indicates a unit base vector.

Now the co-ordinate systems ξ, η, ζ and X, Y, Z are related by a set of direction cosines a_{ij} , such that the unit vectors transform according to the transformation[†]

$$\hat{E}_i = a_{ij} \hat{e}_j. \quad (2-37)$$

Expressing \hat{E}_i in terms of \hat{e}_j , and equating coefficients, equation (2-35) yields

$$\begin{aligned} x^* + u - u_1 &= (X^* + U) a_{11} + (Y^* + V) a_{21} + W a_{31} \\ y^* + v - v_1 &= (X^* + U) a_{12} + (Y^* + V) a_{22} + W a_{32} \\ w - w_1 &= (X^* + U) a_{13} + (Y^* + V) a_{23} + W a_{33}. \end{aligned} \quad (2-38)$$

Grouping all known quantities on the left hand side and recognizing that $x^* = X^*$ and $y^* = Y^*$, we define the modified global displacements \bar{u} , \bar{v} and \bar{w} by the relations

$$\begin{aligned} \bar{u} &= u - u_1 + (1 - a_{11})X^* - a_{21}Y^* = a_{11}U + a_{21}V + a_{31}W \\ \bar{v} &= v - v_1 - a_{12}X^* + (1 - a_{22})Y^* = a_{12}U + a_{22}V + a_{32}W \\ \bar{w} &= w - w_1 - a_{13}X^* - a_{23}Y^* = a_{13}U + a_{23}V + a_{33}W. \end{aligned} \quad (2-39)$$

Equations (2-39) define the transformation between the modified global displacements and the local displacements. Since this transformation is orthogonal, the local displacements are defined by the relation

$$\begin{Bmatrix} U \\ V \\ W \end{Bmatrix} = \begin{bmatrix} a_{11} & a_{12} & a_{13} \\ a_{21} & a_{22} & a_{23} \\ a_{31} & a_{32} & a_{33} \end{bmatrix} \begin{Bmatrix} \bar{u} \\ \bar{v} \\ \bar{w} \end{Bmatrix} \quad (2-40)$$

[†] See Appendix D for the method of determining a_{ij} .

Evaluating this relationship at the nodal points determines the nodal displacements in the local system in terms of the nodal displacements in the global system.

To complete the evaluation of local nodal quantities it is necessary to evaluate the local nodal rotations $\{\phi_{Xi}, \phi_{Yi}\}$. We assume that the nodal rotations in the global system $\{\theta_{xi}, \theta_{yi}\}$ are known. These rotations are related to the first derivatives of the displacements by the equations

$$\begin{aligned} \frac{\partial w}{\partial \xi} &= -\tan^{-1} \theta_y & \frac{\partial w}{\partial \eta} &= \tan^{-1} \theta_x \\ \phi_x &= \tan \frac{\partial W}{\partial Y} & \phi_y &= -\tan \frac{\partial W}{\partial X} \end{aligned} \quad (2-41)$$

The first derivatives are now related by partial differentiation, assuming that the displacements are functions of the original location with respect to the displaced local co-ordinate system, i.e.,

$$U = U(X^*, Y^*) \quad V = V(X^*, Y^*) \quad W = W(X^*, Y^*) \quad (2-42)$$

The details of carrying out the differentiation are developed in Appendix D. This results in equations of the form,

$$\begin{aligned} & (a_{11} X_x^* + a_{21} Y_x^* + a_{11} U_{XE} + a_{21} V_{XE}) (\underline{a_{31}} + a_{33} \underline{\frac{\partial w}{\partial \xi}}) \\ & + a_{12} X_x^* + a_{22} Y_x^* + a_{12} U_{XE} + a_{22} V_{XE}) (\underline{a_{32}} + a_{33} \underline{\frac{\partial w}{\partial \eta}}) \end{aligned} \quad (2-43)$$

$$\frac{\partial W}{\partial X} = \frac{\quad}{1 - a_{31} (\underline{a_{31}} + a_{33} \underline{\frac{\partial w}{\partial \xi}}) - a_{32} (\underline{a_{32}} + a_{33} \underline{\frac{\partial w}{\partial \eta}})}$$

where terms not previously defined are defined in Appendix D. Evaluating at the nodal points, the underlined quantities become the nodal slopes in the global system, and equations of type (2-43) define the nodal slopes in the local system. The nodal rotations are then determined by equations (2-41).

The transformation of nodal rotations developed above is nonlinear and therefore cannot be put in matrix form. It is because this nonlinear geometric transformation is not restricted to small slopes and angle changes* that it is possible to deal with problems which are outside of the range of the classical plate formulation.

2.8 Evaluation of Element Forces

The preceding section described how local nodal displacements are derived from global nodal displacements. Since local nodal displacements are small quantities, they may be used in conjunction with the small displacement stiffness matrix developed in Section 2.4 and evaluated in Appendix C. We now change the order of the vector of nodal forces and define $\{\bar{R}_e\}$ in the local co-ordinate system,

$$\{\bar{R}_e\}^T = \langle \{\bar{R}_1\}^T \{\bar{R}_2\}^T \{\bar{R}_3\}^T \rangle = \quad (2-44)$$

$$\langle P_{x1} \ P_{y1} \ P_{z1} \ M_{x1} \ M_{y1} \mid P_{x2} \ P_{y2} \ P_{z2} \ M_{x2} \ M_{y2} \mid P_{x3} \ P_{y3} \ P_{z3} \ M_{x3} \ M_{y3} \rangle$$

where $\{\bar{R}_1\}$, $\{\bar{R}_2\}$ and $\{\bar{R}_3\}$ represent the nodal forces at the respective nodes. In the following two sections the subscript e is used to distinguish the ordering of the nodal quantities in (2-44) from that of section 2.4, and the bar is used to differentiate local from global vectors. The corresponding vector of nodal displacements in the local co-ordinate system is defined as $\{\bar{r}_e\}$,

† Note that there is a practical limit to beyond which these transformations cannot be used. When the inclination of the element approaches 90° with respect to the x-y plane of the global co-ordinate system, $\partial w / \partial \xi$ and $\partial w / \partial \eta$ become indefinitely large. However problems have been solved for cases where rotations have exceeded 60° (see section 2.11).

$$\begin{aligned} \{\bar{r}_e\}^T &= \langle \{\bar{r}_1\}^T \quad \{\bar{r}_2\}^T \quad \{\bar{r}_3\}^T \rangle \\ &= \langle U_1 \quad V_1 \quad W_1 \quad \phi_{x1} \quad \phi_{y1} \mid U_2 \quad V_2 \quad W_2 \quad \phi_{x2} \quad \phi_{y2} \mid U_3 \quad V_3 \quad W_3 \quad \phi_{x3} \quad \phi_{y3} \rangle \end{aligned} \quad (2-45)$$

where $\{\bar{r}_1\}$, $\{\bar{r}_2\}$, and $\{\bar{r}_3\}$ represent the nodal displacements at the respective nodes. Then the element forces can be established from the set of element displacements by the relation

$$\{\bar{R}_e\} = [K] \{\bar{r}_e\} \quad (2-26)$$

where $[K]$ is the stiffness matrix in equation (2-26), section 2.4, with the elements rearranged to conform to the ordering established in definitions (2-44) and (2-45).

2.9 Global Transformation, Assembly and Iteration

The equilibrium equations and the assembled stiffness matrices for the overall structure, described in section 2.3, are referred to the global axes. It is therefore necessary to transform the element resisting forces of section 2.8, and the stiffness of section 2.4, to the global co-ordinate orientation before assembling.

The transformation of nodal forces is accomplished at each corner of the element by the relation

$$\begin{Bmatrix} P_x \\ P_y \\ P_z \\ M_x \\ M_y \end{Bmatrix} = \begin{bmatrix} a_{11} & a_{12} & a_{13} & \cdot & \cdot \\ a_{21} & a_{22} & a_{23} & \cdot & \cdot \\ a_{31} & a_{32} & a_{33} & \cdot & \cdot \\ \cdot & \cdot & \cdot & a_{11} & a_{12} \\ \cdot & \cdot & \cdot & a_{21} & a_{22} \end{bmatrix} \begin{Bmatrix} P_2 \\ P_3 \\ P_3 \\ M_x \\ M_y \end{Bmatrix} \quad (2-47)$$

Denoting the corner transformation matrix above as $[T_c]$ this relation becomes,

$$\{\bar{R}_i\} = [T_c] \{R_i\}, \quad i = 1, 2, 3 \quad (2-48)$$

where i is the corner index, and $\{R_i\}$ is the corresponding vector of corner forces in the global system.

Considering now infinitesimal displacements, the transformation relation (2-48) implies that

$$\{\bar{r}_i\} = [T_c] \{r_i\}, \quad i = 1, 2, 3 \quad (2-49)$$

where $\{\bar{r}_i\}$ and $\{r_i\}$ are the displacements corresponding to $\{\bar{R}_i\}$ and $\{R_i\}$.

Therefore equation (2-46) can be written as,

$$\bar{R}_e = \begin{Bmatrix} \{\bar{R}_1\} \\ \{\bar{R}_2\} \\ \{\bar{R}_3\} \end{Bmatrix} = \begin{bmatrix} T_c & \cdot & \cdot \\ \cdot & T_c & \cdot \\ \cdot & \cdot & T_c \end{bmatrix} \begin{Bmatrix} \{R_1\} \\ \{R_2\} \\ \{R_3\} \end{Bmatrix} = [\bar{K}] \begin{bmatrix} T_c & \cdot & \cdot \\ \cdot & T_c & \cdot \\ \cdot & \cdot & T_c \end{bmatrix} \begin{Bmatrix} \{r_1\} \\ \{r_2\} \\ \{r_3\} \end{Bmatrix}$$

from which, because of the orthogonality of $[a_{ij}]$ we can write

$$\begin{Bmatrix} \{R_1\} \\ \{R_2\} \\ \{R_3\} \end{Bmatrix} = \begin{bmatrix} T_c^T & \cdot & \cdot \\ \cdot & T_c^T & \cdot \\ \cdot & \cdot & T_c^T \end{bmatrix} [\bar{K}] \begin{bmatrix} T_c & \cdot & \cdot \\ \cdot & T_c & \cdot \\ \cdot & \cdot & T_c \end{bmatrix} \begin{Bmatrix} \{r_1\} \\ \{r_2\} \\ \{r_3\} \end{Bmatrix} \quad (2-50)$$

or

$$\{R_e\} = [K_e]\{r_e\} \quad (2-51)$$

where $[K_e]$ is defined as the triple matrix product in equation (2-50), and $\{R_e\}$ and $\{r_e\}$ are the nodal vectors of element forces and displacements in the global system, in corner order.

Assembly now proceeds, in the manner described in section 2.3.4, by identifying the nodal displacements and forces of the element with the corresponding nodal displacements and forces of the structure. The summation of the element forces at any particular node yields the force required to equilibrate the current structural configuration. These forces are then subtracted from the total applied nodal force to determine the unbalanced force at the nodes. This set of unbalanced forces becomes the loading on the current structural configuration for the present iterate, and the increments in displacement resulting from these forces are then added to the current nodal locations to produce the next estimate of the structural configuration. The entire process of evaluating stiffness and unbalanced forces, and solving for displacement increments, is then repeated until an equilibrium balance is achieved.

Some comments on the transformation to global orientation, carried out in equations (2-47) and (2-50), should now be made.

- (1) The transformation (2-47) is incomplete in the sense that the moment component M_z is not computed. This situation arises because the elements possess only five degrees of freedom per corner. No stiffness coefficients are therefore available which will allow for computation of rotational deformation about the normal to the element.

In effect this means that the equilibrium equation to bring the sum of the moments about the vertical axis, through a node, into balance, cannot be written. It must be assumed that this unbalance is small and has little influence on the behavior of the plate. This assumption appears to be justified by the results presented in section 2.11.

- (2) The matrices in equation (2-50) which premultiply and postmultiply the matrix $[K]$ are displacement transformation matrices. We recall the effort involved in section (2-7) to transform nodal displacements from the global description to the displaced local description. The difference in the transformations arises because the displacement transformation matrices associated with the stiffness matrix need only apply for infinitesimal nodal displacements.
- (3) The element stiffness, as developed in section (2-4), is uncoupled. The coupling of the in-plane and out-of-plane problem is accomplished by the transformations in this section.

2.10 Solution of Equations

The equilibrium equations resulting from the assembly procedure discussed in section 2.9 are solved for the increments in nodal displacements resulting from the unbalanced forces. This requires the solution of $5m$ simultaneous algebraic equations for every iterate, where m is the number of nodal points.

The solution is based on a Gauss elimination procedure but the subroutine is specialized to triangularize a banded symmetric matrix. This results in a very efficient solution of the equations. The subroutine

was originally developed by Wilson* and modified by Felippa.†

2.11 Applications

In this section the method developed in this chapter is applied to some typical problems. Most of the problems have been selected on the basis of two considerations:

- (a) to illustrate the various types of problem to which the method is applicable, and
- (b) to compare the results of this method with the results achieved by more conventional methods.

A list of the problems and the PLATES in which results are illustrated is given in Table 2.1.

2.11.1 Inextensional Bending

A section from an infinite length of plate, 10 inches wide, 0.1 inches thick, clamped along the left edge and free along the right edge was subjected to a pure moment along the free edge. The applied moment and elastic properties were chosen to give a radius of curvature of 9 inches. Since the moments are constant throughout the plate and curvature occurs in one direction only, membrane forces are not induced. The deflection for the plate can therefore be checked against the co-ordinates of a circular arc with 9 inch radius and 10 inch length.

The results of the solution (without the correction for difference between arc length and chord length discussed in Appendix D) are shown in Plate 2-1. Note that the slope at the free edge is approximately 64° and

* Prof. E. L. Wilson, University of California, Berkeley, California

† Dr. C. A. Felippa, University of California, Berkeley.

TABLE 2.1
LIST OF PLATES FOR CHAPTER 2

SUBJECT	PLATE NO.	TITLE
Cantilevered Plate	2-1	Profile of Inextensional Plate Bending
Cylindrical Bending	2-2	Load-Deflection for Cylindrical Bending
	2-3	Stresses for Cylindrical Bending
Simply Supported Square Plate	2-4	Load-Deflection of Simply Supported Square Plate
	2-5	Membrane Stresses in Simply Supported Square Plate
	2-6	Bending Stresses in Simply Supported Square Plate
Clamped Square Plate	2-7	Load-Deflection of Clamped Square Plate for Low Loads
	2-8	Load-Deflection of Clamped Square Plate for High Loads
Post-Buckling of a Cantilevered Plate	2-9	Post-Buckling Load-Deflection of Cantilevered Plate
	2-10	Post-Buckling Profile of Cantilevered Plate
Stress Results for Simply Supported Square Plate	2-11	Comparison of Bending Stresses for Simply Supported Square Plate
	2-12	Distribution of Stresses in Simply Supported Square Plate

the horizontal motion of the free edge is approximately 2 inches. It is this horizontal motion which induces the membrane effect in plates which are not free to move at the supports.

Although this example was solved primarily to check the geometric transformations, it corresponds to the type of plate problems to which the inextensional approximate theory (see section 1.3.6.d) can be applied.

2.11.2 Cylindrical Bending

One of the few types of large deflection plate problems which has been successfully solved in closed form is the case of cylindrical bending. The development of the equations, together with charts and tables required for the solution are given in the first chapter of Timoshenko [6].

In order to check the finite element method with published results, a problem with extreme nonlinearities was selected. The problem consists of an infinite strip of plate, 20 inches wide, 0.5 inches thick, and simply supported on unyielding supports along each edge. A modulus of elasticity of 30×10^6 psi and a Poisson's ratio of 0.3 were used. The loading was increased in 8 increments from 0 to 5000 psi. Under simple beam theory the calculated deflection at the centerline of the span is approximately 30.5 inches.

The load vs. center deflection plot is shown in Plate 2-2. Notice the pronounced nonlinearity. Membrane and bending stresses are plotted in Plate 2-3 for the center section. Stresses of these magnitudes could not be attained in a real material but illustrate the influence of the membrane action. Notice the comparison with the simple plate theory bending stress. Agreement with Timoshenko results are excellent in view of the fact that these results were obtained, from the table on page 18, by interpolation from values with only two significant figures [6].

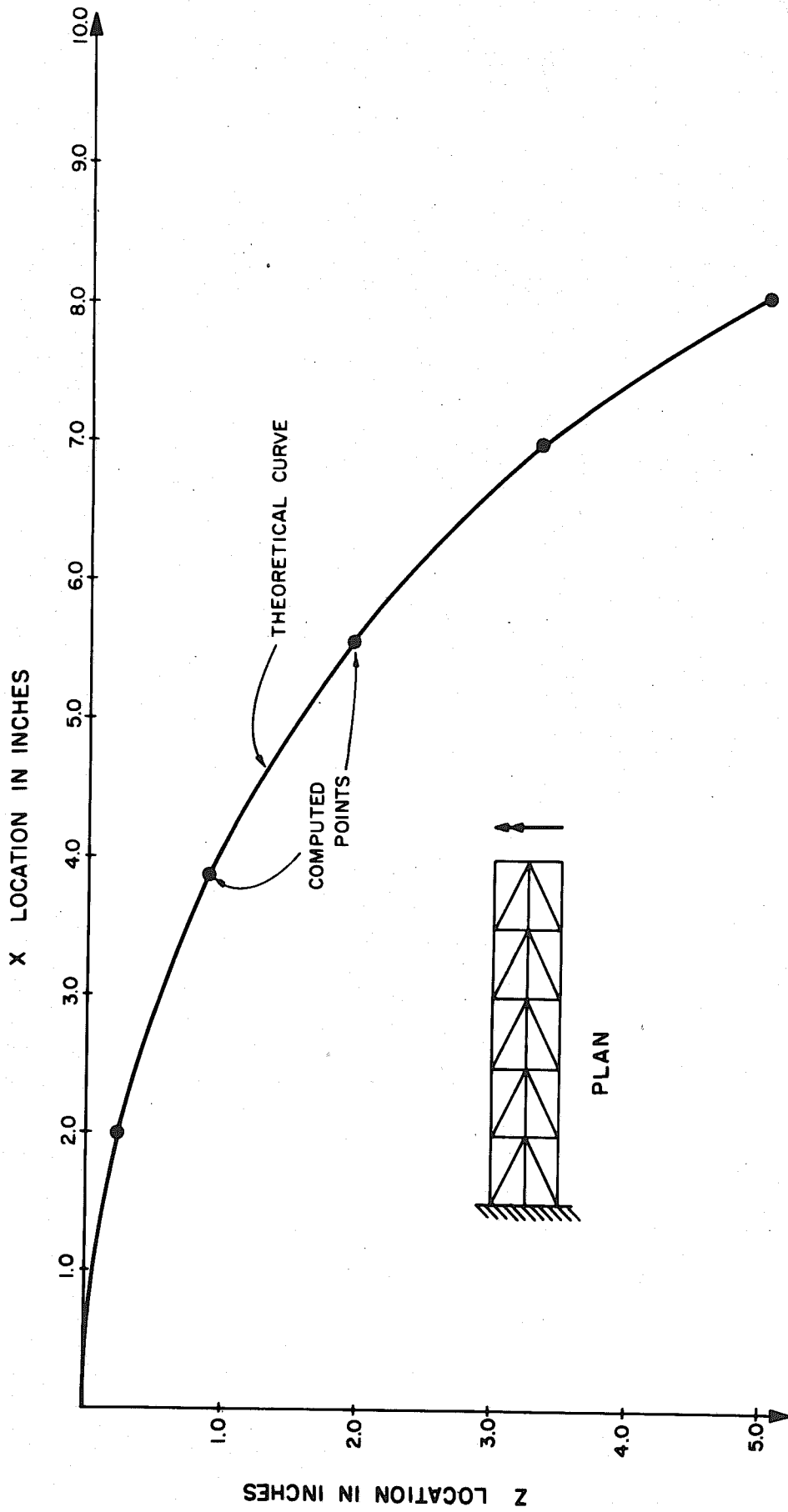


PLATE 2-1 PROFILE OF INEXTENSIONAL PLATE BENDING

2.11.3 Simply Supported Plate - Uniform Load

To check the method for plates developing double curvature, a solution was carried out for a 16 inch square plate, 0.1 inches thick, which was simply supported on unyielding supports on all sides. These results can be compared with those obtained by Levy [15]. Levy solved the von Karman equations (see section 1.3.6.b) consisting of two coupled equations in which the dependent variables were the stress function and out-of-plane displacement. The dependent variables were approximated by a truncated trigonometric series and convergence was examined as more terms were added. The first six nonzero terms were included in the solution.

The plate was assumed to have a modulus of elasticity of 30×10^6 psi and a Poisson's ratio of 0.316.[†] The uniform load was varied from 0 to 15 psi in 5 increments.

The load vs. center deflection plot is shown in Plate 2-4. Note the excellent agreement of the solution.

The plot of membrane stress and bending stress is shown in Plates 2-5 and 2-6, respectively, for various locations on the plate. The agreement of bending stress results with Levy's solution is not as good as for deflections. An accurate determination of stresses from a displacement model is always more difficult to achieve than a determination of displacements. The same phenomenon of course occurs with the series solution. Stress results for this particular example are discussed in detail in section 2.12.

[†] The value of 0.316 was selected to agree with that in Levy's solution. Levy was primarily interested in aluminum and therefore adopted this value. However the modulus of elasticity in Levy's solution appears only in the nondimensionalized form Pa^4/Eh^4 and thus may be varied.

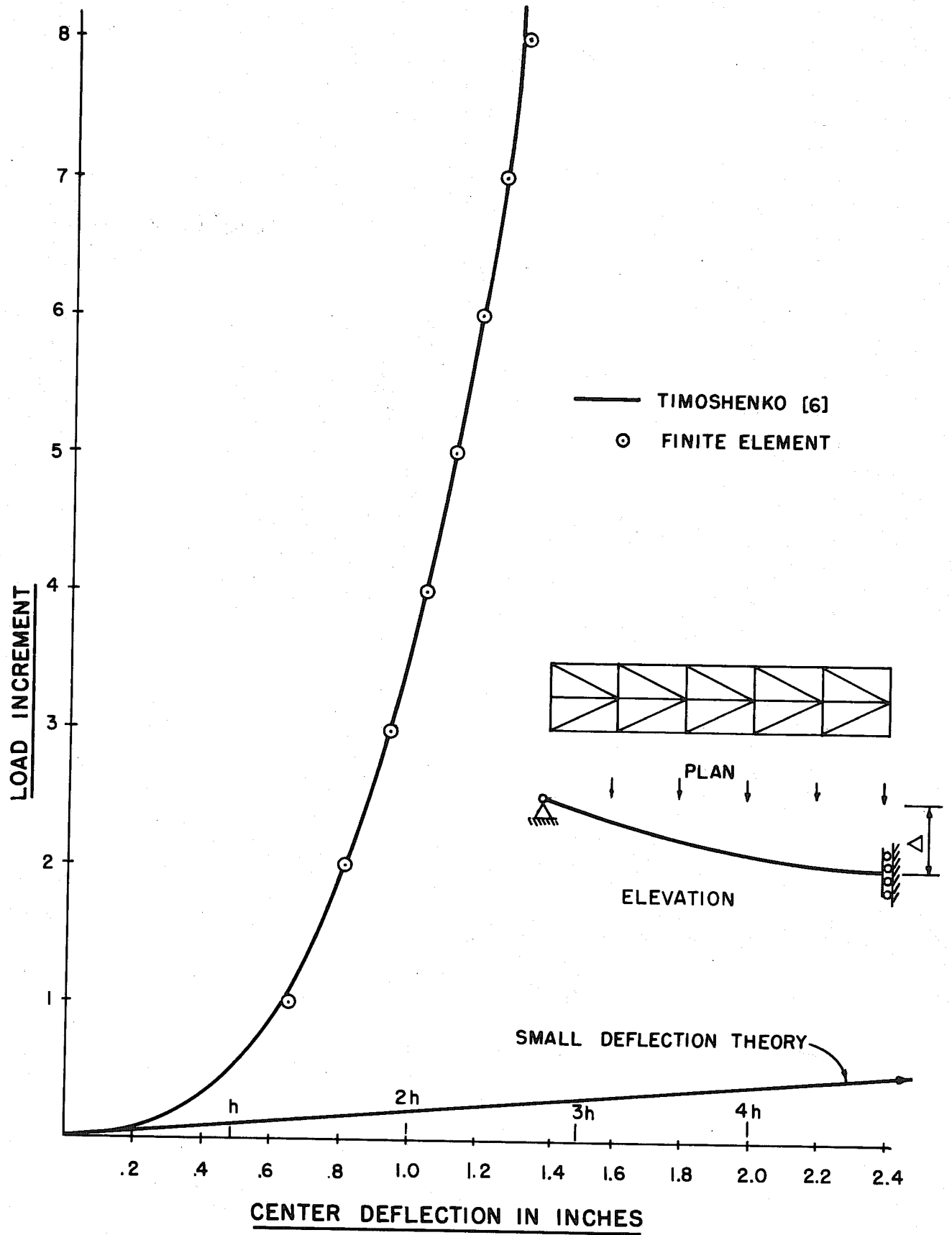


PLATE 2 - 2 LOAD-DEFLECTION FOR CYLINDRICAL BENDING

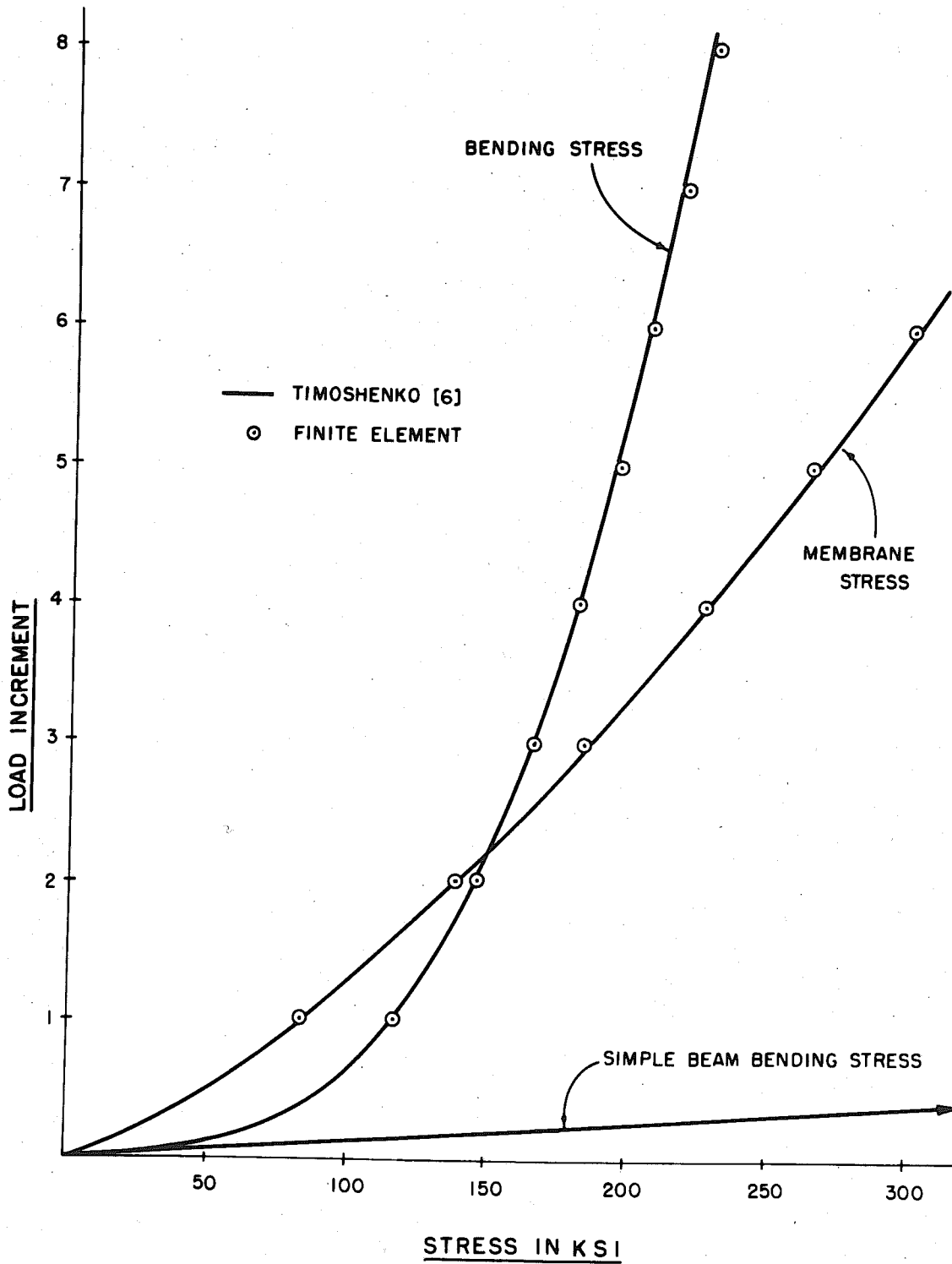


PLATE 2-3 STRESSES FOR CYLINDRICAL BENDING

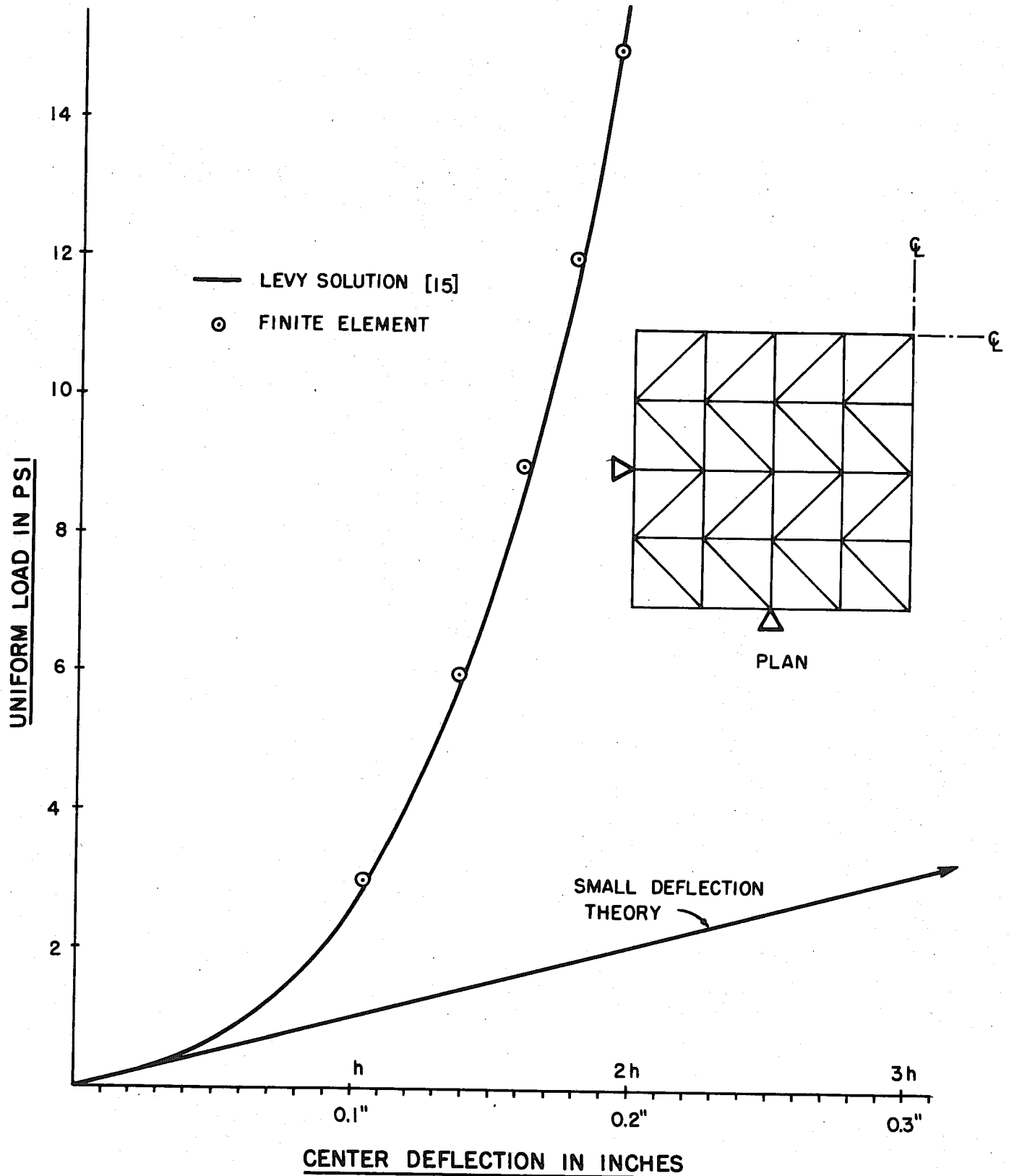


PLATE 2-4 LOAD DEFLECTION OF SIMPLY SUPPORTED SQUARE PLATE

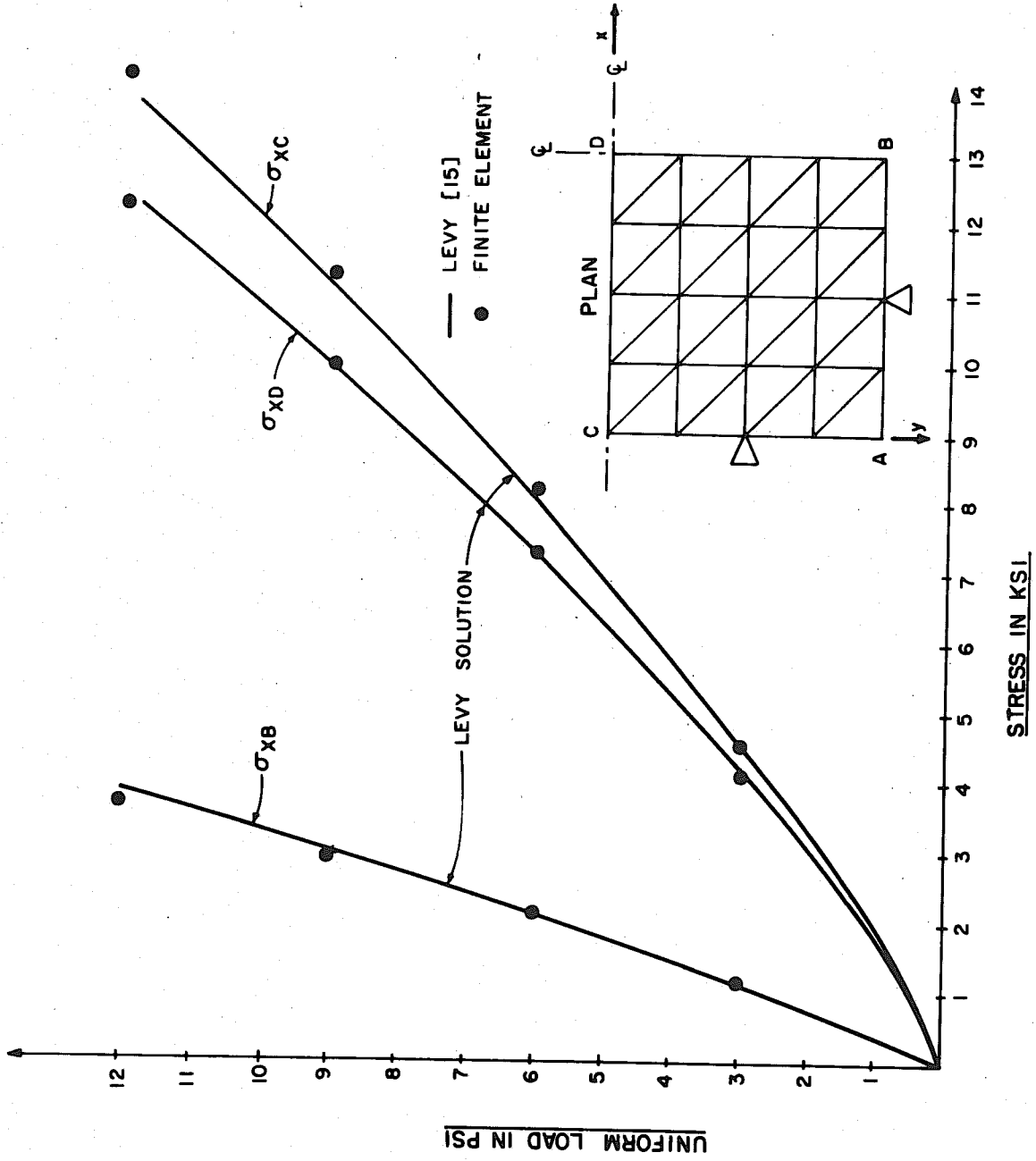


PLATE 2-5 MEMBRANE STRESSES IN SIMPLY SUPPORTED SQUARE PLATE

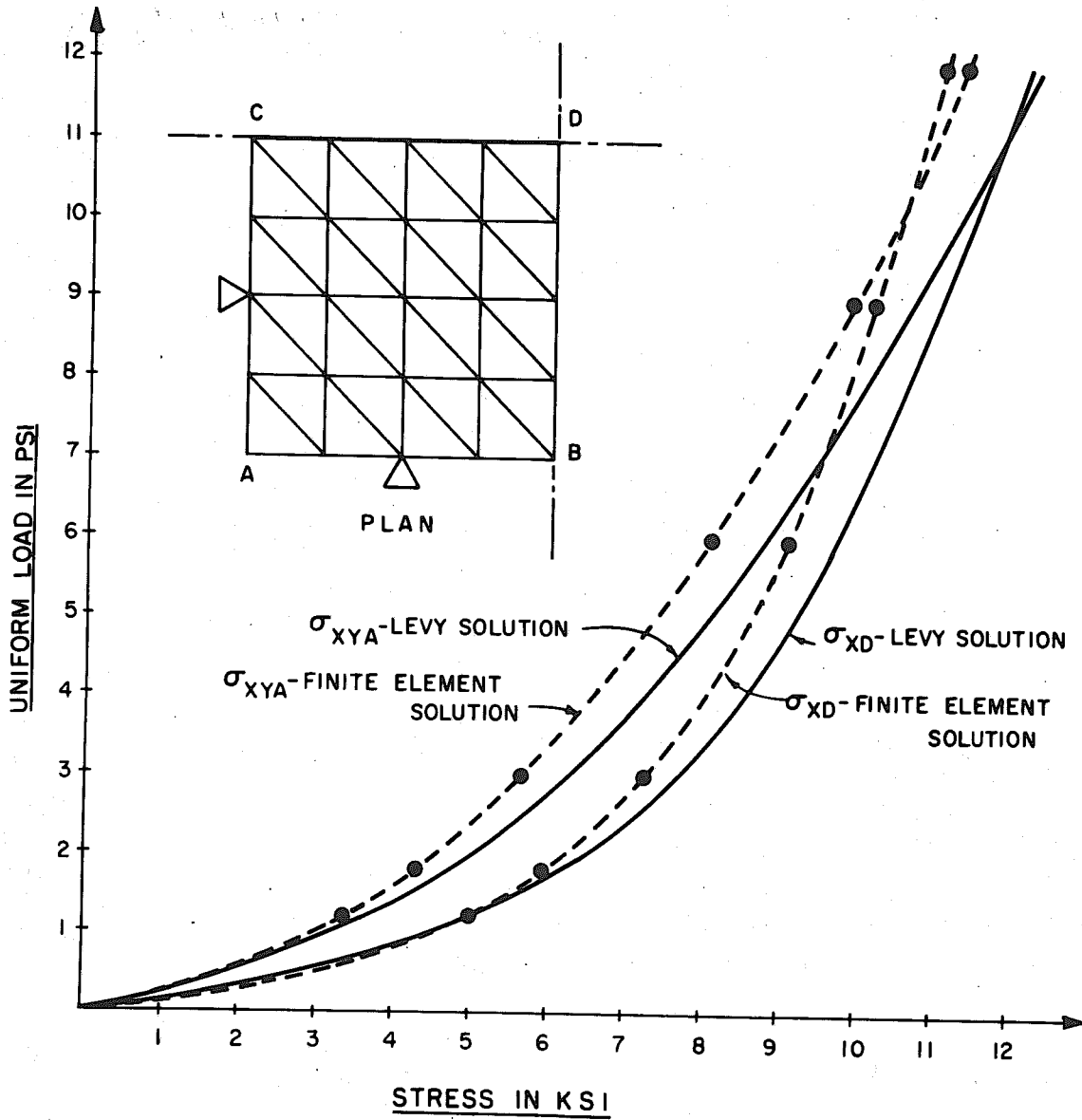


PLATE 2-6 BENDING STRESSES IN SIMPLY SUPPORTED SQUARE PLATE

2.11.4 Clamped Square Plate - Uniform Load

The same plate as was analyzed in section 2.11.3 was analyzed with clamped edges. Plate 2-7 is a plot of center deflection vs. load. The maximum loading on this plot is 15 psi, as it was for the simply supported plate. To illustrate the fact that the method has a greater capacity, the loading was continued to 140 psi. This plot is shown in Plate 2-8. The limit of Levy's work [16] is shown on the same plot to be slightly less than 20 psi.

2.11.5 Post-Buckling Behavior of a Cantilevered Plate

The previous examples have considered plate behavior in which the system becomes stiffer as the load increases. For plates in which the in-plane forces are compressive and increase in magnitude as the loading progresses, the system "softens." The most extreme example of this is an infinite strip of plate subjected to in-plane compressive loads. This problem corresponds to the classical "elastica" problem of column buckling.

The same plate layout as used in section 2.11.1 was selected with the exception that a modulus of elasticity of 30×10^6 psi and a Poisson's ratio of 0.3 were used. The plate was loaded with a compressive line load, parallel to the middle surface of the plate but with an eccentricity of 0.01 inches (which is one-tenth of the plate thickness) so that large deflections would initiate when the load approached the critical load.

The load vs. free edge deflection plot is shown in Plate 2-9. The theoretical elastic solution for a concentrically loaded strip is taken from Timoshenko [17] where the solution is achieved through the use of elliptic integrals. Agreement seems sufficiently close for engineering purposes. Notice that the essentially flat range of deflections is not easily determined by this technique and a better solution is presented

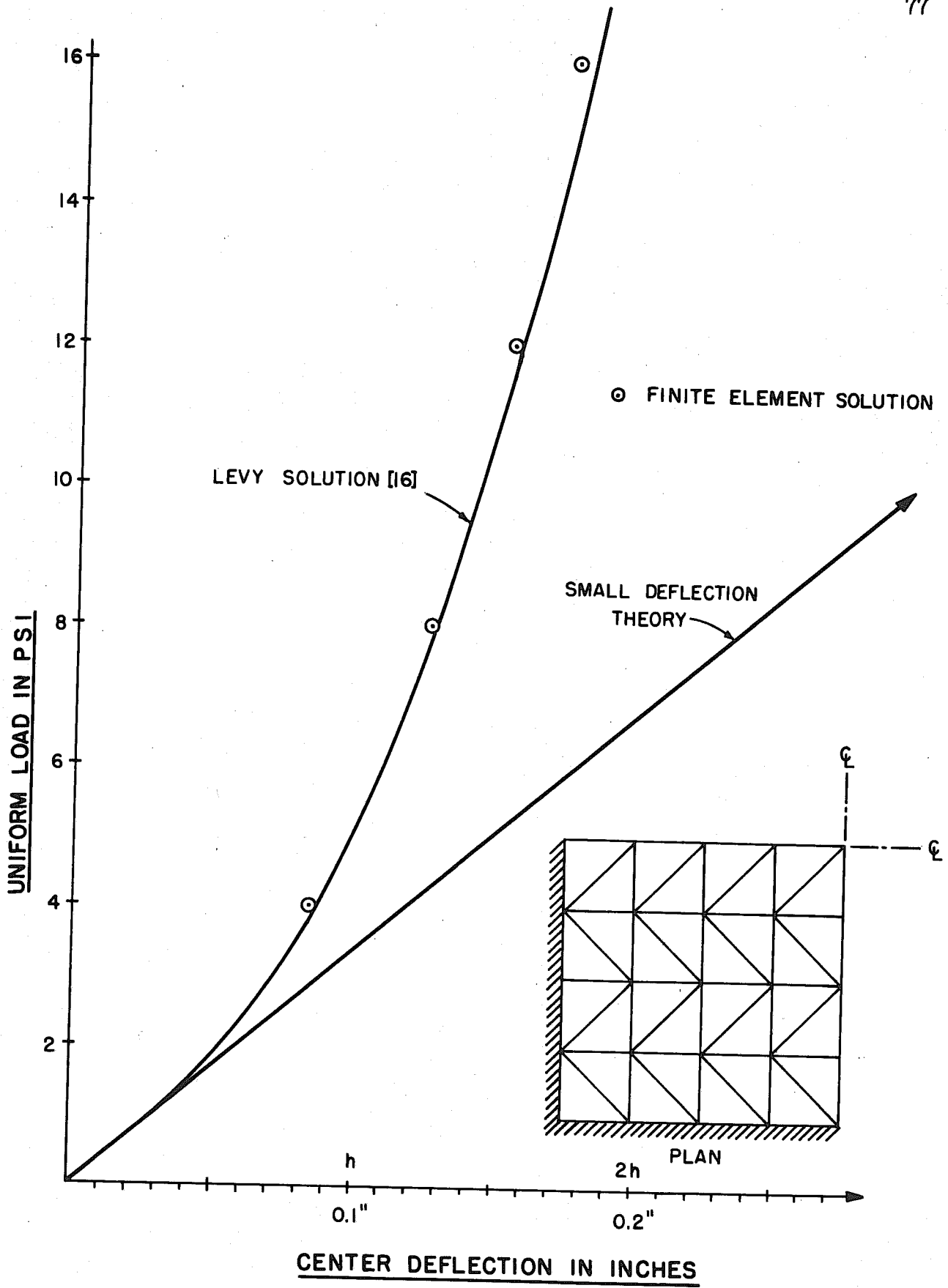


PLATE 2-7 LOAD DEFLECTION OF CLAMPED SQUARE PLATE AT LOW LOADS

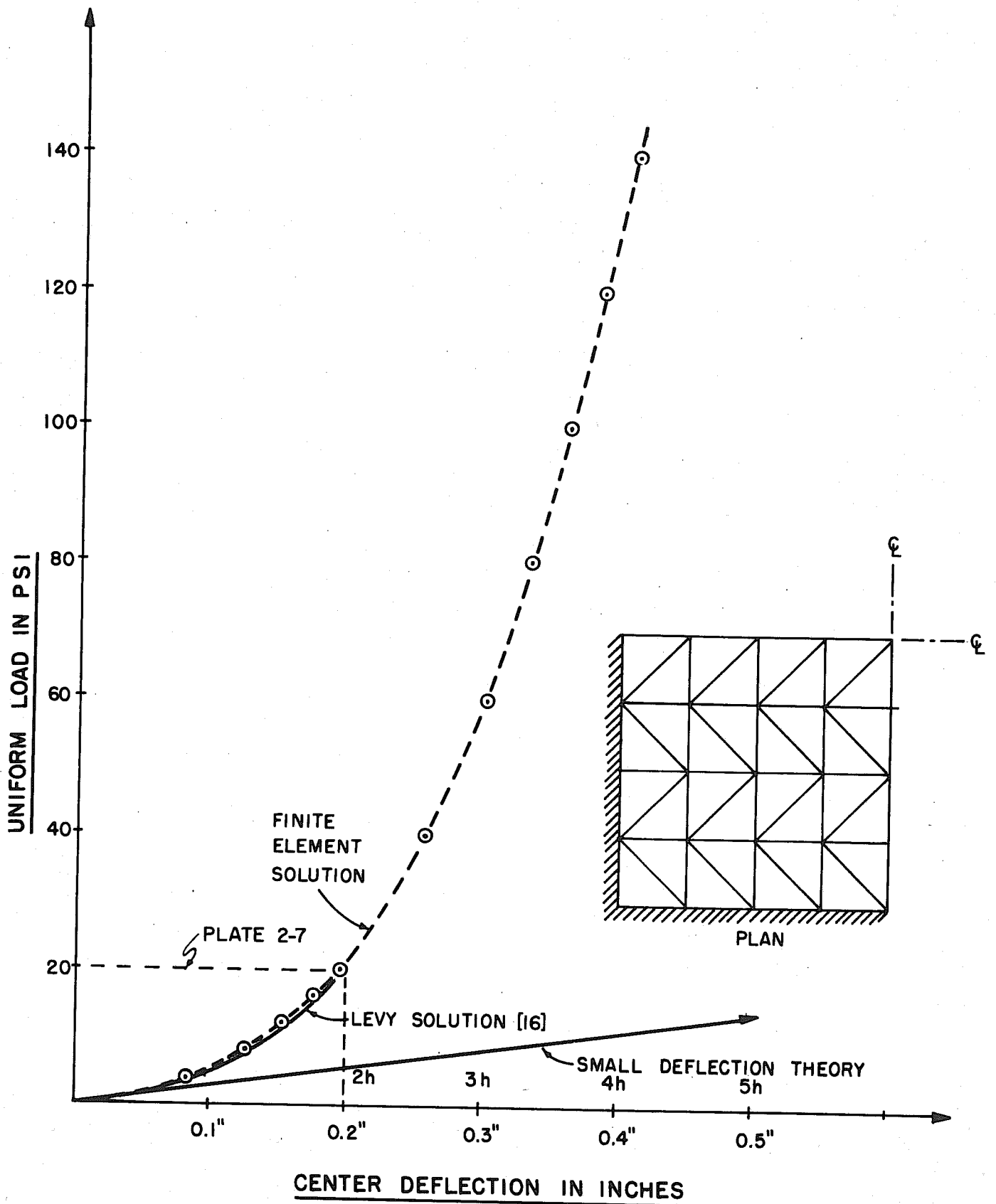


PLATE 2-8 LOAD DEFLECTION OF CLAMPED SQUARE PLATE AT HIGH LOADS

in Chapter 3. A discussion of this point is undertaken below. To illustrate the magnitude of deformations that are involved in this type of problem a profile of deflected configuration for a load greater than the buckling load is shown in Plate 2-10. Notice that the vertical deflection is approximately 4-1/2 inches and the horizontal deflection is approximately 7 inches. Since these deflections occur in a plate of 10 inch length they represent a severe condition.

It was noted above that the "flat" region on the plot in Plate 2-9 is not easily determined by this technique. The reason for this is that the approximate stiffness which was adopted in section 2.3.3 becomes a poor estimate of the actual stiffness of the structure in this range. For this reason it is desirable to consider an evaluation of the geometric stiffness. This is done in Chapter 3.

2.12 Discussion of Results - Stresses

The previous section has presented the solutions for a number of plate problems and compared the results with solutions achieved by other means. The problems have included examples involving large geometric displacements and rotations, various types of boundary conditions and the presence of large in-plane forces. It can be seen that the macroscopic structural behavior is generally well represented by the model and results are sufficiently accurate for engineering purposes. It should be emphasized that the same technique and formulation have been used for all of these problems and can be applied to plates of arbitrary geometry and boundary conditions for which no classical solutions exist.

It was noted in section 2.11.3 that agreement with Levy solution stress results was not as good as for deflections. Stress results from

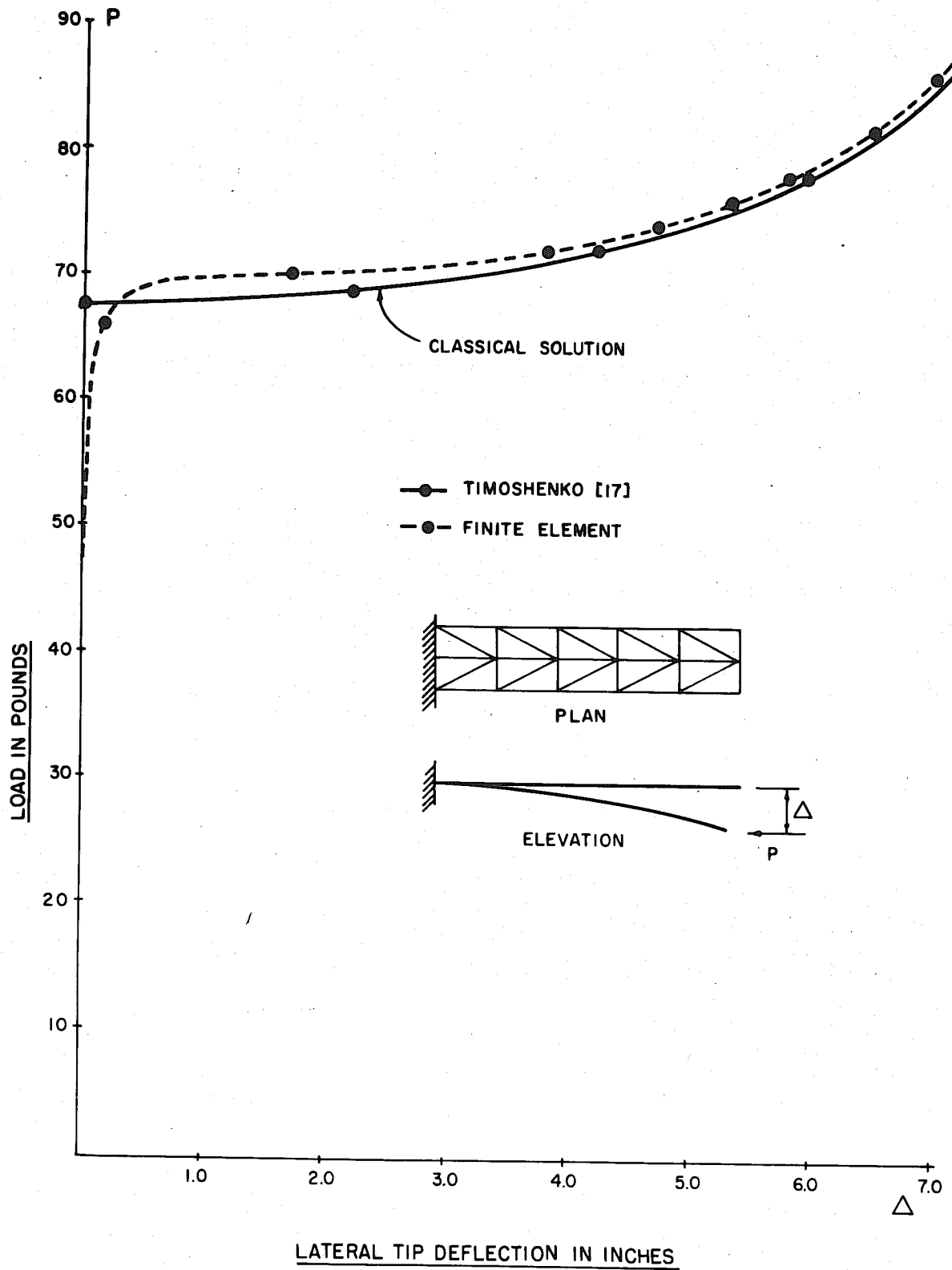


PLATE 2-9 POST-BUCKLING LOAD-DEFLECTION OF CANTILEVERED PLATE

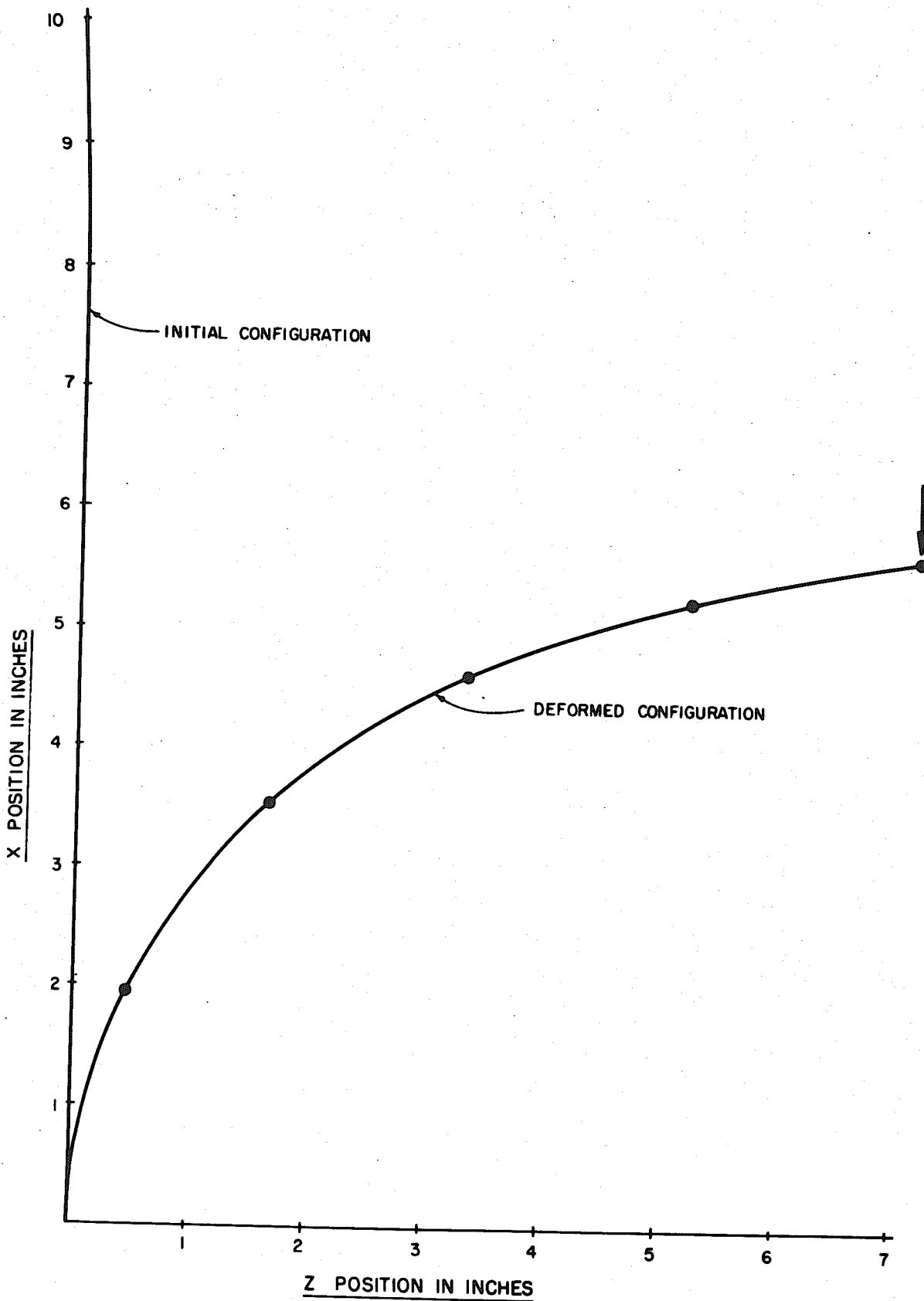


PLATE 2-10 POST-BUCKLING PROFILE OF CANTILEVERED PLATE

the finite element approach must be interpreted carefully. As an illustration of stress results, the example of the simply supported plate of section 2.11.3 is examined in detail. Two element layouts are compared which have roughly the same number of degrees of freedom. These element layouts are shown in Fig. 2.8 and will be referred to as "single diagonal" and "double diagonal" subdivisions, respectively.

Figure 2.7 gives the numerical results for deflections and stresses, for single and double diagonal subdivisions, for both small deflection and large deflection plate theory, for a load of 3 psi. The maximum deflection at the center is 2.78 times the plate thickness as determined by small deflection theory so that this condition is well beyond the applicable limit of small deflection theory. However small deflection theory results are proportional to the loading so that a comparison of the small deflection theory finite element results with conventional theory can be made. The bending stress comparison is shown in Plate 2-11, and indicates that the finite element results are within 4 per cent of the conventional solution* except at the free edge where a self equilibrating set of element moments produces an average stress of approximately ten per cent of the maximum bending stress. The stresses plotted on Plate 2-11 are average stresses at the nodal points. The displacement model maintains normal slope compatibility along the element interfaces but curvatures are discontinuous. Therefore stresses are discontinuous. Figure 2.9 indicates the stress couples, m , at the corner of each element, from which the average stresses were computed. It should be noted that the stress couples at each corner

* Page 118, Timoshenko [6].

are averages in themselves since curvatures are also discontinuous within the element (Appendix C).

The numerical values of stresses and deflections, for a load of 3 psi, for the large deflection solution are also shown in Fig. 2.7 and stresses are plotted on Plate 2-11. Note that the membrane effect reduces the maximum bending stress to approximately $1/3$ of its former value while the locked in stress at the free edge is reduced by a factor of less than two. This results in a greater ratio of free edge stress to maximum stress than occurs for the small deflection solution. The element stress couples are again shown in Fig. 2.9.

Figure 2.8 gives numerical values of stresses and deflections as the load is increased from 3 psi to 15 psi. Stress results are plotted on Plate 2-12. Note that (a) the location of maximum stress and maximum bending stress shifts away from the center of the plate as the load is increased, (b) the membrane stress remains approximately constant across the width of the plate but achieves its highest value at the free edge, and (c) the membrane stress begins to dominate at higher loads. As the load increases the ratio of locked in free edge bending stress to maximum bending stress continues to increase and becomes close to 30 per cent at the maximum loading condition.

However in view of the results on Plate 2-11 it appears that the locked in stresses on the boundary do not detract from the reliability of results in the interior of the plate. It should be noted that the free edge of the plate is the portion of the plate subjected to the greatest moment gradient and that as the deflections became larger this moment gradient is accentuated with respect to gradients in other portions of the plate.

It has been noted that the locked in stresses on the free edge of the plate for a small deflection solution are in the order of 10 per cent (for the present subdivision and the LCCT-9). Fellipa [3] has applied a linear curvature compatible triangle with 12 degrees of freedom (LCCT-12) and found that the free edge stresses are in the order of 5 per cent. It can be expected that considerable improvement in this aspect of stress results can therefore be achieved by incorporating higher order elements into the method. It is interesting to note that Levy's trigonometric series solution also indicates a stress result on the free edge in the order of 10 per cent of the maximum bending stress. Plate 2-6 shows that the finite element bending stresses are approximately 10 per cent lower than those predicted by Levy's series solution. Levy states that "in the case of center deflection, the convergence is oscillatory" for the trigonometric solution and indicates that for large pressures it may be necessary to consider more terms in the series in order to determine the center deflection to within 1 per cent. Since convergence is slower for the second derivative of a series solution than for the series itself, an error in bending stress of 10 per cent appears quite possible with the truncated series which was employed. This is not meant to imply that the finite element bending stresses are a better solution than the series solution but merely to indicate that approximations are present in both solutions and, in the context of this problem, a discrepancy of 10 per cent does not appear unreasonable.

A few remarks should also be made with respect to membrane stresses. The model is based on a uniform membrane stress throughout the entire element. By utilizing an averaging procedure suggested by Wilson [2] membrane stresses may also be estimated at the nodal points. Numerical

membrane stress results are given in Fig. 2.10, and element membrane stresses are plotted in Plate 2-12. The averaged nodal stresses produce results slightly lower than element stresses and are considered less accurate. Stresses plotted in Plate 2-5 were therefore obtained from Plate 2-12 which utilizes element, rather than nodal point stresses and show good agreement with Levy results.

The results of this chapter indicate that the finite element seems to be well adapted to obtaining solutions, which are sufficiently accurate for engineering purposes, to a wide variety of plate problems.

FIG. 2.7. STRESS COMPARISON FOR
16 x 16 x 0.1 PLATE FOR $q = 3$ psi

Distance Along ζ From Free Edge		Finite Element Stresses ($\nu = 0.316$)				
		Single Diagonal		Double Diagonal		
		SD	LD	SD	LD1	LD
0	σ_x	2104	1258	2011	2330	1214
	σ_y	1787	728	2097	2269	871
0.25a	σ_x	11,128	5076			
	σ_y	9834	3619			
1/3a	σ_x			13,789	13,726	6197
	σ_y			11,817	11,722	4365
0.5a	σ_x	17,489	6877			
	σ_y	16,640	5851			
2/3a	σ_x			20,088	20,061	7351
	σ_y			19,314	19,295	6630
0.75a	σ_x	20,766	7162			
	σ_y	20,632	6952			
1.0a	σ_x	21,817	7249	21,833	21,830	7281
	σ_y	21,817	7249	21,833	21,830	7281
0	w	0	0	0	0	0
0.25a	w_6	.1106	.0435			
1/3a	w_{11}			.1450	.1450	.0572
0.5a	w_{11}	.2007	.0771			
2/3a	w_{18}			.2454	.2454	.0938
0.75a	w_{16}	.2585	.0928			
1.0a	w	.2782	.1039	.2805	.2805	.1057

- Notes: (1) a = one half of side length of plate
 (2) SD = small deflection theory
 (3) LD = large deflection theory
 (4) LD1 = first iterate of large deflection solution.

FIG. 2.7 (Continued)

Stress Type	Timoshenko Stresses [5] ($\nu = 0.3$)				
	0.2a	0.4a	0.6a	0.8a	1.0a
σ_x	9650	15,810	19,530	21,500	22,100
σ_y	7750	13,980	18,430	21,150	22,080

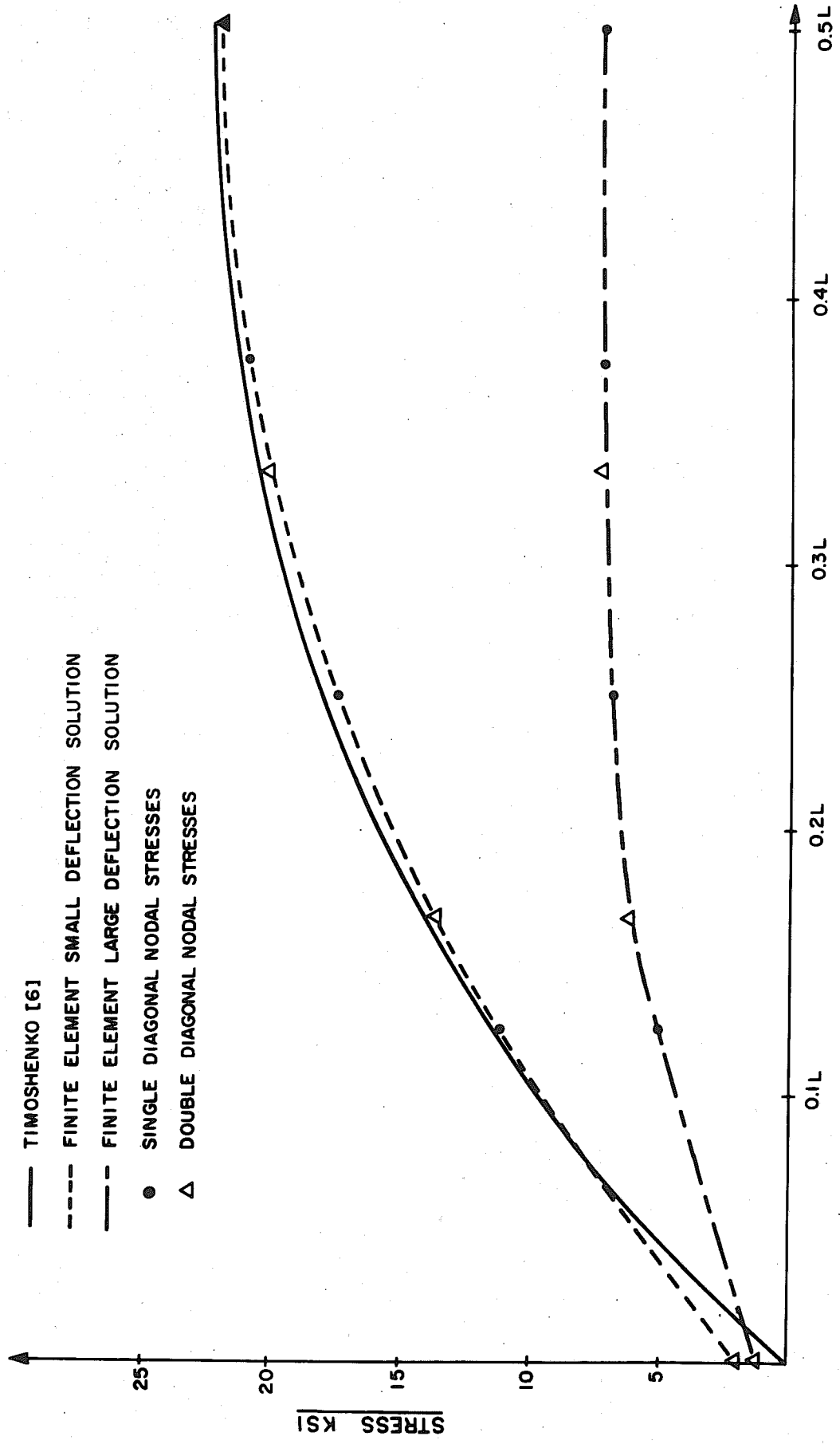
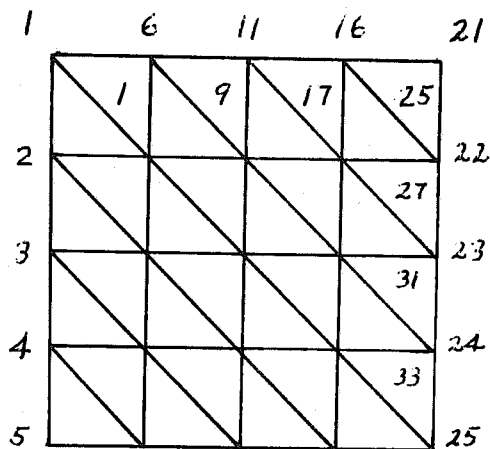
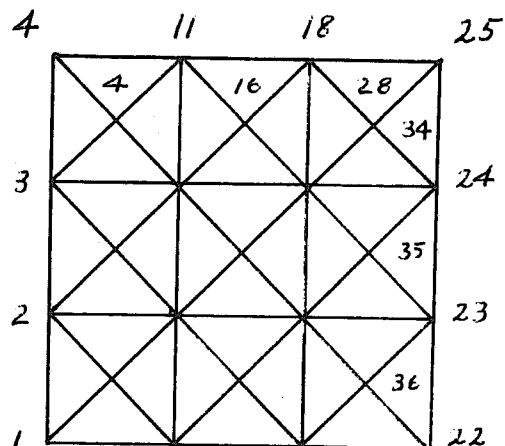


PLATE 2-11 COMPARISON OF BENDING STRESSES IN SIMPLY SUPPORTED SQUARE PLATE FOR UNIFORM LOAD OF 3 PSI

Single Diagonal SubdivisionDouble Diagonal SubdivisionSingle Diagonal

q	w_1	w_6	w_{11}	w_{16}	w_{21}	σ_{x1}	σ_{x6}	σ_{x11}	σ_{x16}	σ_{x21}	σ_{xy5}
3	0	.04345	.07711	.09725	0.1039	1258	5076	6877	7162	7249	5670
6	0	.0588	.1033	.1291	.1373	2012	7309	9260	9098	9058	8081
9	0	.0694	.1210	.1504	.1597	2610	8296	10856	10322	10183	9680
12	0	.0776	.1348	.1669	.1770	3119	10231	12086	11250	11035	11323
15	0	.0846	.1464	.1807	.1915	3568	11341	13108	12014	11739	12590

Double Diagonal

q	w_4	w_{11}	w_{16}	w_{21}	σ_{x4}	σ_{x11}	σ_{x18}	σ_{x25}	σ_{xy1}
3	0	.0572	.0938	.1057	1214	6197	7351	7281	6022
6	0	.0773	.1248	.1399	1969	8809	9555	9092	8640
9	0	.0909	.1457	.1627	2587	10654	10979	10224	10590
12	0	.1017	.1619	.1804	3216	12115	12064	11088	12207
15	0	.1106	.1754	.1952	3612	13338	12958	11806	13615

Figure 2.8

16 x 16 x 0.1 BENDING STRESSES AND DEFLECTIONS

7.435	15.945	23.271	28.489	31.914	34.693	35.543	36.361
-1.421	19.464	16.425	31.089	27.045	35.947	33.594	35.841
3.236	12.17	19.125	24.281	28.070	31.051	32.853	34.019
5.996	14.735	21.861	26.285	29.868	30.534	33.156	30.187
-1.010	17.273	14.450	27.067	24.319	25.138	30.172	27.503
2.245	9.819	15.571	19.803	22.888	24.387	26.814	25.509
4.674	11.671	17.227	10.610	23.259	24.387	25.595	25.509
-1.235	12.541	10.920	18.460	18.431	20.075	22.697	19.645
1.035	5.635	9.761	10.385	14.496	14.692	16.943	16.589
2.378	5.922	9.401	10.318	12.487	12.083	13.603	12.934
0	3.670	6.098	4.415	9.714	11.464	11.464	4.430
0	0	1.577	0.518	2.589	4.247	3.173	1.525

SMALL DEFLECTION

m_x
q = 3 psi

3.188	7.358	10.225	11.870	12.239	12.568	12.026	12.082
1.005	8.460	7.796	12.895	10.276	13.201	11.212	12.048
1.941	6.397	8.971	10.551	10.797	11.344	11.029	11.316
2.829	7.193	10.111	11.605	11.836	11.976	11.548	11.393
.306	8.309	6.403	12.233	9.335	9.635	10.316	10.650
1.430	5.512	7.742	9.155	9.323	11.887	9.467	4.437
2.507	6.418	8.733	9.938	9.923	9.842	9.433	9.168
-1.473	7.007	5.559	9.172	7.863	8.317	8.467	9.168
0.697	3.379	5.372	5.661	6.576	5.863	6.735	7.266
0	1.449	3.428	5.272	5.281	4.991	4.911	6.029
0	2.233	0.892	2.202	4.662	1.581	5.366	4.797
0	0	0.358	1.232	0.772	1.356	1.019	1.407

ITERATED VALUES OF m_x
EQUILIBRIUM POSITION
FOR q = 3 psi

FIG. 2.9
LOCAL STRESS COUPLES m_x

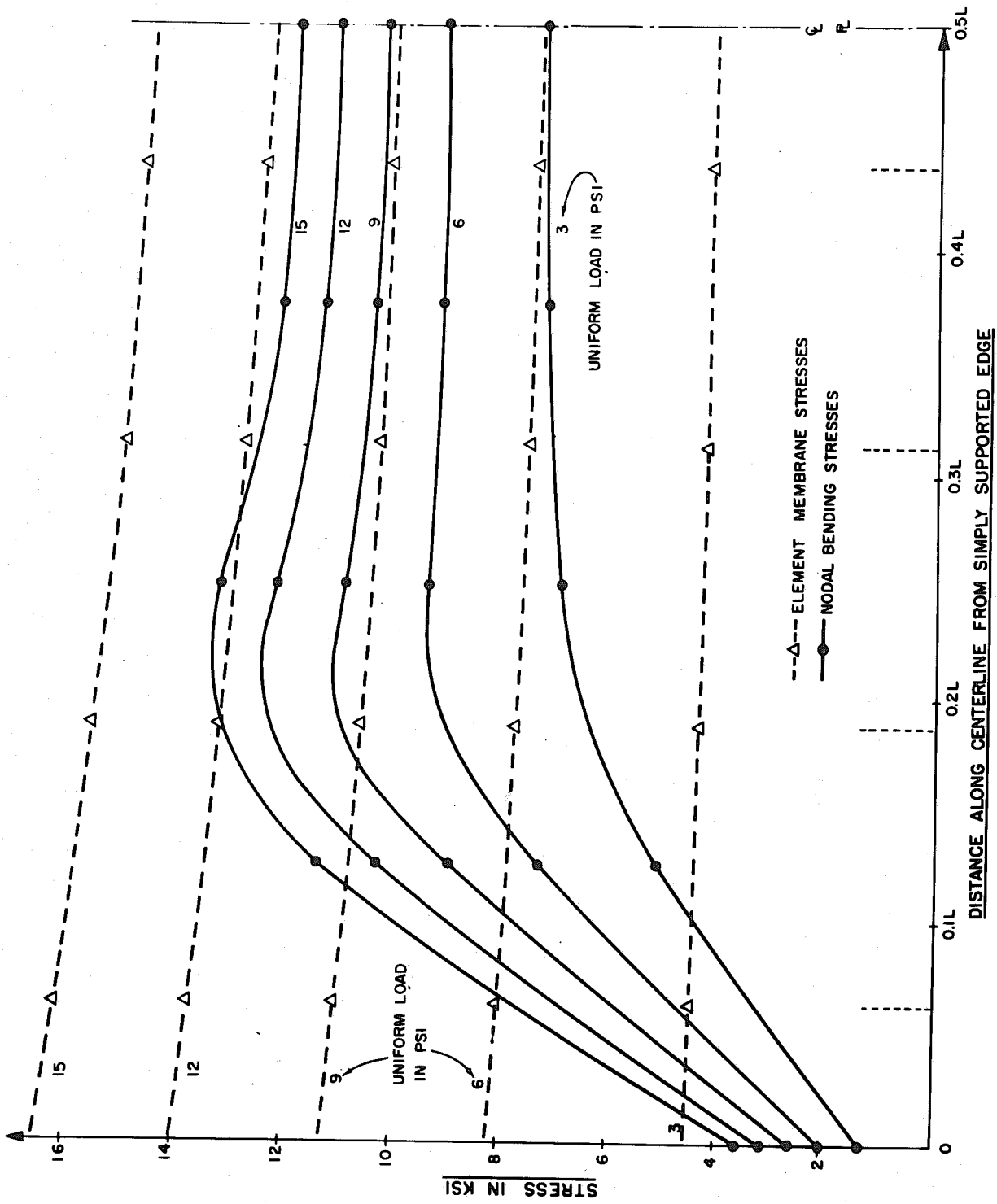


PLATE 2-12 DISTRIBUTION OF STRESSES IN SIMPLY SUPPORTED SQUARE PLATE

(i) Single Diagonal Nodal Stresses

q	σ_{x1}	σ_{x6}	σ_{x11}	σ_{x16}	σ_{x21}	σ_{y16}	σ_{y11}	σ_{y26}	σ_{y1}
3	4221	4194	4088	4049	4160	3777	2927	1857	1370
6	7607	7522	7288	7181	7355	6719	5295	3423	2505
9	10474	10327	9971	9799	10019	9185	7310	4782	3481
12	13040	12830	12358	12124	12382	11379	9117	6013	4362
15	15400	15129	14549	14256	14547	13393	10784	7157	5177

(ii) Single Diagonal Element Stresses

q	σ_{x1}	σ_{x9}	σ_{x17}	σ_{x25}	σ_{x27}	σ_{x29}	σ_{x31}
3	4455	4319	4212	4160	3781	2832	1741
6	8012	7714	7477	7356	6734	5145	3222
9	11016	10562	10204	10019	9210	7119	4510
12	13700	13098	12628	12382	11413	8892	5680
15	16167	15424	14848	14547	13436	10529	6768

(iii) Double Diagonal Nodal Stresses

q	σ_{x4}	σ_{x11}	σ_{x18}	σ_{x25}	σ_{y18}	σ_{y11}	σ_{y4}
3	4364	4303	4143	4056	3403	1980	1378
6	7870	7716	7374	7200	6113	3657	2513
9	10834	10590	10077	9825	8400	5110	3486
12	13485	13153	12482	12158	10442	6427	4361
15	15920	15506	14686	14296	12319	7649	5169

(iv) Double Diagonal Element Stresses

q	σ_{x4}	σ_{x16}	σ_{x28}	σ_{x34}	σ_{x35}	σ_{x36}
3	4429	4293	4122	3860	2720	1557
6	7972	7656	7312	6864	4947	2883
9	10960	10472	9974	9377	6845	4035
12	13630	12977	12340	11612	8550	5080
15	16087	15274	14507	13662	10122	6052

Figure 2.10

16 x 16 x 0.1 INCH MEMBRANE STRESS RESULTS FOR q = 3 psi

3. THE GEOMETRIC STIFFNESS

The formulation and results presented in Chapter 2 were based on approximating the stiffness of the structure by the stiffness of a stress free structure in the deformed configuration. This approach has been successful in solving many practical problems. However, as was pointed out in section 2.3.2, an "exact" evaluation of the stiffness of the structure at any time must include the effects of existing stress conditions. For some types of problem it is advantageous to obtain a more exact estimate of the stiffness. This is particularly true (a) when using a solution technique which is not iterative and (b) when predicting structural behavior in the region of buckling. The object of this chapter is to develop a "complete" formulation of the "geometric stiffness" (see section 2.3.2) of a two dimensional model and to evaluate the significant terms of this formulation for this particular model.

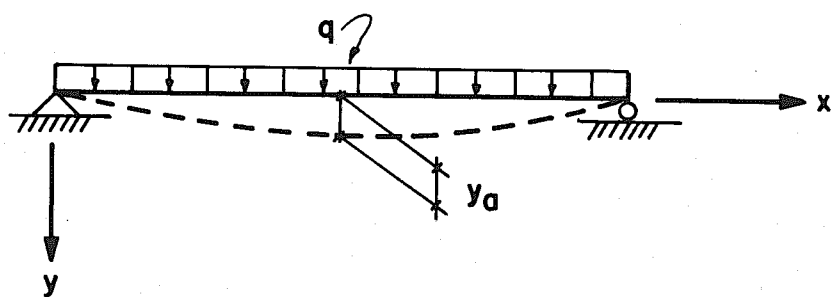
3.1 Introduction

The term "geometric stiffness" is a relatively new one in engineering literature. However the concept has had a long and extensive history. In its simplest form this concept can be illustrated by a simple beam-column. If we refer to Fig. 3.1, the equation of equilibrium for the beam can be written as

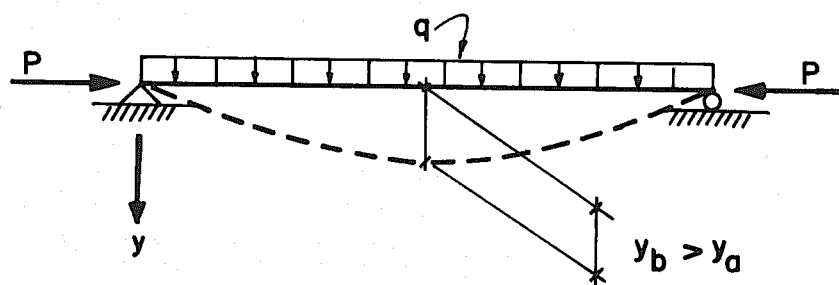
$$EI \frac{d^4 y}{dx^4} = q.$$

However if the beam has an axial load P , at the time of application of the load q , the equation of equilibrium is [17]

$$EI \frac{d^4 y}{dx^4} + P \frac{d^2 y}{dx^2} = q.$$



(a) BEAM



(b) BEAM - COLUMN

FIG. 3.1

The quantity q corresponds to the external "applied load" and the quantity EI is the conventional beam "stiffness." The term $P \frac{d^2y}{dx^2}$ corresponds to a "geometric stiffness," because it effectively reduces the stiffness of the structure with respect to the loads q . The geometric stiffness depends only on the initial stress condition, P , and second order geometric effects. Physically it represents an effective lateral load resulting from a constant initial stress when the beam is subjected to a change in configuration. The concept of effective lateral load can be used to arrive at the terms on the right hand side of equation (1-27) when formulating the equilibrium equations of the plate.[†] In the derivation of the geometric stiffness which follows, it is the forces arising from this effect which are being evaluated.

A systematic and rigorous development of the behavior of a continuum for incremental effects when subjected to initial stress has been undertaken by Biot [18]. In the field of finite elements, the most elegant treatment is probably that of Felippa [1]. However Argyris [5, 19], Matrin [20, 21], and Hartz [22, 23], are among those who have formulated geometric stiffnesses for particular applications. The terms "initial stress" matrix and "stability" matrix are also used for the geometric stiffness matrix.

3.2 Formulation of a "Complete" Geometric Stiffness for Two-Dimensional Elements

The derivation of the expression for the geometric stiffness has been carried out in Appendix B. It arises from the first term in expression (B1-8), namely

[†] See Timoshenko [5], p. 378.

$$\int_{V_0} \bar{\sigma}_{ij0} \frac{1}{2} \delta \{ (\Delta \bar{u}_k)_{,i} (\Delta \bar{u}_k)_{,j} \} dV_0. \quad (3-1)$$

This integral was developed with reference to the global co-ordinate system but the integrand is invariant with respect to co-ordinate transformation so that it may be referred to the local co-ordinate system. The engineering strains and all displacement gradients may be assumed small with reference to this system of co-ordinates so that we may specialize to the two dimensional description and use small deflection plate theory. In the remainder of this chapter we will therefore

- (a) drop the Δ symbol, with the understanding that a u stands for a small increment in displacement
- (b) use lower case letters with the understanding that they refer to the local co-ordinate system. This is consistent with the nomenclature adopted in developing the stiffness matrices in sections 2.4, 2.5 and Appendix C.

We evaluate the integral for one element only, in accordance with the direct stiffness technique.

Expression (3-1) may be written as[†]

$$\sum_{i=1}^3 \sum_{j=1}^3 \int_{V_k} \frac{\bar{\sigma}_{ij0}}{2} \delta \{ \bar{u}_{,i} \bar{u}_{,j} + \bar{v}_{,i} \bar{v}_{,j} + \bar{w}_{,i} \bar{w}_{,j} \} dV \quad (3-2)$$

[†] In the remainder of this section the summation convention will be suppressed. In addition, since only infinitesimal displacements are considered, 0 subscripts for integration are dropped.

or

$$\sum_{i=1}^3 \sum_{j=1}^3 \int_{V_K} \frac{\tilde{\sigma}_{i,jc}}{2} \delta \left[\{\tilde{u}_{,i}\}^T \{\tilde{u}_{,j}\} \right] dV. \quad (3-3)$$

where $\{\tilde{u}\}$ is as defined in section 2.3.

Substituting equation (2-15) into equation (2-14) of section 2.4, establishes the relations for $\{\tilde{u}\}$

$$\{\tilde{u}\} = \begin{Bmatrix} \tilde{u} \\ \tilde{v} \\ \tilde{w} \end{Bmatrix} = \begin{bmatrix} \{\phi_u\}^T & \cdot & -z\{\phi_{w,x}\}^T \\ \cdot & \{\phi_v\}^T & -z\{\phi_{w,y}\}^T \\ \cdot & \cdot & \{\phi_w\}^T \end{bmatrix} \begin{Bmatrix} \{u\} \\ \{v\} \\ \{w\} \end{Bmatrix}, \quad (3-4)$$

where terms are defined in section 2.4. According to the definition of that section we may also designate the nodal vector as $\{r_E\}$.

We use the indexes α, β with a range from 1 to 2 in the following and evaluate the derivatives,

$$\begin{Bmatrix} \frac{\partial \tilde{u}}{\partial x_\alpha} \\ \frac{\partial \tilde{v}}{\partial x_\alpha} \\ \frac{\partial \tilde{w}}{\partial x_\alpha} \end{Bmatrix} = \begin{bmatrix} \{\phi_{u,\alpha}\}^T & \cdot & -z\{\phi_{w,x\alpha}\}^T \\ \cdot & \{\phi_{v,\alpha}\}^T & -z\{\phi_{w,y\alpha}\}^T \\ \cdot & \cdot & \{\phi_{w,\alpha}\}^T \end{bmatrix} \{r_E\} = [\tilde{\Lambda}_\alpha]^T \{r_E\} \quad (3-5)$$

and

$$\begin{Bmatrix} \frac{\partial \tilde{u}}{\partial z} \\ \frac{\partial \tilde{v}}{\partial z} \\ \frac{\partial \tilde{w}}{\partial z} \end{Bmatrix} = \begin{bmatrix} \cdot & \cdot & -\{\varphi_{w,x}\}^T \\ \cdot & \cdot & -\{\varphi_{w,y}\}^T \\ \cdot & \cdot & \cdot \end{bmatrix} \{r_E\} = [\tilde{\Lambda}_z]^T \{r_E\} \quad (3-6)$$

where $[\tilde{\Lambda}_\alpha]$ and $[\tilde{\Lambda}_z]$ are defined by these expressions.

Expression (3-3) can now be written as

$$\begin{aligned} \frac{1}{2} \delta \left\{ \{r_E\}^T \int_V \left[\sum_{\alpha=1}^2 \sum_{\beta=1}^2 [\tilde{\Lambda}_\beta] \sigma_{\alpha\beta} [\tilde{\Lambda}_\alpha]^T + \sum_{\alpha=1}^2 [\tilde{\Lambda}_\alpha] \sigma_{\alpha z_0} [\tilde{\Lambda}_z]^T \right. \right. \\ \left. \left. + \sum_{\beta=1}^2 [\tilde{\Lambda}_z] \sigma_{z\beta_0} [\tilde{\Lambda}_\beta]^T + [\tilde{\Lambda}_z] \sigma_{zz_0} [\tilde{\Lambda}_z]^T \right] dV \{r_E\} \right\}. \quad (3-7) \end{aligned}$$

Since the stress tensor is symmetric, and the summation index is arbitrary, the center two terms can be combined into the sum

$$\sum_{\alpha=1}^2 [\tilde{\Lambda}_\alpha] \sigma_{\alpha z_0} [\tilde{\Lambda}_\alpha]^T \quad (3-7a)$$

where

$$\begin{aligned} [\tilde{\Lambda}_\alpha] &= [\Lambda_\alpha] + [\Lambda_z] \\ &= \begin{bmatrix} \{\varphi_{u,\alpha}\} & \cdot & \cdot \\ \cdot & \{\varphi_{v,\alpha}\} & \cdot \\ \{-\varphi_{w,x}\} + z\{\varphi_{w,x\alpha}\} & -\{\varphi_{w,y}\} + z\{\varphi_{w,y\alpha}\} & \{\varphi_{w,z}\} \end{bmatrix} \quad (3-8) \end{aligned}$$

Since all terms in the matrix sum of (3-7) are now in symmetric form, expression (3-7) can be written symbolically as

$$\frac{1}{2} \delta \left[\{r_E\}^T [K_G] \{r_E\} \right], \quad (3-9)$$

for when the variation is carried out it yields

$$\frac{1}{2} \{ \delta r_E \}^T [K_G] \{ r_E \} + \frac{1}{2} \{ r_E \}^T [K_G] \{ \delta r_E \},$$

and since the matrix sum $[K_G]$ is symmetric this can be written as $\{ \delta r_E \}^T [K_G] \{ r_E \}$, where $[K_G]$ can be identified as the geometric stiffness, as defined in Appendix B, for this element.

We now form the matrix products of the first and last terms in the integral (3-7) and of expression (3-8), and integrate through the thickness. In order to do this, we define

$$\int_{-\frac{h}{2}}^{\frac{h}{2}} \langle \sigma_{\alpha\beta} \quad \sigma_{\alpha 3} \rangle dz = \langle N_{\alpha\beta} \quad Q_{\alpha} \rangle \quad (3-10)$$

and

$$\int_{-\frac{h}{2}}^{\frac{h}{2}} -z \sigma_{\alpha\beta} dz = M_{\alpha\beta}.$$

In performing the integration the following assumptions have been made:

(a) $\int_{-\frac{h}{2}}^{\frac{h}{2}} z \sigma_{\alpha 3} dz = 0$. This can be justified if we consider that $\sigma_{\alpha 3}$ is an even function with respect to the middle surface.

(b) $\int_{-\frac{h}{2}}^{\frac{h}{2}} \sigma_{33} dz = 0$. This is consistent with the assumptions in section (1.3.4) where the smallness of σ_{33} was used to justify the plane stress constitutive law.

$$(c) \int_{-\frac{h}{2}}^{\frac{h}{2}} z^2 \sigma_{\alpha\beta} dz = \frac{h^2}{12} N_{\alpha\beta}. \text{ This follows if } \sigma_{\alpha\beta} \text{ is a linear function of } z.$$

Integration then yields,

$$K_G = \int_A \sum_{\alpha=1}^2 \sum_{\beta=1}^2 \begin{bmatrix} \{\phi_{u,\alpha}\} N_{\alpha\beta} \{\phi_{u,\beta}\}^T & \cdot & \{\phi_{u,\alpha}\} M_{\alpha\beta} \{\phi_{w,\beta}\}^T \\ \cdot & \{\phi_{v,\alpha}\} N_{\alpha\beta} \{\phi_{v,\beta}\}^T & \{\phi_{v,\alpha}\} M_{\alpha\beta} \{\phi_{w,\beta}\}^T \\ \{\phi_{w,\alpha}\} M_{\alpha\beta} \{\phi_{u,\beta}\}^T & \{\phi_{w,\alpha}\} M_{\alpha\beta} \{\phi_{v,\beta}\}^T & \{\phi_{w,\alpha}\} N_{\alpha\beta} \{\phi_{w,\beta}\}^T + \Psi_1 \end{bmatrix} \\ + \sum_{\alpha=1}^2 \begin{bmatrix} \{\phi_{u,\alpha}\} Q_{\alpha} \{\phi_{u,\alpha}\}^T & \cdot & -\{\phi_{u,\alpha}\} Q_{\alpha} \{\phi_{w,\alpha}\}^T \\ \cdot & \{\phi_{v,\alpha}\} Q_{\alpha} \{\phi_{v,\alpha}\}^T & -\{\phi_{v,\alpha}\} Q_{\alpha} \{\phi_{w,\alpha}\}^T \\ -\{\phi_{w,\alpha}\} Q_{\alpha} \{\phi_{u,\alpha}\}^T & -\{\phi_{w,\alpha}\} Q_{\alpha} \{\phi_{v,\alpha}\}^T & \{\phi_{w,\alpha}\} Q_{\alpha} \{\phi_{w,\alpha}\}^T + \Psi_2 \end{bmatrix} dA \quad (3-11)$$

where

$$\Psi_1 = N_{\alpha\beta} \frac{h^2}{12} \left[\{\phi_{w,\alpha}\} \{\phi_{w,\beta}\}^T + \{\phi_{w,\gamma}\} \{\phi_{w,\beta}\}^T \right]$$

and

$$\Psi_2 = Q_{\alpha} \left[\{\phi_{w,\alpha}\} \{\phi_{w,\alpha}\}^T + \{\phi_{w,\gamma}\} \{\phi_{w,\gamma}\}^T \right] \\ + \frac{h^2}{12} Q_{\alpha} \left[\{\phi_{w,\alpha\alpha}\} \{\phi_{w,\alpha\alpha}\}^T + \{\phi_{w,\gamma\alpha}\} \{\phi_{w,\gamma\alpha}\}^T \right]. \quad (3-12)$$

Equation (3-11) represents the geometric stiffness matrix for a plate element subjected to an initial stress condition which has stress resultants $\{N_{\alpha\beta}, Q_{\alpha}\}$ and stress couples $\{M_{\alpha\beta}\}$. All terms can be given a (nominally) physical interpretation. For instance the terms in the top line of the matrices may be respectively interpreted as:

- (a) The rate of change of the x forces, with respect to u displacements, resulting from the initial stress resultants $N_{\alpha\beta}$
- (b) The rate of change of x forces, with respect to w displacements, resulting from the initial stress couples $M_{\alpha\beta}$
- (c) The rate of change of x forces, with respect to u and w displacements respectively, resulting from the initial shear forces Q_{α} .

We note that the second matrix sum in (3-11) could be put in terms of moment gradients by using the equilibrium equations of the type

$$\frac{\partial M_{xx}}{\partial x} + \frac{\partial M_{yx}}{\partial y} = -Q_x \quad (1-26)$$

3.3 Geometric Stiffness Matrix for Influence of In-Plane Forces on Bending Stiffness

From a practical point of view it is unnecessary to evaluate the "complete" geometric stiffness matrix developed in the previous section. Since the incremental displacements gradients are small, most terms are of higher order. The most significant term is the term in the lower right hand corner of the first matrix of equation (3-11). The geometric stiffness matrix may therefore be approximated as

$$[K_G] = \int_A \sum_{\alpha=1}^2 \sum_{\beta=1}^2 \begin{bmatrix} \cdot & \cdot & \cdot \\ \cdot & \cdot & \cdot \\ \cdot & \cdot & \{\phi_{w,\alpha}\} N_{\alpha\beta} \{\phi_{w,\beta}\}^T \end{bmatrix} dA \quad (3-13)$$

To evaluate this term we use a technique similar to that used in evaluating the stiffness matrix for bending that was discussed in Appendix C. Since the derivatives of the displacement functions are of lower degree than the displacement functions themselves, the numerical work of integration can be reduced by evaluating these derivatives at a selected set of nodal points such that interpolation functions of the minimum degree necessary, may be used. This matrix is evaluated in Appendix C.

3.4 Applications

Although the geometric stiffness matrix can be incorporated into all large deflection problems it has only been applied here to problems where the number of iterates required, using the method of Chapter 2, becomes excessive.

A list of the problems discussed, and the Plates on which results are plotted, is given in Table 3.1.

3.4.1 Post-Buckling of a Cantilevered Plate

The problem of the infinite strip of plate with loads applied in the plane of the plate, discussed in section 2.11.5, was repeated with the geometric stiffness included in the analysis. This problem again corresponds to the "elastica" problem.

Load deflection results are shown in Plate 3-1 and compared with the solution in Timoshenko [17]. The problem was solved in two ways:

- (a) incrementing loading, and
- (b) incrementing in-plane displacements of the free edge.

In the latter case the out-of-plane deflection was initiated by a small constant load applied normal to the plane of the plate at the free edge. Note the excellent agreement of both techniques with the theoretical

TABLE 3.1
LIST OF PLATES FOR CHAPTER 3

PROBLEM	PLATE NO.	TITLE
Post-buckling of a Cantilevered Plate	3-1	Post-Buckling Load-Deflection of Cantilevered Plate
Post-buckling of a Square Simply Supported Plate	3-2	Post-Buckling Load-Deflection of Square Plate-Low Loads
	3-3	Post-Buckling Load-Deflection of Square Plate-High Loads
	3-4	Reactive Boundary Forces for Buckled Square Plate
Post-buckling of a Flange Plate	3-5	Post-Buckling Load-Deflection of a Flange Plate
	3-6	Profile of Buckled Flange Plate
Post-buckling of a Rectangular Simply Supported Plate with an Aspect Ratio of 1.75	3-7	Post-Buckling Load-Deflection of a Rectangular Simply Supported Plate
	3-8	Post-Buckling Centerline Profile of a Rectangular Simply Supported Plate

solution. The displacement technique is the more efficient of the two from the point of view of computer time but it is more difficult to select a sequence of displacements which will properly cover the range of interest.

3.4.2 Post-Buckling Behavior of a Square Plate

The 16-inch square plate discussed in section 2.11.3 was investigated to determine its post-buckling behavior. This plate is simply supported on all four sides. Displacements of one side were incremented and two solutions were carried out. One solution maintained zero in-plane nodal forces on the sides perpendicular to the direction of loading. The other solution maintained zero displacement at nodal points on these sides.

Load-deflection results are plotted in Plate 3-2 and Plate 3-3. The Levy solution [15] is given for comparison. These results are rather interesting. The convenient boundary condition for Levy's solution was a straight edge with zero average in-plane force. It can be seen that the finite element solution with zero nodal forces agrees reasonably well with this solution as long as out-of-plane displacements do not exceed the thickness of plate (Plate 3-2). But for greater displacements, the edge in the finite element is free to warp and therefore does not develop as high a membrane effect in the transverse direction. This results in greater flexibility at higher loads (Plate 3-3).

On the other hand the finite element solution for zero edge displacements in the transverse direction predicts a considerably lower "buckling" load (Plate 3-2). This results because the in-plane forces induced in the transverse direction, by the Poisson's ratio effect, reduce the critical load. However when the out-of-plane displacements become large (Plate 3-3), the membrane forces developed in the transverse direction exceed those that

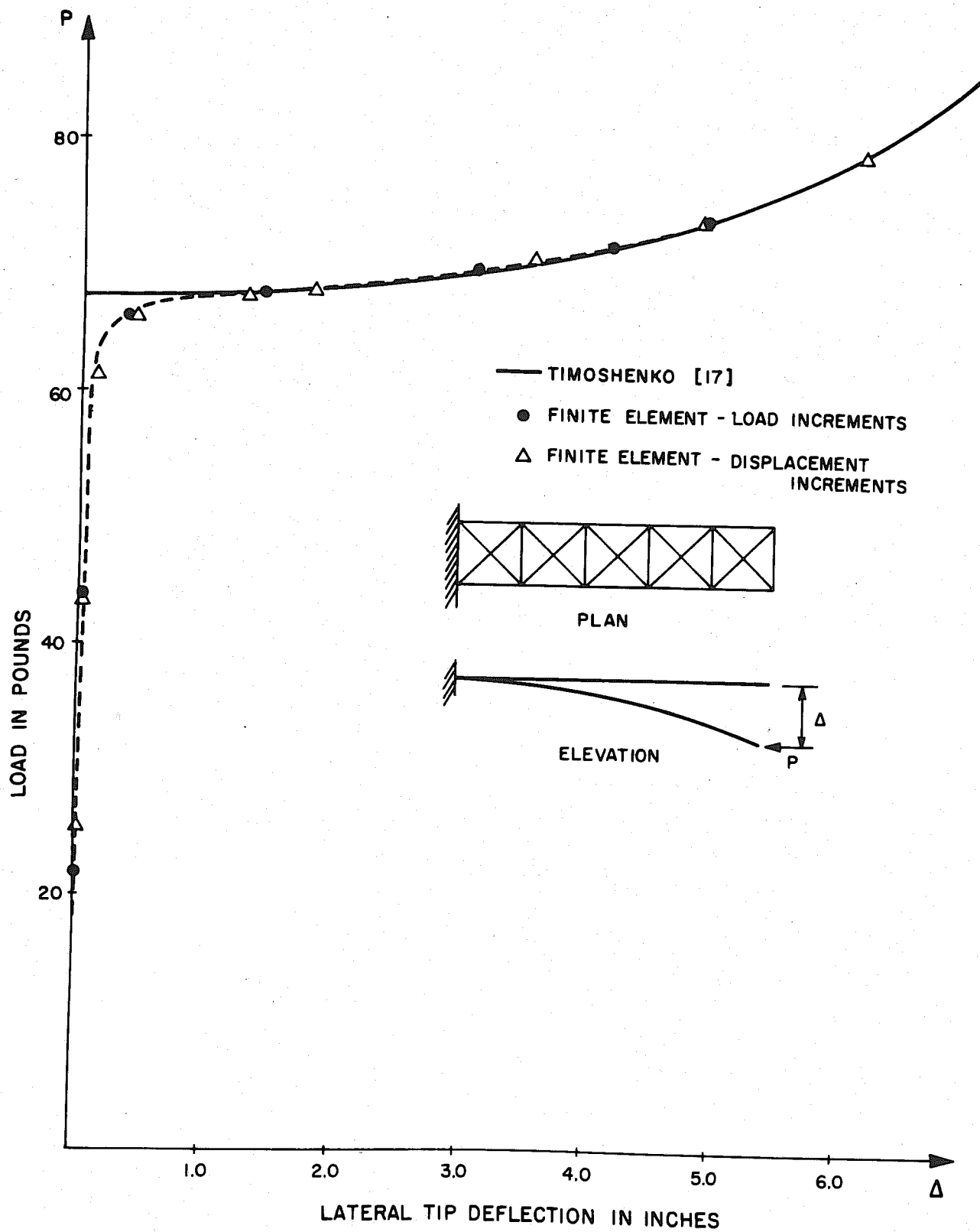


PLATE 3-1 POST-BUCKLING LOAD-DEFLECTION OF CANTILEVERED PLATE

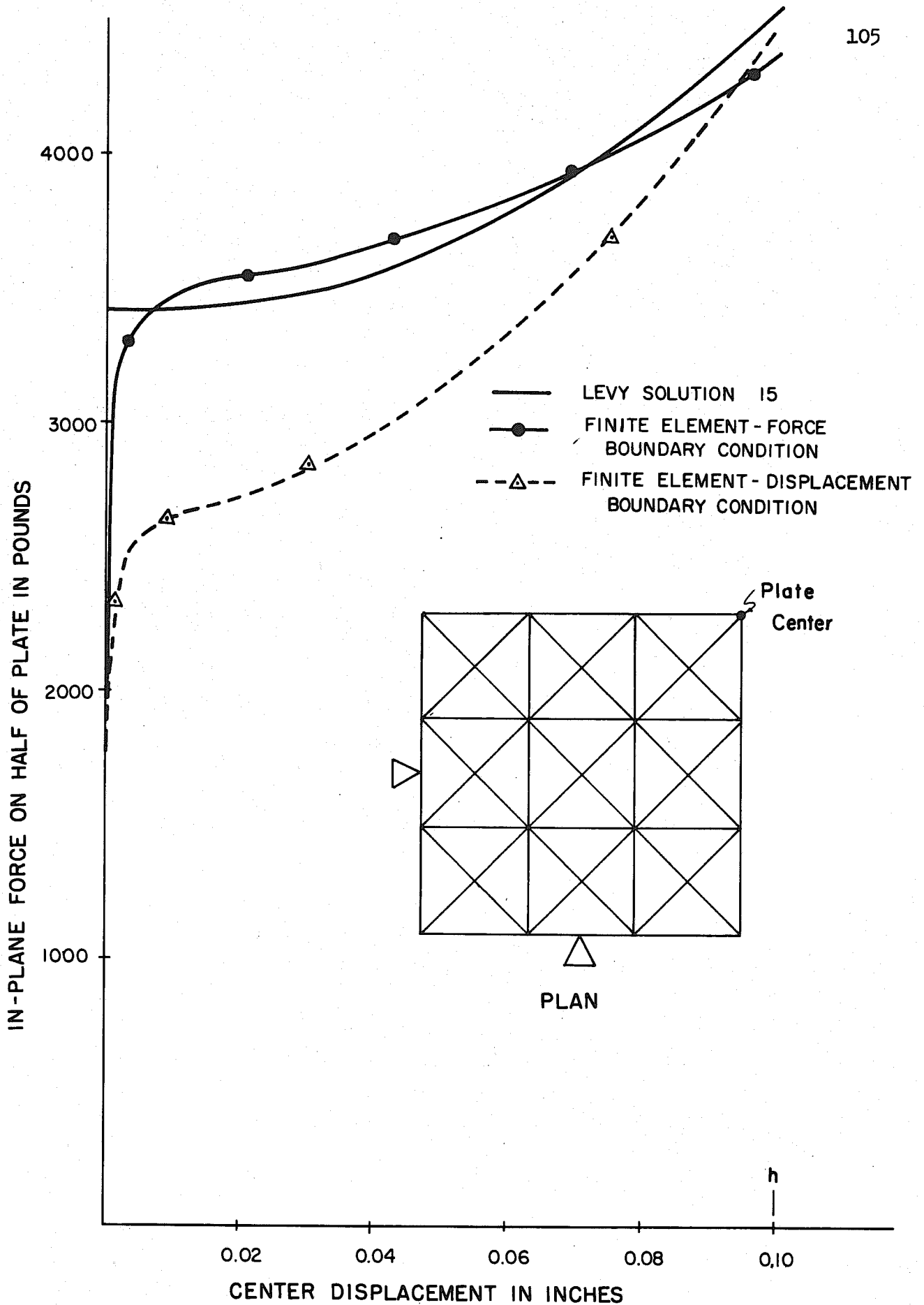


PLATE 3-2 POST-BUCKLING LOAD-DEFLECTION OF SQUARE PLATE AT LOW LOADS

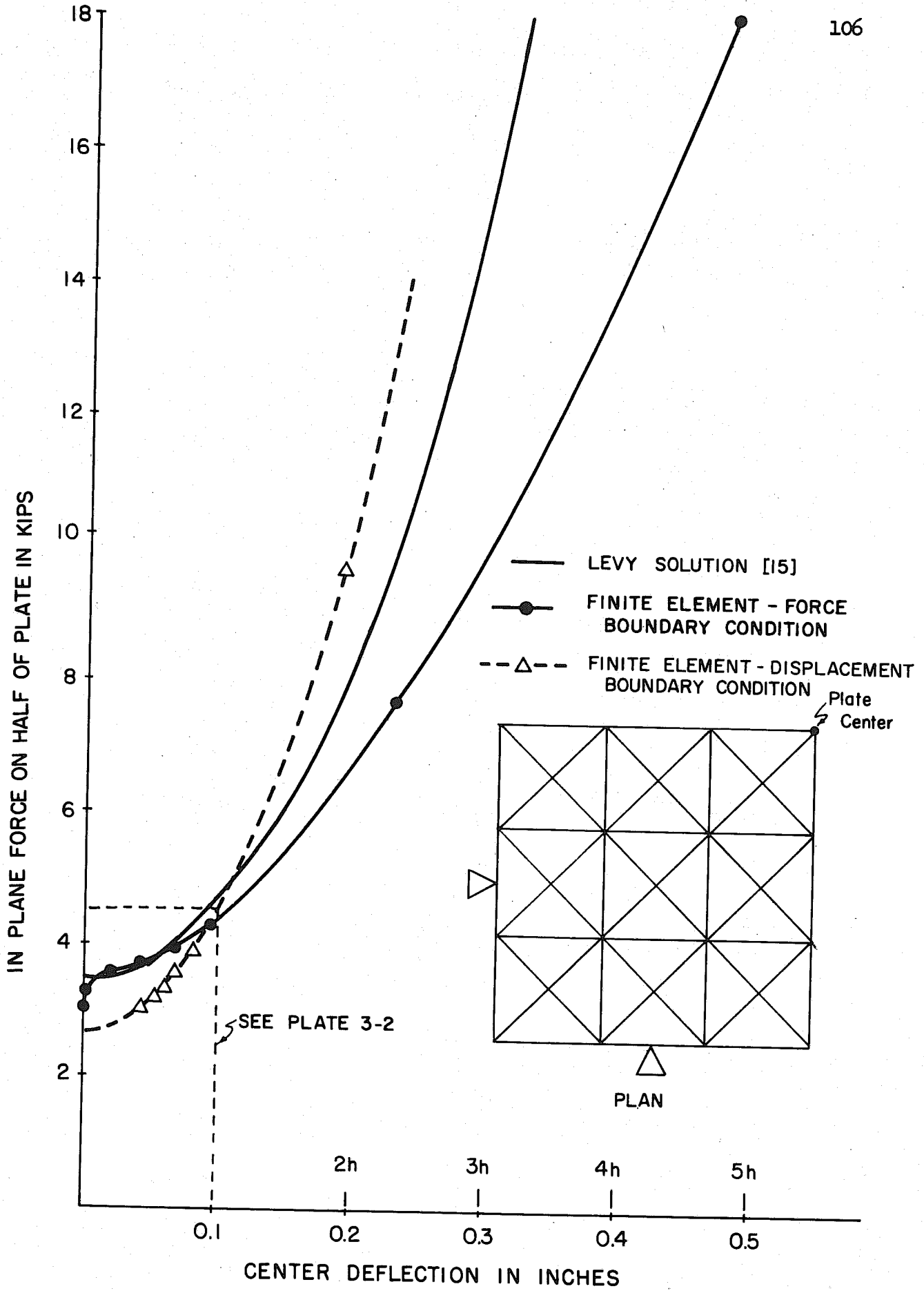


PLATE 3-3 POST BUCKLING LOAD DEFLECTION OF SQUARE PLATE AT HIGH LOADS

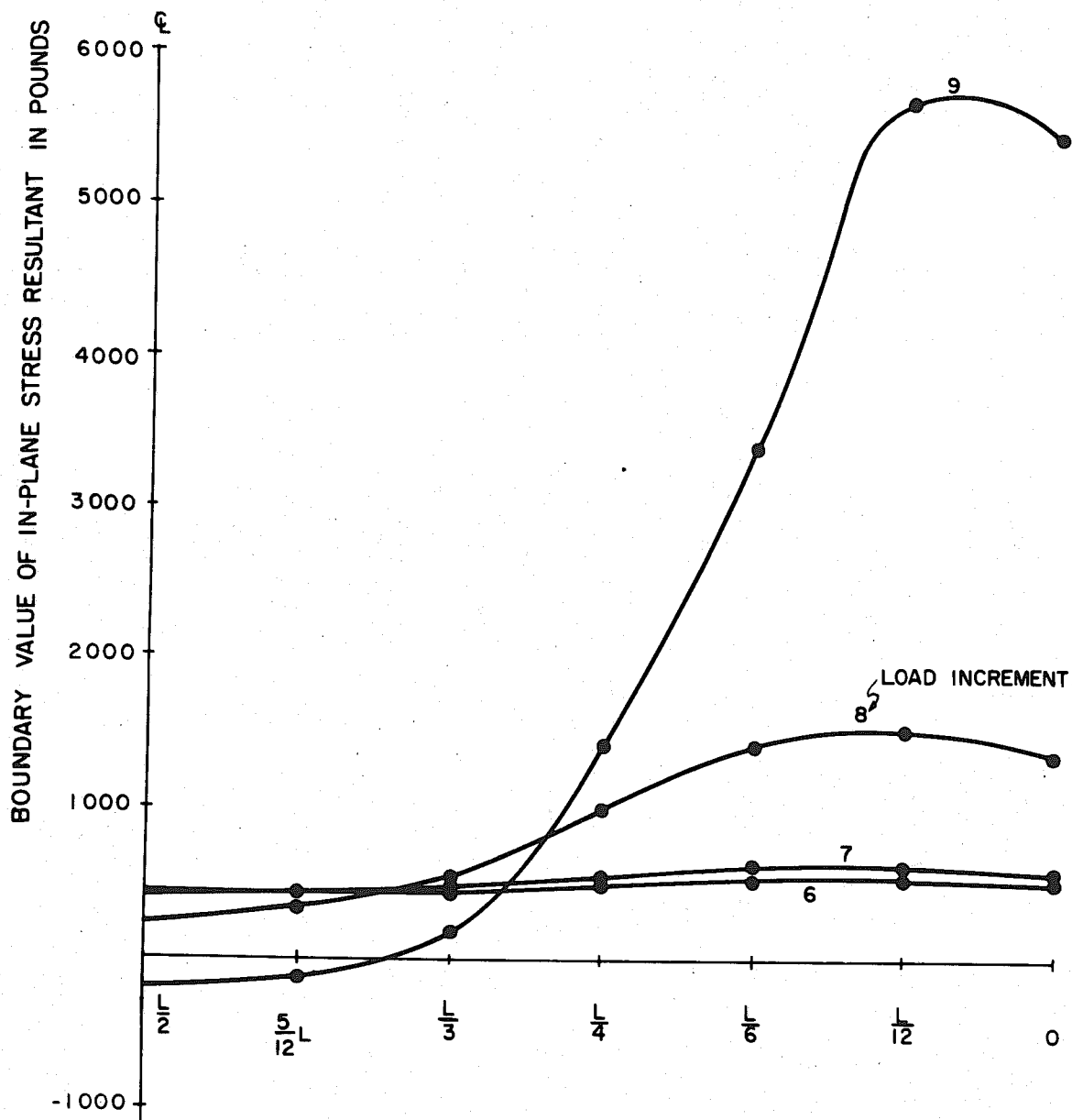


PLATE 3-4 REACTIVE BOUNDARY FORCES FOR BUCKLED SQUARE PLATE

would be developed under Levy's assumption and this results in a stiffer behavior. Levy's solution is therefore effectively bounded. It would be possible to reproduce boundary conditions similar to Levy's, in the finite element solution, but this would be very time consuming from a computational standpoint.

The results of this problem also illustrate two points that are worth repeating:

- (i) the large post-buckling capacity of plates with relatively little out-of-plane deflection. (Compare Plate 3-3 with Plate 3-1.)
- (ii) the effect of boundary conditions cannot always be anticipated prior to a solution, and this effect may be large.

Plate 3-4 shows the distribution of the in-plane stress resultant normal to the edge of the plate on which displacements were incremented, for various loading conditions for the case zero lateral in-plane force. Notice that the center strip of the plate develops tensile membrane forces, even in this direction, under large displacements.

3.4.3 Post-Buckling of a Simulated Flange Plate

In order to illustrate the versatility of the method a section of plate simulating the approximate conditions of a flange of a wide flange beam was examined for post buckling behavior. The plate had a length of 14 inches, a width of 4 inches and a thickness of $1/4$ inches. It was simply supported along one edge, free on one edge, free on one end and clamped on the opposite end.

The load deflection plot is shown on Plate 3-5 and the configuration of the free edge for various post-buckling conditions is shown on Plate 3-6. Notice that, unlike the simply supported plate, the load-deflection curve begins to drop off for large deflections.

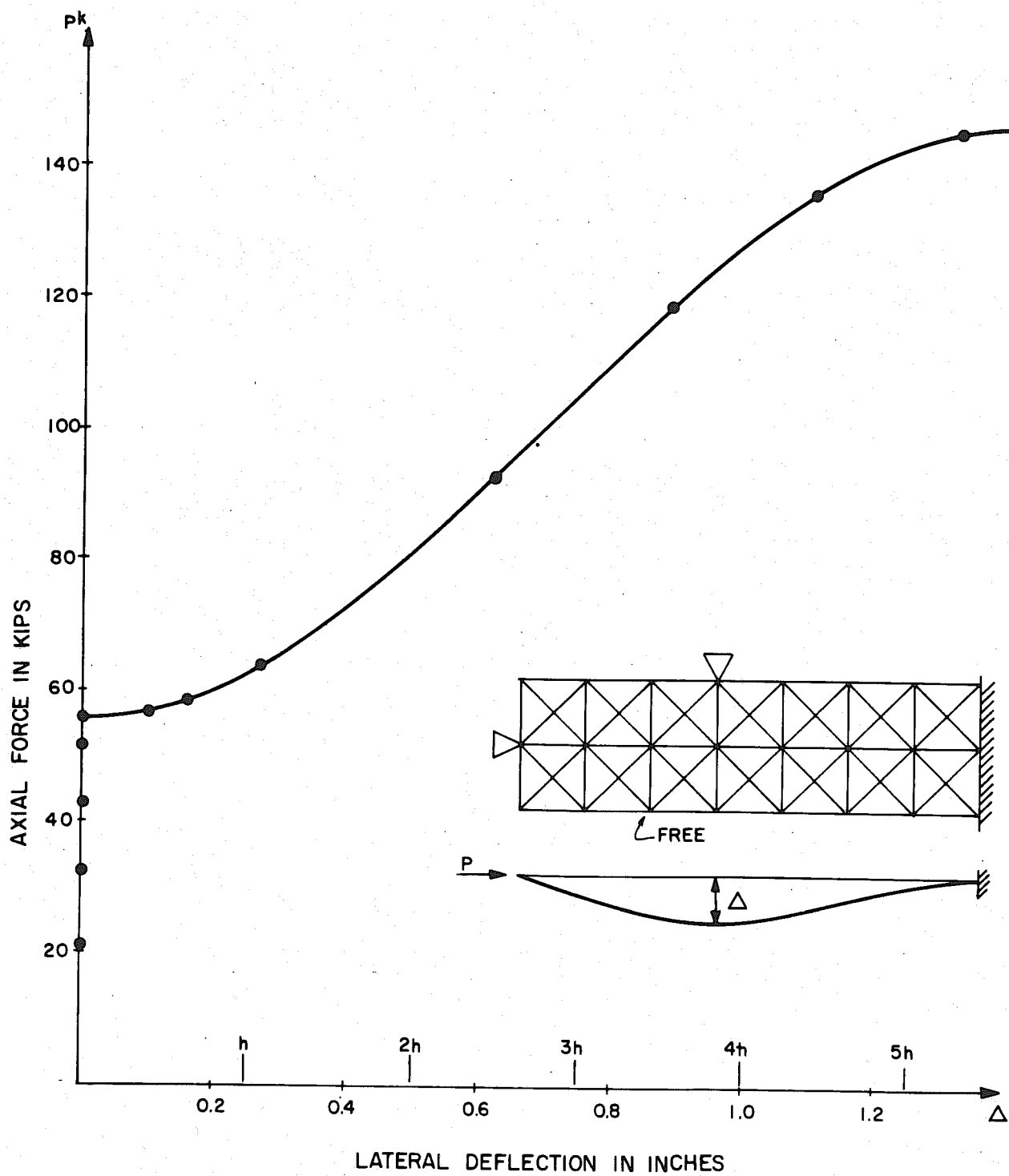


PLATE 3-5 POST-BUCKLING LOAD-DEFLECTION
OF A FLANGE PLATE

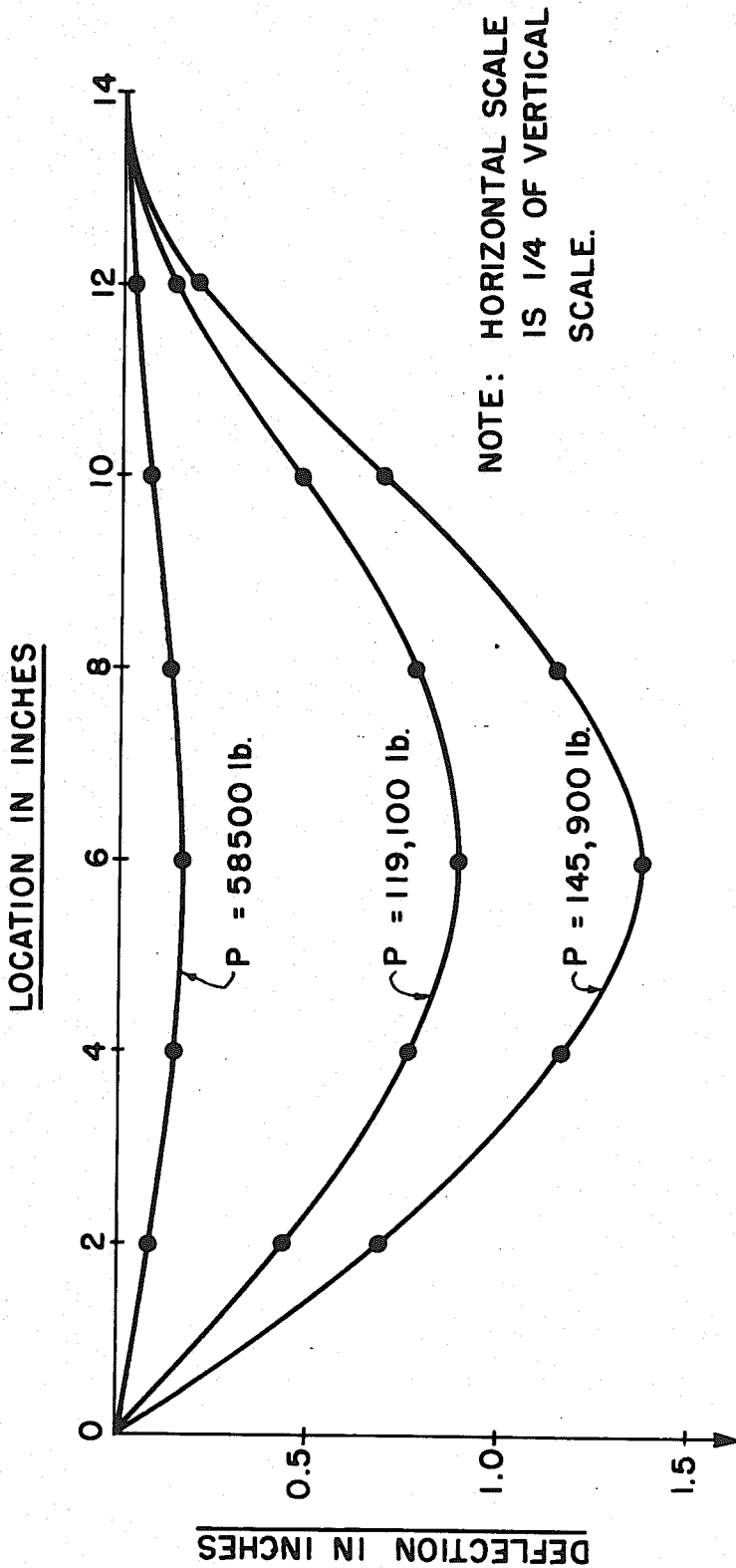


PLATE 3-6 PROFILE OF FREE EDGE OF BUCKLED FLANGE PLATE

Since the writer is unaware of any solutions for this type of problem, even in the small deflection range, it is not possible to obtain a comparison of this solution with one achieved by other techniques.

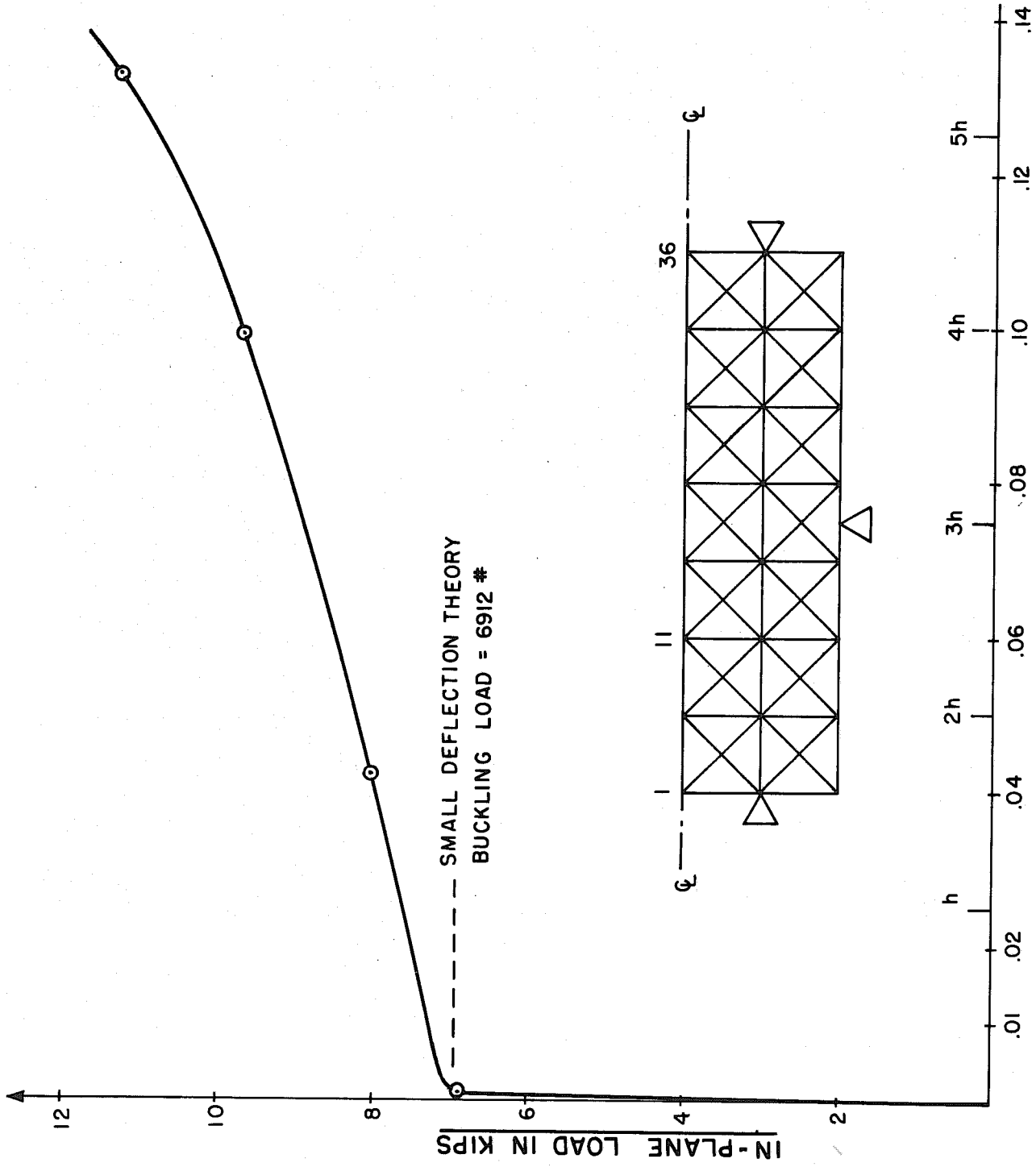
3.4.4 Post-Buckling of a Simply Supported Rectangular Plate With an Aspect Ratio of 1.75

To illustrate that the method is capable of selecting the critical buckling load, when it consists of more than one "half-wave," and simply supported plate 8 inches wide, 14 inches long and one-tenth of an inch in thickness was used. The load-deflection plot is shown in Plate 3-7 and the displacement of the plate along the centerline is shown in Plate 3-8.

As in the other examples, out-of-plane displacement was initiated by applying a small lateral force. In this case a load of one-half a pound was applied at nodal point 11. On Plate 3-8, the solution for the first load increment indicates all displacements in the same direction. For the second load increment, which is just slightly below the classical buckling load (see Plate 3-7), a very small reversal of displacement occurred in the right half of the plate. Subsequent loading produced the symmetric, buckling pattern of two half waves. This pattern agrees with the small deflection buckling pattern and it can be seen from Plate 3-7, that the large deflection finite element solution correlates well with the critical load from the linearized theory.

3.4.5 Discussion

The ability of the finite element method to analyze elastic behavior of plate structures in the post-buckling range has been demonstrated by the examples of this section. The type of problems that can be solved are unrestricted by boundary conditions or plate configuration, and the application of the method in this way therefore represents an extension of



--- SMALL DEFLECTION THEORY
BUCKLING LOAD = 6912 #

LATERAL DEFLECTION IN INCHES

PLATE 3-7 POST-BUCKLING LOAD-DEFLECTION OF SIMPLY SUPPORTED
RECTANGULAR PLATE WITH ASPECT RATIO 1.75

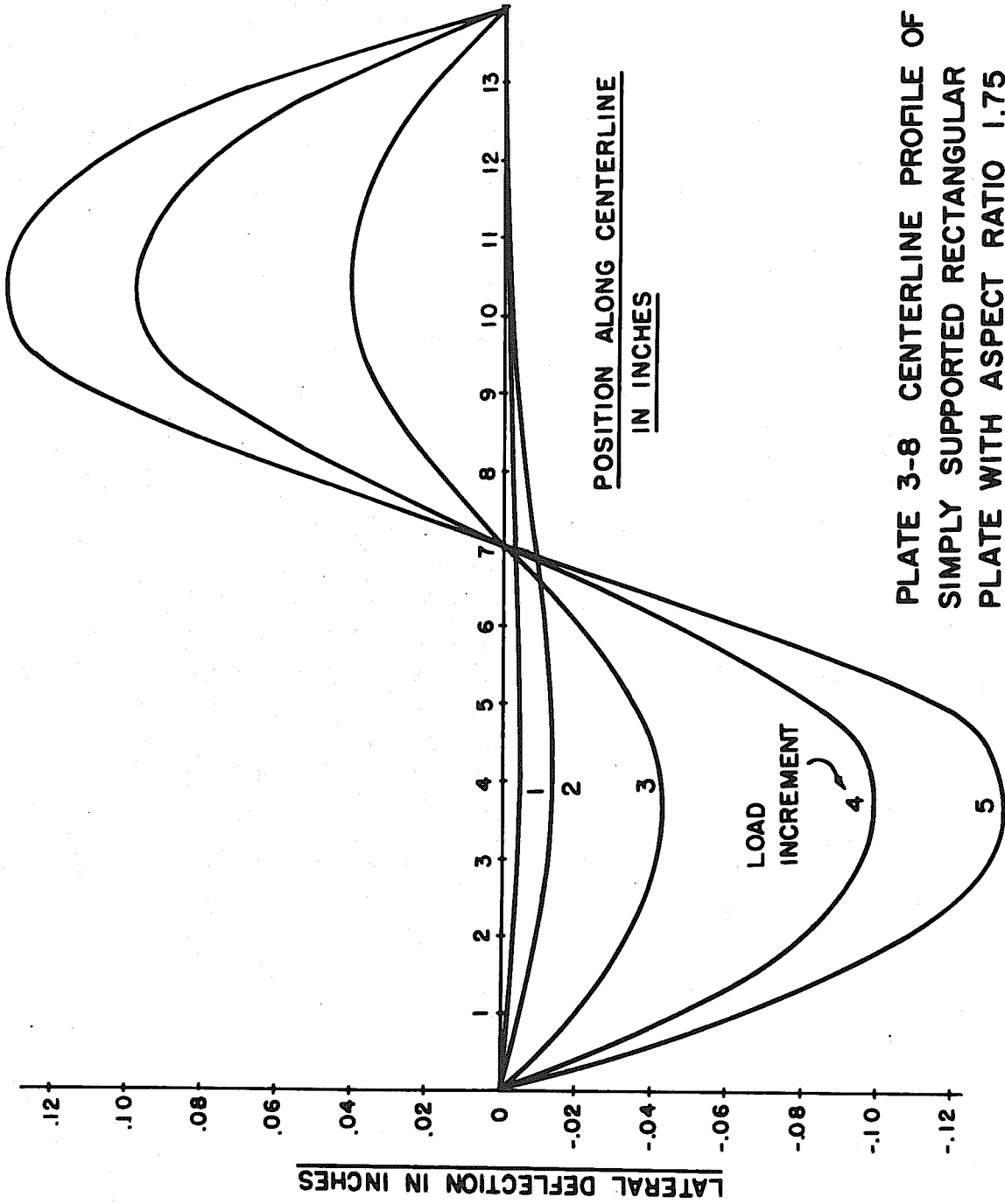


PLATE 3-8 CENTERLINE PROFILE OF
SIMPLY SUPPORTED RECTANGULAR
PLATE WITH ASPECT RATIO 1.75

analysis into an area which has not previously been effectively explored.

The major difficulty encountered in this type of analysis is the computational effort that must be expended. However the technique is capable, in principle, of investigating a large number problems of practical interest. When combined with nonlinear material behavior, such problems as local buckling, the influence of residual stress on buckling, lateral-torsional buckling, and tension field behavior are susceptible to study.

4. VARIABLE MATERIAL PROPERTIES

4.1 Introduction

The incorporation of variable material properties, in large deflection finite element analyses, presents no difficulties in principle. Solutions have been developed for nonlinear material effects for plane stress problems [1, 5], axisymmetric shell problems [24], and small deflection plate problems.[†] However practical difficulties arise in attempting to obtain an efficient solution procedure to realistic plate problems.

Some of the factors which should be considered before developing a solution procedure are:

- (1) Lack of knowledge of real material properties,
- (2) Numerical computations,
- (3) The displacement model.

4.1.a Material Properties

When dealing with materials, certain rules of material behavior are hypothesized, in the form of constitutive relations, and an analysis is developed which is consistent with these rules. A large number of constitutive hypotheses are available. Hypoelastic, hyperelastic, elastic-perfectly plastic, elastic-plastic with various hardening rules, and visco-elastic are only a few of the hypotheses which define idealized materials. In most cases the constants or functional parameters required by the hypothesis are determined experimentally from simple stress states and then are inserted into the more general constitutive relation. However, real materials seldom behave in a manner completely consistent with the

[†] An elastic-plastic solution of the small deflection plate bending problem for work-hardening materials was developed by C. A. Felippa in 1966 but has not been published.

constitutive hypothesis and, in view of the approximations involved in representing material behavior, the question arises as to whether our knowledge in this area justifies an elaborate analytical technique in order to maintain pointwise consistency with the material hypothesis.

4.1.b Numerical Computations

Once the material response becomes nonlinear the derivation of stiffness can seldom be accomplished in closed form and therefore it is usually necessary to resort to numerical integration over the volume of the element. An alternative procedure is to derive interaction relationships by integrating, in closed form, through the thickness, and then integrating numerically over the area to complete the evaluation. In the case of a plate there are six independent strain and stress resultant variables. Interaction relationships of these quantities are complex unless one proceeds to the extreme case of limit analysis.

For a problem such as the plate problem the derivation of element stiffnesses requires a large amount of numerical computation for any analysis with a nonlinear constitutive hypothesis.

4.1.c The Displacement Model

The displacement models used in finite element analysis are based on the assumption that a linear combination of the shape functions can closely approximate the shape of the subregion of the real structure. Since nonlinearity of material properties usually produces high gradients of strain in relatively localized areas, a fine mesh may be required in order to obtain a good representation of behavior. In statically determinate and stress concentration problems this does not usually present a problem since the regions of high gradients can be predicted prior to analysis. However, in complex indeterminate structures the locations of high gradients are not

always evident. Reference to limit analysis of plates illustrates that the regions of high gradient may be distributed throughout the plate and of indeterminate location [25].[†] Since an extremely fine mesh throughout the entire structure may require too great a computational effort, a realistic solution would probably have to be based on a series of solutions which (a) first locate the areas of high gradient and then (b) introduce finer subdivisions in these areas. As the loading is incremented, new areas of high gradient will be introduced as a result of redistribution and changing stress patterns.

4.1.d Discussion

Nonlinear constitutive relations may be incorporated into the basic procedure described in Chapters 2 and 3 with very little modification. However the construction of the stiffness matrix must be modified in such a way that the variation of constitutive parameters throughout the element volume is accounted for and this greatly increases the numerical computations.

The modifications required in the derivation of stiffness are discussed in section 4.2 and a description of a scheme for developing a stiffness matrix for an elastic-plastic hardening material is given in section 4.3. Referring to the discussions of sections 2.1 and 2.12 we note that, although experience has shown that nodal stresses converge in the mean, the particular model used in this investigation cannot be expected to produce point-wise convergence of stress and strain values because the displacement pattern produces discontinuities in both the bending and in-plane strains.

[†] See, for instance, page 266, where the yield line pattern for a simply supported plate is illustrated.

Since the constitutive coefficients are usually functions of the strains, a direct application of the type described in section 4.3 should await the development of an extension of the method to higher order elements in which strain compatibility is maintained.

The procedure of section 4.3 could be applied to the present model by relating the constitutive coefficients to the average strains at the nodal points. However this gives rise to a situation where the constitutive parameters are pointwise inconsistent with the element strains. Nevertheless the approximation would probably give a reasonable representation of overall behavior. However the computational effort involved in such a solution is large since the stiffness of each element for each iterate must be determined by numerical integration through the volume.

Because of the lack of pointwise strain convergence, the lack of knowledge of real material behavior and the magnitude of numerical computations involved, the method of section 4.3 does not appear to be justified for the displacement model developed in this work. An approximate method is therefore developed in section 4.4. This method assumes that the material properties for the entire element may be related to the strains at the centroid of the element. The technique results in a great reduction of computational effort in determining element stiffness but, in order to represent a reasonable approximation of the plate behavior, requires a fine mesh in areas of nonlinear behavior.

4.2 Stiffness Formulation for Variable Material Properties

4.2.1. The Element Stiffness

If, in the derivation of the expression for element stiffness, it is not assumed that the constitutive coefficients are constant throughout the element thickness, all terms of equations (2-23) are nonvanishing. From

section 2.4 we have

$$\begin{aligned} \{r_E^*\}^T \{R_E\} &= \int_V \{\tilde{\epsilon}_0^*\}^T [\tilde{C}] \{\tilde{\epsilon}_0\} dV - \int_V z \{\tilde{\epsilon}_0^*\}^T [\tilde{C}] \{\tilde{\epsilon}\} dV \\ &\quad - \int_V z \{\tilde{\epsilon}^*\}^T [\tilde{C}] \{\tilde{\epsilon}_0\} dV + \int_V z^2 \{\tilde{\epsilon}^*\}^T [\tilde{C}] \{\tilde{\epsilon}\} dV \end{aligned} \quad (2-23)$$

Integrating over the element volume yields

$$\begin{aligned} \{r_E^*\}^T \{R_E\} &= \{r_P^*\}^T [K_P] \{r_B\} - \{r_P^*\}^T [K_{PB}] \{r_B\} \\ &\quad - \{r_B^*\}^T [K_{BP}] \{r_P\} + \{r_B^*\}^T [K_B] \{r_B\} \end{aligned} \quad (4-1)$$

or

$$\{r_E^*\}^T \{R_E\} = \begin{Bmatrix} \{r_P^*\} \\ \{r_B^*\} \end{Bmatrix}^T \begin{bmatrix} K_P & -K_{PB} \\ -K_{BP} & K_B \end{bmatrix} \begin{Bmatrix} \{r_P\} \\ \{r_B\} \end{Bmatrix} \quad (4-1)$$

where

$$\begin{aligned} [K_P] &= \int_V [\tilde{B}_P]^T [\tilde{C}] [\tilde{B}_P] dV, \\ [K_{PB}] &= \int_V [\tilde{B}_P]^T [\tilde{C}] [\tilde{B}_B] dV, \\ [K_{BP}] &= \int_V [\tilde{B}_B]^T [\tilde{C}] [\tilde{B}_P] dV, \end{aligned} \quad (4-2)$$

and

$$[K_B] = \int_V [\tilde{B}_B]^T [\tilde{C}] [\tilde{B}_B] dV.$$

The matrices $[\tilde{B}_P]$ and $[\tilde{B}_B]$ have been defined in section 2.4.

Since the virtual displacements are arbitrary, equation (4-1) may be written as

$$\{R_E\} = [K] \{r_E\} \quad (4-3)$$

where $[K]$ is the element stiffness, as defined by equations (4-1) and (4-2), for any variation of the constitutive matrix throughout the element.

If $[\tilde{C}]$ is a function of the spatial coordinates only, and not of the strains, the evaluation of the stiffness submatrices need only be performed once in solving a particular problem. For a constant $[\tilde{C}]$ the coupling terms vanish, as in section 2.4, and no numerical integration is required. If $[\tilde{C}]$ is a function of z only, as in the case of laminated plates (see, for example Dong, Pister, Taylor [26]), numerical integration is required in only one direction. If $[\tilde{C}]$ is a function of all three spatial co-ordinates, a three dimensional numerical integration is required.

For nonlinear materials the constitutive matrix is usually a function of the strains or strain-history. In this case a numerical integration is required for every load increment if a proper tangent stiffness is to be evaluated.

4.2.2 Incremental Stiffness, Geometric Stiffness and Stress Determination

An examination of the expression for geometric stiffness indicates that it is dependent only on the "initial" stress state and the geometry of deformation and is therefore independent of the constitutive relation (see Felippa [1]). Equation (3-13) therefore remains valid for the geometric stiffness and can be used directly in the solution of problems involving nonlinear material behavior. The combination of the geometric stiffness matrix with the element "tangent stiffness" matrix of section 4.2.1 yields the "incremental" stiffness matrix.

Stress determination is more complex than for a linear material. If the stresses are single valued functions of the element strains (nonlinear elastic or deformation theory of plasticity) the element forces may be determined for a particular deformed configuration by utilizing secant

constitutive values in equations (4-2), and evaluating a "secant stiffness" matrix. If the stress is a function of the strain history (incremental plasticity), the stress must be determined by adding the stress increments to the previous stress state.

4.3 A General Solution Technique Including Nonlinear Material Effects

We illustrate a general solution technique for nonlinear material problems by discussing the case of an elastic-plastic hardening material. Relationships for this constitutive hypothesis have been put in a form suitable for finite element application by Khojasteh [24]. Although this reference deals with a problem for which the principal directions of stress and strain remain constant, and for which numerical integration is two dimensional rather than three dimensional, the basic equations can be extended without difficulty to the plate problem.

Khojasteh's technique consists of establishing an incremental stress-strain relationship of the form

$$\begin{Bmatrix} \Delta \sigma_x \\ \Delta \sigma_y \\ \Delta \sigma_{xy} \end{Bmatrix} = [P] \begin{Bmatrix} \Delta \epsilon_x \\ \Delta \epsilon_y \\ \Delta \gamma_{xy} \end{Bmatrix} \quad (4-4)$$

where $[P]$ is determined on the basis of:

- (a) a flow rule which maintains normality of the plastic strain increment to a subsequent yield surface defined by a loading function,
- (b) a hardening rule which specifies the loading function in terms of the previous plastic strains, and
- (c) the elastic stress-strain relationship,

$$\begin{Bmatrix} \Delta \sigma_x \\ \Delta \sigma_y \\ \Delta \sigma_{xy} \end{Bmatrix} = [C] \begin{Bmatrix} \Delta \epsilon_x^E \\ \Delta \epsilon_y^E \\ \Delta \gamma_{xy}^E \end{Bmatrix} \quad (4-5)$$

In addition, the plastic strains can be determined from the total strains by a relation of the form

$$\begin{Bmatrix} \Delta \varepsilon_x^P \\ \Delta \varepsilon_y^P \\ \Delta \gamma_{xy}^P \end{Bmatrix} = [A] \begin{Bmatrix} \Delta \varepsilon_x \\ \Delta \varepsilon_y \\ \Delta \gamma_{xy} \end{Bmatrix} \quad (4-6)$$

Various solution procedures can be followed but the procedure outlined below is based on the concepts of section 2.2 in which a plate configuration is sought which satisfies the constitutive relationships (4-4) and (4-6) and is in equilibrium with the applied load.

Assume an equilibrium position Γ_t^* is known and the following information associated with this position is also known:

- (a) the nodal locations, x_t^* , y_t^* , z_t^* , θ_{xt}^* , θ_{yt}^*
- (b) for each element,
 - (i) the tangent stiffness, $[K_{Tt}^*]$
 - (ii) the incremental stiffness, $[K_{\Delta t}^*] = [K_{Tt}^*] + [K_{Gt}^*]$
 - (iii) the local element deformations, $\{U_t^*\}$.
- (c) point values of the following quantities, at a sequence of points through the thickness at each node in each element,
 - (i) the effective strain $\bar{\varepsilon}_t^{P*}$
 - (ii) the effective stress $\bar{\sigma}_t^*$
 - (iii) the stress vector $\{\sigma_t^*\}$
 - (iv) the matrix of equation (4-6), $[A^*]$.

The procedure of Table 4.1 may then be regarded as an algorithm for determining the next equilibrium position Γ_{t+1}^* and the quantities associated with it. The algorithm is essentially that of section 2.2, generalized for this material.

TABLE 4.1. General Procedure for Solving
Elastic-Plastic Hardening Problem

- A. Assumed Known for Equilibrium Position Γ_t^* :
- (a) The nodal locations x_t^* , y_t^* , z_t^* , θ_{xt}^* , θ_{yt}^*
 - (b) The element quantities K_{Tt}^* , $K_{\Delta t}^* = K_{Tt}^* + K_{Gt}^*$, U_t^*
 - (c) At a sequence of points through the thickness, at each node each element, the quantities $\bar{\epsilon}_t^*$, $\bar{\sigma}_t^*$, $\{\sigma_t^*\}$, $[A_t^*]_t$
- (See section 4.3 for definitions of these quantities.)
- B. Apply a load increment, ΔR_t
1. Assume an approximate configuration Γ_s .
 2. Compute element deformations, U_s .
 3. Compute increments in element deformations from position Γ_t^*

$$\Delta U_s = U_s - U_t$$
 4. Compute unbalanced loads, $R_{Us} = \Delta R_t - K_{Tt}^*(\Delta U_s)$
 5. Assemble stiffness for current geometry

$$K_s = \Sigma(K_{\Delta t}^*)_{\Gamma_s}$$
 6. Solve for increments in nodal displacements, Δr_s , and compute new nodal locations $\Gamma_{s+1} = \Gamma_s + \Delta r_s$.
 7. Repeat steps 1 to 6 until an equilibrium position, is determined.
- C. The new equilibrium position Γ_{t+1}^* has been determined but it is necessary to determine the quantities in A, and the stresses, before the next load increment. The procedures is as follows.
1. Using nodal locations x_{t+1}^* , y_{t+1}^* , z_{t+1}^* , θ_{xt+1}^* , θ_{yt+1}^* compute element deformations U_{t+1} .
 2. For each point through the thickness and at each node in each element compute:

TABLE 4.1. Continued

$$(a) \{\Delta \varepsilon_t^P\} = [A^*]_t \{\Delta \varepsilon\}$$

$$(b) \{\Delta \sigma_t\} = [C] \{\Delta \varepsilon - \Delta \varepsilon_t^P\}$$

$$(c) \{\sigma_{t+1}^*\} = \{\sigma_t^*\} + \{\Delta \sigma_t\}$$

$$(d) \bar{\sigma}_{t+1}^* = \bar{\sigma}_t^* + \Delta \bar{\sigma}_t, \quad \bar{\varepsilon}_t^{P*} = \bar{\varepsilon}_t^{P*} + \Delta \bar{\varepsilon}_t^P$$

(e) Using the quantities above determine $[P^*]_{t+1}$ of equation (4-4), and $[A^*]_{t+1}$.

3. Integrate equations (4-2), numerically, using the constitutive matrix $[P^*]_{t+1}$ to determine $[K_T^*]_{t+1}$ for each element.
4. Determine $[K_G^*]_{t+1}$ and add to $[K_T^*]_{t+1}$ to determine $[K_\Delta^*]_{t+1}$ for each element.

D. Apply the loading increment ΔR_{t+1} and return to B.1.

4.4 An Approximate Method of Including Nonlinear Material Effect

In view of the numerical complexity of the analysis described in section 4.3 and the discussion of section 4.1, the general approach was not considered justified for the present model. The following is an approximate analysis which assumes material properties may be defined for the entire element in terms of the strains at the centroid of the area of the element. The method is formulated for a particular nonlinear elastic material hypothesis which is described in section 4.4.a.

4.4.a A Nonlinear Elastic Constitutive Relationship

While many references deal with a general formulation for nonlinear elastic materials, very few state a specific relationship. We adopt here a form suggested by Wilson [27].

Since the initiation of yielding of metals has been shown to be essentially independent of the dilatation, the yield surface for plasticity theory is generally related to the strain invariant,

$$\begin{aligned}\pi_{\epsilon} &= (\epsilon_1 - \epsilon_2)^2 + (\epsilon_2 - \epsilon_3)^2 + (\epsilon_3 - \epsilon_1)^2 \\ &= (\epsilon_x - \epsilon_y)^2 + (\epsilon_y - \epsilon_z)^2 + (\epsilon_z - \epsilon_x)^2 + \frac{3}{2} (\gamma_{xy}^2 + \gamma_{yz}^2 + \gamma_{zx}^2).\end{aligned}\tag{4-7}$$

For an elastic-plastic hardening material, an effective plastic strain, $\bar{\epsilon}^P$, is defined as

$$\bar{\epsilon}^P = \frac{\sqrt{2}}{3} \sqrt{\pi_{\epsilon}^P}\tag{4-8}$$

which is arrived at by equating the invariant π_{ϵ}^P for a general strain condition with that for a uniaxial tension test. A similar definition holds for effective stress, with the factor $\frac{\sqrt{2}}{3}$ replaced by $\frac{1}{\sqrt{2}}$.

It seems reasonable to use the same approach for nonlinear elasticity and hypothesize that the modulus of elasticity relates effective stress to effective strain. Proceeding in the same way as in the preceding paragraph we define the effective strain for elastic materials as

$$\bar{\epsilon} = \frac{1}{\sqrt{2}(1+\nu)} \sqrt{\pi_{\epsilon}} \quad (4-9)$$

The effective stress is

$$\bar{\sigma} = \frac{1}{\sqrt{2}} \sqrt{\pi_{\sigma}} \quad (4-10)$$

which is identical to that used in plasticity.

We assume the general constitutive relations may then be expressed as

$$\{\sigma\} = \frac{E_s}{E} [\underline{C}] \{\epsilon\}$$

and

$$\{\Delta\sigma\} = \frac{E_T}{E} [\underline{C}] \{\Delta\epsilon\} \quad (4-11)$$

where the tangent modulus, E_T , and the secant modulus, E_s , are obtained from a uniaxial stress-strain plot and $[\underline{C}]$ is the constitutive matrix for the corresponding problem in linear elasticity.

Specializing equations (4-9) and (4-10) for plane stress, we obtain

$$\bar{\epsilon} = \frac{1}{1-\nu^2} \sqrt{(1-\nu+\nu^2)(\epsilon_x^2 + \epsilon_y^2) - (1-4\nu+\nu^2)\epsilon_x\epsilon_y + \frac{3}{4}(1-\nu^2)\delta_{xy}^2} \quad (4-12)$$

and

$$\bar{\sigma} = \sqrt{\sigma_x^2 - \sigma_x\sigma_y + \sigma_y^2 + 3\sigma_{xy}^2} \quad (4-13)$$

Equation (4-12) may be used to determine $\bar{\epsilon}$ for any strain condition. E_T and E_S are then determined from the uniaxial tension test and equations (4-11) may then be utilized upon identifying $[C]$ with the constitutive matrix of linear elasticity for plane stress. Except for the fact that Poisson's ratio is not $1/2$, the above procedure is analagous to a deformation theory of plasticity.

4.4.b Derivation of Element Stiffness Matrix

The stiffness of the element is obtained by performing the integration in equations (4-2). However it is assumed that the material properties are defined by the strains at the centroid of the area of the element and therefore are only functions of the spatial coordinate z . Under these circumstances the element stiffness can be determined directly from the stiffnesses $[K_P]$ and $[K_B]$ of a linear elastic material. The procedure, suggested by Wilson,[†] is as follows.

Equation (2-23), in its original form, states

$$\{r_E^*\}^T \{R_E\} = \int_V \{ \tilde{\epsilon}_0^* \} - z \{ \tilde{\chi}^* \} \}^T [C] \{ \tilde{\epsilon}_0 \} - z \{ \tilde{\chi} \} \} dV. \quad (2-23)$$

Since the integration can be referred to any arbitrary plane we may define the variable η , measured from the plane $z = c$, as

$$\eta = z - c \quad (4-14)$$

or

$$z = \eta + c.$$

Expressing the variable z in equation (2-23) in terms of the variable η yields.

[†] Professor E. L. Wilson, University of California, Berkeley, California.

$$\begin{aligned}
\{r_E^*\}^T \{R_E\} &= \int_V \{ \{\tilde{\epsilon}_0^*\} - c \{\tilde{\mathcal{X}}^*\} \}^T [\tilde{C}] \{ \{\tilde{\epsilon}_0\} - c \{\tilde{\mathcal{X}}\} \} dV \\
&\quad + \int_V \eta^2 \{\tilde{\mathcal{X}}^*\}^T [\tilde{C}] \{\tilde{\mathcal{X}}\} dV \\
&\quad - \int_V \eta \{\tilde{\mathcal{X}}^*\}^T [\tilde{C}] \{ \{\tilde{\epsilon}_0\} - c \{\tilde{\mathcal{X}}\} \} dV - \int_V \eta \{ \{\tilde{\epsilon}_0^*\} - c \{\tilde{\mathcal{X}}^*\} \}^T [\tilde{C}] \{\tilde{\mathcal{X}}\} dV.
\end{aligned} \tag{4-15}$$

Now $[C]$ is a function of η only and has the form given in equation (4-11) where $E_S(\eta)$ or $E_T(\eta)$ is the only variable. If c is defined such that*

$$c = \frac{\int_h \eta E(z) dz}{\int_h E(z) dz},$$

then

$$\int_h \eta E(z) dz = 0$$

and

$$\int_h \eta \frac{E(\eta)}{E} [C] d\eta$$

is therefore a zero matrix. Consequently the last two terms of equation (4-15) vanish. In addition the vector $\{ \{\tilde{\epsilon}_0\} - c \{\tilde{\mathcal{X}}\} \}$ represents the strains on the surface $z = c$ and therefore may be written as $\{\tilde{\epsilon}_c\}$. Equation (4-15) therefore becomes

$$\{r_E^*\}^T \{R_E\} = \int_V \{ \{\tilde{\epsilon}_c^*\} \}^T [\tilde{C}] \{ \{\tilde{\epsilon}_c\} \} dV + \int_V \eta^2 \{\tilde{\mathcal{X}}^*\}^T [\tilde{C}] \{\tilde{\mathcal{X}}\} dV. \tag{4-16}$$

Using equations (2-19) and (2-20)[†] to express $\{\tilde{\epsilon}_c\}$ and $\{\tilde{\mathcal{X}}\}$,

* When $E(\eta)$ or $E(z)$ is not subscripted it is to be understood that it can be either E_T or E_S depending on the particular application.

[†] It is assumed here that the in-plane interpolation functions apply on the surface $z = c$ and not on the surface $z = 0$.

$$\{\tilde{\epsilon}_c\} = [\tilde{B}_p] \{r_{p_c}\}$$

and

$$\{\tilde{x}\} = [\tilde{B}_B] \{r_B\},$$

and integrating, equation (4-16) becomes

$$\{r_E^*\}^T \{R_E\} = \begin{Bmatrix} \{r_{p_c}^*\} \\ \{r_B^*\} \end{Bmatrix}^T \begin{bmatrix} \underline{K}_P & \cdot \\ \cdot & \underline{K}_B \end{bmatrix} \begin{Bmatrix} \{r_{p_c}\} \\ \{r_B\} \end{Bmatrix} \quad (4-17)$$

where

$$[\underline{K}_P] = \int_V [\tilde{B}_p]^T [\tilde{C}] [\tilde{B}_p] dV \quad (4-18)$$

and

$$[\underline{K}_B] = \int_V [\tilde{B}_B]^T [\tilde{C}] [\tilde{B}_B] dV. \quad (4-18)$$

The matrices $[\underline{K}_P]$ and $[\underline{K}_B]$ can be evaluated by integrating through the thickness and are then directly related to the matrices $[K_P]$ and $[K_B]$ of linear elasticity by the equations

$$[\underline{K}_P] = \frac{\int E(z) dz}{E h} [K_P]$$

and

$$[\underline{K}_B] = \frac{12 \int \eta^2 E(\eta) d\eta}{E h^3} [K_B]. \quad (4-19)$$

The stiffness matrix in equation (4-17) has become uncoupled because the reference plane $z = c$ is the "neutral plane" or "center of stiffness" for the particular variation of $E(z)$. On this surface, in-plane displacements produce no bending and bending produces no in-plane displacements.

In order to utilize this stiffness matrix it is now necessary to relate the vector of displacements $\{r_{pc}\}$ on the right hand side of equation (4-17) to the nodal displacements $\{r_p\}$ on the middle surface. This relationship is

$$\{r_{pc}\} = \{r_p\} - c \begin{Bmatrix} \{\theta_y\} \\ \{-\theta_x\} \end{Bmatrix} = \{r_p\} - c\{\theta\} \quad (4-20)$$

in which the vector $\{\theta\}$ is composed of nodal rotations contained in the vector $\{r_B\}$. Substituting (4-20) into (4-17) yields

$$\{r_E^*\}^T \{R_E\} = \{r_E^*\}^T \begin{bmatrix} \underline{K}_P & -c \underline{K}_{P\theta} \\ -c \underline{K}_{\theta P} & \underline{K}_B + c^2 \underline{K}_{\theta\theta} \end{bmatrix} \begin{Bmatrix} \{r_p\} \\ \{r_B\} \end{Bmatrix} \quad (4-21)$$

where $[\underline{K}_P]$ and $[\underline{K}_B]$ have been defined in equations (4-19), and $[\underline{K}_P]$, $[\underline{K}_{\theta P}]$, $[\underline{K}_{\theta\theta}]$ are all identical to $[\underline{K}_P]$ but with rows or columns of zeros inserted, and with the appropriate sign changes from equation (4-20), so that the elements of $\{\theta\}$ are identified with the corresponding elements of $\{r_B\}$.

The matrix in equation (4-21) can now be identified with the matrix of equation (4-11) or (4-3) and represents the stiffness matrix of the element for the assumptions made in this section.

4.5 Solution Procedure

The solution procedure used for structures with nonlinear elastic properties is identical with that used for structures with linear elastic properties, described in section 2.2, with the exception that the secant stiffness is used to compute the element resisting forces while the tangent stiffness is used to evaluate the assembled stiffness matrices.

Since the assembled stiffness matrix need only be approximate, tangent stiffnesses are evaluated on the basis of the previous equilibrium position. However the unbalanced forces should be evaluated as accurately as possible since they are the basis of the convergence criterion. The element secant stiffnesses are therefore modified every iterate. The solution scheme is illustrated schematically in Fig. 4.1.

4.6 Application

The approximate formulation of section 4.4 was applied, using the procedure outlined in section 2.5 and the bilinear elastic material properties illustrated in Fig. 4.2, to some simple problems for which curvature occurs in only one direction. A list of plates on which the results are presented is given in Table 4.1. We shall refer to the material response for strains exceeding an effective strain of 0.00135 as "soft," as illustrated in Fig. 4.2. Point A will be referred to as the "softening point."

4.6.1 Moment Curvature

The moment curvature diagram for a plate $\frac{1}{2}$ inch thick is shown in Plate 4.1 to a curvature of 16 times the softening curvature. Strains in the y direction were prevented. By combining in-plane and out-of-plane forces, numerical interaction curves could be determined (see section 4.1.6).

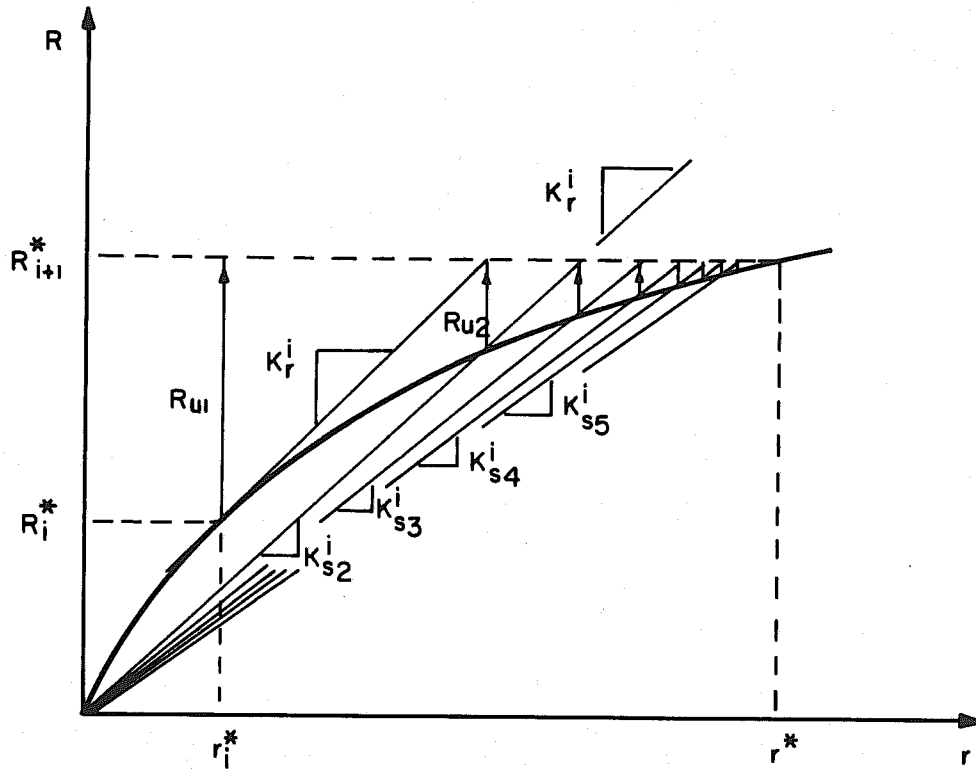


FIG. 4.1 SOLUTION PROCEDURE FOR NONLINEAR MATERIAL PROPERTIES

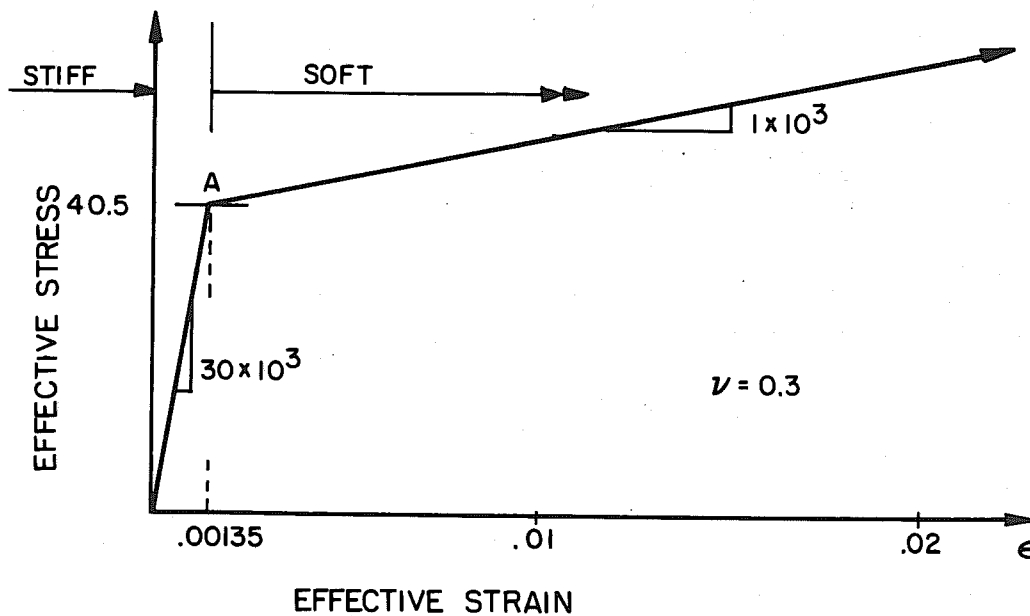


FIG. 4.2 ASSUMED MATERIAL PROPERTIES

TABLE 4.1. LIST OF PLATES FOR CHAPTER 4

SUBJECT	PLATE NO.	TITLE
Moment curvature	4-1	Moment curvature for $\frac{1}{2}$ " plate
Cylindrical bending of an infinite strip of $\frac{1}{2}$ " plate with 14" span	4-2	Force-deflection for cylindrical bending of $\frac{1}{2}$ inch plate strip
	4-3	Stresses and profiles for cylindrical bending of $\frac{1}{2}$ inch plate strip
Cylindrical bending of an infinite strip of 0.1" plate with 14" span	4-4	Force-deflection for cylindrical bending of 0.1 inch plate strip
	4-5	Stresses and profiles for cylindrical bending of 0.1 inch plate strip

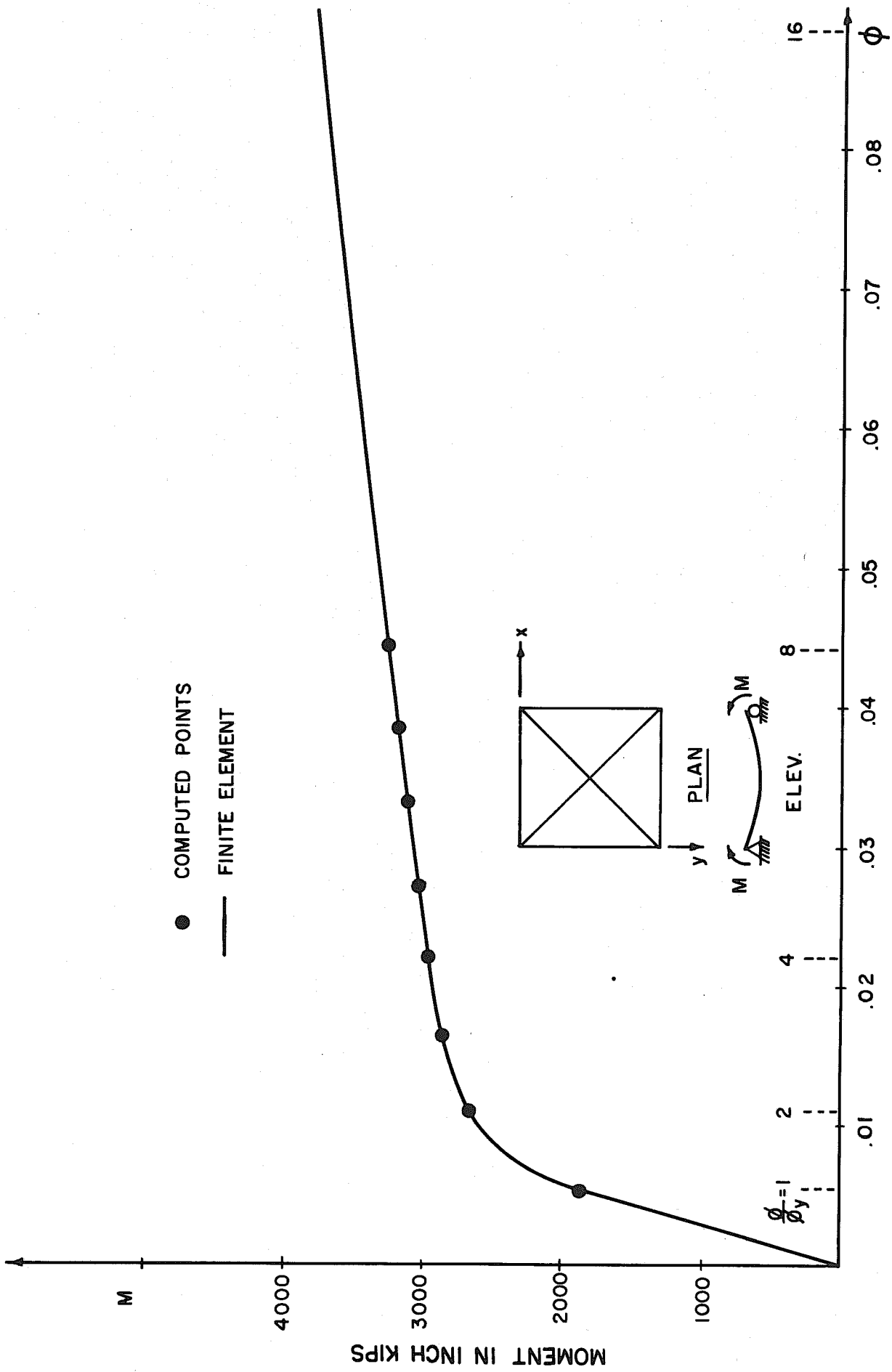


PLATE 4-1 MOMENT CURVATURE FOR $\frac{1}{2}$ " PLATE

4.6.2 Cylindrical Bending of $\frac{1}{2}$ inch Plate

Force-deflection relations for a 14" wide infinite strip of plate, $\frac{1}{2}$ inch thick, are plotted in Plate 4.2. The loading corresponds to a line load along the center of the plate strip. The center moment increases linearly for the first load increments and then drops off at higher loads when the membrane effect becomes dominant. The softening of the material produces only a slight irregularity in the load deflection curve.

Distribution of stresses over the depth of the plate and regions of softened material are shown in Plate 4.3. The profiles indicate the concentration of curvature in the center of the span at high loads.

4.6.3 Cylindrical Bending of 0.1 inch Plate

The same problem as discussed in section 4.6.2 was repeated with a plate thickness of 0.1 inch. In this case the entire plate except for the small shaded area at the top, shown in Plate 4.5, had softened at a deflection of 0.5 inch. For a deflection of 0.3 inch only the shaded area at the bottom of the plate had softened. The membrane effect here is completely dominant and the profile for load increment 7 indicates that the plate is acting essentially as a mechanism with moment resistance having only a minor effect. Since the moments are relatively small and complete convergence was not achieved for the two highest load conditions the last two points on the moment curve in the force-deflection plots on Plate 4.4 are sensitive and only their relative magnitude is significant.

4.7 Discussion of Analysis for Nonlinear Materials

The analysis of problems involving nonlinear material properties by the method presented in the previous sections is time consuming in spite

of simplifying assumptions. This is not primarily due to the increase in number of numerical computations but is a result of slower convergence of the unbalanced forces which necessitates a greater number of iterates.

For linear materials the unbalanced forces can continue to be reduced to arbitrarily small quantities. However for nonlinear material there seems to be a point beyond which it is difficult to achieve further reduction.

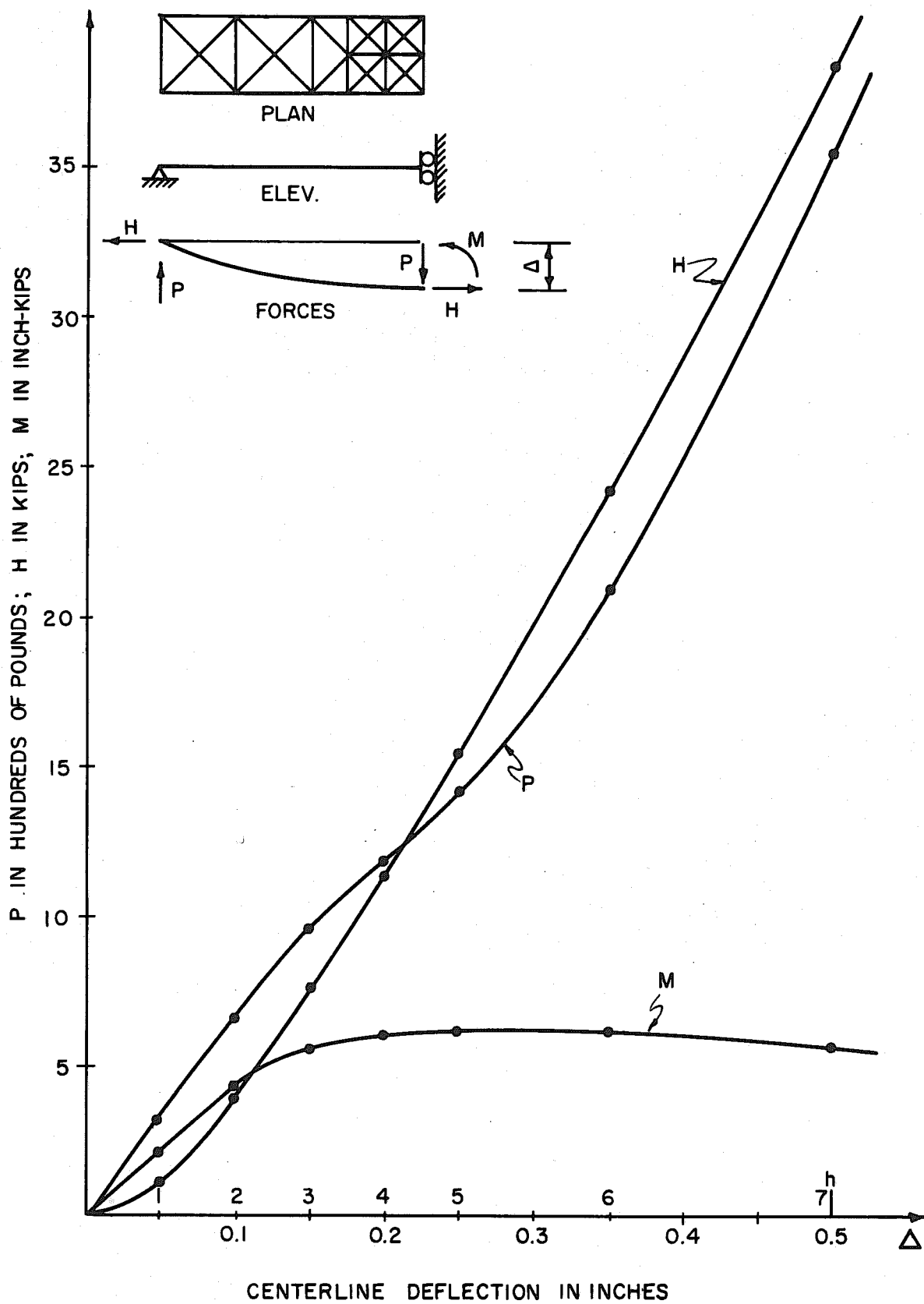
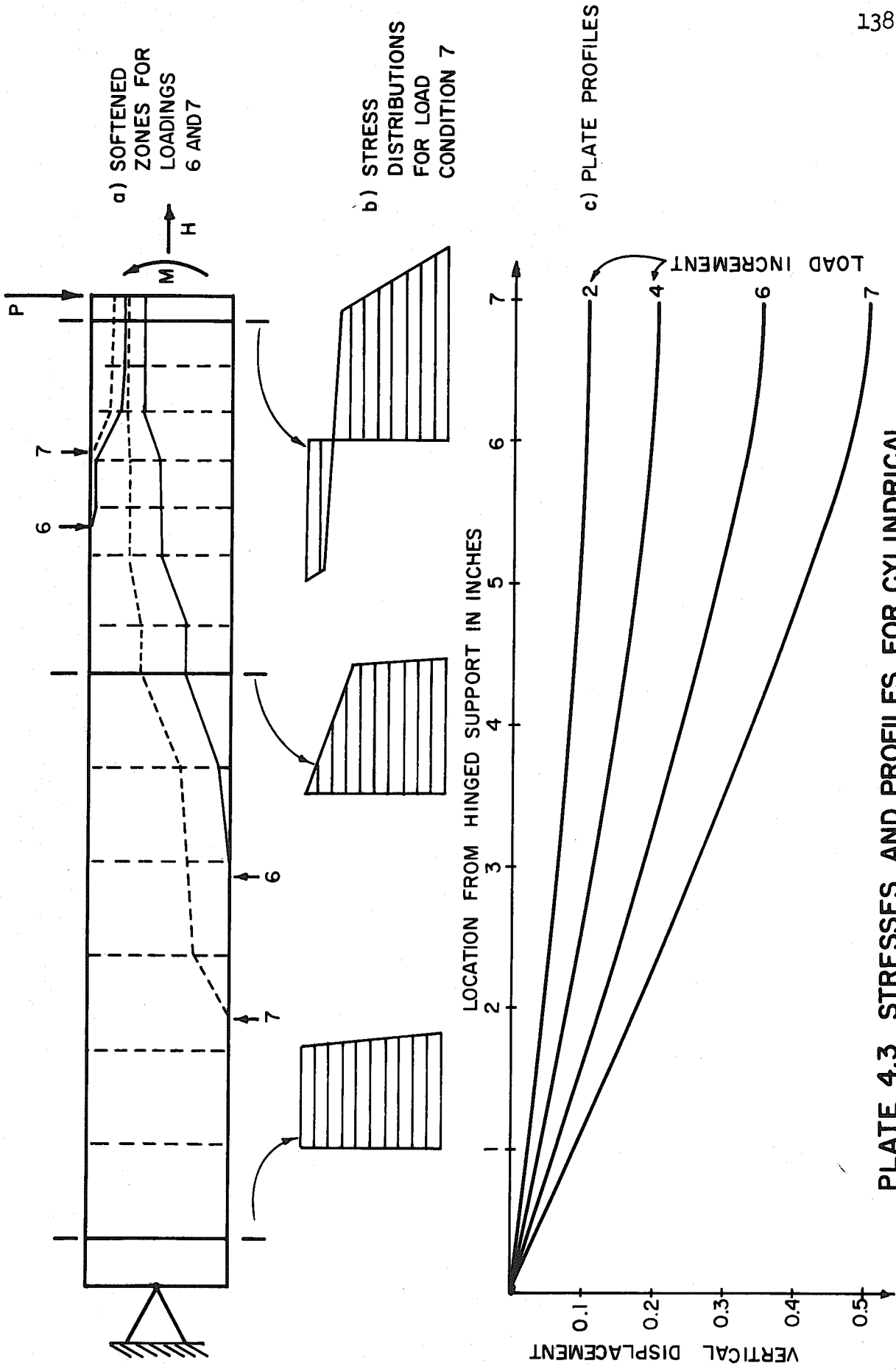


PLATE 4-2 FORCE DEFLECTION FOR CYLINDRICAL BENDING OF 2x14x0.5" PLATE



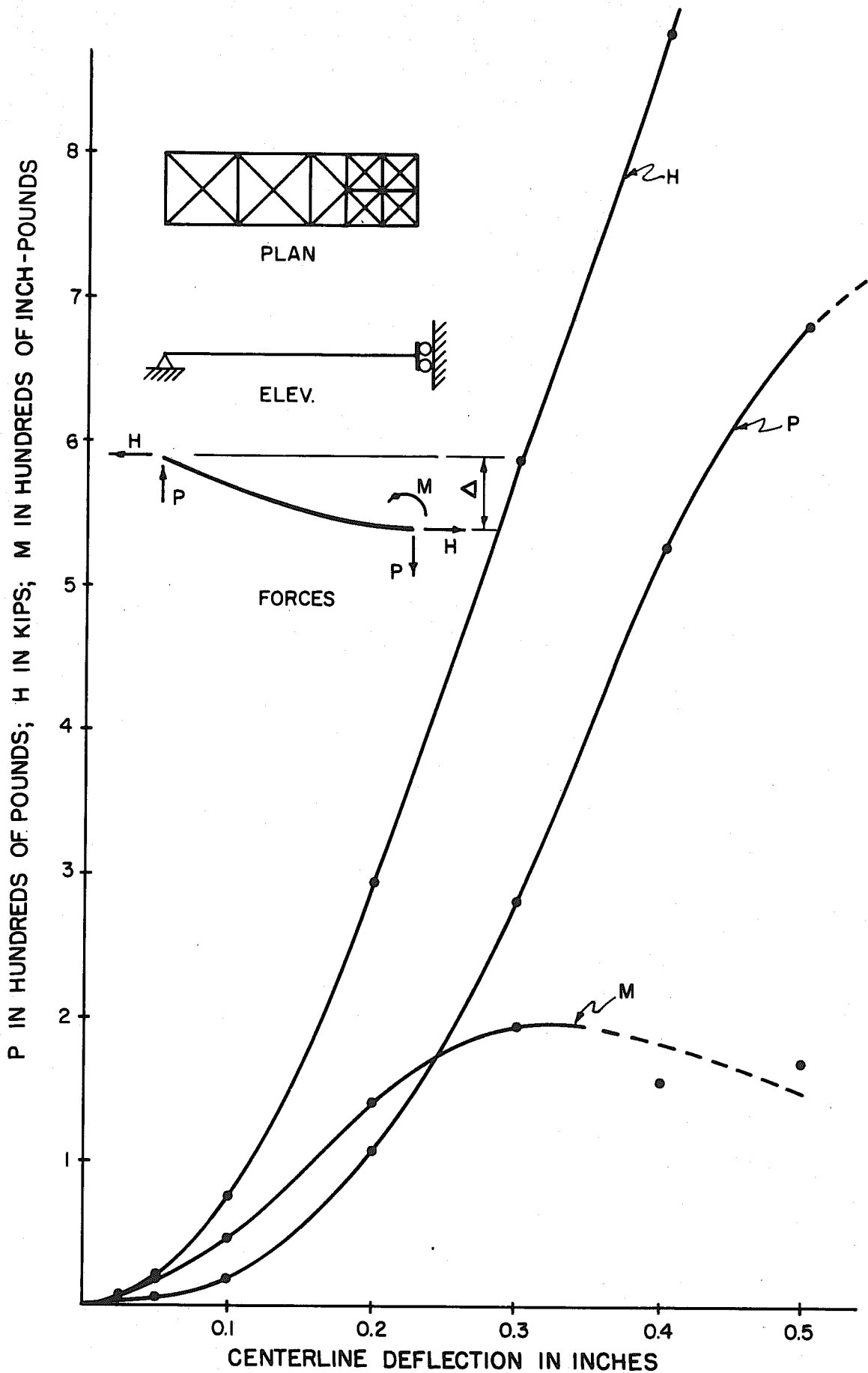
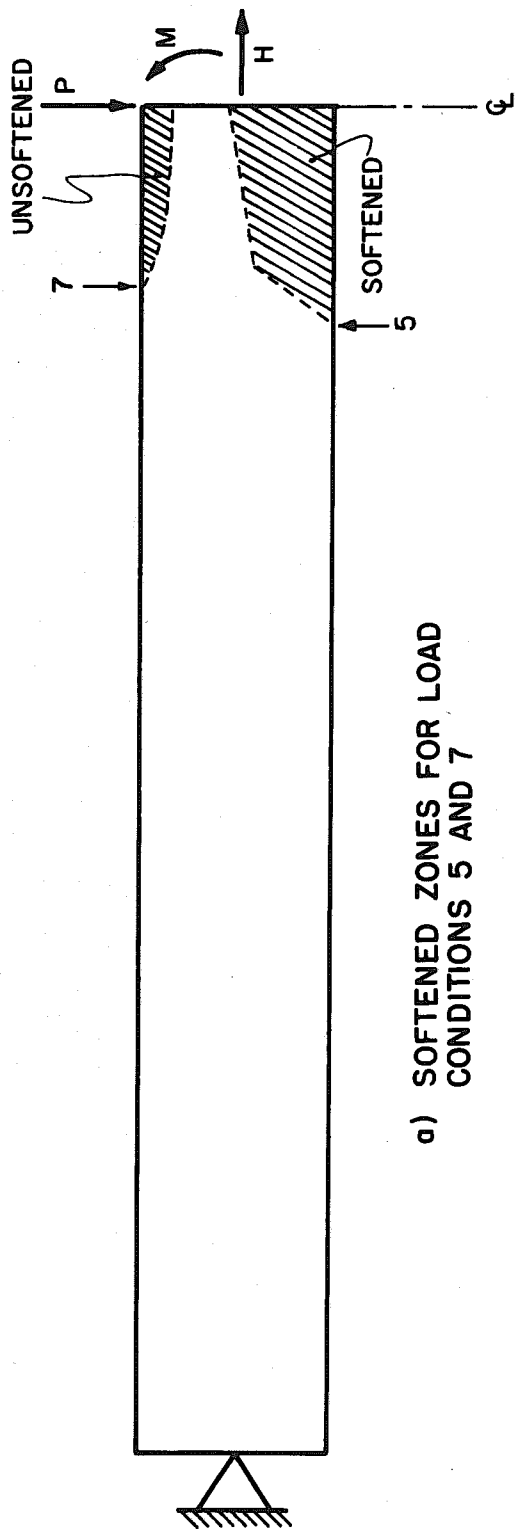
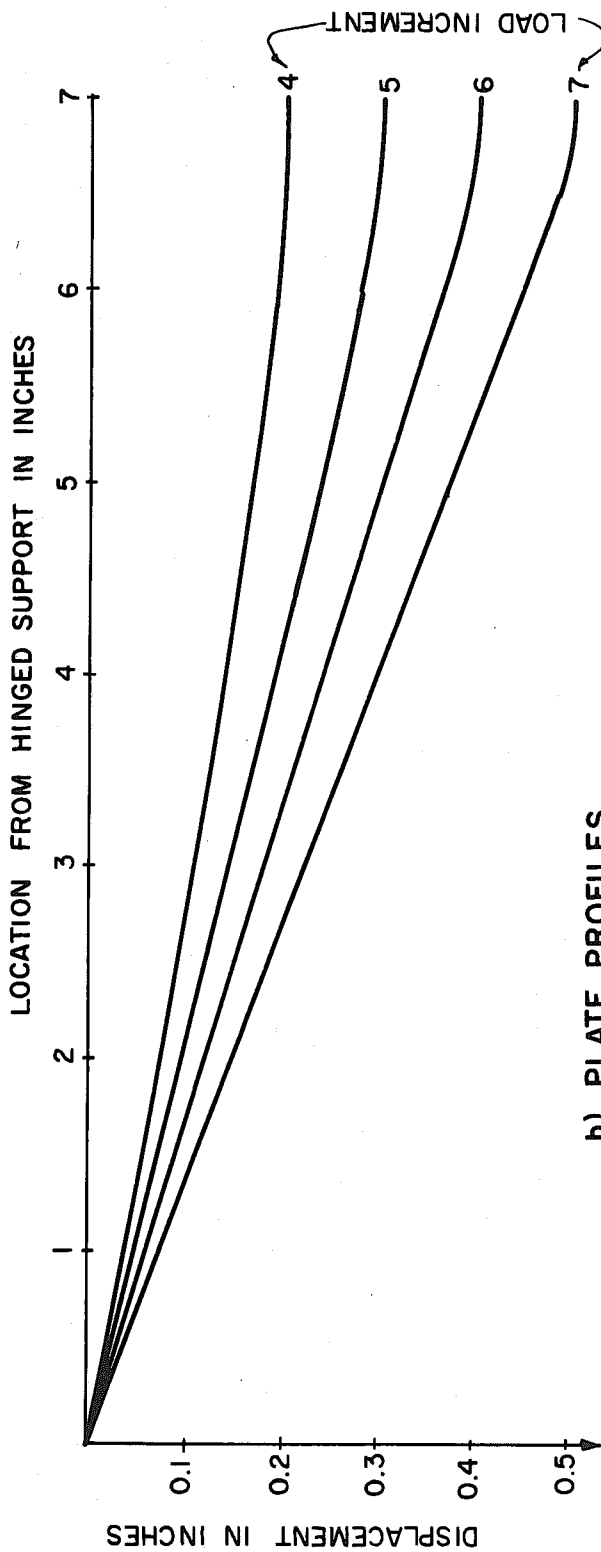


PLATE 4-4 FORCE DEFLECTION FOR CYLINDRICAL BENDING OF 2x14x0.1 INCH PLATE



a) SOFTENED ZONES FOR LOAD CONDITIONS 5 AND 7



b) PLATE PROFILES

PLATE 4-5 SOFTENED ZONES AND PROFILES FOR CYLINDRICAL BENDING OF 2x14x0.1 INCH PLATE

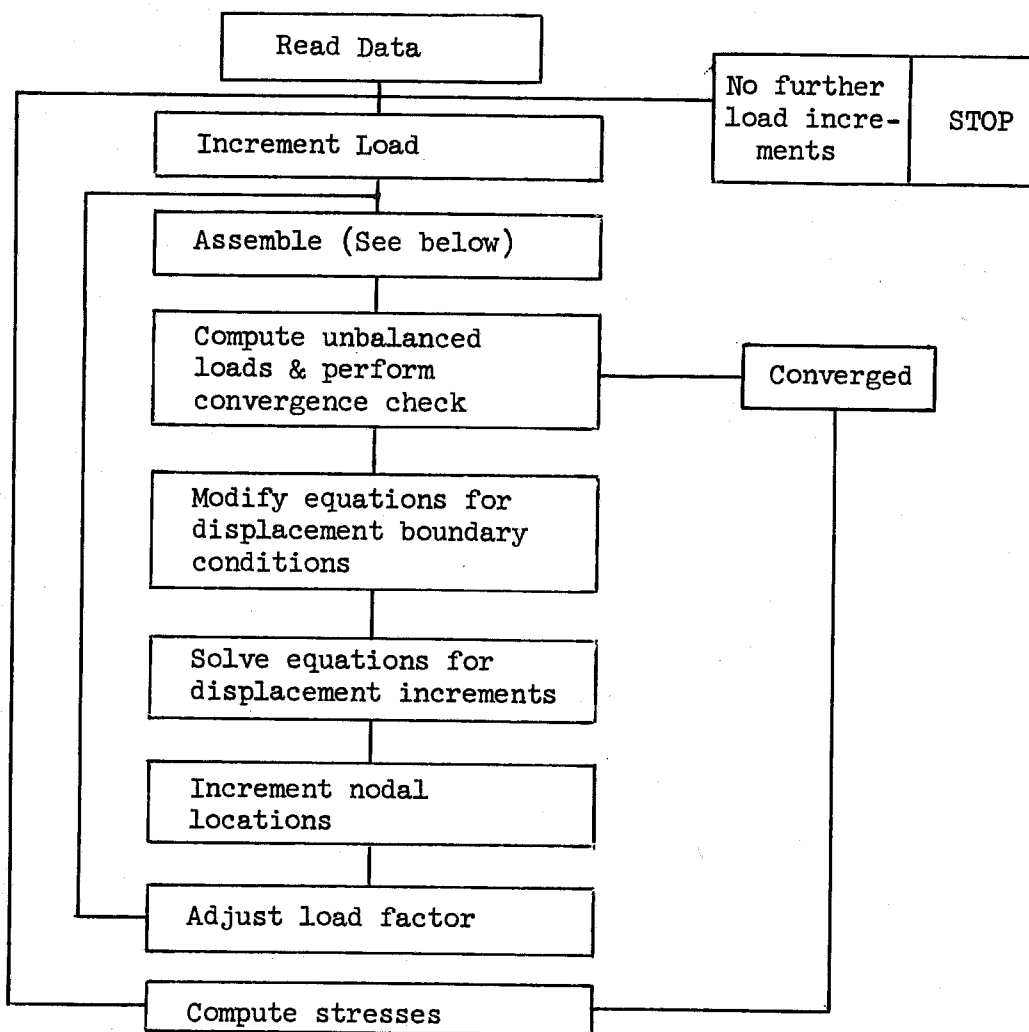
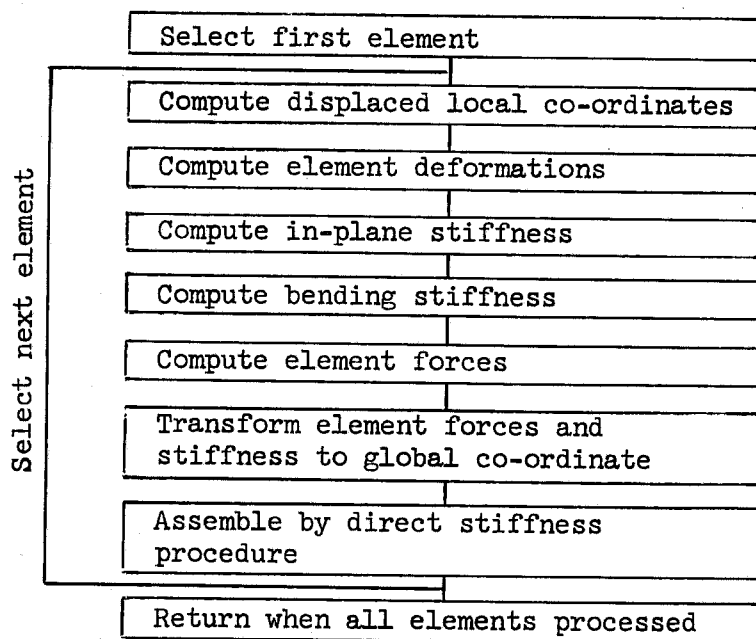
5. PROGRAMMING

The computer programs utilized in this investigation were limited in capacity to maintain an in-core solution. Computations were carried out on the CDC 6400 machine at the University of California Computing Center in Berkeley. Throughout the investigation effort was concentrated on developing an operating program which could produce solutions to the problems under consideration. However no effort was devoted to optimizing numerical computations and the program cannot therefore be considered as a "production program." For this reason a listing is not given and only an outline of the arrangement of subprograms and their functions is included.

5.1 Program Outline

An outline of the program for linear elastic materials is shown in Fig. 5.1. The program for nonlinear material properties is identical except that:

- (a) The element stiffnesses for a linear elastic material are computed prior to the first load increment and stored on tape.
- (b) The element secant stiffness are computed in ASSEMBLE by evaluating the multiplication factors in equations (4-19) and using the taped stiffness matrices. These are used for computing the element forces.
- (c) The element tangent stiffnesses are computed in ASSEMBLE in the same way as the secant stiffnesses but the multiplication factors in equations (4-19) are determined only for each equilibrium position, during the computation of stresses. The element tangent stiffnesses are used in assembling the structure stiffness.

Fig. 5.1 Outline of Program for Linear Elastic MaterialOutline of Assemble

5.2 Computational effort

The time requirements for the CDC 6400 solutions may be estimated approximately on the following basis:

Solution Procedure	Approximate Time per element per iterate in seconds
Without Geometric Stiffness	1/5 → 1/4
With Geometric Stiffness	3/10 → 3/8

Some typical times for solutions carried out in this investigation are:

Problem Type	Total iterates	CP time in minutes
Simply supported square plate large deflection solution (Plate 2-4)	25	4.0
Simply supported square plate post-buckling solution (Plate 3-2)	64	14.3
Nonlinear cylindrical bending (Plates 4-4 and 4-5)	99	9.2

The total solution time depends, of course, on the number of elements, the number of load conditions, and the convergence criterion. In general the convergence criterion was to make the sum of the absolute values of all unbalanced forces less than 0.1 times the number of nodal points. The program for linear materials was limited to 40 nodal points and 60 elements while the program for nonlinear materials was limited to 32 nodal points and 60 elements.

6. SUMMARY AND CONCLUSIONS

A general approach to large deflection problems has been presented and a finite element analysis of the large deflection plate problem has been developed. It has been demonstrated that this analysis is capable of solving a variety of problems for which the in-plane and out-of-plane behavior is coupled and that the results are sufficiently accurate for engineering purposes.

A geometric stiffness matrix has been formulated, and derived in detail for this particular model, which facilitates the study of post buckling behavior. It has been demonstrated that the analysis is capable of predicting post-buckling behavior of plates for a variety of boundary conditions.

An approximate method of incorporating variable material properties has been included. This technique has only been formulated for nonlinear elastic material and exhibits poorer convergence characteristics than for linear elastic materials.

This work has demonstrated the feasibility of solving these types of problems and developed a technique for their analysis. However further developments are required in many directions, some of which may be itemized as follows:

- (a) Optimization of numerical computations.
- (b) Refinement of the displacement model or development of equilibrium models.
- (c) Improvement of the convergence characteristics for nonlinear material properties and development of the analysis to handle more general types of material behavior.

REFERENCES

- [1] Felippa, C. A., "Refined finite element analysis of linear and nonlinear two-dimensional structures," SESM Report 66-22, University of California, Berkeley, 1966.
- [2] Wilson, E. L., "Finite element analysis of two-dimensional structures," SESM Report 63-2, University of California, Berkeley, 1963.
- [3] Felippa, C. A., "Refined finite element analysis of linear and nonlinear two-dimensional structures, Section II, Plate Bending Problems," Ph.D. Dissertation, University of California, Berkeley, 1966.
- [4] Fung, Y. C., "Foundations of solid mechanics," Prentice-Hall, 1965.
- [5] Argyris, J. H., "Continua and discontinua," in "Matrix methods in structural mechanics," Wright-Patterson Air Force Base, Ohio, 1966.
- [6] Timoshenko, S. P., and Woinowsky-Krieger, S., "Theory of plates and shells," second edition, Mc-Graw Hill, 1959.
- [7] Mansfield, W. H., "The bending and stretching of plates," Pergamon Press, 1964.
- [8] Borg, S. F., "An introduction to matrix tensor methods in theoretical and applied mechanics," J. W. Edwards, 1956.
- [9] deVeubeke, B. M. F., "Upper and lower bounds in matrix structural analysis," in "Matrix methods of structural analysis," Agardograph 72, Pergamon Press, 1964.
- [10] Sokolnikoff, I. S., "Mathematical theory of elasticity," second edition, McGraw-Hill, 1956.
- [11] Clough, R. W., and Tocher, J. L., "Finite element stiffness matrices for analysis of plate bending," in "Matrix methods in structural mechanics," Wright-Patterson Air Force Base, Ohio, 1966.

- [12] Bogner, F. K., Fox, R. L., and Schmit, L. A., "The generation of interelement, compatible stiffness and mass matrices by the use of interpolation formulas," in "Matrix methods in structural mechanics," Wright-Patterson Air Force Base, Ohio, 1966.
- [13] Carr, A. J., "A refined finite element analysis of thin shell structures including dynamic loadings," SESM Report 67-9, University of California, Berkeley, 1967.
- [14] Breuleux, R., "Large deflections in plane frames," SESM Graduate Student Report 238, University of California, Berkeley, 1966.
- [15] Levy, S., "Bending of rectangular plates with large deflections," NACA Technical Note 846, 1942.
- [16] Levy, S., "Square plate with clamped edges under normal pressure," NACA Technical Note 847, 1942.
- [17] Timoshenko, S. P., and Gere, J. M., "Theory of elastic stability," second edition, McGraw-Hill, 1961.
- [18] Biot, M. A., "Mechanics of incremental deformations," John Wiley and Sons, 1965.
- [19] Argyris, J. H., Kelsey, S., and Kamel, H., "Matrix methods of structural analysis," Agardograph 72, Pergamon Press, 1964.
- [20] Martin, H. C., "On the derivation of stiffness matrices for the analysis of large deflection and stability problems," Department of Aeronautics and Astronautics Report 66-4, University of Washington, 1966. (Also in Wright-Patterson Air Force Base Conference Proceedings, 1966.)
- [21] Martin, H. C., "Large deflection and stability analysis by the direct stiffness method," Jet Propulsion Laboratory, Technical Report No. 32-931, Pasadena, 1965.

- [22] Hartz, B. J., "Matrix formulation of structural stability problems," Proc. ASCE, V. 91, ST. 6, 1965.
- [23] Kapur, K. K., Hartz, B. J., "Stability of plates using finite element method," Proc. ASCE, V. 92, EM 2, April. 1966.
- [24] Khojasteh-Bakht, M., "Analysis of elastic-plastic shells of revolution under axisymmetric loading by the finite element method," SESM Report 67-8, University of California, Berkeley, 1967.
- [25] Hodge, P. G., "Plastic analysis of structures," McGraw-Hill, 1959.
- [26] Dong, S. B., Pister, K. S., and Taylor, R. L., "On the theory of laminated isotropic shells and plates," J. of Aerospace Sciences, Vol. 29, No. 8, August 1962.
- [27] Wilson, E. L., "A digital computer program for the finite element analysis of solids with nonlinear material properties," Aerojet Report, Sacramento, 1965.

APPENDIX A

STRESS TENSORS FOR LAGRANGIAN DESCRIPTION OF
LARGE DEFLECTION PROBLEMSA.1 Introduction

Three different stress tensors are used in deriving large deflection equations in the Lagrangian description. These are nicely dealt with by Fung [4] and details may be found in that reference. However it is advantageous to summarize the pertinent relationships here since many engineers using plate theory have not been exposed to these concepts and also because a more complete physical interpretation with respect to the plate problem can be attempted. Physical interpretations which follow are illustrated in two dimensions in Figs. A1 and A3.

A.2 The Lagrangian Stress Tensor and the Equilibrium Equations

Consider an element from a plate before and after deformation as shown in Fig. A1. Consider a set of rectangular cartesian axes such that x_i specify the position of a point before deformation and X_i specify the position of a point after deformation. The stress tensor defined per unit of area in the deformed body with respect to this set of axes is called the Eulerian stress tensor. We denote it by σ_{ij} . The requirements of equilibrium for an infinitesimal element are

$$\frac{\partial \sigma_{ij}}{\partial X_i} + \rho F_j = 0$$

and

$$\sigma_{ij} = \sigma_{ji} .$$

If we now consider a general body such as shown in Fig. A2, the equilibrium requirement may be written for the deformed configuration as

$$\int_V F_i \rho dV + \int_S \sigma_{ji} v_j dS = 0. \quad (\text{A-1})$$

However the shape of the deformed body is unknown prior to obtaining a solution. Assuming the body force per unit of mass does not change during deformation we can say

$$\int_V F_i \rho dV = \int_{V_0} F_{i0} \rho_0 dV_0 \quad (\text{A-2})$$

where the subscript 0 indicates initial configuration, and F_i , ρ , and dV are the body force per unit of mass, the density and the element of volume, respectively.

The resulting surface traction on an area dS is represented by a force vector dT_i ,

$$dT_i = \sigma_{ji} v_j dS \quad (\text{A-3})$$

where v_j is the normal to the surface element dS . We now define the Lagrangian stress tensor, T_{ij} , and the surface traction, $dT_{0i}(L)$, such that (see Fig. A1)

$$\sigma_{ji} v_j dS = dT_i = dT_{0i}^{(L)} = T_{ji} v_{0j} dS_0 \quad (\text{A-4})$$

where dS_0 and v_0 are the area and normal in the initial configuration associated with the same material points which comprise dS in the final configuration. By means of this definition the forces acting on a surface of the deformed body can be evaluated in terms of an integral over the corresponding area in the original configuration. Thus

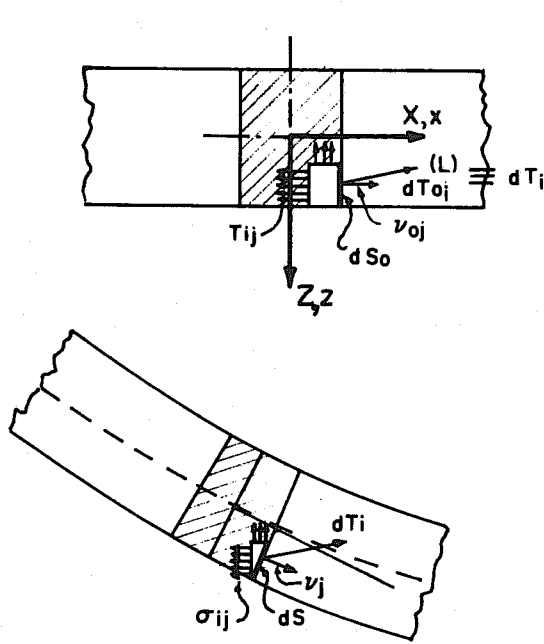


FIG. A1 - LAGRANGIAN AND EULERIAN STRESS TENSORS, T_{ij} AND σ_{ij}

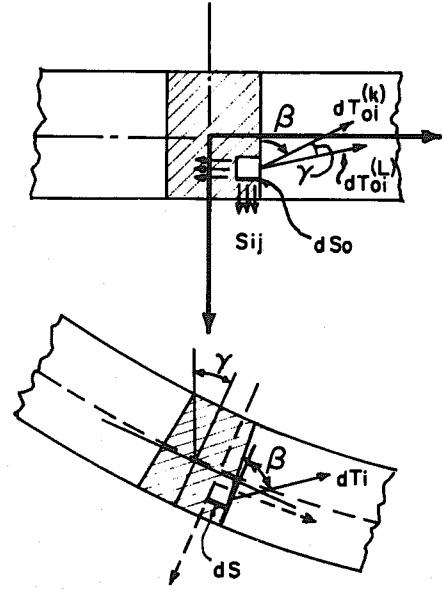


FIG. A3 - KIRCHHOFF STRESS TENSOR, S_{ij}

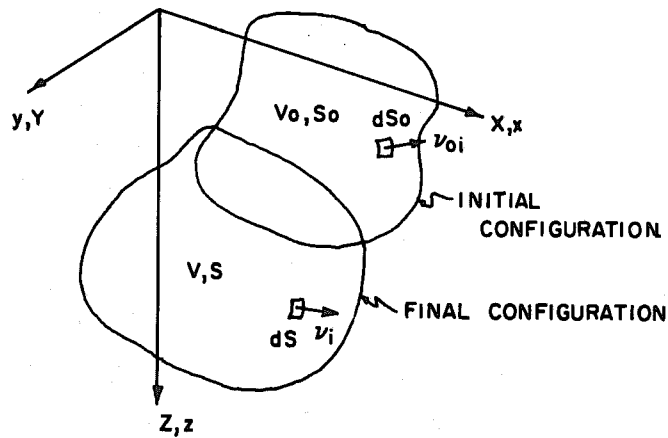


FIG. A2

$$\int_S dT_i = \int_{S_0} dT_{0i}^{(L)} \quad (\text{A-5})$$

By substituting the definition of $dT_{0i}^{(L)}$ into equation (A-5) and using equation (A-2); the equilibrium equation (A-1) becomes

$$\int_{V_0} F_{i0} \rho_0 dV_0 + \int_{S_0} T_{ji} v_{0j} dS_0 = 0. \quad (\text{A-6})$$

Applying Gauss's theorem

$$\int_{S_0} T_{ji} v_{0j} dS_0 = \int_{V_0} \frac{\partial T_{ji}}{\partial x_j} dV_0$$

and equation (A-6) becomes

$$\int_{V_0} \left(F_{i0} \rho_0 + \frac{\partial T_{ji}}{\partial x_j} \right) dV_0 = 0.$$

Since this equation must be satisfied for an arbitrary volume element, the integrand must vanish everywhere and therefore

$$\frac{\partial T_{ji}}{\partial x_j} + F_{i0} \rho_0 = 0 \quad (\text{A-7})$$

becomes the equation expressing the equilibrium requirement of the deformed configuration in terms of quantities referred to the original configuration.

Thus the Lagrangian stress tensor is the stress tensor which appears in the equilibrium equations when these equations are referred to the original configuration. It should be noted that the Lagrangian stress tensor is unsymmetric (see section A1.4) but since equation (A-7) expresses

the equilibrium conditions in the deformed configuration in terms of a stress tensor defined on the original configuration this is not an inconsistent property.

A.3 The Kirchoff Stress Tensor and the Constitutive Relations

We start by recalling the definition of Green's strain tensor. The physical interpretation of this quantity is most easily understood if developed by means of vector concepts. Considering a line element of length ds_0 originally orientated in the direction of the x axis, the measure of change in length associated with component E_{xx} is obtained by taking the vector dot product before and after deformation and evaluating

$$\frac{ds^2 - ds_0^2}{2 ds_0^2} = \frac{(ds_0 + \delta(ds_0))^2 - ds_0^2}{2 ds_0^2} = \frac{\delta(ds_0)}{ds_0} + \frac{1}{2} \left(\frac{\delta(ds_0)}{ds_0} \right)^2 \equiv E_{xx}.$$

The quantity $\frac{\delta(ds_0)}{ds_0}$ is the engineering strain and thus, providing the engineering strain is small with respect to one, E_{xx} is an accurate measure of this strain. This interpretation applies to a line element in any orientation. Note that the line element may have a final orientation in a radically different direction, but the measure remains valid. A similar interpretation shows that the off-diagonal terms of Green's strain tensor are an accurate representation of engineering shear strain provided the engineering strains remain small. This is true regardless of the magnitudes of the displacement gradients.

Consider now a line element ds as shown in Fig. A3. Logically, the final length of this line should be related to the component of stress oriented in the direction of the line element in its final position. If the force vector on the element surface shown in Fig. A3 is dT_i , and a

force vector referred to the original position is desired which produces stress components having the same relative magnitudes with respect to the element, then the force vector must be rotated through the same angle as the line element when referring to the original configuration. This gives rise to the Kirchoff stress tensor, S_{ij} , which is defined such that it produces a traction $dT_{O_i}^{(K)}$ having the same orientation with respect to the element. The definition is

$$dT_{O_i}^{(K)} = dT_{\alpha} \frac{\partial x_i}{\partial X_{\alpha}} = S_{ji} \nu_{j0} dS_0.$$

The Kirchoff stress tensor therefore represents the state of stress in the final configuration when referred to the original dimensions and orientation of the element. Since the strains are specified in terms of this original configuration it is natural to relate the strains to the Kirchoff stress tensor. The constitutive equation for an isotropic linear elastic material therefore becomes

$$S_{ij} = \lambda E_{\alpha\alpha} \delta_{ij} + 2\mu E_{ij}. \quad (\text{A-8})$$

A.4 Relations Between Stress Tensors

It can be shown [4] that the three stress tensors are related as follows

$$T_{ji} = \frac{\rho_0}{\rho} \frac{\partial x_i}{\partial X_m} \sigma_{mi}$$

$$S_{ji} = \frac{\rho_0}{\rho} \frac{\partial x_i}{\partial X_{\alpha}} \frac{\partial x_j}{\partial X_{\beta}} \sigma_{\beta\alpha}$$

$$T_{ij} = \frac{\partial X_j}{\partial x_{\alpha}} S_{i\alpha}$$

$$S_{ji} = \frac{\partial x_i}{\partial X_{\alpha}} T_{j\alpha}$$

$$\sigma_{ji} = \frac{\rho}{\rho_0} \frac{\partial X_i}{\partial x_{\alpha}} T_{\alpha j}$$

$$\sigma_{ji} = \frac{\rho}{\rho_0} \frac{\partial X_i}{\partial x_{\alpha}} \frac{\partial X_j}{\partial x_{\beta}} S_{\beta\alpha}.$$

The symmetry of S_{ji} can be seen from its relationship to $\sigma_{\beta\alpha}$ which is a symmetric tensor.

A.5 Final Remarks

In formulating equations it is desirable to use only one of the stress tensors. The most convenient is the Kirchoff stress tensor. The constitutive equations and the equilibrium equations, suitable for large deflection problems, therefore become

$$S_{ij} = \lambda E_{\alpha\alpha} \delta_{ij} + 2\mu E_{ij} \quad (\text{A-8})$$

and

$$\frac{\partial}{\partial x_j} \left[S_{jk} \left(\delta_{ij} + \frac{\partial u_i}{\partial x_k} \right) \right] + \rho_0 F_{0i} = 0. \quad (\text{A-9})$$

Since we are concerned here with a problem in which the engineering strains are small, the Kirchoff stress tensor may be interpreted as representing the Eulerian stresses in the final configuration if properly orientated with respect to the element (see Fig. A3).

APPENDIX B

VIRTUAL WORK AND STRAIN ENERGY RELATIONSHIPS

B.1 Derivation of Incremental Virtual Work Equation[†]

We refer to Fig. B1. Consider a typical structure in configuration Γ_0 , specified by displacements $\{r_0\}$, which is an equilibrium with loads $\{R_0\}$. We consider this configuration as the "initial" configuration for a load increment. The application of a load increment $\{\Delta R\}$ leads to a new equilibrium configuration, $\Gamma = \Gamma_0 + \Delta\Gamma$, specified by the displacements $\{r_0\} + \{\Delta r\}$, which is in equilibrium with the loads $\{R_0\} + \{\Delta R\}$. We seek a virtual work equation which relates the increments in loads $\{\Delta R\}$ to the increments in displacement $\{\Delta r\}$. The initial stress σ_{ij0} , the strain increment ΔE_{ij} , and the stress increment ΔS_{ij} are all referred to the "initial" configuration, Γ_0 .

The "initial" stress tractions arising from the loads $\{R\}$ are assumed to remain of constant magnitude and maintain the same orientation with respect to the infinitesimal element axes for subsequent incremental deformations. The initial stress tensor is therefore conjugate* to the strain increments ΔE_{ij} in the sense that the product $\sigma_{ij}(\Delta E_{ij})$ is work. Similarly ΔS_{ij} is conjugate to ΔE_{ij} . These expressions for work are only valid for small increments of engineering strain.

The virtual work equation for the position Γ therefore becomes

[†] The incremental stiffness is developed in a more elegant way by Felippa [1], page 119, and is also developed by Biot [15], page 80.

* See Biot [15], page 61.

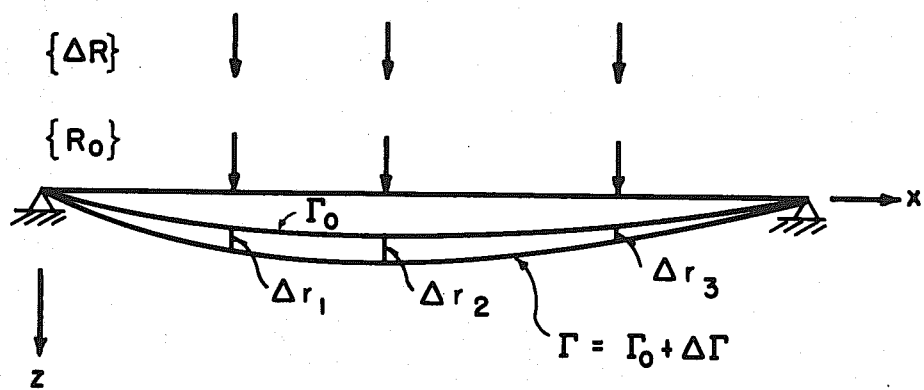


FIG. B1

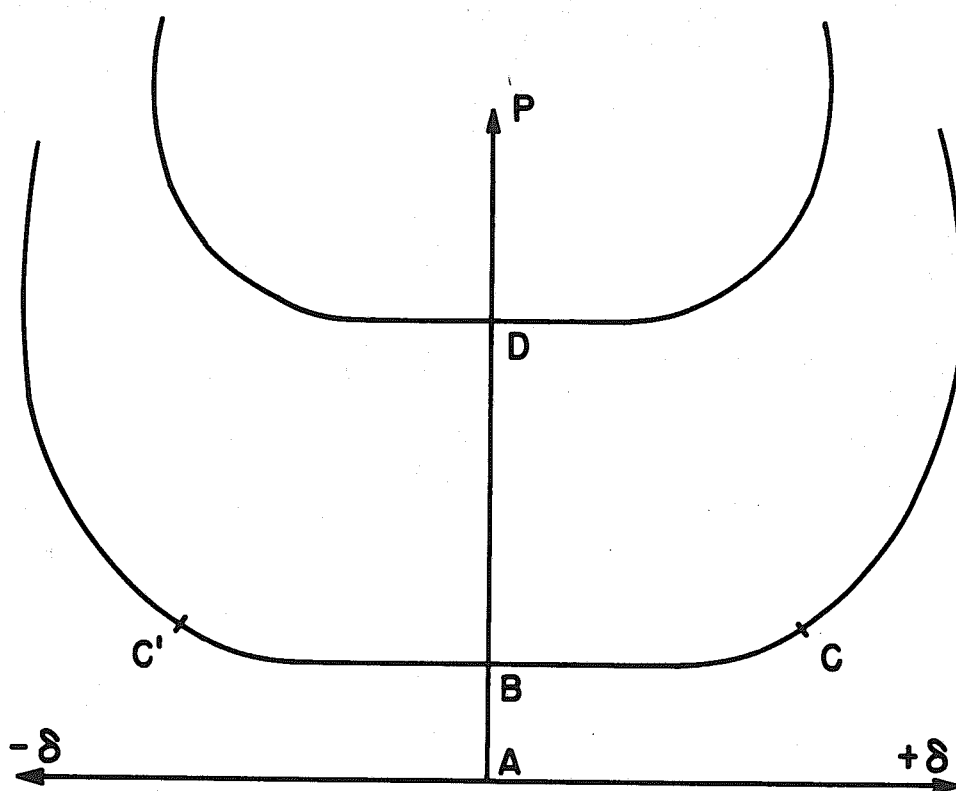


FIG. B2 SCHEMATIC REPRESENTATION OF SOLUTION TO "ELASTICA" PROBLEM

$$\int_{V_0} \{ \tilde{\sigma}_{ij0} + \Delta \tilde{\sigma}_{ij} \} \delta(\Delta \tilde{E}_{ij}) dV_0$$

$$= \int_{S_{\sigma_0}} \left\{ d\tilde{T}_{i0}^{\nu_0} + d\tilde{T}_{i0}^{\nu_0(L)} \right\} \delta(\Delta \tilde{u}_i) + \int_{V_0} \rho_0 \tilde{F}_{i0} \delta(\Delta \tilde{u}_i) dV_0 \quad (\text{B-1})$$

where the subscript 0 refers to the "initial" configuration (see Appendix A).

In equation (B-1), the surface vector is defined by the relation

$$d\tilde{T}_i^{\nu_0} = \tilde{\sigma}_{ji} \nu_j dS = (\tilde{\sigma}_{ji0} + \Delta \tilde{\sigma}_{ji}) \nu_{j0} dS_0 = d\tilde{T}_{i0}^{\nu_0} + \Delta d\tilde{T}_{i0}^{\nu_0(L)} = d\tilde{T}_{i0}^{\nu_0(L)}$$

i.e.,

$$d\tilde{T}_{i0}^{\nu_0} = \tilde{\sigma}_{ji0} \nu_{j0} dS_0 \quad \Delta d\tilde{T}_{i0}^{\nu_0(L)} = \tilde{\sigma}_{ji} \nu_j dS - \tilde{\sigma}_{ji0} \nu_{j0} dS_0.$$

Now, the structure is also in equilibrium in the "initial" configuration.

Therefore, the virtual work equation for position Γ_0 states

$$\int_{V_0} \tilde{\sigma}_{ij0} \delta(\Delta \tilde{E}_{ij}) dV_0 = \int_{S_{\sigma_0}} d\tilde{T}_{i0}^{\nu_0} \delta(\Delta \tilde{u}_i) \quad (\text{B-2})$$

$$+ \int_{V_0} \rho_0 \tilde{F}_{i0} \delta(\Delta \tilde{u}_i) dV_0.$$

Evaluating $\Delta \tilde{E}_{ij}$,

$$\Delta \tilde{E}_{ij} = \frac{1}{2} \left\{ (\Delta \tilde{u}_i)_{,j} + (\Delta \tilde{u}_j)_{,i} + (\Delta \tilde{u}_k)_{,i} (\Delta \tilde{u}_k)_{,j} \right\} \quad (\text{B-3})$$

Taking the variation of $\Delta \tilde{E}_{ij}$,

$$\delta(\Delta \tilde{E}_{ij}) = \frac{1}{2} \left\{ (\delta \Delta \tilde{u}_i)_{,j} + (\delta \Delta \tilde{u}_j)_{,i} \right. \quad (\text{B-4})$$

$$\left. + (\delta \Delta \tilde{u}_k)_{,i} (\Delta \tilde{u}_k)_{,j} + (\Delta \tilde{u}_k)_{,i} (\delta \Delta \tilde{u}_k)_{,j} \right\}$$

Therefore equation (B-1) becomes

$$\begin{aligned}
& \int_{V_0} \left\{ \tilde{\sigma}_{ij0} + \Delta \tilde{S}_{ij} \right\} \frac{1}{2} \left\{ (\delta \Delta \tilde{u}_i)_{,j} + (\delta \Delta \tilde{u}_j)_{,i} \right. \\
& \left. + (\delta \Delta \tilde{u}_k)_{,i} (\Delta \tilde{u}_k)_{,j} + (\Delta \tilde{u}_k)_{,i} (\delta \Delta \tilde{u}_k)_{,j} \right\} dV_0 \\
& = \int_{S_{\sigma_0}} \left\{ d\tilde{T}_{i0}^{V_0} + \Delta d\tilde{T}_{i0}^{V_0(L)} \right\} (\delta \Delta \tilde{u}_i) + \int_{V_0} \rho_0 \tilde{F}_{i0} (\delta \Delta \tilde{u}_i) dV_0 .
\end{aligned} \tag{B-5}$$

Equation (B-2) becomes, noting that $\Delta \tilde{u}_i$, $\Delta \tilde{S}_{ij}$ and $\Delta d\tilde{T}_{i0}^{V_0(L)} = 0$,

$$\begin{aligned}
& \int_{V_0} \tilde{\sigma}_{ij0} \cdot \frac{1}{2} \left\{ (\delta \Delta \tilde{u}_i)_{,j} + (\delta \Delta \tilde{u}_j)_{,i} \right\} dV_0 \\
& = \int_{S_{\sigma_0}} d\tilde{T}_{i0}^{V_0} (\delta \Delta \tilde{u}_i) + \int_{V_0} \tilde{F}_{i0} \rho_0 (\delta \Delta \tilde{u}_i) dV_0 .
\end{aligned} \tag{B-6}$$

Subtracting equation (B-6) from equation (B-5) yields

$$\begin{aligned}
& \int_{V_0} \tilde{\sigma}_{ij0} \cdot \frac{1}{2} \left\{ (\delta \Delta \tilde{u}_k)_{,i} (\Delta \tilde{u}_k)_{,j} + (\Delta \tilde{u}_k)_{,i} (\delta \Delta \tilde{u}_k)_{,j} \right\} dV_0 \\
& + \int_{V_0} \Delta \tilde{S}_{ij} \cdot \frac{1}{2} \left\{ (\delta \tilde{u}_i)_{,j} + (\delta \tilde{u}_j)_{,i} + (\delta \Delta \tilde{u}_k)_{,i} (\Delta \tilde{u}_k)_{,j} \right. \\
& \left. + (\Delta \tilde{u}_k)_{,i} (\delta \Delta \tilde{u}_k)_{,j} \right\} dV_0 = \int_{S_{\sigma_0}} \Delta d\tilde{T}_{i0}^{V_0(L)} (\delta \Delta \tilde{u}_i) .
\end{aligned} \tag{B-7}$$

This can be written as

$$\begin{aligned}
& \int_{V_0} \tilde{\sigma}_{ij0} \cdot \frac{1}{2} \delta \left\{ (\Delta \tilde{u}_k)_{,i} (\Delta \tilde{u}_k)_{,j} \right\} dV_0 + \int_{V_0} \Delta \tilde{S}_{ij} \delta (\Delta \tilde{E}_{ij}) dV_0 \\
& = \int_{S_{\sigma_0}} \Delta d\tilde{T}_{i0}^{V_0(L)} (\delta \Delta \tilde{u}_i)
\end{aligned} \tag{B-8}$$

If we now adopt the vector notation for \tilde{u}_i specified in equation (2-3) and write

$$\{\Delta \tilde{u}\} = [\tilde{D}_\Delta] \{\Delta r\} \quad \text{and} \quad \{\Delta \tilde{u}_{,i}\} = [D_{\Delta,i}] \{\Delta r\} ,$$

where $[\tilde{D}_\Delta]$ is the functional relationship specifying the infinitesimal displacement field in terms of infinitesimal nodal displacements, the first term of equation (B-8) can be written as

$$\begin{aligned}
& \int_{V_0} \tilde{\sigma}_{ij_0} \cdot \frac{1}{2} \delta \left[\Delta \tilde{u}_{,i} \right]^T \left[\Delta \tilde{u}_{,j} \right] dV_0 \\
&= \int_{V_0} \tilde{\sigma}_{ij_0} \cdot \frac{1}{2} \delta \left[\Delta r \right]^T \left[\tilde{D}_{\Delta,i} \right]^T \left[\tilde{D}_{\Delta,j} \right] \left[\Delta r \right] dV_0 \\
&= \int_{V_0} \tilde{\sigma}_{ij_0} \cdot \frac{1}{2} \left\{ \Delta r \right\}^T \left[\tilde{D}_{\Delta,i} \right]^T \left[\tilde{D}_{\Delta,j} \right] + \left[\tilde{D}_{\Delta,j} \right]^T \left[\tilde{D}_{\Delta,i} \right] \left\{ \Delta r \right\} dV_0 \\
&= \left\{ \Delta r \right\}^T \cdot \frac{1}{2} \int_{V_0} \sum_{i=1}^3 \sum_{j=1}^3 \tilde{\sigma}_{ij_0} \left[\tilde{D}_{\Delta,i} \right]^T \left[\tilde{D}_{\Delta,j} \right] + \left[\tilde{D}_{\Delta,j} \right]^T \left[\tilde{D}_{\Delta,i} \right] dV_0 \left\{ \Delta r \right\}.
\end{aligned}$$

The summation has been written in full in the last expression so the nature of the term can be seen. The quantity inside the square brackets is called the "geometric stiffness" or "initial stress stiffness" matrix and is designated as $[K_G]$.

The second term on the left hand side of equation (B-8) represents the virtual work done by the increments in stress arising from deformation and can be identified with the conventional stiffness matrix. Since it represents the stiffness in the displaced configuration we designate it as $[K_D]$, and this term becomes

$$\left\{ \Delta r \right\}^T [K_D] \left\{ \Delta r \right\}.$$

The term on the right hand side represents the virtual work done by the increments in surface forces and can be written as

$$\left\{ \Delta r \right\}^T \left\{ \Delta R \right\}.$$

Equation (B-8) therefore becomes

$$\left\{ \Delta r \right\}^T [K_G + K_D] \left\{ \Delta r \right\} = \left\{ \Delta r \right\}^T \left\{ \Delta R \right\}. \quad (\text{B-9})$$

Since all virtual displacements are arbitrary, this requires that

$$[K_G + K_D] \{\Delta r\} = \{\Delta R\} \quad (\text{B-10})$$

which is the relation between incremental displacements and incremental forces required if the structure is to pass from one equilibrium configuration to another.

B.2 Some Notes on Uniqueness

In solid mechanics there are two general approaches to uniqueness proofs.

- (a) Direct approach.* Given the governing differential equation and the boundary conditions and (for dynamics) initial conditions of the problem, assume two solutions u_1 and u_2 , $u_1 \neq u_2$. Then show that the function $\Delta u = u_1 - u_2$ is also a solution and is identically zero. Such proofs depend upon the linear properties of the differential equation and the positive definiteness of the strain energy function.
- (b) Variational approach. In the variational approach it is first necessary to show the equivalence of the differential equation formulation with the conditions for a stationary value of an integral, say I . In other words it is necessary to show that a stationary value of I implies the differential equation and boundary conditions are satisfied; and satisfaction of the differential equation and boundary conditions implies a stationary value of the integral. The uniqueness of the solution can then be studied on the basis of the properties of the integral. Since this approach is not confined to linear equations we use it as a basis for discussion.

* See, for example, Fung [4], p. 160, or Sokolnikoff [10], p. 86.

Although there are many recent developments in variational theorems, the two traditional variational approaches that can be shown to yield the equations of elasticity are the principle of stationary potential energy and the principle of stationary complementary energy.

For a linear elastic material and infinitesimal deformations the potential energy is a quadratic form. Under these conditions the principle of stationary potential becomes the principle of minimum potential energy[†] and a unique solution is assured. If nonlinear elastic material is considered the potential energy is no longer a quadratic form and therefore it cannot be shown that there is an absolute minimum value of the integral, I. It can however be shown that there is a "relative minimum in the neighborhood of a stable natural (i.e., stress and strain free) state"^{*} where the strain energy is a positive definite function. The proof is restricted to apply to a natural state since the effect of initial stress is not included in the formulation and is restricted to a neighborhood of this state since infinitesimal strain-displacement relationships are utilized.[‡]

The inclusion of any of the effects, (a) nonlinear material properties (b) large displacement strain-displacement relationships or (c) initial stress states, invalidates the traditional uniqueness proof either by destroying the quadratic form of the strain-energy density or by adding additional terms to give an "effective" strain-energy density term which may not be positive definite. However, the fact that uniqueness cannot be proven in the mathematical problem does not necessarily mean that the

[†] Sokolnikoff, [10], p. 385.

^{*} Fung, [4], p. 287.

[‡] Sokolnikoff, [10], p. 86.

physical problem does not have a solution which for practical purposes can be considered unique. Some remarks on the solutions to the problems contained in this report can be made.

Consider the case of the "elastica" problem for which the finite element solution is given in section 2.12. The theoretical load deflection plot for this problem is illustrated schematically in Fig. B2. From a mathematical standpoint this problem has a multitude of solutions. However, when solved numerically, using an incremental approach, the solution A, B, C will always be obtained. This is the critical solution for the physical problem. When the solution reaches the bifurcation point, B, it will follow the stable branch because there is always sufficient disturbance in the iterative technique so that it will depart from the unstable branch. From a practical point of view, it is immaterial which stable branch it follows although this has been predetermined in the solutions of section 2.11 and 3.4 by introducing a small lateral load.

In the large deflection plate problem that is not subjected to in-plane compressive forces, the membrane force stabilizes the structure and again, although it cannot be shown mathematically, there can be no question of the uniqueness of the solution of the physical problem. For plates with large in-plate compressive forces the same type of argument can be advanced for physical uniqueness as was done for the column above. The results of section 2.11 show that the incremental technique picks out the critical buckling configuration when this consists of two half waves rather than one.

For nonlinear elastic materials the uniqueness proof fails because the strain energy density is no longer a quadratic form and this permits the existence of other relative minima. However, here again, the incremental

solution technique selects the neighboring stable equilibrium position and therefore the one which is physically significant.

In conclusion it may be said that while uniqueness of the mathematical problem does not exist, the incremental solution technique selects a neighboring stable equilibrium position which, for practical purposes, may be considered to be the unique solution of the physical problem which the model is simulating.

APPENDIX C

EVALUATION OF ELEMENT MATRICES

C.1 Co-ordinate Systems and Interpolation Functions[†]

In deriving the stiffness properties of triangular elements it is useful to introduce the concept of triangular co-ordinates. These are the "natural co-ordinates" of a triangular shape in the sense that the co-ordinates of a point are independent of the size, orientation or subsequent deformation of the element and that along each side of the triangle one co-ordinate is always zero. They have the advantages of simplifying integration and simplifying the direct construction of interpolation functions. Direct construction of interpolation functions is advantageous because generalized co-ordinates associated with the interpolation functions can be immediately identified with physical displacement quantities at nodal points.

Referring to Fig. C1, the corners of the triangle are numbered in cyclic order in a counterclockwise manner. A side is identified with the number of the corner opposite to it and distance measured normal to this side is also identified by the same number.

We define the triangular co-ordinates of a point (see Fig. C1b) as

$$\xi_i = \frac{m_i}{h_i} = \frac{A_i}{A}, \quad i = 1, 2, 3,$$

where A_i are subtriangles as indicated in Fig. C1a and A is the area of the total triangle. It follows from definition that for any particular point

[†] The reader is referred to Felippa [1, 3] for details. Basic geometric relationships are derived in Appendix D.4.

$$\zeta_1 + \zeta_2 + \zeta_3 = 1$$

and this relation expresses the linear dependence of one co-ordinate on the other two.

If we now define the projections of the sides l_i on the x and y co-ordinate axes as a_i and b_i , respectively, as indicated in Fig. Clc, the following relationships can be established.

$$a_i = x_j - x_k \tag{C-1}$$

$$b_i = y_k - y_j$$

$$\begin{pmatrix} \zeta_1 \\ \zeta_2 \\ \zeta_3 \end{pmatrix} = \frac{1}{2A} \begin{bmatrix} 2A_{23} & b_1 & a_1 \\ 2A_{31} & b_2 & a_2 \\ 2A_{12} & b_3 & a_3 \end{bmatrix} \begin{pmatrix} 1 \\ x \\ y \end{pmatrix} \tag{C-2}$$

$$\frac{\partial \zeta_i}{\partial x} = \frac{b_i}{2A} \tag{C-3}$$

$$\frac{\partial \zeta_i}{\partial y} = \frac{a_i}{2A}$$

$$\frac{\partial \zeta_j}{\partial m_i} = \frac{d_i - l_i}{2A} \quad \frac{\partial \zeta_k}{\partial m_i} = -\frac{d_i}{2A} \quad \frac{\partial \zeta_i}{\partial m_i} = l_i \tag{C-4}$$

and for, $f = f(\zeta_1, \zeta_2, \zeta_3)$,

$$\frac{\partial f}{\partial m_i} = \frac{1}{2A} \left[l_i \frac{\partial f}{\partial \zeta_i} + (d_i - l_i) \frac{\partial f}{\partial \zeta_j} - d_i \frac{\partial f}{\partial \zeta_k} \right] \text{ (no sum)} \tag{C-5}$$

and

$$\frac{\partial f}{\partial x} = \frac{b_i}{2A} \frac{\partial f}{\partial \xi_i}$$

(C-6)

$$\frac{\partial f}{\partial y} = \frac{a_i}{2A} \frac{\partial f}{\partial \xi_i}$$

where i, j, k are any cyclic combination of 1, 2, 3, A_{ij} is the area of the triangle formed by connecting the origin and the points i and j ; and d_i is defined in Fig. Clc.

The displacement functions used in displacement models for most finite element work consist of linear combinations of polynomials. A linear combination of polynomials in x and y , will not be independent of the orientation of element (i.e., invariant) unless it contains all product terms that are homogeneous to the particular order under consideration. In addition, lower order terms usually must be included if the completeness requirement is to be satisfied (i.e., rigid body modes and uniform strain states). For this reason a systematic method of obtaining displacement functions should be based on linear combinations of the terms in a complete polynomial (here we use the word "complete" in its mathematical sense). There are $\frac{(n+1)(n+2)}{2}$ terms in such a complete polynomial in a two dimensional space. Therefore any linear combination of $\frac{(n+1)(n+2)}{2}$ independent polynomials of degree less than or equal to n forms the complete polynomial of order n . Polynomials in triangular co-ordinates have the property that a linear combination of all terms that are homogeneous of order n , forms the (mathematically) complete polynomial of order n . To construct an n th order displacement function it is only necessary therefore to select $\frac{(n+1)(n+2)}{2}$ nodal points and use the interpolation functions

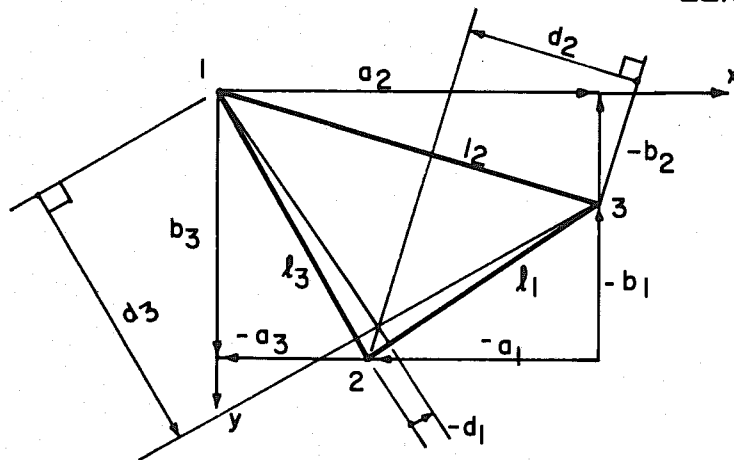
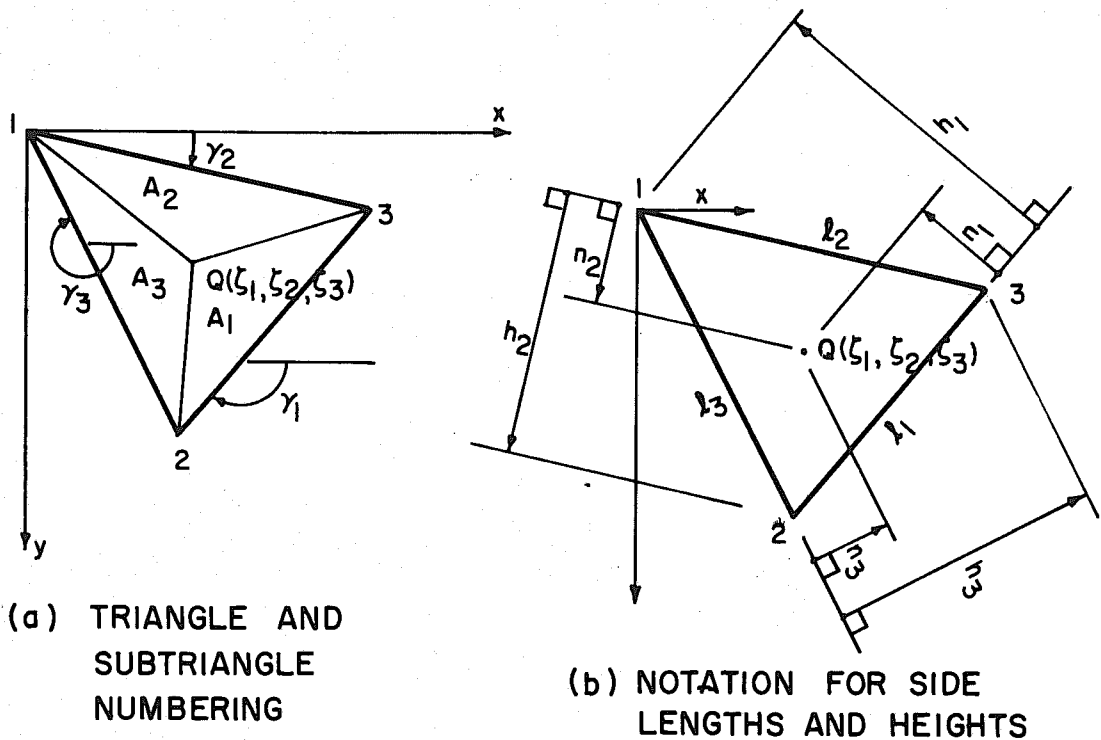


FIG. C1 - DEFINITION OF TRIANGULAR GEOMETRY

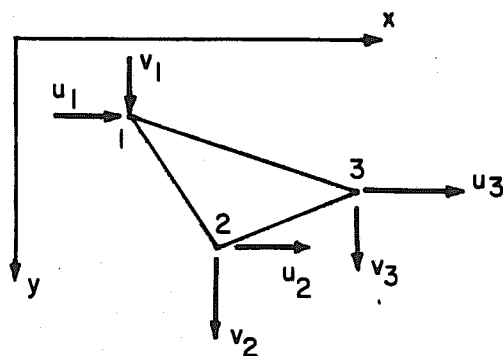


FIG. C2 - NODAL DISPLACEMENTS FOR CST

associated with these points as the shape functions associates with the displacement of these points. These polynomials are automatically linearly independent and the generalized co-ordinates are then the physical nodal displacements. In practice it is often desirable to use two or more physical displacement quantities (i.e., displacement and slope) associated with the same node rather than associate each shape function with a separate node. Interpolation functions of this type are called Hermitian polynomials [12].

C.2 Evaluation of the Stiffness Matrix for In-Plane Deformations

The simplest type of displacement field that can be used for in-plane deformations is a linear displacement field. A complete linear polynomial has $\frac{(1+1)(1+2)}{2} = 3$ independent terms. The nodal system is selected as the three corner points 1, 2, 3 of the triangle as illustrated in Fig. C2. The interpolation functions associated with these corners are ζ_1 , ζ_2 , and ζ_3 , respectively. Consider now the \tilde{u} displacement field. It is specified as the linear combination

$$\tilde{u} = \langle \zeta_1 \quad \zeta_2 \quad \zeta_3 \rangle \begin{Bmatrix} u_1 \\ u_2 \\ u_3 \end{Bmatrix} = \{\zeta\}^T \{u\}. \quad (C-7)$$

Similarly the \tilde{v} displacement is specified as

$$\tilde{v} = \langle \zeta_1 \quad \zeta_2 \quad \zeta_3 \rangle \begin{Bmatrix} v_1 \\ v_2 \\ v_3 \end{Bmatrix} = \{\zeta\}^T \{v\}. \quad (C-8)$$

We can therefore identify the set of interpolation functions $\{\varphi_u\}$ and $\{\varphi_v\}$ of the equations (2-15), section 2-4, with the interpolation vector $\{\zeta\}$ appearing in equations (C-7) and (C-8).

Referring to equation (2-19) and the relations (C-3) we evaluate

$$\{\varphi_{u,x}\}^T = \frac{\partial}{\partial x} \{\xi\}^T = \frac{1}{2A} \langle b_1 \quad b_2 \quad b_3 \rangle$$

and

$$\{\varphi_{u,y}\}^T = \frac{\partial}{\partial y} \{\xi\}^T = \frac{1}{2A} \langle a_1 \quad a_2 \quad a_3 \rangle.$$

Equation (2-19) therefore becomes

$$\{\tilde{\epsilon}_o\} = \frac{1}{2A} \begin{bmatrix} b_1 & b_2 & b_3 & \cdot & \cdot & \cdot \\ \cdot & \cdot & \cdot & a_1 & a_2 & a_3 \\ a_1 & a_2 & a_3 & b_1 & b_2 & b_3 \end{bmatrix} \begin{Bmatrix} \{u\} \\ \{v\} \end{Bmatrix} \quad (\text{C-9})$$

which identifies the matrix $[\tilde{B}_p]$.

Referring now to the evaluation of matrix $[K_p]$ in section 2.5, the matrix $[\tilde{N}]$ can be evaluated as it appears in equation (2-28). We use the constitutive relation for plane stress to obtain

$$[\tilde{N}] = \frac{hE}{(1-\nu^2)} \begin{bmatrix} 1 & \nu & \cdot \\ \nu & 1 & \cdot \\ \cdot & \cdot & \frac{1+\nu}{2} \end{bmatrix} \begin{bmatrix} b_1 & b_2 & b_3 & \cdot & \cdot & \cdot \\ \cdot & \cdot & \cdot & a_1 & a_2 & a_3 \\ a_1 & a_2 & a_3 & b_1 & b_2 & b_3 \end{bmatrix} \frac{1}{2A} \quad (\text{C-10})$$

Since the matrix product in (C-10) does not depend on the co-ordinates, the stress resultants are constant throughout the element and may be determined from equation (2-28) for any set of nodal displacements $\{r_p\}$.

The stiffness matrix $[K_p]$, appearing in equation (2-30), section 2.5, is then evaluated as

$$[K_P] = \int_A \frac{1}{2A} \begin{bmatrix} b_1 & \cdot & a_1 \\ b_2 & \cdot & a_2 \\ b_3 & \cdot & a_3 \\ \cdot & a_1 & b_1 \\ \cdot & a_2 & b_2 \\ \cdot & a_3 & b_3 \end{bmatrix} [\tilde{N}] dA \quad (C-11)$$

Since the integrand is composed of constants, integration over the area simply amounts to multiplying the matrix product in equation (C-11) by the area of the triangle.

C.3 Evaluation of Stiffness Matrix for Out-of-Plane Deformations

The evaluation of stiffness for out-of-plane deformations is a complex task and therefore only an outline is presented here. The reader is referred to Felippa [3] for a more detailed development.

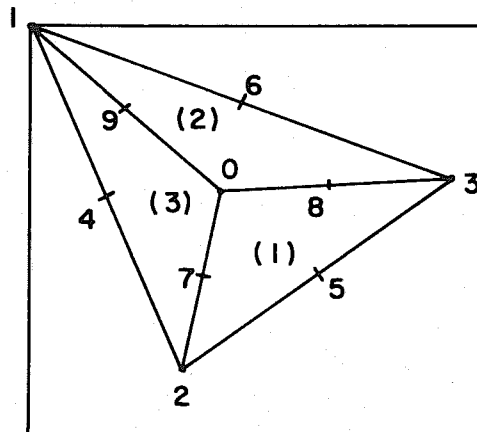
The deflected shape of a beam with a linear variation of moment is a cubic curve. In order to adequately express the deflected shape of an element subjected to different moments at the corners, a cubic polynomial therefore appears to be the minimum expansion. However difficulties arise in maintaining normal slope compatibility with only $\frac{(3+1)(3+2)}{2} = 10$ degrees of freedom. The evolution of a triangular compatible bending element took a number of years and the reader is referred to Clough and Tocher [10] and to Felippa [3] for an account of this period. The simplest solution to the problem requires that a linear variation of normal slope be maintained along the edges. However this cannot be achieved with a single cubic polynomial. The triangle was therefore divided into three sub-triangles as shown in Fig. C3a, and a separate expansion was used in each

subtriangle. The expansion maintained linear variation of normal slope along the particular edge of the subtriangle which was an outside edge of the complete triangle. Although continuity of slope can be maintained along the interior interfaces 1-0, 2-0, and 3-0, there is a discontinuity in curvature along these lines. We outline a development of this stiffness matrix using the technique of Felippa.

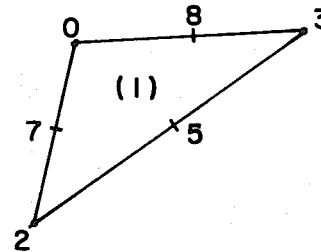
The corners of each subtriangle are mentally numbered so that corner 3 corresponds to node 0 of the complete triangle. In each subtriangle a cubic expansion is desired. This requires 10 degrees of freedom in the subtriangle which in turn requires 10 nodal displacements. The most convenient nodal displacements are those illustrated in Fig. C3c. The interpolation functions associated with these nodal displacements, for subtriangle k , are [3][†]

$$\{\phi_{w1}^k\} = \left[\begin{array}{l} \zeta_1^2(3-2\zeta_1) + 6\mu_3 \zeta_1 \zeta_2 \zeta_3 \\ \zeta_1^2(b_3 \zeta_2 - b_2 \zeta_3) + (b_3 \mu_3 - b_1) \zeta_1 \zeta_2 \zeta_3 \\ \zeta_1^2(a_3 \zeta_2 - a_2 \zeta_3) + (a_3 \mu_3 - a_1) \zeta_1 \zeta_2 \zeta_3 \\ \zeta_2^2(3-2\zeta_2) + 6\lambda_3 \zeta_1 \zeta_2 \zeta_3 \\ \zeta_2^2(b_1 \zeta_3 - b_3 \zeta_1) + (b_2 - b_3 \lambda_3) \zeta_1 \zeta_2 \zeta_3 \\ \zeta_2^2(a_1 \zeta_3 - a_3 \zeta_1) + (a_2 - a_3 \lambda_3) \zeta_1 \zeta_2 \zeta_3 \\ \zeta_3^2(3-2\zeta_3) \\ \zeta_3^2(b_2 \zeta_1 - b_1 \zeta_2) \\ \zeta_3^2(a_2 \zeta_1 - a_1 \zeta_2) \\ -4h_3 \zeta_1 \zeta_2 \zeta_3 \end{array} \right]^k$$

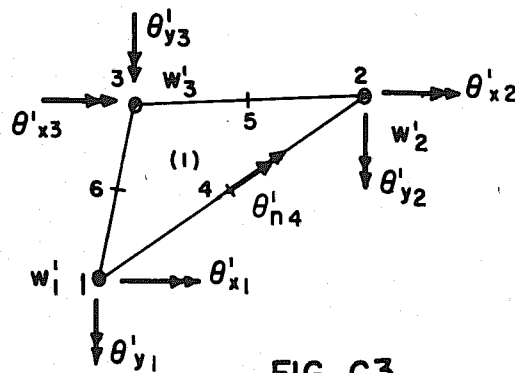
[†] A technique for determining these interpolation functions is described in Appendix D.4.



(a) COMPLETE TRIANGLE



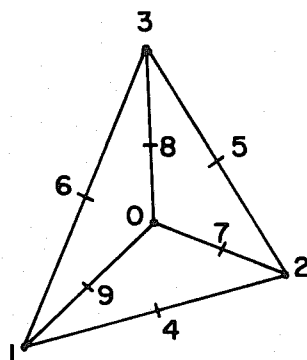
(b) SUBTRIANGLE (1) WITH "COMPLETE TRIANGLE" LETTERING



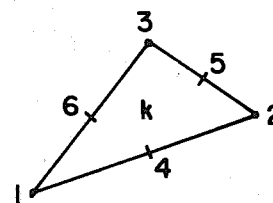
(c) SUBTRIANGLE (1) WITH "SUBTRIANGLE" NUMBERING AND SUBTRIANGLE NODAL DISPLACEMENTS

FIG. C3

NUMBERING SYSTEMS FOR STIFFNESS DERIVATION



(a) COMPLETE TRIANGLE



(b) SUBTRIANGLE NUMBERING SYSTEM

FIG. C4

NUMBERING SYSTEMS FOR GEOMETRIC STIFFNESS DERIVATION

where the nodal vector for the subtriangle is

$$\{r_{BI}^k\}^T = \langle w_1 \quad \theta_{x1} \quad \theta_{y1} \quad w_2 \quad \theta_{x2} \quad \theta_{y2} \quad w_3 \quad \theta_{x3} \quad \theta_{y3} \quad \theta_{n4} \rangle^k$$

and the displacement field within the subtriangle is given by

$$\tilde{w} = \{\psi_{w1}^k\}^T \{r_{BI}^k\}. \quad (C-12)$$

All co-ordinates and the other triangular parameters in equations (C-12) are referred to the subtriangle k . The undefined terms may be specified, with reference to Fig. C1c, as

$$\mu_i = \frac{l_i - d_i}{l_i} \quad \lambda_i = \frac{d_i}{l_i}$$

Since we desire the variation of normal slope to be linear along the edge containing nodal point 4, the nodal displacement θ_{n4} is set equal to $\frac{1}{2}(\theta_{n1} + \theta_{n2})$. Since θ_{n1} and θ_{n2} can be expressed in terms of θ_{x1} , θ_{y1} , θ_{x2} , θ_{y2} , this yields

$$\{\psi_w^k\} = \left[\begin{array}{l} \zeta_1^2 (3 - 2\zeta_1) + 6\mu_3 \zeta_1 \zeta_2 \zeta_3 \\ \zeta_1^2 (b_3 \zeta_2 - b_2 \zeta_3) + (b_3 \mu_3 - b_1 - 2h_3 S_3) \zeta_1 \zeta_2 \zeta_3 \\ \zeta_1^2 (a_3 \zeta_2 - a_2 \zeta_3) + (a_3 \mu_3 - a_1 + 2h_3 C_3) \zeta_1 \zeta_2 \zeta_3 \\ \zeta_2^2 (3 - 2\zeta_2) + 6\lambda_3 \zeta_1 \zeta_2 \zeta_3 \\ \zeta_2^2 (b_1 \zeta_3 - b_3 \zeta_1) + (b_2 - b_3 \lambda_3 - 2h_3 S_3) \zeta_1 \zeta_2 \zeta_3 \\ \zeta_2^2 (a_1 \zeta_3 - a_3 \zeta_1) + (a_2 - a_3 \lambda_3 + 2h_3 C_3) \zeta_1 \zeta_2 \zeta_3 \\ \zeta_3^2 (3 - 2\zeta_3) \\ \zeta_3^2 (b_2 \zeta_1 - b_1 \zeta_2) \\ \zeta_3^2 (a_2 \zeta_1 - a_1 \zeta_2) \end{array} \right]^k \quad (C-13)$$

where S_3 and C_3 are $\sin \gamma_3$, $\cos \gamma_3$ of the subtriangle, respectively, (Fig. Cla), and where the nodal vector of the subtriangle now is

$$\{r_B^k\}^T = \langle \omega, \theta_{x1}, \theta_{y1}, \omega_2, \theta_{x2}, \theta_{y2}, \omega_3, \theta_{x3}, \theta_{y3} \rangle^k \quad (C-14)$$

and the displacement field within the subtriangle is given by

$$\tilde{w} = \{\phi_w^k\}^T \{r_B^k\}.$$

We now assemble the three subtriangles together in such a way that the normal slopes along the interfaces 1-0, 2-0, and 3-0 are compatible. This is done by (a) identifying the corner slopes of the subtriangles with the corner slopes of the main triangle, and (b) determining and equating the normal slopes of adjacent subtriangles at the mid-points of their interfaces. The latter operation leads to the equations

$$\begin{aligned} \left(\frac{\partial w}{\partial n}\right)'_5 + \left(\frac{\partial w}{\partial n}\right)^2_6 &= 0 \\ \left(\frac{\partial w}{\partial n}\right)^2_5 + \left(\frac{\partial w}{\partial n}\right)^3_6 &= 0 \\ \left(\frac{\partial w}{\partial n}\right)^3_5 + \left(\frac{\partial w}{\partial n}\right)'_6 &= 0 \end{aligned} \quad (C-15)$$

where the superscript is the subtriangle number and the subscript is the subtriangle nodal point. These three equations can be expressed in matrix form after identifying the subtriangle displacements with the nodal point displacements of the complete triangle. We express the relationship as

$$\begin{bmatrix} Q_1 & | & Q_0 \\ \hline 3 \times 9 & & 3 \times 3 \end{bmatrix} \begin{Bmatrix} \{r_B\} \\ \{r_0\} \end{Bmatrix} = 0, \quad (C-16)$$

12x1

where $\{r_B\}$ is the nodal vector appearing in equation (2-25) section 2.4

and $\{r_0\}^T = \langle w_0 \theta_{x0} \theta_{y0} \rangle$. This equation can be solved to determine $\{r_0\}$ in terms of $\{r_B\}$.

$$\{r_0\} = - [Q_0]^{-1} [Q_1] \{r_B\}. \quad (C-17)$$

We are now in a position to develop the stiffness matrix of the element in terms of the 12 nodal degrees of freedom associated with points 1, 2, 3 and 0 and then reduce it to one for only nine degrees of freedom by using equations (C-17).

Referring to section 2.6 the relationships which we desire were specified by the equations

$$\begin{aligned} \{\tilde{m}\} &= \int_{-\frac{h}{2}}^{\frac{h}{2}} z^2 [\tilde{C}] \{\tilde{\epsilon}\} dz \\ &= \int_{-\frac{h}{2}}^{\frac{h}{2}} z^2 [\tilde{C}] [\tilde{B}_B] dz \{r_B\} = [\tilde{M}] \{r_B\}, \end{aligned} \quad (2-33)$$

and

$$[K_B] = \int_A [\tilde{B}_B]^T [\tilde{M}] dA, \quad (2-34)$$

where $[\tilde{B}_B]$ arises in the equation

$$\{\tilde{\epsilon}\} = \begin{bmatrix} \{\varphi_{w,xx}\}^T \\ \{\varphi_{w,yy}\}^T \\ \{2\varphi_{w,xy}\}^T \end{bmatrix} \{r_B\} = [\tilde{B}_B] \{r_B\}. \quad (2-20)$$

Since the interpolation functions $\{\varphi_w\}$ are cubic functions, the second derivatives of these functions are linear functions. The labor involved in evaluating the integrals in (2-33) and (2-34) can be considerably reduced if we recognize this fact. We have also seen that the shape functions are independently specified over each of the three subtriangles. The

stiffness matrix can therefore be derived more easily by returning to the basic work equation in the form of equation (2-24), section 2.4. The matrix $[K_B]$ arises from the last term of this equation and, from equation (2-23), this relationship can be written as

$$\{r_B^*\}^T [K_B] \{r_B\} = \int_V z^2 \{\tilde{x}^*\}^T [C] \{\tilde{x}\} dV. \quad (C-18)$$

Also from equation (2-32) of section 2.6 we have the relation

$$\{\tilde{m}\} = \int_{-\frac{h}{2}}^{\frac{h}{2}} z^2 [\tilde{C}] \{\tilde{x}\} dz. \quad (C-19)$$

Therefore equation (C-18) can be written in the form

$$\{r_B^*\}^T [K_B] \{r_B\} = \int_A \{\tilde{x}^*\}^T \{\tilde{m}\} dA \quad (C-20)$$

$$= \sum_{k=1}^3 \int_{A_k} \{\tilde{x}^{k*}\}^T \{m^k\} dA. \quad (C-21)$$

To evaluate this summation, consider first a typical subtriangle. Since the variation of curvature over this subtriangle is linear, the variation of moment will also be linear if $[\tilde{C}]$ is not a function of position in the element. We can therefore write[†]

[†] The superscript, k , will be dropped from the $\{\zeta\}$ vector in all expressions subsequent to equation (C-22) but should be understood to be present. All numerical superscripts appearing on ζ will be exponents. Superscripts on other quantities will indicate the subtriangle number.

$$\{\tilde{x}^k\} = \begin{bmatrix} \{\psi^k\}^T & \cdot & \cdot \\ \cdot & \{\psi^k\}^T & \cdot \\ \cdot & \cdot & \{\psi^k\}^T \end{bmatrix} \begin{Bmatrix} \{x_{xx}^k\} \\ \{x_{yy}^k\} \\ \{2x_{xy}^k\} \end{Bmatrix} \quad (C-22)$$

3×1 3×9 9×1

where $\{\tilde{x}^k\}^T = \langle \tilde{x}_{xx}^k \quad \tilde{x}_{yy}^k \quad 2\tilde{x}_{xy}^k \rangle$,

$$\{x_{xx}^k\}^T = \langle x_{xx1}^k \quad x_{xx2}^k \quad x_{xx3}^k \rangle,$$

and 1, 2, 3, indicate values at the respective nodal points of the sub-triangle. Expressions for $\{x_{yy}^k\}$ and $\{x_{xy}^k\}$ are similar to $\{x_{xx}^k\}$. Similarly

$$\{\tilde{m}^k\} = \begin{bmatrix} \{\psi\}^T & \cdot & \cdot \\ \cdot & \{\psi\}^T & \cdot \\ \cdot & \cdot & \{\psi\}^T \end{bmatrix} \begin{Bmatrix} \{m_{xx}^k\} \\ \{m_{yy}^k\} \\ \{m_{xy}^k\} \end{Bmatrix}$$

3×1 3×9 9×1

Then

$$\int_{A_k} \{\tilde{x}^{*k}\}^T \{\tilde{m}^k\} dA =$$

$$\langle \{x_{xx}^{*k}\}^T \{x_{yy}^{*k}\}^T \{2x_{xy}^{*k}\}^T \rangle \int_{A_k} \begin{bmatrix} \{\psi\} \cdot \cdot \\ \cdot \{\psi\} \cdot \\ \cdot \cdot \{\psi\} \end{bmatrix} \begin{bmatrix} \{\psi\}^T \cdot \cdot \\ \cdot \{\psi\}^T \cdot \\ \cdot \cdot \{\psi\}^T \end{bmatrix} dA \begin{Bmatrix} \{m_{xx}^k\} \\ \{m_{yy}^k\} \\ \{m_{xy}^k\} \end{Bmatrix}$$

$$= \langle \{x_{xx}^{*k}\}^T \{x_{yy}^{*k}\}^T \{2x_{xy}^{*k}\}^T \rangle \begin{bmatrix} [Q] \cdot \cdot \\ \cdot [Q] \cdot \\ \cdot \cdot [Q] \end{bmatrix} \begin{Bmatrix} \{m_{xx}^k\} \\ \{m_{yy}^k\} \\ \{m_{xy}^k\} \end{Bmatrix} \quad (C-23)$$

where

$$[Q] = \frac{A^k}{12} \begin{bmatrix} 2 & 1 & 1 \\ 1 & 2 & 1 \\ 1 & 1 & 2 \end{bmatrix} .$$

Rearranging the order of the nodal quantities, we define the vectors

$$\begin{aligned} & \langle \underbrace{\{m_1^k\}^T}_{1 \times 3} \underbrace{\{m_2^k\}^T}_{1 \times 3} \underbrace{\{m_3^k\}^T}_{1 \times 3} \rangle \\ & = \langle m_{2x1}^k \quad m_{2y1}^k \quad m_{2z1}^k \mid m_{2x2}^k \quad m_{2y2}^k \quad m_{2z2}^k \mid m_{2x3}^k \quad m_{2y3}^k \quad m_{2z3}^k \rangle . \end{aligned}$$

A similar definition holds for \mathcal{X} .

Equation (C-23) can then be written as

$$\begin{aligned} & \int_{A_k} \{\tilde{\mathcal{X}}^{k*}\}^T \{\tilde{m}^k\} dA = \\ & \langle \{\mathcal{X}_1^{k*}\}^T \{\mathcal{X}_2^{k*}\}^T \{\mathcal{X}_3^{k*}\}^T \rangle \frac{A_k}{12} \begin{bmatrix} 2I_3 & I_3 & I_3 \\ I_3 & 2I_3 & I_3 \\ I_3 & I_3 & 2I_3 \end{bmatrix} \begin{Bmatrix} \{m_1^k\} \\ \{m_2^k\} \\ \{m_3^k\} \end{Bmatrix} . \end{aligned} \quad (C-24)$$

We now perform the addition indicated in (C-21). In doing this it is necessary to recognize that the curvature and moments at the center node will be the same for each subtriangle once conditions (C-15) have been imposed [3]. Define the nodal vectors for the complete triangle as

$$\{\mathcal{X}\}^T = \langle \{\mathcal{X}_1^3\}^T \{\mathcal{X}_2^3\}^T \{\mathcal{X}_1^1\}^T \{\mathcal{X}_2^1\}^T \{\mathcal{X}_1^2\}^T \{\mathcal{X}_2^2\}^T \{\mathcal{X}_0\}^T \rangle$$

and

$$\{m\}^T = \langle \{m_1^3\}^T \{m_2^3\}^T \{m_1^1\}^T \{m_2^1\}^T \{m_1^2\}^T \{m_2^2\}^T \{m_0\}^T \rangle .$$

Equation (C-20) then becomes

$$\int_A \{\tilde{x}^{*T}\} \{m\} dA = \{x^{*T}\} \frac{A}{36} \begin{bmatrix} 2I_3 & I_3 & & & & & I_3 \\ I_3 & 2I_3 & & & & & I_3 \\ & & 2I_3 & I_3 & & & I_3 \\ & & I_3 & 2I_3 & & & I_3 \\ & & & & 2I_3 & I_3 & I_3 \\ & & & & I_3 & 2I_3 & I_3 \\ I_3 & I_3 & I_3 & I_3 & I_3 & I_3 & 6I_3 \end{bmatrix} \{m\} \quad (C-25)$$

$$= \{x^{*T}\} \underset{21 \times 21}{[\bar{Q}]} \{m\}. \quad (C-26)$$

and this equation defines the matrix $[\bar{Q}]$.

Equation (2-33) can be used at each node to relate moment to curvature

$$\{m_i^k\} = \frac{h^3}{12} [C] \{x_i^k\}.$$

Therefore, for a constant constitutive relation,

$$\{m\} = \frac{h^3}{12} \begin{bmatrix} [C] & & & & & & \\ & [C] & & & & & \\ & & [C] & & & & \\ & & & [C] & & & \\ & & & & [C] & & \\ & & & & & [C] & \\ & & & & & & [C] \end{bmatrix} = \underset{21 \times 21}{[\bar{C}]} \{x\} \quad (C-27)$$

which defines the matrix $[\bar{C}]$. Using relations (C-3) to differentiate equation (C-13) and evaluating at the corners of the subtriangle, the curvatures $\{x_1^k\}$, $\{x_2^k\}$ and $\{x_3^k\}$ can be evaluated in terms of $\{r_B^k\}$.

Identifying the elements of $\{r_B^k\}$ with the nodal displacements of the main triangle yields an expression of the form

$$\{X\} = \begin{bmatrix} B_e & | & B_o \\ \hline 2 \times 9 & & 2 \times 3 \end{bmatrix} \begin{Bmatrix} \{r_B\} \\ \{r_o\} \end{Bmatrix}.$$

Using relation (C-17) this equation becomes

$$\{X\} = \begin{bmatrix} [B_e] - [Q_o]^{-1}[Q][B_o] \\ \hline 2 \times 9 \end{bmatrix} \{r_B\} = [B] \{r_B\} \quad (C-28)$$

which defines the matrix [B].

Substituting (C-28) into (C-27) gives the nodal moments in terms of the element displacements $\{r_B\}$. Combining (C-27) and (C-28) with (C-26), and identifying the product with equation (C-20), yields

$$\{r_B^*\}^T [K_B] \{r_B\} = \{r_B^*\}^T [B]^T [\bar{Q}] [\bar{C}] [B] \{r_B\}$$

or

$$[K_B] = [B]^T [\bar{Q}] [\bar{C}] [B]. \quad (C-29)$$

The bending stiffness matrix has therefore been determined.

C.4 Evaluation of Geometric Stiffness Matrix for Influence of In-Plane Forces on Bending Stiffness

In section 3.3, the geometric stiffness was approximated as[†]

$$[K_G] = \int_A \sum_{\alpha=1}^2 \sum_{\beta=1}^2 \begin{bmatrix} \cdot & \cdot & \cdot \\ \cdot & \cdot & \cdot \\ \cdot & \cdot & \{ \psi_{\omega,\alpha} \} N_{\alpha\beta} \{ \psi_{\omega,\beta} \}^T \end{bmatrix} dA. \quad (3-13)$$

[†] Throughout this section the summation convention is suppressed.

The purpose of this section is to evaluate this expression for the particular finite element model under consideration.

The nonzero terms in equation (3-13) are associated with the nodal vector $\{r_B\}$ and the virtual work expression associated with these terms is

$$\begin{aligned} & \{r_B^*\}^T \{R_B\} \\ &= \{r_B^*\}^T \left[\int_A \sum_{\alpha=1}^2 \sum_{\beta=1}^2 \{\varphi_{w,\alpha}\} N_{\alpha\beta} \{\varphi_{w,\beta}\}^T dA \right] \{r_B\} \end{aligned} \quad (C-30)$$

$$= \int_A \sum_{\alpha=1}^2 \sum_{\beta=1}^2 \tilde{w}_{,\alpha}^* N_{\alpha\beta} \tilde{w}_{,\beta} dA. \quad (C-31)$$

Recalling that the displacement functions are independently specified over each subtriangle, the virtual work can be evaluated by considering each subtriangle independently and then summing. Therefore

$$\{r_B^*\}^T \{R_B\} = \sum_{k=1}^3 \int_{A_k} \sum_{\alpha=1}^2 \sum_{\beta=1}^2 \tilde{w}_{,\alpha}^k N_{\alpha\beta} \tilde{w}_{,\beta}^k dA_k. \quad (C-32)$$

Now $\{w^k\}$ is specified by the product of the nodal displacements $\{r_B^k\}$ and the interpolation functions $\{\varphi_w^k\}$ of equation (C-13). Since these interpolation functions are cubic polynomials, the slope can be expressed as a linear combination of quadratic polynomials. A quadratic polynomial has $\frac{(2+1)(2+2)}{2} = 6$ independent terms. The nodal system in Fig. C4b is selected as the most convenient for representing this quadratic variation for a typical subtriangle k . Since the $N_{\alpha\beta}$ do not vary throughout

the element they may be treated as constants throughout.

The interpolation functions for this nodal system will be defined as $\{\varphi_s^k\}$, where

$$\{\varphi_s^k\} = \begin{Bmatrix} \zeta_1 (2\zeta_1 - 1) \\ \zeta_2 (2\zeta_2 - 1) \\ \zeta_3 (2\zeta_3 - 1) \\ 4\zeta_1\zeta_2 \\ 4\zeta_2\zeta_3 \\ 4\zeta_3\zeta_1 \end{Bmatrix}^k \quad (C-33)$$

and it is understood that the triangular co-ordinates are those associated with the subtriangle k . The corresponding nodal vector is defined as either $\{w_x\}$ or $\{w_y\}$ where these vectors represent the values of the slope in the x and y directions, respectively, at nodal points 1 through 6. The variation of slope throughout the subelement is therefore expressed by the relation

$$\tilde{w}_{,\alpha}^k = \{\varphi_s^k\}^T \{\omega_\alpha\}. \quad (C-34)$$

The virtual work in one subelement can now be written as

$$\begin{aligned} \{r_B^{k*}\}^T \{R_B^k\} &= \sum_{\alpha=1}^2 \sum_{\beta=1}^2 \int_{A_k} \tilde{w}_{,\alpha}^{k*} N_{\alpha\beta} \tilde{w}_{,\beta}^k dA_k \\ &= \sum_{\alpha=1}^2 \sum_{\beta=1}^2 N_{\alpha\beta} \{\omega_\alpha^{k*}\}^T \int_{A_k} \{\varphi_s^k\} \{\varphi_s^k\}^T dA_k \{\omega_\beta^k\} \end{aligned} \quad (C-35)$$

Carrying out the integration and arranging the summation as a matrix product, equation (C-35) can be written as

$$\begin{aligned}
 & \{r_B^*\}^T \{R_B\} \\
 &= \langle \{\omega_x^{k*}\}^T \{\omega_y^{k*}\}^T \rangle \begin{bmatrix} N_{xx}[L] & N_{xy}[L] \\ N_{yx}[L] & N_{yy}[L] \end{bmatrix} \begin{Bmatrix} \{\omega_x^k\} \\ \{\omega_y^k\} \end{Bmatrix} \quad (C-36)
 \end{aligned}$$

where

$$[L] = \int_{A_k} \{\phi_s^k\} \{\phi_s^k\}^T dA_k = \frac{A_k}{180} \begin{bmatrix} 6 & -1 & -1 & \cdot & -4 & \cdot \\ & 6 & -1 & \cdot & \cdot & -4 \\ & & 6 & -4 & \cdot & \cdot \\ & & & 32 & 16 & 16 \\ \text{SYM.} & & & 32 & 16 & \\ & & & & & 32 \end{bmatrix} \quad (C-37)$$

Identifying the nodal points of the subtriangle with those of the complete triangle (Fig. C.4a) and defining the nodal vectors for the complete triangle as

$$\begin{aligned}
 \{\omega_x\}^T &= \langle \omega_{x1} \ \omega_{x2} \ \omega_{x3} \ \omega_{x4} \ \omega_{x5} \ \omega_{x6} \ \omega_{x7} \ \omega_{x8} \ \omega_{x9} \ \omega_{x0} \rangle \\
 \{\omega_y\}^T &= \langle \omega_{y1} \ \omega_{y2} \ \omega_{y3} \ \omega_{y4} \ \omega_{y5} \ \omega_{y6} \ \omega_{y7} \ \omega_{y8} \ \omega_{y9} \ \omega_{y0} \rangle
 \end{aligned} \quad (C-38)$$

equation (C-30) becomes

$$\begin{aligned}
 & \{r_B^*\}^T \{R_B\} \\
 &= \langle \{\omega_x^*\}^T \{\omega_y^*\}^T \rangle \begin{bmatrix} N_{xx}[L_E] & N_{xy}[L_E] \\ N_{yx}[L_E] & N_{yy}[L_E] \end{bmatrix} \begin{Bmatrix} \{\omega_x\} \\ \{\omega_y\} \end{Bmatrix} \quad (C-39)
 \end{aligned}$$

where

$$[L_E] = \frac{A}{540} \begin{bmatrix} 12 & -1 & -1 & \cdot & \cdot & \cdot & -4 & -4 & \cdot & -2 \\ & 12 & -1 & \cdot & \cdot & \cdot & \cdot & -4 & -4 & -2 \\ & & 12 & \cdot & \cdot & \cdot & -4 & \cdot & -4 & -2 \\ & & & 32 & \cdot & \cdot & 16 & \cdot & 16 & -4 \\ & & & & 32 & \cdot & 16 & 16 & \cdot & -4 \\ & & & & & 32 & \cdot & 16 & 16 & \cdot \\ & & & & & & 64 & 16 & 16 & \cdot \\ & & & & & & & 64 & 16 & \cdot \\ & & & & & & & & 64 & \cdot \\ & & & & & & & & & 18 \end{bmatrix} \quad (C-40)$$

SYM.

The virtual work for the triangle has now been evaluated in terms of the slopes at the nodal points of Fig. C.4a. Since we wish to express this in terms of the nodal displacements, as in equation (C-30), it is now necessary to express the nodal vectors $\{w_x\}$ and $\{w_y\}$ in terms of $\{r_B\}$.

At nodal points 1, 2, 3 of the complete triangle, the slopes appearing in the nodal vectors of equation (C-39) can be identified directly with the nodal rotations. The slopes at point 0 are retained in the nodal vector $\{r_0\}$ [see equation (C-16)] and eliminated later. It is therefore only necessary to evaluate the slopes at nodal points 4 and 5 of each subtriangle to be able to define the nodal vector for the complete triangle. To do this we consider the expression for displacement in a subtriangle, namely

$$\tilde{w}^k = \{\varphi_w^k\}^T \{r_B^k\} \quad (C-41)$$

where $\{\varphi_w^k\}$ and $\{r_B^k\}$ are defined in equations (C-13) and (C-14). Differentiating $\{\varphi_w^k\}$ with respect to x and y results in the expression shown

in Table C1.* Evaluating these expressions at node 4, with co-ordinates $(\frac{1}{2}, \frac{1}{2}, 0)$, and node 5, with co-ordinates $(0, \frac{1}{2}, \frac{1}{2})$, results in the expressions in Table C2. Using these expressions, the slopes for the complete triangle can be expressed by identifying the subtriangle nodal displacements with the nodal displacements of the complete triangle. This results in expressions of the type

$$\{w_x\} = \begin{bmatrix} \bar{W}_{x1} & \bar{W}_{x0} \\ 10 \times 9 & 10 \times 3 \end{bmatrix} \begin{Bmatrix} \{r_B\} \\ \{r_0\} \end{Bmatrix} \quad (C-42)$$

12×1

where $\{r_B\}$ and $\{r_0\}$ are defined as in (C-16). Using equation (C-17) to eliminate $\{r_0\}$ we obtain finally the results

$$\begin{aligned} \{w_x\} &= [W_x] \{r_B\} \\ 10 \times 1 & \quad 10 \times 9 \quad 9 \times 1 & (C-43) \\ \{w_y\} &= [W_y] \{r_B\} \end{aligned}$$

where $[W_x] = [\bar{W}_{x1}] - [\bar{W}_{x0}][Q_0]^{-1}[Q_1]$, and similarly for $[W_y]$.

Substituting equations (C-43) into (C-40) we obtain

$$\{r_B^*\}^T \{R_B\} = \{r_B^*\}^T \begin{bmatrix} [W_x]^T & [W_y]^T \end{bmatrix} \begin{bmatrix} N_{xx}[L_E] & N_{xy}[L_E] \\ N_{yx}[L_E] & N_{yy}[L_E] \end{bmatrix} \begin{bmatrix} [W_x] \\ [W_y] \end{bmatrix} \{r_B\} \quad (C-44)$$

where the matrix product is the evaluation of the nonzero terms in equation (3-13). The geometric stiffness matrix for the influence of in-plane forces on bending stiffness has therefore been determined.

* The relations in Tables C1 and C2 are for a right handed co-ordinate system $x - y - z$, with the z axis directed vertically upward.

TABLE C1

DERIVATIVES OF THE INTERPOLATING FUNCTION $\{\varphi_w\}$

(a)	$2A_k \frac{\partial \{\varphi_w\}}{\partial x} = \underline{b_1} \frac{\partial \{\varphi_w\}}{\partial \xi_1} + \underline{b_2} \frac{\partial \{\varphi_w\}}{\partial \xi_2} + \underline{b_3} \frac{\partial \{\varphi_w\}}{\partial \xi_3}$
	$\underline{b_1} \{2\xi_1(3-2\xi_1) - 2\xi_1^2 + 6\mu_3 \xi_2 \xi_3\} + \underline{b_2} \{6\mu_3 \xi_1 \xi_2 + \underline{b_3} \cdot 6\mu_3 \xi_1 \xi_2$
	$\underline{b_1} \{2\xi_1(b_3 \xi_2 - b_2 \xi_3) + b_3(\mu_3 - b_1) \xi_2 \xi_3 - 2C_3 h_3 \xi_2 \xi_3\} + \underline{b_2} \{\xi_1^2 b_3 +$
	$(b_3 \mu_3 - b_1) \xi_1 \xi_3 - 2C_3 h_3 \xi_1 \xi_3\} + \underline{b_3} \{-b_2 \xi_1^2 + (b_3 \mu_3 - b_1) \xi_1 \xi_2 - 2C_3 h_3 \xi_1 \xi_2\}$
	$\underline{b_1} \{2\xi_1(a_3 \xi_2 - a_2 \xi_3) + (a_3 \mu_3 - a_1) \xi_2 \xi_3 - 2S_3 h_3 \xi_2 \xi_3\} + \underline{b_2} \{\xi_1^2 a_3 +$
	$(a_3 \mu_3 - a_1) \xi_1 \xi_3 - 2S_3 h_3 \xi_1 \xi_3\} + \underline{b_3} \{-a_2 \xi_1^2 + (a_3 \mu_3 - a_1) \xi_1 \xi_2 - 2S_3 h_3 \xi_1 \xi_2\}$
	$\underline{b_1} \{6\lambda_3 \xi_1 \xi_2\} + \underline{b_2} \{2\xi_2(3-2\xi_2) - 2\xi_2^2 + 6\lambda_3 \xi_1 \xi_3\} + \underline{b_3} \{6\lambda_3 \xi_1 \xi_2\}$
	$\underline{b_1} \{-b_3 \xi_2^2 + (b_2 - b_3 \lambda_3) \xi_2 \xi_3 - 2C_3 h_3 \xi_2 \xi_3\} + \underline{b_2} \{2\xi_2(b_1 \xi_3 - b_3 \xi_1) +$
	$(b_2 - b_3 \lambda_3) \xi_1 \xi_3 - 2C_3 h_3 \xi_1 \xi_3\} + \underline{b_3} \{b_1 \xi_2^2 + (b_2 - b_3 \lambda_3) \xi_1 \xi_2 - 2C_3 h_3 \xi_1 \xi_2\}$
	$\underline{b_1} \{-a_3 \xi_2^2 + (a_2 - a_3 \lambda_3) \xi_2 \xi_3 - 2S_3 h_3 \xi_2 \xi_3\} + \underline{b_2} \{2\xi_2(a_1 \xi_3 - a_3 \xi_1) +$
	$(a_2 - a_3 \lambda_3) \xi_1 \xi_3 - 2S_3 h_3 \xi_1 \xi_3\} + \underline{b_3} \{a_1 \xi_2^2 + (a_2 - a_3 \lambda_3) \xi_1 \xi_2 - 2S_3 h_3 \xi_1 \xi_2\}$
	$\underline{b_3} \{2\xi_3(3-2\xi_3) - 2\xi_3^2\}$
	$\underline{b_1} \{b_2 \xi_3^2\} + \underline{b_2} \{-b_1 \xi_3^2\} + \underline{b_3} \{2\xi_3(b_2 \xi_1 - b_1 \xi_2)\}$
	$\underline{b_1} \{a_2 \xi_3^2\} + \underline{b_2} \{-a_1 \xi_3^2\} + \underline{b_3} \{2\xi_3(a_2 \xi_1 - a_1 \xi_2)\}$

$$(b) \quad 2A_k \frac{\partial \{\varphi_w\}}{\partial x} = a_1 \frac{\partial \{\varphi_w\}}{\partial \xi_1} + a_2 \frac{\partial \{\varphi_w\}}{\partial \xi_2} + a_3 \frac{\partial \{\varphi_w\}}{\partial \xi_3}$$

These expressions may be obtained by replacing the underlined b_i in (a) with a_i .

TABLE C2

EVALUATION OF DERIVATIVES AT NODAL POINTS 4 AND 5 OF THE SUBTRIANGLES

(a) Expressions for $2A_i \cdot \partial\{\phi_{\omega}^i\}/\partial x$ (a_i) Evaluation at node 4, with co-ordinates $[1/2, 1/2, 0]$

in terms of subtriangle dimensions	in terms of complete triangle dimensions
$\frac{3}{2}(b_1 + \mu_3 b_3)$	$\frac{1}{2}(b_j + \mu_i b_i)$
$\frac{b_3}{4}(b_1 + \mu_3 b_3) - \frac{1}{2} C_3 h_3 b_3$	$\frac{1}{12} b_i (b_j + \mu_i b_i) - \frac{1}{6} C_i h_i b_i$
$\frac{1}{4} a_3 (b_1 + \mu_3 b_3) - \frac{1}{2} S_3 h_3 b_3$	$\frac{1}{12} a_i (b_j + \mu_i b_i) - \frac{1}{6} S_i h_i b_i$
$\frac{3}{2}(b_2 + \lambda_3 b_3)$	$\frac{1}{2}(b_k + \lambda_i b_i)$
$-\frac{1}{4} b_3 (b_2 + \lambda_3 b_3) - \frac{1}{2} C_3 h_3 b_3$	$-\frac{b_i}{12} (b_k + \lambda_i b_i) - \frac{1}{6} C_i h_i b_i$
$-\frac{1}{4} a_3 (b_2 + \lambda_3 b_3) - \frac{1}{2} S_3 h_3 b_3$	$-\frac{a_i}{12} (b_k + \lambda_i b_i) - \frac{1}{6} S_i h_i b_i$
0	0
0	0
0	0

(a_{ii}) Evaluation at node 5, with co-ordinates $[0, 1/2, 1/2]$

in terms of subtriangle dimensions	in terms of complete triangle dimensions
$\frac{3}{2} b_1 \mu_3$	$\frac{1}{6} (1 + \mu_i) (b_j - b_i)$
$\frac{1}{4} b_1 (\mu_3 b_3 - b_1) - \frac{1}{2} C_3 h_3 b_1$	$\frac{1}{36} (b_j - b_i) \{ (2 + \mu_i) b_i - b_j \} - \frac{1}{18} C_i h_i (b_j - b_i)$
$\frac{1}{4} b_1 (\mu_3 a_3 - a_1) - \frac{1}{2} S_3 h_3 b_1$	$\frac{1}{36} (b_j - b_i) \{ (2 + \mu_i) a_i - a_j \} - \frac{1}{18} S_i h_i (b_j - b_i)$
$\frac{3}{2} (b_2 + b_1 \lambda_3)$	$\frac{1}{2} (b_k - b_i) + \frac{1}{6} (b_j - b_i) (1 + \lambda_i)$
$\frac{1}{4} b_1 (3b_2 - b_3 \lambda_3) - \frac{1}{2} C_3 h_3 b_1$	$\frac{1}{12} (b_j - b_i) \{ b_k - \frac{(4 + \lambda_i) b_i}{3} \} - \frac{1}{18} C_i h_i (b_j - b_i)$
$\frac{1}{4} (b_2 a_1 + b_1 a_2) + \frac{b_1}{4} (a_2 - a_3 \lambda_3) - \frac{1}{2} S_3 h_3 b_1$	$\frac{1}{36} \{ (b_k - b_i) (a_j - a_i) + (b_j - b_i) (a_k - a_i) \} + \Omega_x^+$
$\frac{3}{2} b_3$	$\frac{3}{2} b_i$
$-\frac{1}{2} b_1 b_3$	$-\frac{1}{6} b_i (b_j - b_i)$
$-\frac{1}{4} (b_1 a_3 + b_3 a_1)$	$-\frac{1}{12} \{ (b_j - b_i) a_i + (a_j - a_i) b_i \}$

$$+ \Omega_x = \frac{1}{36} (b_j - b_i) \{ a_k - (2 + \lambda_i) a_i \} - \frac{1}{18} S_i h_i (b_j - b_i)$$

TABLE C2 (Continued)

(b) Expressions for $2A_i \partial(\phi_{\sigma}^i)/\partial y$ (b_i) Evaluation at node 4, with co-ordinates [1/2, 1/2, 0]

in terms of subtriangle dimensions	in terms of complete triangle dimensions
$\frac{3}{2}(a_1 + \mu_3 a_3)$	$\frac{1}{2}(a_j + \mu_i a_i)$
$\frac{b_3}{4}(a_1 + \mu_3 a_3) - \frac{1}{2} C_3 h_3 a_3$	$\frac{b_i}{12}(a_j + \mu_i a_i) - \frac{1}{6} C_i h_i a_i$
$\frac{a_3}{4}(a_1 + \mu_3 a_3) - \frac{1}{2} S_3 h_3 a_3$	$\frac{a_i}{12}(a_j + \mu_i a_i) - \frac{1}{6} S_i h_i a_i$
$\frac{3}{2}(a_2 + \lambda_3 a_3)$	$\frac{1}{2}(a_k + \lambda_i a_i)$
$-\frac{b_3}{4}(a_2 + \lambda_3 a_3) - \frac{1}{2} C_3 h_3 a_3$	$-\frac{b_i}{12}(a_k + \lambda_i a_i) - \frac{1}{6} C_i h_i a_i$
$-\frac{a_3}{4}(a_2 + \lambda_3 a_3) - \frac{1}{2} S_3 h_3 a_3$	$-\frac{a_i}{12}(a_k + \lambda_i a_i) - \frac{1}{6} S_i h_i a_i$
0	0
0	0
0	0

(b_{ii}) Evaluating at node 5, with co-ordinates [0, 1/2, 1/2]

in terms of subtriangle dimensions	in terms of complete triangle dimensions
$\frac{3}{2} a_1 \mu_3$	$\frac{1}{6}(1 + \mu_i)(a_j - a_i)$
$\frac{a_1}{4}(\mu_3 b_3 - b_1) - \frac{1}{2} C_3 h_3 a_1$	$\frac{1}{36}(a_j - a_i)\{(2 + \mu_i)b_i - b_j\} - \frac{1}{18} C_i h_i (a_j - a_i)$
$\frac{a_1}{4}(\mu_3 a_3 - a_1) - \frac{1}{2} S_3 h_3 a_1$	$\frac{1}{36}(a_j - a_i)\{(2 + \mu_i)a_i - a_j\} - \frac{1}{18} S_i h_i (a_j - a_i)$
$\frac{3}{2}(a_2 + a_1 \lambda_3)$	$\frac{1}{2}(a_k - a_i) + \frac{1}{6}(1 + \lambda_i)(a_j - a_i)$
$\frac{1}{4}(a_1 b_2 + a_2 b_1) + \frac{a_1}{4}(b_2 - b_3 \lambda_3) - \frac{1}{2} C_3 h_3 a_1$	$\frac{1}{36}\{(a_j - a_i)(b_k - b_i) + (a_k - a_i)(b_j - b_i)\} + \Omega_{\frac{1}{2}}^{\dagger}$
$\frac{a_1}{4}(3a_2 - a_3 \lambda_3) - \frac{1}{2} S_3 h_3 a_1$	$\frac{1}{12}(a_j - a_i)\{a_k - \frac{(4 + \lambda_i)}{3} a_i\} - \frac{S_i h_i}{18}(a_j - a_i)$
$\frac{3}{2} a_3$	$\frac{3}{2} a_i$
$-\frac{1}{4}(a_1 b_3 + a_3 b_1)$	$-\frac{1}{12}\{(a_j - a_i)b_i + (b_j - b_i)a_i\}$
$-\frac{a_1 a_3}{2}$	$-\frac{a_i}{6}(a_j - a_i)$

$$^{\dagger} \Omega_{\frac{1}{2}} = \frac{1}{36}(a_j - a_i)\{b_k - (2 + \lambda_i)b_i\} - \frac{1}{18} C_i h_i (a_j - a_i)$$

APPENDIX D

GEOMETRIC RELATIONSHIPS

In this appendix the methods of determining the local co-ordinate system, transforming nodal rotations, and modifying in-plane displacements are established.

D.1 Establishment of Local Displaced Co-ordinate System[†]

In section 2.7 it was assumed that the orientation of the local displaced co-ordinate system was known. The operations involved in establishing this co-ordinate system are elementary so that only an outline of the procedure is given here. We refer to Fig. 2.6 of section 2.7. The element before and after deformation is shown in this figure. We also refer to the discussion in section 2.2 for the reasons for following the procedure below to establish this local co-ordinate system.

The quantities which are known prior to the establishment of the local system are the nodal displacements and rotations in the global system. We establish the origin of the local displaced system at point 1'. Taking the vector cross product of $\overline{1' - 2'}$ and $\overline{1' - 3'}$ establishes the "reference plane" (i.e., the X-Y plane) and the direction cosines a_{31} , a_{32} , and a_{33} of the Z axis. To establish an orientation of the X axis, bisect line 2' - 3' to establish point Q' and the vector $\overline{1' - Q'}$. Establish the direction cosines of X by making

$$\sin \beta' = \sin \beta$$

[†] The nomenclature of section 2.7 is used throughout sections D.1 and D.2.

as shown in Fig. 2.6. The factor $\sin \beta$ is computed from the original element configuration by locating Q at the midpoint of line 2-3. The direction cosines of the Y axis are then established by making it normal to X and Z.

Notice that the above procedure effectively eliminates the average element rotation about the normal axis. There is no need therefore to restrict the displacement gradients $\partial u/\partial y$ and $\partial y/\partial x$ providing the engineering strains remain small.

A "reference element" 1' - 2'' - 3'', is now constructed in the reference plane, with 2'' and 3'' having the same co-ordinates with respect to X,Y as 2 and 3 have with respect to x, y. The local nodal displacements are then computed as outlined in section 2.7 and represent the displacements 2' - 2'' and 3' - 3'' of Fig. 2.6. (Note that $U_1, V_1, W_1, W_2,$ and W_3 are all zero.)

D.2 Derivation of Transformation of Nodal Rotations

In section 2.7 the transformation of nodal displacements was derived. The transformation of nodal rotations is accomplished by equations (2-41), providing a relationship between the first derivatives can be established. The co-ordinate systems have been defined in section 2.7 and we repeat the basic relationships here.

$$\begin{aligned} X &= X^* + U \\ Y &= Y^* + V \\ Z &= W \end{aligned} \tag{D-1}$$

$$\begin{aligned} \xi &= x + u = x_1 + x^* + u \\ \eta &= y + v = y_1 + y^* + v \\ \zeta &= w \end{aligned} \tag{D-2}$$

$$\begin{aligned} X^* &= x^* & Y^* &= y^* \end{aligned} \tag{D-3}$$

In addition, equations (2-38) can be written as

$$\begin{aligned} X^* + U &= (x^* + u - u_1) a_{11} + (y^* + v - v_1) a_{12} + (w - w_1) a_{13} \\ Y^* + V &= (x^* + u - u_1) a_{21} + (y^* + v - v_1) a_{22} + (w - w_1) a_{23} \quad (\text{D-4}) \\ W &= (x^* + u - u_1) a_{31} + (y^* + v - v_1) a_{32} + (w - w_1) a_{33} \end{aligned}$$

and we assume

$$U = U(X^*, Y^*) \quad V = V(X^*, Y^*) \quad W = W(X^*, Y^*) \quad (\text{D-5})$$

Using relations (D-2), the last of equations (D-4) may be written as

$$W = (\xi - x_1 - u_1) a_{31} + (\eta - y_1 - v_1) a_{32} + (w - w_1) a_{33}. \quad (\text{D-6})$$

Differentiating (D-6) yields

$$\begin{aligned} \frac{\partial W}{\partial X} &= \left(a_{31} + a_{33} \frac{\partial w}{\partial \xi} \right) \frac{\partial \xi}{\partial X} + \left(a_{32} + a_{33} \frac{\partial w}{\partial \eta} \right) \frac{\partial \eta}{\partial X} \\ \frac{\partial W}{\partial Y} &= \left(a_{31} + a_{33} \frac{\partial w}{\partial \xi} \right) \frac{\partial \xi}{\partial Y} + \left(a_{32} + a_{33} \frac{\partial w}{\partial \eta} \right) \frac{\partial \eta}{\partial Y}. \end{aligned} \quad (\text{D-7})$$

To evaluate $\partial \xi / \partial X$, $\partial \eta / \partial X$, $\partial \xi / \partial Y$ and $\partial \eta / \partial Y$ we use equations (D-2) and (2-38) in the form

$$\begin{aligned} \xi &= x_1 + x^* + u \\ &= x_1 + u_1 + a_{11}(X^* + U) + a_{21}(Y^* + V) + a_{31}W. \end{aligned}$$

Differentiating,

$$\begin{aligned} \frac{\partial \xi}{\partial X} &= a_{11} \frac{\partial X^*}{\partial X} + a_{21} \frac{\partial Y^*}{\partial X} + a_{31} \left(\frac{\partial U}{\partial X^*} \frac{\partial X^*}{\partial X} + \frac{\partial U}{\partial Y^*} \frac{\partial Y^*}{\partial X} \right) \\ &\quad + a_{21} \left(\frac{\partial V}{\partial X^*} \frac{\partial X^*}{\partial X} + \frac{\partial V}{\partial Y^*} \frac{\partial Y^*}{\partial X} \right) + a_{31} \frac{\partial W}{\partial X}. \end{aligned} \quad (\text{D-8})$$

Defining

$$\frac{\partial X^*}{\partial X} = X_X^* \qquad \frac{\partial Y^*}{\partial X} = Y_X^*$$

$$\frac{\partial U}{\partial X^*} \frac{\partial X^*}{\partial X} + \frac{\partial U}{\partial Y^*} \frac{\partial Y^*}{\partial X} = U_{XE} \tag{D-9}$$

$$\frac{\partial V}{\partial X^*} \frac{\partial X^*}{\partial X} + \frac{\partial V}{\partial Y^*} \frac{\partial Y^*}{\partial X} = V_{XE}$$

equation (D-8) can be written as

$$\frac{\partial \xi}{\partial X} = a_{11} X_X^* + a_{21} Y_X^* + a_{11} U_{XE} + a_{21} V_{XE} + a_{31} \frac{\partial W}{\partial X}$$

Similarly

$$\frac{\partial \xi}{\partial Y} = a_{11} X_Y^* + a_{21} Y_Y^* + a_{11} U_{YE} + a_{21} V_{YE} + a_{31} \frac{\partial W}{\partial Y}$$

$$\frac{\partial \eta}{\partial X} = a_{12} X_X^* + a_{22} Y_X^* + a_{12} U_{XE} + a_{22} V_{XE} + a_{32} \frac{\partial W}{\partial X} \tag{D-10}$$

$$\frac{\partial \eta}{\partial Y} = a_{12} X_Y^* + a_{22} Y_Y^* + a_{12} U_{YE} + a_{22} V_{YE} + a_{32} \frac{\partial W}{\partial Y}$$

where all terms can be obtained by analogy with definitions (D-9). Substituting equations (D-10) into equations (D-7) and solving for $\partial W/\partial X$ and $\partial W/\partial Y$ yields

$$\frac{\partial W}{\partial X} = \frac{\left\{ \begin{aligned} &(a_{11} X_X^* + a_{21} Y_X^* + a_{11} U_{XE} + a_{21} V_{XE}) (a_{31} + a_{33} \frac{\partial W}{\partial \xi}) \\ &+ (a_{12} X_X^* + a_{22} Y_X^* + a_{12} U_{XE} + a_{22} V_{XE}) (a_{32} + a_{33} \frac{\partial W}{\partial \eta}) \end{aligned} \right\}}{1 - a_{31} (a_{31} + a_{33} \frac{\partial W}{\partial \xi}) - a_{32} (a_{32} + a_{33} \frac{\partial W}{\partial \eta})} \tag{D-11}$$

and

$$\frac{\partial W}{\partial Y} = \frac{\left\{ \begin{aligned} &(a_{11} X_Y^* + a_{21} Y_Y^* + a_{11} U_{YE} + a_{21} V_{YE}) (a_{31} + a_{33} \frac{\partial W}{\partial \xi}) \\ &+ (a_{12} X_Y^* + a_{22} Y_Y^* + a_{12} U_{YE} + a_{22} V_{YE}) (a_{32} + a_{33} \frac{\partial W}{\partial \eta}) \end{aligned} \right\}}{1 - a_{31} (a_{31} + a_{33} \frac{\partial W}{\partial \xi}) - a_{32} (a_{32} + a_{33} \frac{\partial W}{\partial \eta})}$$

Equations (D-11) are the relations we seek but it remains to evaluate $\partial X^*/\partial X$, $\partial Y^*/\partial X$, $\partial X^*/\partial Y$, $\partial Y^*/\partial Y$ which are required in definitions (D-9).

To evaluate these factors we return to equations (D-1). Recognizing that a line $X^* = C$ is a straight line parallel to the X axis in the reference element before deformation, and the line $X = C$ is a straight line parallel to the X axis after deformation (where C is in an arbitrary constant) we differentiate equations (D-1) with respect to X to obtain

$$\frac{\partial X}{\partial X} = 1 = \frac{\partial X^*}{\partial X} + \frac{\partial U}{\partial X^*} \frac{\partial X^*}{\partial X} + \frac{\partial U}{\partial Y^*} \frac{\partial Y^*}{\partial X}$$

$$\frac{\partial Y}{\partial X} = 0 = \frac{\partial Y^*}{\partial X} + \frac{\partial V}{\partial X^*} \frac{\partial X^*}{\partial X} + \frac{\partial V}{\partial Y^*} \frac{\partial Y^*}{\partial X}$$

Solving these equations for $\partial X^*/\partial X$ and $\partial Y^*/\partial X$ yields

$$\frac{\partial X^*}{\partial X} = \frac{1 + \frac{\partial V}{\partial Y^*}}{\left(1 + \frac{\partial U}{\partial X^*}\right)\left(1 + \frac{\partial V}{\partial Y^*}\right) - \frac{\partial U}{\partial Y^*} \frac{\partial V}{\partial X^*}} \quad (D-12)$$

$$\frac{\partial Y^*}{\partial X} = \frac{-\frac{\partial V}{\partial X^*}}{\left(1 + \frac{\partial U}{\partial X^*}\right)\left(1 + \frac{\partial V}{\partial Y^*}\right) - \frac{\partial U}{\partial Y^*} \frac{\partial V}{\partial X^*}}$$

Similarly

$$\frac{\partial X^*}{\partial Y} = \frac{-\frac{\partial U}{\partial Y^*}}{D}$$

and

$$\frac{\partial Y^*}{\partial Y} = \frac{1 + \frac{\partial U}{\partial X^*}}{D}$$

where D is the denominator appearing in equations (D-12).

The transformation equations above are valid for any shape of element and any set of shape functions. (See footnote in section 2.7.)

If we refer to Appendix C for the shape functions used in this analysis,

$$U = \langle \xi_1 \quad \xi_2 \quad \xi_3 \rangle \begin{Bmatrix} U_1 \\ U_2 \\ U_3 \end{Bmatrix} \quad V = \langle \xi_1 \quad \xi_2 \quad \xi_3 \rangle \begin{Bmatrix} V_1 \\ V_2 \\ V_3 \end{Bmatrix} .$$

The values of $\partial U/\partial X^*$, etc., can therefore be evaluated at the nodes in terms of the local nodal displacements, as

$$\frac{\partial U}{\partial X^*} = \frac{1}{2A} \langle b_1 \quad b_2 \quad b_3 \rangle \begin{Bmatrix} U_1 \\ U_2 \\ U_3 \end{Bmatrix} .$$

The quantities $\partial V/\partial X^*$, $\partial U/\partial Y^*$ and $\partial V/\partial Y^*$ are evaluated in the same way and the equations for transformation of nodal slopes have therefore been completely defined.

D.3 Modification of In-Plane Displacements

In applying this finite element analysis to solution of problems it was found that a reasonable estimate of membrane forces could not be obtained for all problems unless a correction was introduced for the difference between arc length and chord length in the deformed element. This modification is only required for certain element layouts.

We illustrate this by referring to Example 1 of section 2.11. The layout of the problem is given in Fig. D1. Two subdivisions are shown. Results from layout 1 were completely satisfactory for large curvatures. However the same problem, when solved using layout 2 produced high compressive membrane stresses in the shaded elements and high tensile membrane stresses in the unshaded elements. An examination of Fig. D1d indicates

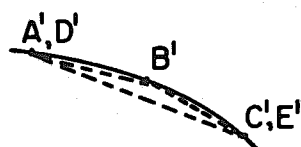
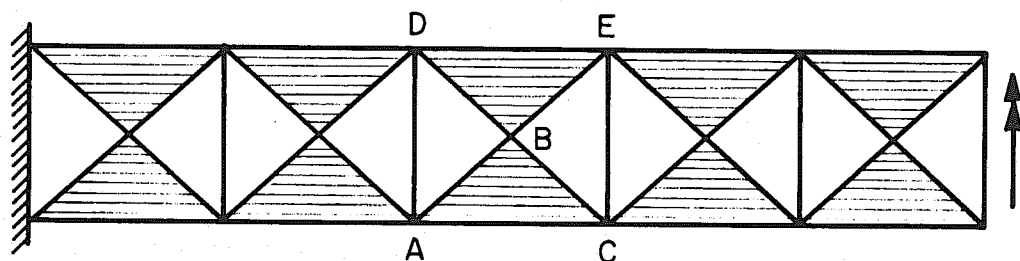
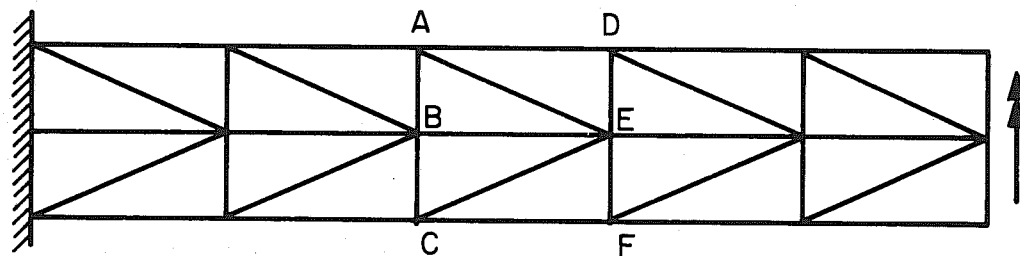


FIG. D1 - CANTILEVER SUBJECTED TO PURE MOMENT

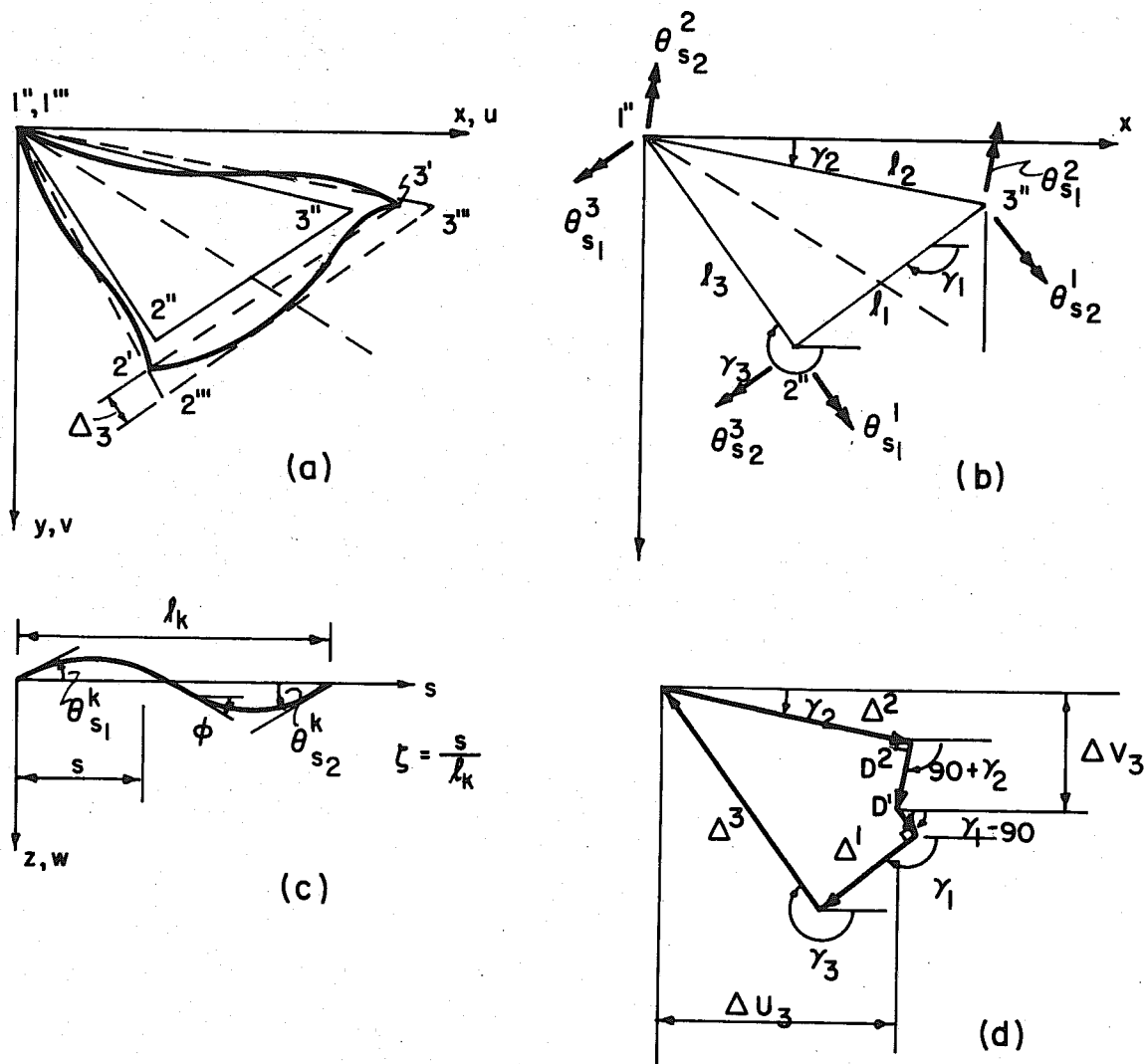


FIG. D2 MODIFICATION OF IN-PLANE DEFORMATIONS

the reason for this discrepancy. Given the proper location of points A', B', C', the difference between the chord length and arc length is much greater for A' C' than for A' B'. Since in-plane deformation is computed with respect to a flat element, this effect would induce a greater compressive stress in elements ABC and DBE than in ABD and CBE. Subsequent iteration produces a set of self balancing internal stresses of which the stress pattern referred to above is characteristic.

The effect is not present in layout 1 since the shortening of all elements is the same and therefore no self balancing stresses are built into the solution.

The above defect in the method would be a serious one if it could not be eliminated since a severe restriction would be placed on element layout. This negates one of the principle advantages of the finite element method, namely the ability to adjust the element layout to pick up more detail in regions of high gradient and to adjust the layout to fit arbitrary shapes. For these reasons the in-plane deformations were modified to correct for the difference between arc length and chord length in the deformed element.

Consider the element shown in Fig. D2. We define the rotation at the end of each side as shown in Fig. D2b. These rotations can be established from the nodal rotations $\{\theta_{xi}, \theta_{yi}\}$, which were determined in the preceding section, by the equation

$$\begin{Bmatrix} \theta_{s1} \\ \theta_{s2} \end{Bmatrix} = \begin{bmatrix} S_i & -C_i & \cdot & \cdot \\ \cdot & \cdot & S_i & -C_i \end{bmatrix} \begin{Bmatrix} \theta_{xk} \\ \theta_{yk} \\ \theta_{xj} \\ \theta_{yj} \end{Bmatrix}, \quad i, j, k \text{ in cyclic order,} \quad (D-13)$$

where $S_i = \sin \gamma_i$, $C_i = \cos \gamma_i$, $\{\theta_{xk}, \theta_{yk}\}$ are the rotations at corner k as established in section D.2, and $\{\theta_{s1}^i, \theta_{s2}^i\}$ are the end rotations of side i .

The profile of a typical side k of the triangle is shown in Fig. D2c. Since the shape functions for the triangle are cubic expansions the deflection from the chord can be expressed as

$$W^k = l_k \langle -\xi(1-\xi^2) \quad \xi^2(1-\xi) \rangle \begin{Bmatrix} \theta_{s1}^k \\ \theta_{s2}^k \end{Bmatrix}$$

then

$$\frac{\partial W^k}{\partial s} = \langle -(1-\xi)(1-3\xi) \quad -\xi(3\xi-2) \rangle \begin{Bmatrix} \theta_{s1}^k \\ \theta_{s2}^k \end{Bmatrix} \quad (D-14)$$

The difference between the arc length and the chord length may be evaluated as

$$\Delta^k = \int_0^{l_k} (1 - \cos \phi) ds \approx \frac{1}{2} \int_0^{l_k} \left(\frac{\partial W}{\partial s} \right)^2 ds \quad (D-15)$$

where the approximation is obtained from the first term of the trigonometric expansion of $\cos \phi$.

Substituting equation (D-14) into (D-15) and integrating yields

$$\Delta^k = \frac{1}{2} \langle \theta_{s1}^k \quad \theta_{s2}^k \rangle \int_0^1 \begin{Bmatrix} (1-\xi)(1-3\xi) \\ -\xi(2-3\xi) \end{Bmatrix} \langle (1-\xi)(1-3\xi) \quad -\xi(2-3\xi) \rangle d\xi \begin{Bmatrix} \theta_{s1}^k \\ \theta_{s2}^k \end{Bmatrix} \quad (D-16)$$

$$= \langle \theta_{s1}^k \quad \theta_{s2}^k \rangle \frac{l_k}{60} \begin{bmatrix} 4 & -1 \\ -1 & 4 \end{bmatrix} \begin{Bmatrix} \theta_{s1}^k \\ \theta_{s2}^k \end{Bmatrix}$$

Evaluating $\langle \theta_{s1}, \theta_{s2} \rangle$ by making use of equations (D-13) yields

$$\Delta^i = \langle \theta_{xk} \theta_{yk} \theta_{xj} \theta_{yj} \rangle \frac{l_i}{60} \begin{bmatrix} 4S_i^2 & -4C_i S_i & -S_i^2 & S_i C_i \\ & 4C_i^2 & S_i C_i & -C_i^2 \\ & & 4C_i^2 & -4S_i C_i \\ & & & 4S_i^2 \end{bmatrix} \begin{Bmatrix} \theta_{xk} \\ \theta_{yk} \\ \theta_{xj} \\ \theta_{yj} \end{Bmatrix} \quad (\text{D-17})$$

which gives the change in length of the three sides of the triangle in terms of the nodal rotations.

Since this change in length represents an increase in length over the chord length, the effective nodal displacements were incremented for the purposes of computing element strains. The increments in nodal displacements were computed as follows:

- (1) The nodal displacements of point 2' were incremented by Δ^3 as shown in Fig. D2a.
- (2) The nodal displacements of point 3' were incremented by combining Δ^1 , Δ^2 , and Δ^3 by a Williot-Mohr approach as shown in Fig. D2d.

This modification of nodal displacements was applied only for the purpose of computing in-plane element strains and is obviously approximate. It reduces but does not eliminate the effect discussed at the first of this section. However the residual stresses are reduced by several orders of magnitude and those remaining are negligible in comparison with the primary stress effects.

D.4 Derivation of Triangular Relationships[†]

D.4.1 Relationships Between Co-ordinate Systems

In dealing with the triangle, three types of co-ordinate systems are useful:

- (a) the "global" or "local" co-ordinate system $x - y$, (Fig. D3a),
- (b) "side" co-ordinates $s_i - n_i$, (Fig. D3b)
- (c) the "triangular" co-ordinate system $\zeta_1, \zeta_2, \zeta_3$, (Fig. D3c).

In this section i, j, k , refer to any cyclic order of the indices 1, 2, 3.

To relate the global and side co-ordinate systems, the s and n co-ordinates of a point may be projected onto the x and y axes, (Fig. D3d), to obtain

$$\begin{Bmatrix} x \\ y \end{Bmatrix} = \begin{bmatrix} \cos \gamma_i & -\sin \gamma_i \\ \sin \gamma_i & \cos \gamma_i \end{bmatrix} \begin{Bmatrix} s_i \\ n_i \end{Bmatrix} + \begin{Bmatrix} x_j \\ y_j \end{Bmatrix} \quad (\text{D-18})$$

which, according to the definitions, (Fig. D3e),

$$a_i = x_k - x_j$$

$$b_i = y_j - y_k$$

can be written as

$$\begin{Bmatrix} x \\ y \end{Bmatrix} = \frac{1}{l_i} \begin{bmatrix} a_i & b_i \\ -b_i & a_i \end{bmatrix} \begin{Bmatrix} s_i \\ n_i \end{Bmatrix} + \begin{Bmatrix} x_j \\ y_j \end{Bmatrix}. \quad (\text{D-19})$$

[†] The co-ordinate systems used in this section are lefthanded co-ordinate systems and do not correspond to those used in the remainder of this work. Formulae cannot therefore be taken directly from this section and applied in other sections. All the relationships developed have been previously established elsewhere. See, for instance, Felippa [1, 3].

Transposition of the corner co-ordinates and inversion then yields the relationships

$$\begin{aligned} \begin{Bmatrix} s_i \\ m_i \end{Bmatrix} &= \begin{bmatrix} \cos \delta_i & \sin \delta_i \\ -\sin \delta_i & \cos \delta_i \end{bmatrix} \begin{Bmatrix} x - x_j \\ y - y_j \end{Bmatrix} \\ &= \frac{1}{l_i} \begin{bmatrix} a_i & -b_i \\ b_i & a_i \end{bmatrix} \begin{Bmatrix} x - x_j \\ y - y_j \end{Bmatrix}. \end{aligned} \quad (\text{D-20})$$

Using the definition of triangular co-ordinates

$$\xi_i = \frac{A_i}{A} \quad (\text{D-21})$$

the derivatives of the triangular co-ordinates may be established

(Fig. D3f)

$$\frac{\partial \xi_i}{\partial x} = \frac{b_i}{2A} \quad \frac{\partial \xi_i}{\partial y} = \frac{a_i}{2A} \quad (\text{D-22})$$

Differentiating equations (D-18) and (D-20) yields

$$\begin{aligned} \frac{\partial x}{\partial s_i} &= \frac{a_i}{l_i} = \frac{\partial y}{\partial m_i} & \frac{\partial s_i}{\partial x} &= \frac{a_i}{l_i} = \frac{\partial m_i}{\partial y} \\ \frac{\partial x}{\partial m_i} &= \frac{b_i}{l_i} = -\frac{\partial y}{\partial s_i} & \frac{\partial m_i}{\partial x} &= \frac{b_i}{l_i} = -\frac{\partial s_i}{\partial y} \end{aligned} \quad (\text{D-23})$$

Starting with the basic relationship between triangular co-ordinates (see section C.1), and the geometric relationships of Fig. D3g, the relationship between triangular and global co-ordinates may be established.

$$\begin{pmatrix} 1 \\ x \\ y \end{pmatrix} = \begin{bmatrix} 1 & 1 & 1 \\ x_1 & x_2 & x_3 \\ y_1 & y_2 & y_3 \end{bmatrix} \begin{pmatrix} \xi_1 \\ \xi_2 \\ \xi_3 \end{pmatrix} \quad (\text{D-24})$$

Inverting the matrix yields

$$\begin{pmatrix} \xi_1 \\ \xi_2 \\ \xi_3 \end{pmatrix} = \frac{1}{2A} \begin{bmatrix} 2A_{23} & b_1 & a_1 \\ 2A_{31} & b_2 & a_2 \\ 2A_{12} & b_3 & a_3 \end{bmatrix} \begin{pmatrix} 1 \\ x \\ y \end{pmatrix} \quad (\text{D-25})$$

where A_{ij} has been defined in section C.1 and

$$2A = a_j b_i - b_j a_i \quad (\text{D-26})$$

is twice the area of the triangle, (Fig. D3h).

Differentiating equation (D-24) yields

$$\frac{\partial x}{\partial \xi_i} = x_i \quad \frac{\partial y}{\partial \xi_i} = y_i \quad (\text{D-27})$$

The side co-ordinates may be expressed in terms of the triangular co-ordinates, by the geometry of Fig. D3k, which yields

$$\begin{pmatrix} 1 \\ s_i \\ x_i \end{pmatrix} = \begin{bmatrix} 1 & 1 & 1 \\ \cdot & l_i & d_i \\ \cdot & \cdot & h_i \end{bmatrix} \begin{pmatrix} \xi_j \\ \xi_k \\ \xi_i \end{pmatrix} \quad (\text{D-28})$$

Inversion yields

$$\begin{pmatrix} \zeta_j \\ \zeta_k \\ \zeta_i \end{pmatrix} = \frac{1}{2A} \begin{bmatrix} 2A & -h_i & d_i - l_i \\ \cdot & h_i & -d_i \\ \cdot & \cdot & l_i \end{bmatrix} \begin{pmatrix} 1 \\ s_i \\ m_i \end{pmatrix}. \quad (\text{D-29})$$

Differentiation of equation (D-29) yields

$$\begin{aligned} \frac{\partial \zeta_j}{\partial s_i} &= -\frac{h_i}{2A} & \frac{\partial \zeta_j}{\partial m_i} &= \frac{d_i - l_i}{2A} \\ \frac{\partial \zeta_k}{\partial s_i} &= \frac{h_i}{2A} & \frac{\partial \zeta_k}{\partial m_i} &= -\frac{d_i}{2A} \\ \frac{\partial \zeta_i}{\partial s_i} &= 0 & \frac{\partial \zeta_i}{\partial m_i} &= \frac{l_i}{2A} \end{aligned} \quad (\text{D-30})$$

If we now consider a general function of the triangular co-ordinates $f(\zeta_1, \zeta_2, \zeta_3)$, equation (D-30) and (D-22) may be used to evaluate the partial derivatives which arise and establish the relations.

$$\begin{aligned} \frac{\partial f}{\partial s_i} &= \frac{1}{l_i} \left(\frac{\partial f}{\partial \zeta_k} - \frac{\partial f}{\partial \zeta_j} \right) \\ \frac{\partial f}{\partial m_i} &= \frac{1}{2A} \left\{ l_i \frac{\partial f}{\partial \zeta_i} + (d_i - l_i) \frac{\partial f}{\partial \zeta_j} - d_i \frac{\partial f}{\partial \zeta_k} \right\} \text{ no sum} \quad (\text{D-31}) \end{aligned}$$

$$\begin{aligned} \frac{\partial f}{\partial z} &= \frac{b_i}{2A} \frac{\partial f}{\partial \zeta_i} \\ \frac{\partial f}{\partial y} &= \frac{a_i}{2A} \frac{\partial f}{\partial \zeta_i} \end{aligned} \quad (\text{D-32})$$

Defining the quantities μ_i and λ_i as

$$\lambda_i = \frac{a_i}{l_i} \quad \text{and} \quad \mu_i = 1 - \lambda_i, \quad (\text{D-33})$$

(see Fig. C1), and using the geometry of Fig. D3l establishes the relations

$$\lambda_i = - \frac{a_i a_k + b_i b_k}{l_i^2}$$

$$\mu_i = - \frac{a_i a_j + b_i b_j}{l_i^2} \quad (\text{D-34})$$

and

$$h_i = \frac{a_i b_k - a_k b_i}{l_i}$$

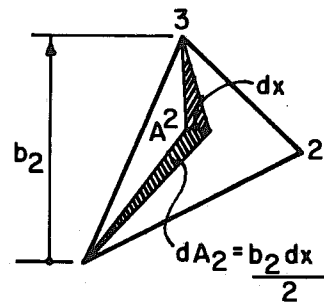
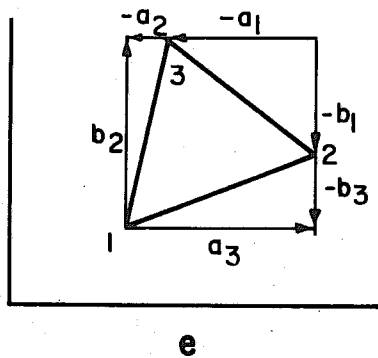
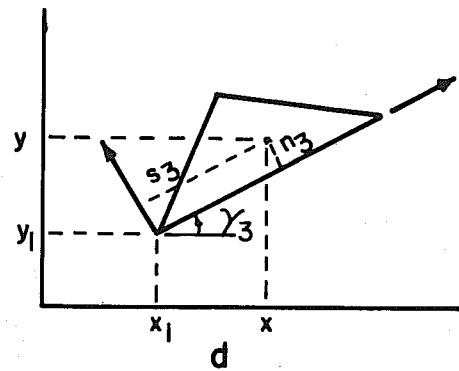
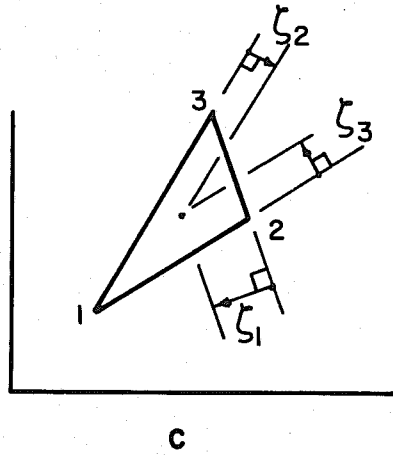
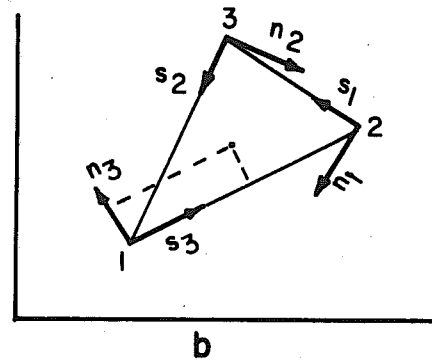
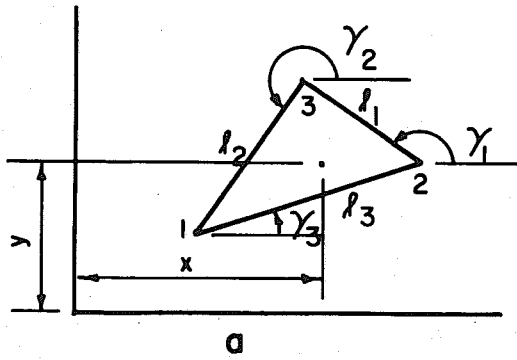
D.4.2 Subtriangle Geometry

In developing the stiffness matrices for the LCCT-9 it is necessary to use relationships between subtriangle geometry and the geometry of the total triangle. In the following, the subtriangles are assumed formed by joining the corner points to the centroid (see Fig. C1). Superscripts refer to the subtriangle number. Referring to Fig. D3m the following relationships are obtained by inspection

$$a_i = a_3^i \quad b_i = b_3^i$$

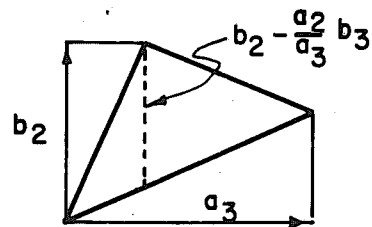
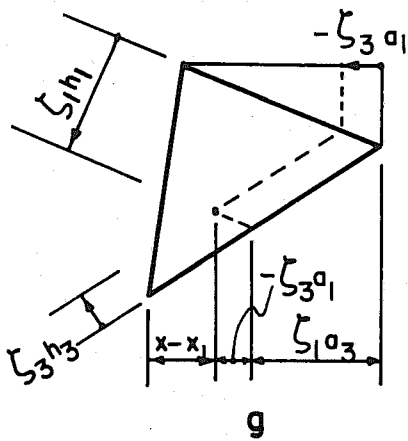
$$a_1^i = -a_2^j \quad b_1^i = -b_2^j \quad (\text{D-35})$$

In addition, from the geometry of Fig. D3n, we obtain



$$\frac{\delta \zeta_2}{\delta x} = \frac{1}{A} \frac{\delta A_2}{\delta x} = \frac{b_2}{2A}$$

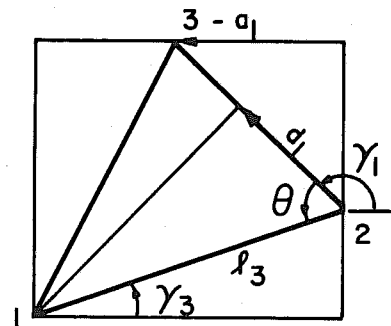
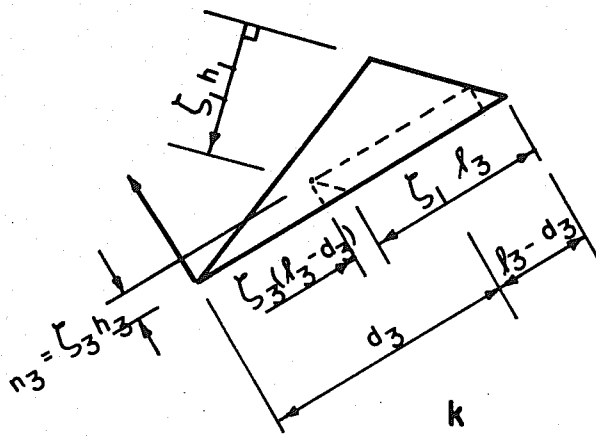
f



$$A = \frac{a_3}{2} (b_2 - \frac{a_2}{a_3} b_3)$$

h

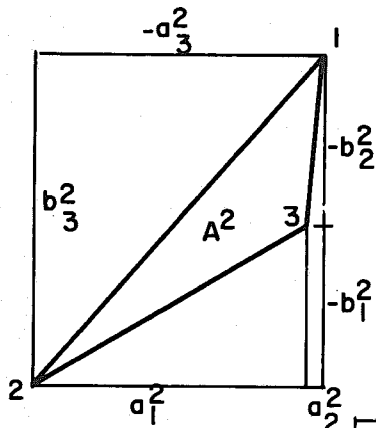
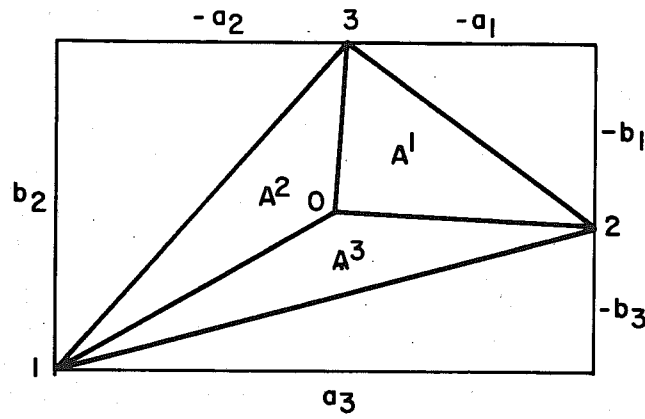
FIG. D3 (Page 1 of 3)



l

$$\sin \gamma_i = \frac{b_i}{l_i}$$

$$\cos \gamma_i = \frac{a_i}{l_i}$$



m

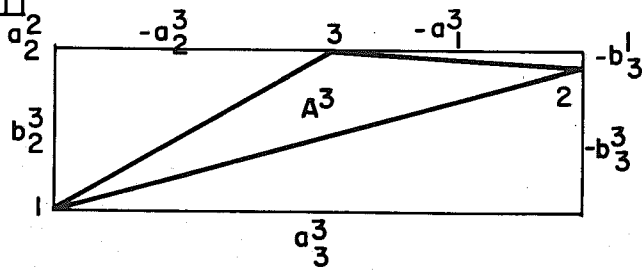
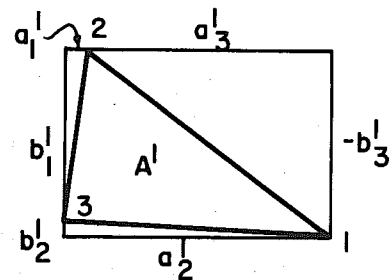
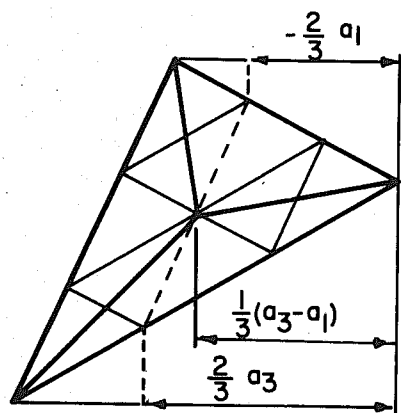
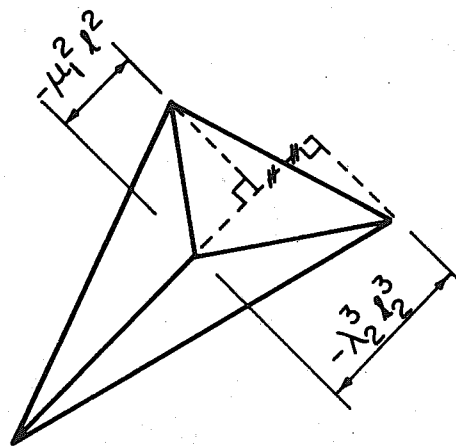


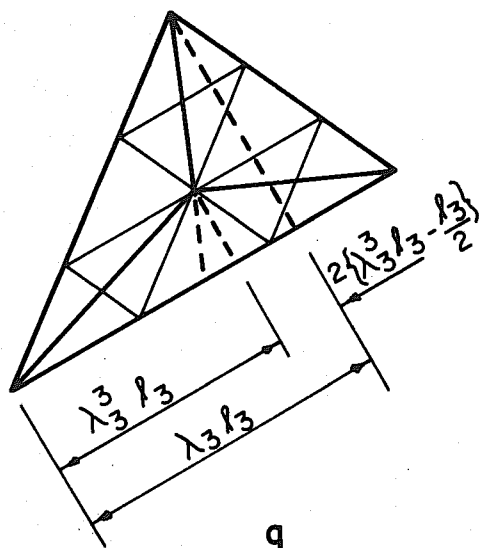
FIG. D3 (Page 2 of 3)



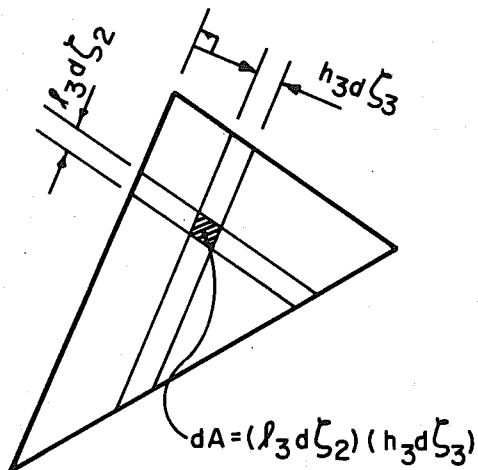
n



p



q



r

FIG. D3 (Page 3 of 3)

$$a_1^i = -a_2^j = \frac{a_j - a_i}{3}$$

$$b_1^j = -b_2^i = \frac{b_j - b_i}{3} \quad (\text{D-36})$$

Also, from the geometry of Fig. D3p, we obtain

$$\mu_1^i + \lambda_2^j = -1 \quad (\text{D-37})$$

and, from the geometry of Fig. D3q, we obtain

$$\lambda_3^i = \frac{1}{3} (1 + \lambda_i) \quad (\text{D-38})$$

and therefore

$$\mu_3^i = \frac{1}{3} (1 + \mu_i) \quad (\text{D-39})$$

D.4.3 Integration

Integration of polynomials in triangular co-ordinates easily accomplished by reducing the terms to products of only two co-ordinates, say ζ_1 and ζ_2 , integrating each from 0 to 1 and using an element of area as shown in Fig. D3r.

D.4.4. Construction of Interpolating Polynomials[†]

The construction of interpolation functions can be most easily

[†] The method of constructing interpolations functions that is outlined here is due to Felippa.

accomplished by visualizing the function as a surface constructed with reference to the plane of the element which is taken as the $z = 0$ plane. Felippa has used this technique and intuitive reasoning to construct interpolation functions for various nodal systems up to the fifth order.

In deriving the geometric stiffness matrix, interpolation functions for a quadratic expansion were used [equation (C-33)]. The complete quadratic polynomial has $\frac{(2+1)(2+2)}{2} = 6$ independent terms (see section C.1). For this purpose the nodal system in Fig. D4a was used. To obtain interpolating functions for this system the following procedure may be used:

- (a) Consider a corner point such as point 1. The interpolation function for this point should have a value of unity for $(1, 0, 0)$ and zero for points 2, 3, 4, 5 and 6. This can be achieved by taking a product of the equations for the lines 3-2 and 4-5. Thus the interpolation function for point 1 should be.

$$k \xi_1 \left(\xi_1 - \frac{1}{2} \right)$$

The constant k is chosen to normalize the function for $(1, 0, 0)$ and therefore is 2.

- (b) Consider the midpoint of a side, say point 4. By identical reasoning to that above the interpolation function is

$$k \xi_1 \xi_2$$

where k must have a value of 4.

In constructing the bending stiffness matrix for the triangle a cubic expansion is used. Fig. D4 shows three alternative sets of nodal quantities that can be used. The actual nodal system employed is that of Fig. D4d but it is useful to start with the nodal system of Fig. D4b to describe the procedure.

The interpolation functions for the nodal system of Fig. D4b are constructed in exactly the same way as described above. Thus, by inspection, the interpolation function for point 1 is

$$k_1 \zeta_1 \left(\zeta_1 - \frac{1}{3} \right) \left(\zeta_1 - \frac{2}{3} \right),$$

for point 4 is

$$k_2 \zeta_1 \zeta_2 \left(\zeta_1 - \frac{1}{3} \right),$$

for point 5 is

$$k_3 \zeta_1 \zeta_2 \left(\zeta_1 - \frac{2}{3} \right),$$

and for point 0 is

$$k_4 \zeta_1 \zeta_2 \zeta_3.$$

The k_i are determined to normalize the values of the functions at the respective points.

The construction of interpolations functions for the nodal quantities of Fig. D4c, can be undertaken as follows:

- (a) Consider displacement of corner 1. The associated interpolation function should
- (i) have a value of unity at (1, 0, 0)
 - (ii) produce zero slope at all corners and zero displacement at corners 2 and 3.
 - (iii) produce zero displacement at the centroid.

To satisfy conditions (ii) it is sufficient, for points 2 and 3, to have a ζ_1^2 in the product. However the function must also have zero slope at (1, 0, 0). This suggest a function of the form

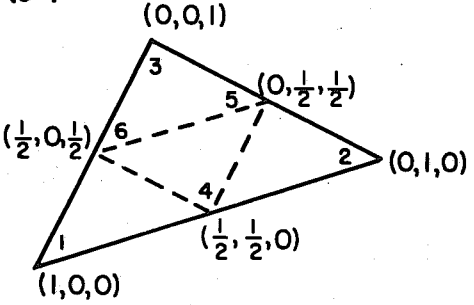
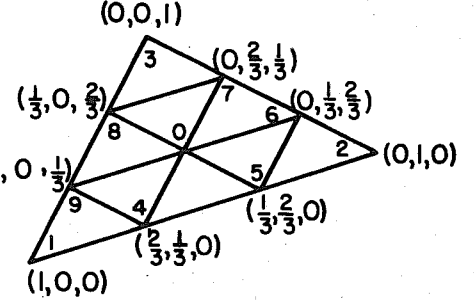
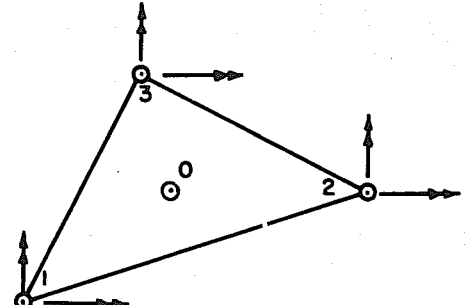
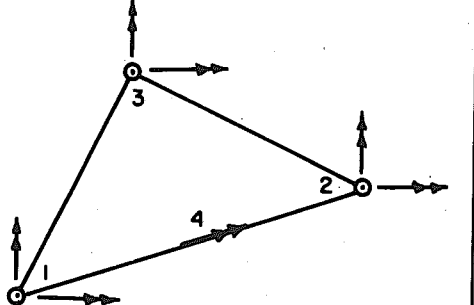
NODAL SYSTEM	NODAL VECTOR	INTERPOLATING FUNCTIONS
<p>(a)</p> 	w_1 w_2 w_3 w_4 w_5 w_6	$\xi_1 (2 \xi_1 - 1)$ $\xi_2 (2 \xi_2 - 1)$ $\xi_3 (2 \xi_3 - 1)$ $4 \xi_1 \xi_2$ $4 \xi_2 \xi_3$ $4 \xi_3 \xi_1$
<p>(b)</p> 	w_1 w_2 w_3 w_4 w_5 w_6 w_7 w_8 w_9 w_{10}	$\xi_1 (3 \xi_1 - 1) (3 \xi_1 - 2)$ $\xi_2 (3 \xi_2 - 1) (3 \xi_2 - 2)$ $\xi_3 (3 \xi_3 - 1) (3 \xi_3 - 2)$ $9 \xi_1 \xi_2 (3 \xi_1 - 1)$ $9 \xi_1 \xi_2 (3 \xi_2 - 1)$ $9 \xi_2 \xi_3 (3 \xi_2 - 1)$ $9 \xi_2 \xi_3 (3 \xi_3 - 1)$ $9 \xi_3 \xi_1 (3 \xi_3 - 1)$ $9 \xi_3 \xi_1 (3 \xi_1 - 1)$ $54 \xi_1 \xi_2 \xi_3$
<p>(c)</p> 	w_1 θ_{x1} θ_{y1} w_2 θ_{x2} θ_{y2} w_3 θ_{x3} θ_{y3} w_0	$\xi_1^2 (\xi_1 + 3 \xi_2 + 3 \xi_3) - 7 \xi_1 \xi_2 \xi_3$ $\xi_1^2 (a_3 \xi_2 - a_2 \xi_3) + (a_2 - a_3) \xi_1 \xi_2 \xi_3$ $\xi_1^2 (b_2 \xi_3 - b_3 \xi_2) + (b_3 - b_2) \xi_1 \xi_2 \xi_3$ $\xi_2^2 (\xi_2 + 3 \xi_3 + 3 \xi_1) - 7 \xi_1 \xi_2 \xi_3$ $\xi_2^2 (a_1 \xi_3 - a_3 \xi_1) + (a_3 - a_1) \xi_1 \xi_2 \xi_3$ $\xi_2^2 (b_3 \xi_1 - b_1 \xi_3) + (b_1 - b_3) \xi_1 \xi_2 \xi_3$ $\xi_3^2 (\xi_3 + 3 \xi_1 + 3 \xi_2) - 7 \xi_1 \xi_2 \xi_3$ $\xi_3^2 (a_2 \xi_1 - a_1 \xi_2) + (a_1 - a_2) \xi_1 \xi_2 \xi_3$ $\xi_3^2 (b_1 \xi_2 - b_2 \xi_1) + (b_2 - b_1) \xi_1 \xi_2 \xi_3$ $27 \xi_1 \xi_2 \xi_3$
<p>(d)</p> 	w_1 θ_{x1} θ_{y1} w_2 θ_{x2} θ_{y2} w_3 θ_{x3} θ_{y3} θ_{z4}	$\xi_1^2 (\xi_1 + 3 \xi_2 + 3 \xi_3) + 6 \mu_3 \xi_1 \xi_2 \xi_3$ $\xi_1^2 (b_3 \xi_2 - b_2 \xi_3) + (b_3 \mu_3 - b_1) \xi_1 \xi_2 \xi_3$ $\xi_1^2 (a_3 \xi_2 - a_2 \xi_3) + (a_3 \mu_3 - a_1) \xi_1 \xi_2 \xi_3$ $\xi_2^2 (\xi_2 + 3 \xi_3 + 3 \xi_1) + 6 \lambda_3 \xi_1 \xi_2 \xi_3$ $\xi_2^2 (b_1 \xi_3 - b_3 \xi_1) + (b_2 - b_3 \lambda_3) \xi_1 \xi_2 \xi_3$ $\xi_2^2 (a_1 \xi_3 - a_3 \xi_1) + (a_2 - a_3 \lambda_3) \xi_1 \xi_2 \xi_3$ $\xi_3^2 (\xi_3 + 3 \xi_1 + 3 \xi_2)$ $\xi_3^2 (b_2 \xi_1 - b_1 \xi_2)$ $\xi_3^2 (a_2 \xi_1 - a_1 \xi_2)$ $-4 h_3 \xi_1 \xi_2 \xi_3$

FIG. D4 INTERPOLATION FUNCTIONS.

$$k_1 \zeta_1^2 (k_2 - \zeta_1)$$

such that k_2 can be evaluated to give zero slope at $(1, 0, 0)$. To satisfy condition (iii) the term

$$k_3 \zeta_1 \zeta_2 \zeta_3$$

can be added. This function produces zero displacement and slope at each corner and k_3 can be evaluated to eliminate displacement at node 0. The final function is therefore

$$k_1 \zeta_1^2 (k_2 - \zeta_1) + k_3 \zeta_1 \zeta_2 \zeta_3$$

with values of k_1, k_2, k_3 determined to satisfy the above conditions.

- (b) Considering an interpolation function for slope at a corner, say for θ_y at corner 1. This function should
- (i) have a unit derivative with respect to x at corner 1.
 - (ii) have a zero derivative with respect to x at corners 2, and 3.
 - (iii) have zero derivative with respect to y and have zero displacement at the three corners.
 - (iv) produce zero displacement at the centroid.

The condition at the centroid is satisfied in the same way as described above. Therefore we concentrate on conditions (i), (ii), and (iii). Since a visualization of the function shows it cannot be a function of ζ_1 alone, it could be of the form,

$$\zeta_1^2 (k_1 \zeta_1 + k_2 \zeta_2 + k_3 \zeta_3).$$

The inclusion of ζ_1^2 satisfies the conditions at corners 2 and 3.

Evaluation at (1, 0, 0) requires that k_1 be zero. The constants k_2 and k_3 may then be evaluated to satisfy the slope requirements at corner 1.

(c) The function

$$k \zeta_1 \zeta_2 \zeta_3$$

satisfies all requirements of the interpolation function for the centroid point 0.

Interpolation functions for the nodal system in Fig. D4d are given in equation (C-12) and may be obtained in the same way as those for the nodal system of Fig. D4c, except that the coefficient of

$$\zeta_1 \zeta_2 \zeta_3$$

is evaluated to make the normal derivative of all interpolating functions, except that for θ_4 , equal to zero at point 4. The function

$$k \zeta_1 \zeta_2 \zeta_3$$

is then the interpolation function for θ_4 but the coefficient is chosen to normalize the slope rather than the deflection at the centroid.